Life cycle assessment of silicon based tandem and advanced silicon solar modules

Author:
Monteiro Lunardi, Marina

Publication Date:
2019

DOI:
https://doi.org/10.26190/unsworks/21226

License:
https://creativecommons.org/licenses/by-nc-nd/3.0/au/
Link to license to see what you are allowed to do with this resource.

LIFE CYCLE ASSESSMENT OF SILICON BASED TANDEM AND ADVANCED SILICON SOLAR MODULES

Marina Monteiro Lunardi

A THESIS IN FULFILMENT OF THE REQUIREMENTS FOR THE DEGREE OF

DOCTOR OF PHILOSOPHY

School of Photovoltaic and Renewable Energy Engineering

Faculty of Engineering

The University of New South Wales

January 2019

INCLUSION OF PUBLICATIONS STATEMENT

UNSW is supportive of candidates publishing their research results during their candidature as detailed in the UNSW Thesis Examination Procedure.

Publications can be used in their thesis in lieu of a Chapter if:

- The student contributed greater than 50% of the content in the publication and is the "primary author", ie. the student was responsible primarily for the planning, execution and preparation of the work for publication
- The student has approval to include the publication in their thesis in lieu of a Chapter from their supervisor and Postgraduate Coordinator.
- The publication is not subject to any obligations or contractual agreements with a third party that would constrain its inclusion in the thesis

Please indicate whether this thesis contains published material or not.

☐ *This thesis contains no publications, either published or submitted for publication (if this box is checked, you may delete all the material on page 2)*

☒ *Some of the work described in this thesis has been published and it has been documented in the relevant Chapters with acknowledgement (if this box is checked, you may delete all the material on page 2)*

☐ *This thesis has publications (either published or submitted for publication) incorporated into it in lieu of a chapter and the details are presented below*

CANDIDATE'S DECLARATION

I declare that:

- I have complied with the Thesis Examination Procedure
- where I have used a publication in lieu of a Chapter, the listed publication(s) below meet(s) the requirements to be included in the thesis.

Name	Signature	Date (dd/mm/yy)

Postgraduate Coordinator's Declaration (to be filled in where publications are used in lieu of Chapters)

I declare that:

- the information below is accurate
- where listed publication(s) have been used in lieu of Chapter(s), their use complies with the Thesis Examination Procedure
- the minimum requirements for the format of the thesis have been met.

PGC's Name	PGC's Signature	Date (dd/mm/yy)

THE UNIVERSITY OF NEW SOUTH WALES

Thesis/Dissertation Sheet

Surname or Family name: **Monteiro Lunardi**

First name: **Marina**   Other name/s: -

Abbreviation for degree as given in the University calendar: **PhD**

School: **School of Photovoltaic and Renewable Energy Engineering**   Faculty: **Engineering**

Title: **Life cycle assessment of silicon based tandem and advanced silicon solar modules**

Abstract 350 words maximum:

Electricity generation from renewable sources has increased greatly in recent years. The use of photovoltaic (PV) solar modules is constantly studied and improved. Silicon (Si) solar cells dominate the current market share, because Si is abundant, non-toxic, stable and has benefited from developments in the semiconductor industry. However, the PV single-junction solar cell limiting energy conversion efficiency is approximately 30% (depending on specific assumptions). Tandem technology is based in multiple solar cells that are each optimized for a part of the spectrum and can achieve higher efficiencies compared to single junction solar cells. Considering a Si bottom cell, there are also a few enhancements that can be made to achieve even higher efficiencies for tandem solar cells. Especially for crystalline Si (c-Si) wafer solar cells, there are many variations in the existing production processes to improve module performance, such as the passivated emitter and rear cell (PERC) technology, which is replacing the recently-dominant screen-printed aluminium back surface field (Al-BSF) technology in the future.

Environmental analysis should complement the development of new PV technologies. Life cycle assessment (LCA) is a methodology that assesses environmental impacts through the inputs and outputs associated with all the stages of a product's life cycle, from the raw material extraction to the end of life. A significant quantity of inventory data is necessary to build a model as close as possible to reality to perform a realistic LCA and the availability of relevant and recent data is the greatest challenge for all LCA practitioners, independently of methodological approaches.

The goal of this research is to undertake a comparison of several environmental impacts of different Si-tandem solar module technologies through the LCA method. Besides that, this research aims to partially address the inventory gap issue by developing life cycle inventory (LCI) data of some PV technologies and methods of production.

Conducting LCAs on new technologies is indispensable in the search for materials and processes that have the lowest environmental impacts possible, as has been reinforced in this thesis. The energy use during the Si treatment is the main contributor to the majority of the ecological effects assessed.

FOR OFFICE USE ONLY   Date of completion of requirements for Award:

COPYRIGHT STATEMENT

Signed: …………………………   Date: …………………………………

AUTHENTICITY STATEMENT

'I certify that the Library deposit digital copy is a direct equivalent of the final officially approved version of my thesis. No emendation of content has occurred and if there are any minor variations in formatting, they are the result of the conversion to digital format.'

Signed: …………………………   Date: …………………………………

ORIGINALITY STATEMENT

'I hereby declare that this submission is my own work and to the best of my knowledge it contains no materials previously published or written by another person, or substantial proportions of material which have been accepted for the award of any other degree or diploma at UNSW or any other educational institution, except where due acknowledgement is made in the thesis. Any contribution made to the research by others, with whom I have worked at UNSW or elsewhere, is explicitly acknowledged in the thesis. I also declare that the intellectual content of this thesis is the product of my own work, except to the extent that assistance from others in the project's design and conception or in style, presentation and linguistic expression is acknowledged.'

Signed: …………………………   Date: …………………………………

Table of Contents

Abbreviations and Symbols

ADP	Abiotic depletion potential
Al	Aluminium
Al-BSF	Aluminium back surface field
a-Si	Amorphous silicon
a-Si:H	Hydrogenated amorphous silicon
AZTS	Ag_2ZnSnS_4
B	Boron
BOS	Balance of system
CdS	Cadmium sulfide
CdTe	Cadmium telluride
$CH_3NH_3PbI_3$	Methylammonium lead triiodide perovskite
CIGS	Copper indium gallium diselenide
CIS	Copper indium diselenide or disulphide
c-Si	Crystalline silicon
CZTS	Copper zinc tin sulfide
DC	Direct current
DSSC	Dye-sensitised solar cells
EGS	Electronic grade silicon
EoL	End-of-life
EPBT	Energy payback time
Fe	Iron
FEcP	Freshwater ecotoxicity potential
FEuP	Freshwater eutrophication potential
FU	Functional unit
GaAs	Gallium arsenide
GHG	Greenhouse gases
GWP	Global warming potential
HJS	Silicon-based heterojunction solar cells
HTP-CE	Human toxicity potential - cancer effects
HTP-nCE	Human toxicity potential – non-cancer effects
IEA	International Energy Agency
ISO	International Organization for Standardization
LCA	Life cycle assessment

LCI	Life cycle inventory
MGS	Metallurgical grade silicon
mono-Si	Monocrystalline silicon
multi-Si	Multicrystalline silicon
N	Nitrogen
OPV	Organic photovoltaics
P	Phosphorous
Pb	Lead
PECVD	Plasma-enhanced chemical vapour deposition
PERC	Passivated emitter and rear cell
PR	Performance ratio
PV	Photovoltaic
PVPS	Photovoltaic Power Systems Programme
SGS	Solar grade silicon
Si	Silicon
SiHCl$_3$	Trichlorosilane
S-Q	Shockley-Queisser
UMG-Si	Upgraded metallurgical silicon
W	Watts

List of Figures

List of Tables

Acknowledgements

I would like to express my gratitude to those who were with me, here in Australia and far away, during this long period. I'm glad to have such incredible people in my life, and it is because of them that I could accomplish this important step in my professional journey.

I couldn't start with anyone but my beautiful parents, Deise and Álvaro, who dedicated their life to my sister and me and helped us to be who we are today. Even from the other side of the world, they were present in every step of this journey giving me the support and love that I needed always to keep going. I love you unconditionally. Thanks to my sister, Gabriela, for her care and presence here in Australia. You are a brilliant person, and you inspire me every day. A special thanks to my grandmother, Elza, for teaching me how to be a strong woman and for never letting me give up.

During these 4 years of PhD, I also had a lot of support from all my friends from Brazil and the ones that I met here in Australia. I believe in the power of friendship, and they prove me that it is true. Thank you for my friends from Porto Alegre Natália Eifler, Sofia Bezerra, Luisa Silveira, Luisa Pires, Clarisse Dornelles, Laura Pressi and Aline Kintchner that were far away but so close at the same time. I would also like to thank my friends from Sydney Patrícia Parreira, Juliana Souza, Polyana Moura, Anita Amorim, Daniele Leão e Nayara Tanin and many others that made my life happier here. A special thanks to my best friend and partner, Daniel Castello, who was part of the good and bad moments of this journey, and kept me strong to keep going. I love you all very much.

1 Introduction

The global demand for electricity rises every day as a consequence of constant and rapid population growth and development. This growth has become a great challenge. The dependence of non-renewable fossil fuels as an energy source is widely debated since these sources are finite and also proven to damage the existing environment, putting humans, fauna and flora at risk. The hazards caused by non-renewable sources of energy, in addition to the new economic opportunities provided by the transition to the clean-energy era, have driven many countries to target the reduction of their harmful emissions [1].

Consequently, electricity generation from renewable sources has increased greatly in recent years and photovoltaic (PV) technology is a frequent preference worldwide. Solar PV was the world's leading source of additional (net of decommissioning) power generating capacity in 2017 [2]. The annual market increased approximately 50% to at least 75 gigawatts – equivalent to more than 31 thousand solar modules installed per hour – raising the global total to at least 303 gigawatts in the same year [2].

The use of PV solar modules as a source of electricity is constantly studied and improved. Silicon (Si) solar cells dominate the current market share [3] because Si is abundant, non-toxic, stable and has benefited from developments in the semiconductor industry. This technology is proven, modules are robust, and the manufacturing costs are low and falling. However, the search for new materials and designs is also being carried out looking for cost and performance improvements.

Based on the Shockley-Queisser (S-Q) detailed-balance model, even with improvements, the PV single-junction solar cell limiting energy conversion efficiency is approximately 30% (depending on specific assumptions), for a band gap of 1.1 eV and

considering an AM 1.5 solar spectrum [4]. The tandem technology is based in multiple solar cells that are optimized for each part of the spectrum and either connected electrically in series (two-terminal tandem) or kept electrically separate (four-terminal tandem, if a two-cell stack), achieving higher efficiencies when compared with single junction solar cells [5, 6]. Therefore, tandem solar cells are expected to be of increasing interest.

Tandem technology is not new [7] and has previously been efficaciously applied for solar cells in several combinations as dye-sensitized solar cells / Si solar cells [8], organic solar cells / Si solar cells [9], 3-junction tandem amorphous silicon solar cells [10], micromorph tandem solar cells [11] and triple junction tandems using III-V solar cells [12], for example. A Si-based tandem solar cell uses a top cell with a higher bandgap than Si. Thus, the top cell absorbs the higher energy photons and generates a voltage that is approximately twice what Si can generate [13, 14].

Thin-film materials have been developed, providing potentially low cost, flexible geometries and using relatively small material quantities. Thin-film technologies have led to three main options for PV modules: amorphous and microcrystalline Si films ("micromorph cells"); chalcogenide compounds such as cadmium telluride (CdTe), copper indium diselenide or disulphide (CIS), copper indium gallium diselenide (CIGS); and, more recently, perovskite solar cells. The possibility of a high band gap makes thin-film technologies attractive for using them on top of a Si base cell in tandem solar cells [15].

It is believed by some that a possible path for implementation of tandem solar cells on an industrial scale would be using perovskite and c-Si [16]. Some experiments have been made combining these two materials in a tandem structure [17, 18]. In a two-junction tandem solar cell, the higher bandgap cell (e.g., 1.5eV for methylammonium lead triiodide perovskite ($CH_3NH_3PbI_3$) perovskite) is placed such that it absorbs higher

energy photons first, followed by a lower bandgap cell (e.g., 1.1eV for a Si cell) for the lower energy part of the spectrum [19]. Various demonstrations of two-terminal perovskite-Si tandems, which involve the fabrication of a perovskite solar cell directly on a Si solar cell, have been reported [20-22].

The CIGS technology can also achieve high band gaps and be a good possibility for Si-based tandem solar cells. It has a chalcopyrite crystal structure which allows its band gap to be tuned between 1.0 and 2.4 eV by varying the In/Ga and Se/S ratios [15]. A problem with CIGS is the relative scarcity of indium in Earth's crust [23]. Researchers are showing that copper zinc tin sulfide (CZTS) is the most promising alternative to CIGS [24]. Development of tandem structures using CZTS on Si cells started with demonstrating CZTS epitaxy on Si, which has already been confirmed [25-27]. However, CZTS has lower efficiency than CIGS [28]. Recently, new alternatives have been proposed where either Zn or Cu is replaced by other elements in order to generate higher band gaps [29]. One example is Ag_2ZnSnS_4 (AZTS), wherein Ag replaces Cu [30]. The AZTS solar cells can achieve a direct band gap of 2.0 eV [31], making AZTS/Si tandem solar cells a promising future technology.

Considering the bottom cell as Si, there are also a few enhancements that can be made to achieve even higher efficiencies for tandem solar cells. Especially for crystalline Si (c-Si) wafer solar cells, there are many variations in the existing production processes that are intended to improve module performance [32]. The screen-printed aluminium back surface field (Al-BSF) sequence [33] is the current industry standard process but, in particular, the passivated emitter and rear cell (PERC) technology [34] is gaining significant share of the world market, and it will probably mostly replace Al-BSF technology in the future [32].

In recent years cost reduction has been a huge focus for the PV industry [32]. One possibility to reduce the overall costs of PV modules is the use of low-cost Si

feedstock, such as upgraded metallurgical Si (UMG-Si) [35], which produces lower quality wafers than Si made by the usual Siemens process but requires less energy and less financial investment [36, 37]. Additionally, the higher potential efficiency for tandems is particularly significant regarding costs because the cost to install solar modules – considering the installation, support frames, cabling, etc. – depends strongly on the number of modules installed which, in turn, is dependent on the module efficiency [38].

Complementary to the development of PV technologies, there should be environmental analyses of these new processes. Life cycle assessment (LCA) is a methodology that assesses the environmental impacts through the inputs and outputs associated with all the stages of a product's life cycle, considering raw material extraction, materials processing, manufacture, distribution, use, repair and maintenance, and end of life [21]. The LCA method has the benefit of involving different disciplines and a broad variety of techniques.

Although the environmental impacts of PV solar modules are not yet totally determined, there has already been some research carried out on this subject. These LCA studies evaluate potential environmental impacts associated with the raw materials, production processes, use phase and disposal of solar cells and modules during their assumed lifetimes, considering several assumptions, depending on the technology and production method. The depth of detail of an LCA study varies with each study and depends on the goal and scope definition [39].

A significant quantity of high-quality inventory data is necessary to build a model as close as possible to reality to perform a detailed LCA to be able to achieve realistic results. The availability of relevant and recent data is the greatest challenge for all LCA practitioners, independently of methodological approaches, which has led to the development of different databases. The most common inventory file used for LCA

studies related to energy generation is the Ecoinvent database [40]. However, there are still substantial data gaps in relation to renewable sources of energy such as PV, for example. Particularly for new technologies (e.g. perovskite), there is a very limited inventory, and most of these values are from laboratory experiments, so they cannot necessarily be considered as realistic for industrial mass production.

The goal of this research is to undertake a comparison of several environmental impacts of different Si-tandem solar module technologies through the LCA method, with the aid of GaBi LCA software [41]. The analyses focus on six crucial categories: global warming (GWP), human toxicity - cancer effects (HTP-CE), human toxicity – non-cancer effects (HTP-nCE), freshwater eutrophication (FEuP), freshwater ecotoxicity (FEcP) and abiotic depletion potential (ADP). It is also an objective of this thesis to calculate the EPBT of the chosen cells and module structures. Besides that, this research aims to partially address the inventory gap issue by developing life cycle inventory (LCI) data of some PV technologies and methods of production.

1.1 Motivations and Significance

In this thesis, we perform an analysis of the environmental impacts of specific solar cell and module structures, considering various sets of assumptions and different scenarios. There are several publications about possible environmental impacts of various types of solar cells. The International Energy Agency (IEA), for example, publishes regularly the "Life Cycle Inventories and Life Cycle Assessments of Photovoltaic Systems" through the Photovoltaic Power Systems Programme (PVPS) [42]. This document contains important data about inventories and impacts of the main commercial solar modules technologies; namely, monocrystalline Si (mono-Si), multicrystalline Si (multi-Si), and CdTe. However, there remains room for improvements in inventory collection and study of new technologies.

The advance of PV technologies and structures requires comprehensive LCA studies to guide manufacture's and policy makers to the best choice of technology. This thesis uses the LCA method to compare the environmental impact results from the production processes of perovskite/Si and chalcogenide/Si tandem solar modules, considering different Si technologies and possible improvements.

This LCA study can assist in sustainable technology development by focusing on the life cycle environmental consequences of fresh technologies that are still in the early stages of development. The advance of PV technologies and structures requires comprehensive LCA studies to develop the knowledge to find the best environmental choices of materials and technology. The LCA results help to identify opportunities to improve the ecological aspects of PV devices at various points in their lifecycle, as well as bring enough discussion to aid decision-making in industry, governmental or non-governmental organisations, selection of relevant indicators of environmental performance and marketing.

The results are in reasonable agreement with those already presented in the literature and encourage further studies, particularly related to the end-of-life (EoL) of these modules.

Besides, as the technologies keep evolving, the inventories for LCA studies are continuously changing. This thesis presents new data for tandem production processes, and for the innovative Si technologies of PERC and specific hydrogenation processes.

1.2 Research Limitations

The objective of this thesis is to provide realistic results for the environmental impacts from new PV technologies. However, there are uncertainties associated with the data

required and the assumption made throughout this work that might limit the precision of the results.

The majority of technologies chosen in this study are well known and the inventories, consequently, are complete and reliable. However, because the PV technologies are evolving, the inventory might be considered old and not account for the most recent developments. Some technologies are still being studied in laboratory scale and, because of that, there is only a small quantity of data available. Hence, a few values had to be estimated. These assumptions are based in specific publications and personal communication with experts on these processes and materials.

Additionally, several environmentally based suggestions are made regarding the ecological problems detected in this research. The goal of this work is not related to providing a solution for the environmental problems identified but to guide the research community and the industry on where to focus. In other words, this work provides a critical assessment of the environmental risks and impacts associated with using specific materials and production processes.

1.3 Thesis Outline

This thesis is divided into four main sections. The first part is a literature review of LCA studies focused on PV devices and possible recycling processes for the main technologies. Secondly, the methodology is described in detail, including the functional unit (FU) and other assumptions made and the scenarios considered. The third section is focused on the environmental impacts and the interpretation of each. Lastly, the final part discusses and concludes this thesis, presenting suggestions for future work.

Chapter 2 is a literature review. It starts with a background of PV technologies, and then focuses on the LCA studies made on the main technologies known, including single junction c-Si, perovskite, chalcogenide, advanced Si solar cells and tandem

structures. Besides that, a review of possible recycling processes for the main PV technologies is also accomplished.

Chapter 3 describes the concepts involved in the LCA methodology. This chapter includes a detailed explanation of the goal and scope chosen, as well as the functional unit, system boundaries and other important assumptions made. It evaluates the existing inventories (input and output data for each process step) and includes data collected for new technologies. And finally, it establishes the impact categories to be calculated and explains their importance related to the calculation of environmental impacts from energy sources.

Chapters 4, 5 and 6 investigate the environmental impacts. In these chapters, the results for GWP, HTP (cancer and non-cancer effects), FEuP, FEcP and ADP are interpreted through the LCA methodology, identifying the main focus of impacts from each production process and suggesting environmental improvements. It is also an objective of this thesis to calculate the EPBT.

Finally, *Chapter 7* summarises and discusses the key results and conclusions of this thesis and *Chapter 8* presents suggestions for future studies and some preliminary results for the environmental impacts of PV module recycling processes.

2 Literature Review

The intensity of the search for renewable sources of electric energy is increasing rapidly. The major challenge is to find technologies that can be as effective as non-renewable technologies and are able to be produced at a competitive price. Solar energy is one of the most highly developed renewable energy sources currently known [43]. PV conversion is the direct conversion of sunlight into electricity without using any heat engine or fossil source [44].

This chapter aims to review the existing knowledge of PV technologies and their environmental impacts, detecting the potential gaps that are significant for future investigation. First, a review on PV technologies is made, with a historical perspective, including a description of the possible materials for solar cells and modules and an outlook for future dominant technologies. Secondly, the concept of LCA methodology is introduced and explained. Finally, the LCA approach for PV technologies is described, with particular emphasis on the environmental impacts from production, use and end-of-life processes of different tandem solar cells and modules, which is the focus of this thesis.

2.1 Historical Perspective of Photovoltaics

The PV effect was first discovered, by accident, in 1839 by Becquerel. His work was focused on the behaviour of solids in electrolytes [45]. He immersed a metal plate in a solution and exposed it to light and observed that a small voltage and current were produced. This effect was called the PV effect [46].

In 1877, Adams and Day observed this effect in solid selenium [44]. Later, in 1883, Fritz developed the first thin-selenium PV cell with an efficiency of approximately 1%

[46, 47]. The development of this technology was increasing, and new materials were discovered. In 1927 a copper (Cu) and semiconductor Cu oxide PV cell was developed with an efficiency as low as the first solar cell, less than 1% [44]. The Si-based solar cell was discovered after that, in 1941, by Ohl — who produced the cell by impurity variation during crystal growth [46] — and with additional silicon refinement, this type of solar cell reached an efficiency of 6% under direct sunlight exposure. In 1954, in Bell Laboratories, the efficiency increased to 11% [47].

Since the 1950s the PV technology has advanced quickly. Small-scale use such as telephone repeaters requiring tens of Watts were traditional primary markets [46, 48, 49]. The first real impacts were realised for space applications [46].

The first practical PV device was first produced in 1958. The Vanguard satellite employed a PV generator (1W). With the space program increasing, improvements of PV power generation were required. In the 1960s the scientists needed to focus on the possibilities of improving the electrical power generation from the solar cells [50]. In the same decade, researchers discovered other PV materials, such as gallium arsenide (GaAs), that could be operated in higher temperatures then Si-based solar cells, but this type of cell was much more expensive [51].

In the 1970s Dr. Elliot Berman and the Exxon Corporation designed a significantly less costly solar cell based on selenium. Solar cells began to power many different applications. In 1972 France installed a cadmium sulfide (CdS) PV system to operate an educational television in Niger. In 1972 the Institute of Energy Conversion is established at the University of Delaware to perform research and development on thin-film PV and solar thermal systems, becoming the world's first laboratory dedicated to PV research and development [52].

Concern about the environment has increased and research about renewable sources of energy became ever more important, making the study of PV modules even more significant. Besides, the decision of exploring PV technology potential for terrestrial applications is also a consequence of the oil crises of 1973. Considering that, the researchers started to look towards PV technology for large-scale energy generation and use both in stand-alone and grid-connected (without storage) configurations [53].

In the 1980s, companies attempted to scale up thin-film PV technologies such as amorphous Si (a-Si) and CIGS, which had achieved >10% efficiency for small area (1 cm^2) devices [52]. From the early 1990s, there was significant research interest in thin-film cells, mainly because of their flexibility and cheap fabrication, compared with Si cells. However, by 2013, the thin-film cells were generally still not performing enough well in terms of efficiency, compared with Si solar cells [54]. In consequence, nowadays only a few companies are still manufacturing thin-film solar cells, which are CdTe cells and CIGS cells, representing a PV market share of below 10% [32].

After a long period of research and market growth, the costs for solar power are reducing every year, and the search for new materials and processes can reduce the prices even more, which increases the PV share in the world's energy market [32].

2.2 Photovoltaic Technologies

PV is a technology that produces direct current (DC) electrical power, which can be measured in Watts (W), from semiconductor materials when photons illuminate them. The radiation comes from sunlight, an abundant source of photons. The solar cells produce energy only while they are being illuminated [32], but PV devices require very little maintenance during use [55].

A simplified process of the production of electricity from a PV module is shown in Figure 1.
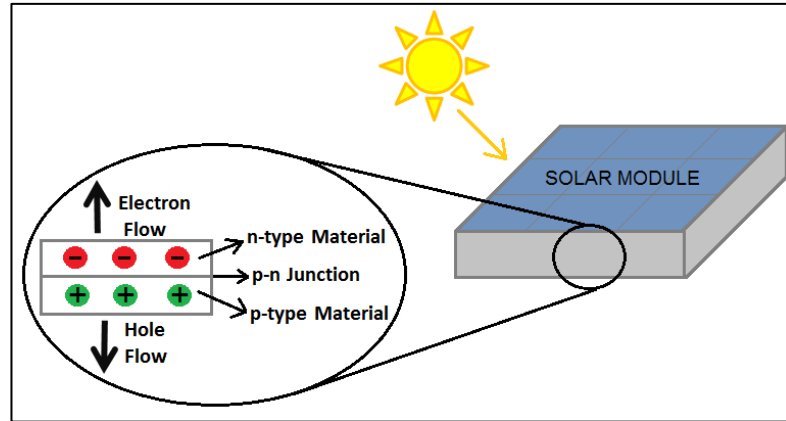
Figure 1: Summarised process of production of electricity from a PV module.

The energy conversion through PV solar cells consists of two main steps. The first one is the absorption of light from the sun, which generates an electron-hole pair. The second is the separation of the electron and hole by an imbalance within the device (electrons to the negative side and holes to the positive side), which generates electrical current [56].

The energy difference between the top of the valence (outer electron) band and the bottom of the conduction (free electron flow) band is called the "band gap", which determines the photon energy ranges for which the material is absorbing/transparent. Change carriers move by drift within an electric field and by diffusion.

The industry uses PV semi-conductor cells alone, in consumer products (solar powered watches, calculators, etc.) or assembled and encapsulated in solar modules. Solar cells have benefitted from intensive research and development efforts, leading to three main commercial technologies [57].

2.2.1 Crystalline Silicon Technologies

c-Si technology currently dominates the PV market, representing above 90% of the total [32]. Si wafers, in the form of either mono-Si or multi-Si, are the most studied technologies and, after decades of research and manufacturing, scientists and engineers are still improving the performance of Si-wafer PV [43]. Al-BSF (Figure 2) [33] is the current industry standard process [32] but there are many variations of the existing production processes for c-Si solar cells and modules, that are intended to improve module performance and/or reduce costs [32].
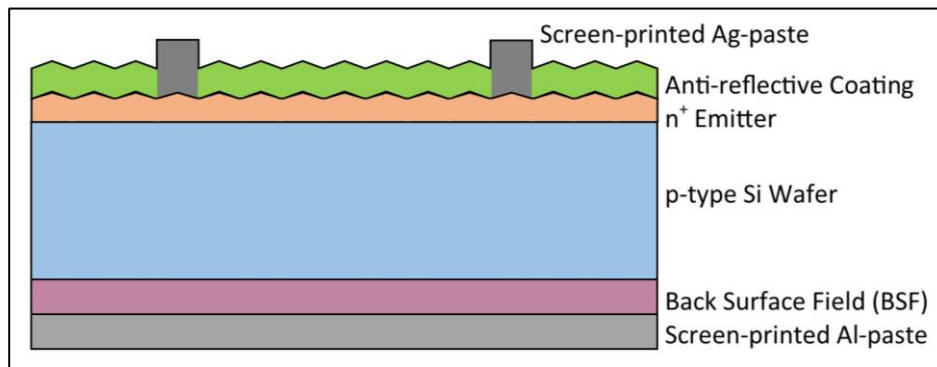
Figure 2: Basic structure of a aluminium Back Surface Field (Al-BSF) cell.

Silicon-based heterojunction solar cells (HJS) (Figure 3), for example, offer high efficiencies and several advantages in the production process compared to conventional crystalline silicon solar cells. The key point of that technology is the displacement of highly recombination-active contacts from the crystalline surface by insertion of a film with wide band gap [58], commonly amorphous Si.
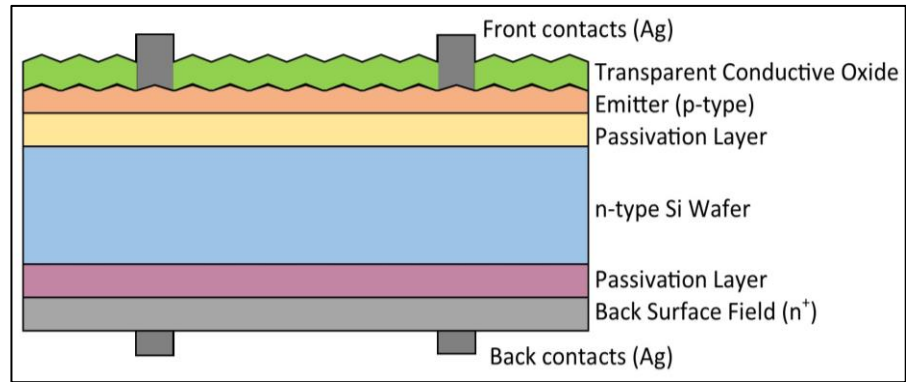
Figure 3: Basic structure of a Silicon-based heterojunction solar cells (HJS) cell.

The PERC technology [5] (Figure 4) is another example of high performance solar cells. This technology is gaining significant share in the world's PV market and is expected to replace Al-BSF as the dominant technology in the future (expected around 60% share in 2027) [3]. The PERC process has already been implemented in the industry [5] and the efficiency a p-type PERC cell has achieved $25.0 \pm 0.5\%$ [59].
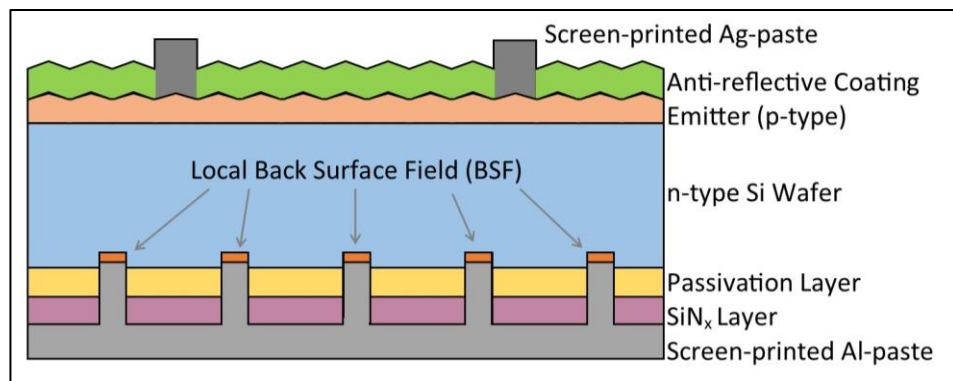
Figure 4: Basic structure of a Passivated Emitter and Rear Cell (PERC) cell.

Also, the interactions of impurities and defects within Si with hydrogen (H) have been intensely studied for decades [60]. The hydrogenation process has recently become better understood and more controllable and offers improvements to the electrical

performance of Si solar cells from different feedstocks, and can allow complete stabilisation of specific degradation mechanisms in solar cells [61].

Besides that, to avoid the wafering of Si ingots (which will be further explained in this chapter), attempts for developing Si sheets have been made. The Si ribbon sheets had already reached a small fraction of the market with some companies in the past, but this technology uses an expensive and wasteful process [56] has fallen from favour. This technology will not be discussed in this thesis.

The benefits of c-Si solar cells include their maturity, performance, reliability and material non-toxicity, stability and abundance. It is considered a semi-mature technology and there is a substantial amount of information on evaluating the safety and robustness of the c-Si designs. The performance of c-Si solar cells and modules is high compared with other mass-produced single-junction devices. Also, since c-Si cells reach module lifetimes of more than 25 years, it can be considered a reliable source of electricity. Finally, as Si is the second most abundant element in Earth's crust, after oxygen, this technology uses the most appropriate material among the PV devices [43].

There are several variations in the c-Si technology, but the main processes remain the same. The first step for produce energy from a c-Si solar module is mining raw materials, which is mainly quartz sand. To fabricate solar cells, the Si needs to achieve a high purity, because of that, the mining of this material is followed by further processing and purification stages, which typically entails a large amount of energy consumption [42].

The mining of quartz or sand is a well-known technology and used not just for solar cells manufacture, but also for other uses. Thus, this technology is not expected to change much in the future [62]. The silica in the quartz sand is reduced with carbon ($SiO_{2(l)} + 2\ C_{(s)} = Si_{(l)} + 2\ CO_{(g)}$) in an arc furnace to reduce impurities. Liquid Si is then

collected at the bottom of the furnace, drained and cooled, resulting in metallurgical grade silicon (MGS), which is about 98.5% pure. It needs to be further purified mainly because concentrations of B and P dopant impurities are much too high [63].

Two different routes can be taken in the latter step. The Si feedstock necessary to fabricate c-Si solar cells can be electronic, solar or upgraded metallurgical grade Si (EGS, SGS and UMG-Si, respectively).

EGS is a highly-purified version of the MGS with extremely low impurities. The most common method to purify MGS into EGS is by the Siemens process, which can be broken down into three main steps: the production of trichlorosilane ($SiHCl_3$) from MGS in a fluid-bed-reactor; the purification of $SiHCl_3$; and the reduction or thermal decomposition of $SiHCl_3$ into solid polysilicon. During this reactions impurities such as iron (Fe), aluminium (Al), and boron (B) react to form their halides (e.g. $FeCl_3$, $AlCl_3$, and BCl_3) [64].

Similar to EGS, the typical method for producing SGS involves conversion MGS to intermediate Si-based compounds, purification of these intermediate species and then reduction or thermal decomposition of these species into high purity Si. The most important of these is also the Siemens process, which accounts for approximately 90% of worldwide polysilicon production, but SGS undergoes less refinement and has lower quality [65].

UMG-Si is a low-cost alternative to SGS and EGS, which requires less equipment and energy than the Siemens process [66, 67]. UMG-Si generally prepared by a relatively simple chemical refining process, which is approximately 5–10 times cheaper than SGS. Unfortunately, the power conversion efficiency of a solar cell based on UMG silicon is lower compared with other Si feedstocks [36].

The next step is sawing into wafer form. In this process, there are typically 50% material losses [68]. With this in mind, sawing costs are a large part of the wafer production cost and thus contribute considerably to the total module cost [32]. Different methods of slicing ingots have been studied, but ,mainly, two have been used in the industry: slurry based and electroplated diamond wires [32]. Currently, the slurry based sawing method is the dominant technology, but diamond wire sawing is gaining a greater market share and is expected to lead to a significant improvement regarding process cost reduction [32].

Si is usually doped with B and phosphorous (P) to produce the p–n junction [69] in Al-BSF cells, during the treatment processes as already mentined. For solar cells, p–n junction is an interface between two oppositely-doped regions of semiconductor material. The n-type side has an excess of mobile "free" electrons, while the p-type side contains an excess of mobile holes. This combination (p-n) allows current to flow readily in one direction (forward biased) but not in the other (reverse biased), creating a basic diode. Typically, the base is doped in forming the boulle or ingot, and the emitter is doped in the cell making process.

Next, the wafers (mono and multi-Si) are treated with chemicals to enhance optical and electrical properties. Besides that, anti-reflection coating layers are formed on the cells aiming to moderate reflection losses at its front surface. Front and back electrical contacts are added to complete the solar cell [70].

HJS solar cells are also based on Si wafers. However, instead of a p-n junction formation in conventional c-Si solar cells, this junction is made by deposition of doped a-Si in heterojunction cells. This modification reduces recombination and decreases the thermal budget and therefore the energy required for cell production, resulting in potential reduction in environmental impacts [71].

2.2.2 Thin-film technologies

The most widely commercialised thin-film solar cells use thin films of a-Si, CdTe and chalcogenides, such as CIS or CIGS [57]. The main characteristic of these technologies is that they have a direct band gap, which allows strong light absorption and the use of thin layers. Other materials and processes, such as dye-sensitised solar cells (DSSC), organic photovoltaics (OPV) technology, and the emerging thin-film technologies, perovskite and CZTS solar cells [72], have also been studied.

2.2.2.1 Amorphous-Si technology

Hydrogenated amorphous silicon (a-Si:H) (Figure 5) can work with low-temperature supporting materials (mainly glass) and is deposited by plasma-enhanced chemical vapour deposition (PECVD) process at about 200°C [73, 74]. Different configurations of a-Si:H were developed, either in a single or tandem junction configurations [75-77]. The low average efficiency (6% or less) of large-area single-junction a-Si PV modules is the main reason why this technology has not confirmed to occupy a significant PV market. Researchers and industry have been continuously trying to find ways to increase a-Si solar cells and modules efficiency but the prospects seem limited [78].
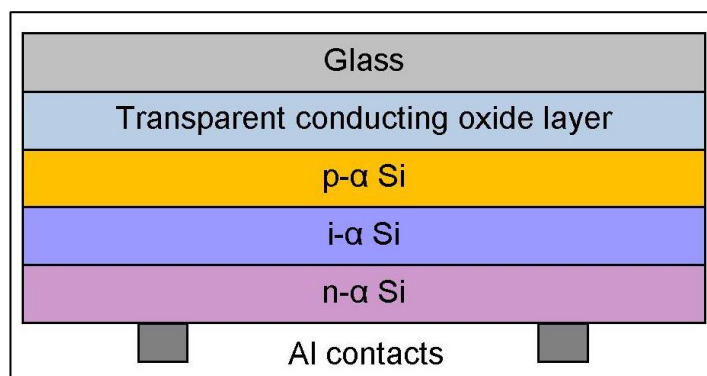
Figure 5: Basic structure of a Hydrogenated amorphous silicon (a-Si:H) cell.

2.2.2.2 Cadmium telluride technology

The CdTe technology (Figure 6) represents around 5% of the current PV world market share [79].

Glass
Transparent conducting oxide layer
CdS
CdTe
Back contact (metal)
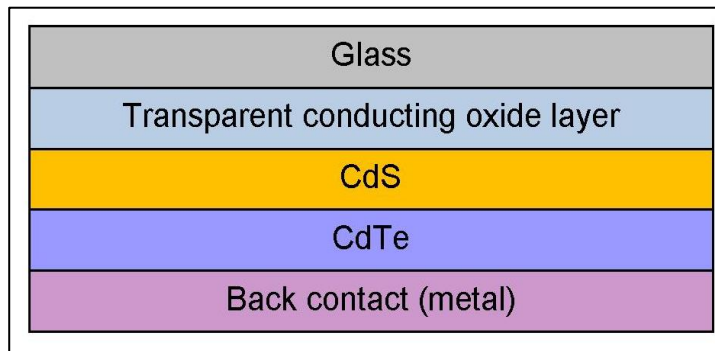
Figure 6: Basic structure of a Cadmium telluride (CdTe) cell.

These solar cells can be manufactured by quick and cheap processes, usually on a glass superstrate which doubles as the cover glass, providing a low-cost alternative to Si-based technologies [80]. Differently from a-Si, these cells can achieve efficiencies of more than 20% [28]. The main technical problem of that technology is the relatively light doping of the CdTe back contact layer, which reduces the long-term stability of the cells [81], as well as the scarcity of Te and toxicity of Cd.

2.2.2.3 Chalcogenide technologies

The fabrication of CIS and CIGS modules is made from back to front (substrate configuration), which allows the cells to be independent of transparent supporting materials, giving flexibility regarding the choice of the substrate [52]. The confirmed terrestrial CIGS cell efficiency (measured under the global AM1.5 spectrum (1000 W/m^2) at 25°C) is 21.0 ± 0.6 % [28], but a problem with CIGS is the scarcity of In [82].

CZTS is very similar to CIGS in optoelectronic and crystallographic properties and methods of fabrication, but it has lower efficiency than CIGS (10.0 ± 0.2 % [28]). Nevertheless, researchers are showing that CZTS is the most promising alternative to CIGS [24], in order to avoid the use of indium. Additionally, CZTS/Si tandem cells are expected to be of increasing interest [25-27]. Options to CZTS have also been proposed, in search of better efficiencies, where either Zn or Cu is replaced by other elements to produce higher band gaps [29]. One example is AZTS, wherein Ag replaces Cu [30].

2.2.2.4 Dye-sensitised technology

DSSC solar cells (Figure 7) emerged as a new class of low-cost energy conversion devices with simple manufacturing procedures compared to a-Si semiconductors. This technology incorporates dye molecules and wide band gap semiconductor electrodes to produce a photoelectrochemical effect [83].

Glass
Transparent conducting oxide layer
Catalyst layer
Mediator (Electrolyte)
Photoactive mesoporous oxide with coated dye
Transparent conducting oxide layer
Glass
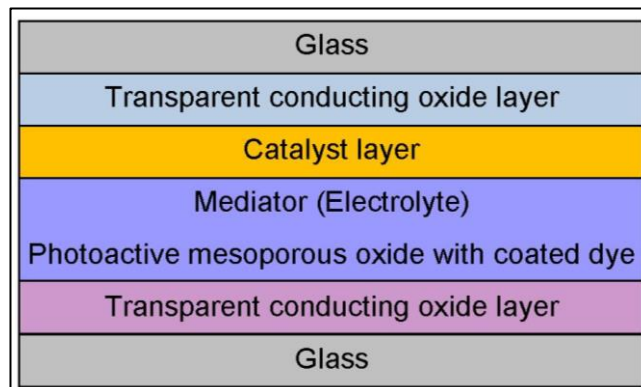
Figure 7: Basic structure of a dye-sensitised solar cell (DSSC).

The manufacturing process for DSSC solar cells is modest, typically low-cost, and uses environmentally friendly materials. They have a record efficiency of 11.9 ± 0.4% [28], which is not very competitive, compared with other PV technologies. Besides, a

significant disadvantage is the temperature sensitivity of these cells, hence a lot of research is going on to improve their stability [84]. Currently, stability and performance are the main problems with this technology and are the reasons why they are not as competitive as other thin-film solar cells [84].

2.2.2.5 Organic photovoltaics technology

Instead of creating free charge carriers (electron and hole) when a photon is absorbed, in OPV (Figure 8) materials excitons (neutral pairs of electrons/holes) are formed.
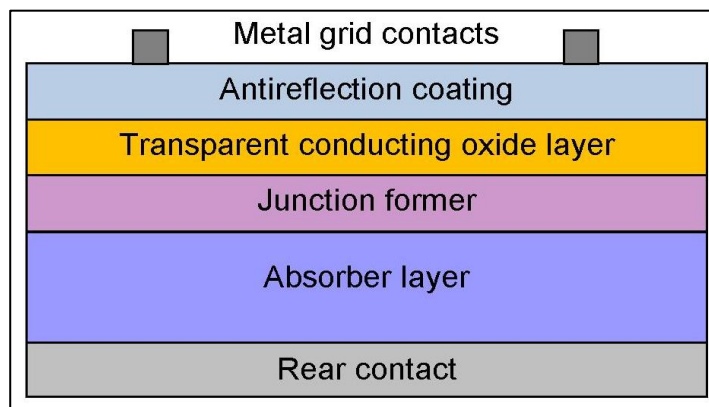
Figure 8: Basic structure of an organic photovoltaic (OPV) cell.

The dissociation of these excitons is what generates electrical energy [85]. In the standard configuration of OPV devices, a translucent substrate (most commonly glass or plastic) is coated with a transparent conductor and, in between, there are hole-transport and electron-transport materials, followed by reflective materials.

There are still many improvements that need to occur before possible industrial scale manufacturing of OPV, advances need to be made in increasing device efficiency and lifetime, and the cost of devices needs to be lowered [86]. Even with some recent improvements on the cells efficiency, such as 12.3% for a small area 0.09 cm^2 bulk

heterojunction organic solar cell [28] and 14.08% for a ternary organic solar cell using fullerene in the active layer [87], the stability of OPV cells still needs further development [88].

2.2.2.6 Organic-inorganic halide perovskite technology

Solar cells based on organic-inorganic lead halide perovskite (Figure 9) are the most recent thin-film technology, and it has gained considerable attention for the past few years [89]. Perovskite solar cells demonstrated a certified solar energy conversion efficiency of 22.7 ± 0.8% [90] and its rapid progress suggests even higher values in the future. The use of low-cost materials and simple fabrication process make them even more attractive [91].

| Metal contact |
| Spiro-OMeTAD |
| Perovskite layer |
| TiO_2 |
| Glass |
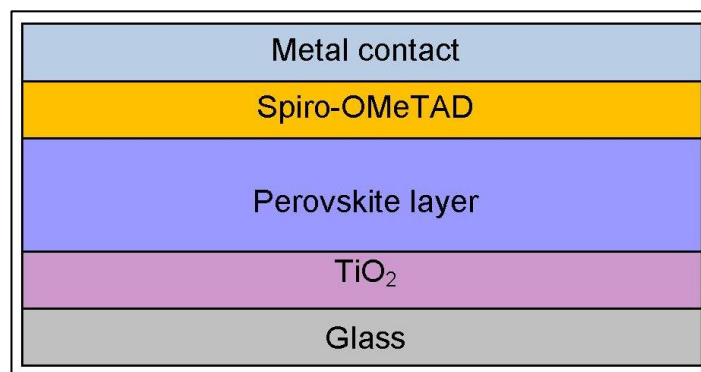
Figure 9: Basic structure of an organic-inorganic halide perovskite cell

On the other hand, stability and challenges in upscaling the manufacture of this device are serious concerns that must be addressed for its future commercialisation [92]. Besides that, in the case of lead(Pb)-based perovskites, the use and toxicity of soluble Pb salts is also a concern regarding environmental impacts [93].

2.2.3 Tandem Solar Cell Technologies

Developed by Shockley and Queisser in 1961, the detailed balance principle has been the standard method of calculating the limiting efficiency of a solar cell. Based on that model, the PV single-junction solar cell limiting energy conversion efficiency is 30%, for a band gap of 1.1 eV and considering an AM 1.5 solar spectrum [4].

The search for high power conversion and lower costs motivates researchers to investigate new PV technologies and materials. With this in mind, tandem solar cells appear as a method to combine efficiency increase and long-term price reductions of PV modules [16].

The illumination first interacts with the high band gap absorber, because the high bandgap allows absorption of the high energy photons. This material is transparent to low energy photons, allowing them to pass through to the next absorber with lower band gap [94]. In other words, tandem solar cells are layered from short wavelength material on top (high band gap) to high wavelength material on bottom (low band gap).

Tandem solar cells can be formed by either connecting them electrically in series, to form a two-terminal tandem or making separate connections to the individual cells (Figure 10).
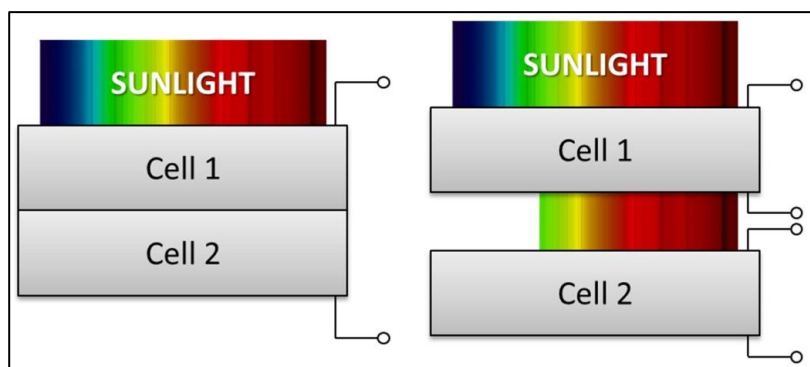
Figure 10: Possible tandem solar cell configurations: two-terminal (left) and multi-terminal (right).

The fabrication of series connected cells is simpler but the current is necessarily the same though each cell, which makes the choices of band gaps and layer thicknesses more restricted. The most common arrangement for series connected tandem cells is to grow all the cells as subsequent layers on the substrate to connect the individual cells, which is called monolithic growth [94].

The monolithic design has some restrictions, such as requirement of current matching and restricted design and material selections, such as thermal expansion coefficient and lattice constant. In contrast, the mechanically stacked configuration offers a more generic approach way of realizing multi-junction solar cells.

A different configuration of tandem solar cells is mechanical stacking or wafer bonding, which are fabricated by stacking individual solar cells (top and bottom cells are individually fabricated first) with intermediate adhesive layers that must be electrically conductive to produce electrical current for the two (or more) cells [95]. This approach allows more freedom on cell design and material choice [96].

Tandem solar cells have achieved high efficiencies mostly using III-V cells. The InGaP/GaAs/InGaAs multijunction cell, for example, can reach up to more than 43% efficiency in specific conditions [97].

Experiments have shown that a Si substrate is likely to give the quickest path to affordable high efficiency for tandem solar cells in different configurations, reaching an efficiency of more than 30% in Si-based tandem device [5] until now. The theoretical efficiency of a two-cell tandem device with a 1.6 to 1.8 eV band gap top cell and a 1.0 to 1.2 eV band gap bottom cell (e.g. Si) can exceed 30% [52]. Nevertheless, a variety of possibilities have been studied and have previously been applied for solar cells in several combinations such as DSSC/Si solar cells [8] or OPV/Si solar cells [9], for example.

CIGS is a semiconductor with a chalcopyrite crystal structure, that allows its band gap to vary between 1.0 and 2.4 eV by varying the In/Ga and Se/S ratios [15] (with efficiency of approximately 15.7 ± 0.5 % for high band gap cells [28]). The possibility of a high band gap makes CIGS an attractive material for use on top of a Si base cell in a tandem solar cell [15]. Alternatively, CZTS and AZTS also present the possibility of high band gaps (up to 2.0 eV for both [31]), which makes CZTS/Si and AZTS/Si tandem solar cells interesting candidates.

The emergence of perovskite solar cells was also followed by interest in experimenting with this technology in a tandem form. Essentially, it is believed by some researchers that the most likely way for the perovskite technology to be processed on an industrial scale would be on the top of a Si cell, configuring a tandem cell structure [16]. Stacking a perovskite cell on a multi-Si screen-printed cell can, for example, reach an efficiency value of above 22% and if stacked on UMG-Si (low-cost) it can achieve above 20% efficiency [17, 18].

2.2.4 Possibilities for Future Photovoltaic Developments

The Al-BSF [33] is the current industry standard Si cell process, but there are many variations of existing production processes that aim to develop better c-Si cell and module efficiency and performance [32].

The PERC technology [34] is gaining significant share in the world market and is expected to displace Al-BSF as the dominant technology in the future (estimated around 60% share in 2027) [32]. The PERC process has already been industrialised [34], and in 2016 the efficiency of a p-type monocrystalline cell using this technology achieved 20.6% for a commercial cell [98]. Another example of improving the photoconversion efficiency of c-Si solar cells is the HJS. This technology allows for Si

solar cells with record-efficiency energy conversion of over 26% with a 180.4 cm^2 designated area [99].

The technology that appears to be the most promising solution for achieving high-efficiency values and small costs compared to fairly static module costs such as those of module encapsulation, frames and junction boxes, is the tandem structure. As Si-based tandem solar cells offer the potential for a high-efficiency product at a low price per unit power or energy output, they are expected to appear in mass production operation after 2019 and also gain a worldwide PV market share of 10% by 2028 [32]. In fact, tandem cells are crucial to the success of thin-film technologies, which might lead to a faster learning curve and reduced costs [52].

2.3 Life Cycle Assessment of Photovoltaic Technologies

Most aspects of the use of PV panels has been intensively studied and improved, and although their environmental impacts are not yet fully determined, there is already a great number of works carried out on this subject. LCA is a method used to evaluate potential environmental impacts associated with the production, use phase and disposal of a product during its lifetime. The depth of detail in LCA studies depends on the goal and scope definition and the assumptions made [39], so the results can vary for the same technology.

LCA is a methodology used to analyse any product or process from an environmental perspective [21]. The initial step is defining the goal and scope of the study. The next phase is to produce an inventory, followed by the impact assessment, where the inventory data is translated into environmental impacts. Finally and based on the results, recommendations are made to guide choices for lower environmental impacts [100].

The IEA, for example, occasionally publishes the "Life Cycle Inventories and Life Cycle Assessments of Photovoltaic Systems" through the PVPS, which contains inventories and impact data for the main commercial solar module types (mono-Si, multi-Si, and CdTe) [42].

LCA publications on PV technologies started to appear in the mid-1970s [101, 102] and are being continuously updated following the rapid improvements and industrialisation of these devices. The results from LCA studies vary mainly due to the PV system configuration (module design, efficiency assumed, cell technology, etc.) and the application of the methodology (system boundaries, functional unit and other assumptions). More aspects of this field have been the subject of reviews. In 2012 Kim et al. [103] reviewed 109 studies harmonising the life cycle greenhouse gas emissions of commercial thin-film PV technologies, including a-Si, CdTe, and CIGS, by aligning the assumptions, parameters, and system boundaries. In the same year Hsu et al. [104] published scientific literature reviewing 397 LCA studies estimating life cycle greenhouse gas emissions of residential and utility-scale solar PV, particularly c-Si technology and focusing on LCAs that met minimum standards of quality, transparency, and relevance. Recently, Bhandari in 2015 [105] and Louwen et al. in 2016 [106] also published reviews of PV technologies. Bhandari [105] focused his analysis on EPBT and energy return on energy invested (EROI) of solar PV systems and Louwen et al. [106] assessed 40 years of PV development analysing the net energy production and greenhouse gas emissions avoidance progress.

Although there are impact categories recommended for LCA on PV technologies [107], most of the publications focus on GWP — also called greenhouse gases (GHG) emissions — and EPBT, as it has been considered that these categories can substantially assess the sustainability and environmental performance of PV systems.

PV technologies directly generate electricity from solar energy, with no fossil energy consumption in the use phase, however, during the cells' production, they consume a large amount of primary energy. Therefore, there are no GHG emission during their operation, but they produce important environmental impacts related to these emissions during manufacturing processes, module assembly, material and product transportation, and other steps of their whole lifecycle [42]. Compared with fossil-based power plants, PV power systems have an advantage in their potential to mitigate GHG emissions and, because of that, GWP is the most frequently calculated environmental impact in LCA studies of PV systems.

The EPBT for PV systems is defined as the time, normally in years, required for a system to generate the same amount of energy to compensate for the primary energy input requirements during the system's manufacturing, assembly, transportation, installation, operation and maintenance [108]. The EPBT relates the total primary energy input of the PV module, which can include the balance of system (BOS) or not. The BOS refers to the components and equipment that move direct current energy produced by solar panels through the conversion system (not including land occupation), which, in turn, produces alternating current electricity, such as inverters and racking, cables/wires, switches, enclosures, fuses, ground fault detectors etcetera.

The result of an EPBT calculation depends on several factors such as the type of PV module, manufacturing technologies, module conversion efficiency, installation location, etcetera [109]. F

These two categories are the most commonly included in LCA studies of PV technologies, so the major focus of the next section is on GWP and EPBT impacts. However, there are a few other impacts that are also often considered important. The use of toxic substances, heavy metals and other hazardous materials during the manufacturing of all parts of a PV system should also be assessed. These materials

can affect human health, fauna and flora. HTP, FEcP and FEuP are comprehensive indicators to assess these impacts [110]. Besides that, the use of some natural resources, such as metals and the ingredients of glass, and the decreasing availability of most of the associated raw materials should also be assessed. The ADP is the category used to investigate this latter impact, relating the annual production and the reserves of natural resources [111]. Section 3.3, Impact assessment, discusses it.

2.3.1 Life Cycle Assessment of Silicon Technologies

Currently, PV production is dominated by single-junction solar cells based on silicon wafers including multi-Si and mono-Si [79]. Consequently, a significant number of LCA studies focus on these technologies.

2.3.1.1 Multicrystalline silicon technology

Multi-Si has the most significant share in the current PV market, so the majority of LCA studies of Si PV modules have analysed this technology [32]. Table 1 presents a summary of LCA published on multi-Si (from the year 2000).

Table 1: Summary of LCA published of multicrystalline silicon (from the year 2000). Colours identify the different FU.

Technology/System	Year	Impacts	FU	System boundaries	Assumptions				Main results	Ref
					Insolation (kWh/m²/yr)	PR	Eff. (%)	Lifetime (years)		
multi-Si	2000	GWP EPBT	1 kWh	Production of the PV system	1700	0.75	13	30	GWP: 46 gCO$_{2eq}$/kWh EPBT: 2.5 yrs	[112]
multi-Si roof-top installation	2000	GWP EPBT	1 kWh	Production of the PV system	1700	0.75	13	30	GWP: 60 gCO$_{2eq}$/kWh EPBT: 3.2 yrs	[113]
Very largescale PV power generation	2003	GWP EPBT Others	1 kWh	Manufacturing transport and installation.	1675	0.78	12.8	30	GWP: 12 gCO$_{2eq}$/kWh EPBT: 1.7 yrs	[114]
multi-Si integrated system	2005	GWP EPBT	1 kWh	Production (BOS), transp. and disposal	1530	0.8	10.7	30	GWP: 463 gCO$_{2eq}$/m² EPBT: 3.3 yrs	[115]
multi-Si Large-scale PV System	2006	GWP EPBT	1 kWh	Installation and use phase.	1702	0.7	12.8	30	GWP: 12.1 gCO$_{2eq}$/kWh EPBT: 1.9 yrs	[116]
multi-Si modules	2007	GWP EPBT	1 kWh	Production (BOS), install. and use phase	1359	-	12.9	30	GWP: 72.4 gCO$_{2eq}$/kWh EPBT: 7.5 yrs	[117]
Commercial multi-Si PV modules	2010	GWP Others	1 kWh	Production (BOS) and use phase	-	-	12.5	30	GWP: 63 gCO$_{2eq}$/kWh	[118]
multi-Si modules (roof top)	2011	EPBT	1 kWh	Production (BOS), install. and use	1408.8 - 1930.9	-	-	20 - 30	EPBT: 3.67–4.94 yrs	[119]
multi-Si ground-mounted PV	2012	GWP EPBT Others	1 kWh	Production (BOS) to EoL	-	-	14.4	25	GWP: 8.74 gCO$_{2eq}$/kWh EPBT: 4.17 yrs	[120]
multi-Si systems	2016	GWP EPBT Others	1 kWh	Raw materials, production and system (BOS)	1000 - 2300	0.80	16	30	GWP: 28–33 gCO$_{2eq}$/kWh EPBT: 0.9-2.1 yrs	[121]
multi-Si roof-mounted	2006	GWP EPBT Others	1 kWp	Production and use phase	1700	0.75	13.2	30	GWP: 30–45 gCO$_{2eq}$/kWh EPBT:1.7–2.7yrs	[122]
multi-Si modules	2015	GWP EPBT Others	1 kWp	From silica to module fabrication	1300	0.75	16	25	GWP: 51 gCO$_{2eq}$/kWh EPBT: 2.2-6.1 yrs	[123]
multi-Si PV cell	2016	GWP Others	1 kWp	Transp., Prod., disposal	1300	-	12.7	25	GWP: 56.2 gCO$_{2eq}$/kW h	[124]
PV cell grid-connected PV systems	2005	GWP EPBT Others	3 kWp	Production (BOS) and use phase	-	-	13.2	30	GWP: 136–100 gCO$_{2eq}$/kWh EPBT: 3–6 yrs	[125]
PV cell modules	2008	GWP EPBT	0.65 m²	Production and use phase	Several	-	16	28	GWP: 39 - 49 gCO$_{2eq}$/kWh EPBT: 3.5–7 yrs	[126]
PV cell Tracking system	2012	GWP EPBT Others	1 MWh	Production and use phase	-	-	13.8	30	GWP: 44.7 gCO$_{2eq}$/kWh EPBT: 5.5 yrs	[127]
Crystalline PV production	2011	GWP Others	1 kWh	Production process	1300	-	15	30	CO$_2$ emissions: direct < indirect	[128]

Comparing the LCA reports analysed, two studies from 2000 [113] and 2011 [119], have similar scopes, but the inventories (as well as the production processes) are updated from one to another. The comparison of these studies shows that more recent production processes and recent inventories result in lower GWP and EPBT impacts, mainly due to the use of less energy use and more efficient processes. The results were 60 gCO_{2eq}/kWh and 3.2 years in the first LCA [113] and 46 gCO_{2eq}/kWh and 2.5 years in the LCA made in 2011 [119].

Recent studies, made in China, analysing multi-Si PV cells and modules assume insolation of 1300 kWh/m^2/yr, a lifetime of 25 years and 1 kWp as the FU. These LCAs provide different results based on their system boundary set up. One of these studies considered the processes from raw materials extraction to module fabrication, including transportation [124], while the other also included the infrastructure, production and disposal phases [123]. The results for the latter show that the GWP from the LCA [123], is lower than in the other study, however they considered different insulations.

Studies using very specific assumptions produce different results, which makes the comparison between them very difficult. In 2005, for example, an LCA of a multicrystalline building integrated PV system was conducted considering insolation of 1530 kWh/m^2/yr, a performance ratio of 0.8, a module efficiency of 10.7 % and a lifetime of 30 years. The results from this study for GWP and EPBT were 463 gCO_{2eq}/m^2 module and 3.3 years, respectively [115], which are very different to those from the previous studies analysed in this review, mainly because of the dissimilar FU.

An LCA of a large-scale PV power plant also shows contradictory results. This study included in the system boundaries the manufacturing, transportation and installation processes and the assumed values for insolation, performance ratio, efficiency and lifetime were 1675 kWh/m^2/yr, 0.78, 12.8 % and 30 years, respectively. Based on a 1

kWh FU, the results presented a GWP impact of 12 gCO_{2eq}/kWh and an EPBT of 1.7 years, which seems to be very small compared with the other studies reviewed [114].

An LCA conducted in 2011 analysed the CO_2 emissions from crystalline Si PV production. The conclusion was that the direct emissions (emissions from sources that are owned or controlled by the reporting entity) are lower than the indirect emissions (emissions that are a consequence of the activities of the reporting entity, but occur at sources owned or controlled by another entity) from the production processes [30]. This particular study does not present quantitative results and cannot be considered to have the same reliability as the other studies.

A study made in 2016 uses more recent and realistic assumptions, mainly for efficiency [121]. This study considered different PV technologies, including multi-Si. The system boundaries include the raw materials, production of the cells, modules and BOS components (PV system). The assumptions for insolation, performance ratio, efficiency and lifetime were 1000 – 2300 kWh/m^2/yr, 0.80, 16 % and 30 years, respectively. The results from this LCA study for GWP and EPBT were 28 – 33 gCO_{2eq}/kWh and 0.9 – 2.1 years, respectively. Compared with the other studies (taking into consideration their assumptions), this updated LCA shows substantial reductions of the environmental impacts analysed (GWP and EPBT), and the conclusion from the referred study [121] describe this reduction of impacts as a consequence of the improvements in module efficiency and manufacturing process yields.

2.3.1.2 Monocrystalline silicon technology

A summary of LCA studies of mono-Si cells (2000 or later) and modules is shown in Table 2 and are described and discussed in this section.

Table 2: Summary of LCA published of monocrystalline silicon (from the year 2000). Colours identify the different FU.

Technology/ System	Year	Impacts assessed	FU	System boundaries	Assumptions				Main results	Ref.
					Insolation (kWh/m^2/yr)	PR	Eff. (%)	Lifetime (years)		
mono-Si grid connected	2000	GWP EPBT	1 kWh	Production phase	1700	0.75	14	30	GWP: 60 gCO$_{2eq}$/kWh EPBT: 3.2 years	[113]
mono-Si	2000	GWP EPBT	1 kWh	Production of PV system	1700	0.75	14	30	GWP: 63 gCO$_{2eq}$/kWh EPBT: 3.1 years	[112]
mono-Si solar modules	2005	GWP EPBT Others	1 kWh	Production and BOS.	1700	0.75	13.7	30	GWP: 41 gCO$_{2eq}$/kWh EPBT: 2.6 years	[129]
mono-Si frameless, on-roof	2009	GWP EPBT	1 kWh	Production (BOS), install., use and landfill	1700	0.75	14	30	GWP: 30 gCO$_{2eq}$/kWh EPBT: 1.75 years	[130]
mono-Si systems	2016	GWP EPBT Others	1 kWh	Raw materials, production and system (BOS)	1000 - 2300	0.80	17	30	GWP: 37-50 gCO$_{2eq}$/kWh EPBT: 1.2-2.8 yrs	[121]
mono-Si grid-connected PV systems	2005	GWP EPBT Others	3 kWp	Production (BOS) and use phase	-	-	14.8	30	GWP: 136–100 gCO$_{2eq}$/kWh EPBT: 3–6 years	[125]
mono-Si roof-mounted	2006	GWP EPBT Others	1 kWp	Production and use	1700	0.75	14	30	GWP:30–45gCO$_{2eq}$/kWh EPBT: 1.7–2.7 years	[122]
mono-Si tracking system	2012	GWP EPBT Others	1 MWh	Production and use	-	-	13.8	30	GWP:44.7gCO$_{2eq}$/kWh EPBT: 5.5 years	[127]
mono-Si façade PV	2012	GWP EPBT	1 kWh	Production (not cells) and use	766	0.66 0.64	-	30	GWP:10.2gCO$_{2eq}$/kWh EPBT: 3.8 years	[131]

Comparing the main results it can be seen that the GWP is not very different when the authors use the same assumptions, but the efficiency and the type of system analysed influence the final results.

Two studies [112, 113] for mono-Si consider the production phases of all the PV system components and assume the same insolation (1700 kWh/m^2/yr), performance ratio (0.75), efficiency (14 %) and lifetime (30 years). The GWP and EPBT results are similar (60 and 63 gCO$_{2eq}$/kWh and 3.2 and 3.1 years, respectively), which shows the consistency between studies.

Using similar assumptions but more recent data, an LCA of mono-Si solar modules presented lower impacts, compared with the two previous studies, for mono-Si technology, considering the production process and including the BOS components [129]. The GWP and EPBT results were 41 gCO$_{2eq}$/kWh and 2.6 years, respectively, which are lower than in previous studies, mainly due to the improvement in the

manufacturing processes. Even lower results were found considering a frameless mono-Si solar module (FU of 1kWh, insolation of 1700 kWh/m^2/yr, performance ratio of 0.75 and a lifetime of 30 years) [130]. The calculated GWP is 30 gCO$_{2eq}$/kWh and the EPBT 1.75 years, which are lower than the earlier studies, mainly because of the assumption of a frameless module.

Different results were calculated based on case studies. In 2005 an LCA study of a mono-Si grid-connected PV system was conducted using 3 kilowatt-peak (kWp) of power production as the FU and included the whole production (including the BOS) and the use phases [125]. The GWP and EPBT outcomes are 136–100 gCO$_{2eq}$/kWh and 3–6 years, respectively, which are not similar to the previous studies. In 2006 an LCA for mono-Si roof-mounted modules used 1 kWp of power production as the FU, and the results for GWP and EPBT were 30–45 gCO$_{2eq}$/kWh and 1.7–2.7 years [122], which is comparable to the previous studies. Later, in 2012, and using more recent data, a study of a mono-Si tracking system using 1 MWh as the FU presented a GWP of 44.7 gCO$_{2eq}$/kWh and an EPBT of 5.5 years [127].

A case study analysed the impacts from a specific façade–integrated PV system in the USA. This LCA calculated a GWP of 10.2 gCO$_{2eq}$/kWh and an EPBT of 3.8 years considering 1 kWh as the FU and insolation of 766 kWh/m^2/yr [131]. These results are different compared to the other studies, which is expected because this is a case study and uses distinct assumptions, compared with the other LCA studies analysed in this review.

In 2016 an LCA study considered recent and more realistic assumptions compared with the previous studies analysed [121]. The system boundaries assumed for production of a mono-Si module included raw materials and production of the cells, modules and BOS components (PV system). The results from this LCA study for GWP and EPBT were 37-50 gCO$_{2eq}$/kWh and 1.2-2.8 years, respectively, assuming an

insolation varying from 1000 to 2300 kWh/m^2/yr, a 0.80 performance ratio, an efficiency of 17% and 30 years of lifetime. The improvement in the LCA assumption to more recent data shown positive effects regarding to reductions of GWP and EPBT impacts.

2.3.1.3 Other silicon technologies

LCA studies in other Si technologies are shown in Table 3.

Table 3: Summary of LCA published of specific silicon technologies (from the year 2000). Colours identify the different FU.

Technology/ System	Year	Impacts	FU	System boundaries	Assumptions				Main results	Ref.
					Insolation (kWh/m^2/yr)	PR	Eff. (%)	Lifetime (years)		
Ribbon Si roof mounted	2006	✓GWP ✓EPBT ✓Others	1 kWp	Production and use phase	1700	0.75	11.5	30	GWP: 30–5gCO$_{2eq}$/kWh EPBT: 1.7–2.7 years	[122]
HJS solar cell	2014	✓GWP ✓EPBT	1 kWh	Production (BOS) and use.	1700	0.75	18.4	30	GWP: 32 gCO$_{2eq}$/kWh EPBT: 1.5 years	[132]

An LCA of a ribbon Si roof-mounted system, using 1 kWp of power production as FU and a module efficiency of 11.5 %, presented GWP values of 30–45 gCO$_{2eq}$/kWh and EPBT of 1.7–2.7 years, considering the production and use phases [122]. This technology is different from mono-Si and multi-Si but presented similar results for GWP and EPBT. This result undermines the main intended benefits of such waferless technologies, the environmental savings from the avoidance of sawing.

A complete study on Si heterojunction solar cells was conducted in 2014. The results for GWP and EPBT are 32 gCO$_{2eq}$/kWh and 1.5 years, respectively [132]. This study considered 1 kWh as the FU, the system boundaries were from the production processes (including the BOS) until the use phase, which is in accordance with LCA studies for other types of Si technologies.

2.3.2 LCA of Thin-films Technologies

Thin-films are single-junction devices that are intended to use less material and, at the same time, preserve similar efficiencies achieved by silicon-based solar cells. This result can be accomplished by using materials that can absorb the solar spectrum much more efficiently than mono-Si or multi-Si and use a smaller amount of active material. Thin film technologies are, for example, chalcogenide (CIS, CIGS and CZTS), CdTe, a-Si, DSSC, OPV and perovskite [133]. However, for most of these technologies the efficiency is unlikely to be close to c-Si values.

A summary of LCAs published on the above technologies is shown in this section. There aren't as many studies as there are for c-Si technologies, due to their smaller share in the PV market [32].

2.3.2.1 Chalcogenide (CIS, CIGS and CZTS) technologies

The LCA studies for CIS, CIGS and CZTS technologies are shown in Table 4.

Table 4: Summary of LCA published of CIS and CIGS technologies (from the year 2000). Colours identify the different FU.

Technology/ System	Year	Impacts	FU	System boundaries	Assumptions				Main results	Ref.
					Insolation (kWh/m²/yr)	PR	Eff. (%)	Lifetime (years)		
CIS Large-scale PV System	2006	✓GWP ✓EPBT	1 kWh	Installation and use phase.	1702	0.7	11.0	30	GWP: 10.5 gCO₂eq/kWh EPBT: 1.6 years	[116]
CIS PV modules	2007	✓GWP ✓EPBT	1 kWh	Module production (BOS)	1700	0.75	11.0	20	GWP: 95 gCO₂eq/kWh EPBT: 2.8 years	[134]
CIGS PV modules	2009	✓GWP ✓EPBT	1 m²	Production (BOS), installation, use and end-of-life.	1700	0.75	10.5	30	GWP: 65 gCO₂eq/m² EPBT: 1.8 years	[130]
CZTS PV cells	2014	✓GWP ✓Others	1 kWh	Raw materials, cells and module production	1700	0.75	10.0	30	GWP: 38 gCO₂eq/kWh	[135]
CZTS PV systems	2016	✓GWP ✓EPBT ✓Others	1 kWh	Raw materials, production and system (BOS)	1000 - 2300	0.80	14	30	GWP: ≈ 20 gCO₂eq/kWh EPBT: 0.8-1.9 yrs	[121]
CZTS (vacuum processing)	2018	✓GWP ✓Others	1 m2	Raw materials, production and materials deposition.	1700	0.75	15.0	30	GWP: 360 gCO₂eq/m² GWP*:0.09 gCO₂eq/kWh	[136]
CZTS (non-vacuum proc.)			1 m2						GWP: 501 gCO₂eq/m² GWP*:0.8 gCO₂eq/kWh	
*Assumptions made for a large scale production, with production of 1 GW per year.										

In 2007 an LCA study considered a CIS module production process (including the BOS). The results for GWP and EPBT from this LCA are 95 gCO$_{2eq}$/kWh and 2.8 years, respectively [134]. Another assessment, conducted in 2006, calculated the impacts from a CIS large-scale PV system, considering the installation and use phases. The outcomes from this LCA are a GWP of 10.5 gCO$_{2eq}$/kWh and an EPBT of 1.6 years [116]. These LCA studies used the same insolation, efficiency and lifetime valued, but different system boundaries. The results demonstrate the influence of the system boundaries in an environmental study showing that dissimilar assumptions result in a wide range of GWP and EPBT impacts.

In 2009 an analysis of CIGS PV modules was conducted. The functional unit chosen was 1 m^2, which is not very common for PV systems environmental assessments. This LCA calculated GWP and EPBT impacts based on the analysis of the production process (including the BOS), installation, use phase and end-of-life. The results were 65 gCO$_{2eq}$/m^2 and 1.8 years, respectively [130].

The CZTS technology aims to overcome the challenges of production costs, material availability, and toxicity of a PV mass deployment, replacing the CIGS technology. CZTS technology is most likely to be used in tandem cell concept with existing high-efficiency c-Si cells, in particular, because CZTS uses earth-abundant semiconductor materials [137]. A cradle to gate LCA was conducted in 2014, considering the impacts from raw materials, cells and module production. This LCA used a FU of 1 kWh, insolation of 1700 kWh/m^2/yr, performance ratio of 0.75 and a lifetime of 30 years. Their results for GWP were 38 gCO$_{2eq}$/kWh [135].

In 2018 another LCA study made for the CZTS technology compared two different processes: cells fabricated via vacuum and non-vacuum processing. Firstly, this LCA used a FU of 1 m^2 of cell fabricated. Assuming a lifetime of 30 years and an efficiency of 15% the results from this study for GWP were 360 and 510 gCO$_{2eq}$/m^2, respectively.

According to the assumption made in this LCA, the results in gCO_{2eq}/kWh would be approximately 6.4 and 8.8, respectively. Secondly, they assumed a large-scale production process and their results were calculated based on 1 kWh of electricity generated (FU), insolation of 1700 kWh/m^2/yr and performance ratio of 0.75. Assuming the same efficiency and lifetime the results for a large scale production of CZTS were 0.09 and 0.8 gCO_{2eq}/kWh, respectively, which are much lower than the lab scale production, which is expected [136].

A GWP of approximately 20 gCO_{2eq}/kWh and a EPBT value of 0.8-1.9 years was calculated with data used for a 2016 publication, considering a CIGS efficiency of 14 % [121], which is more realistic than earlier values, considering the recent improvements on this technology. The assumptions for insolation, performance ratio and lifetime were 1000 – 2300 kWh/m^2/yr, 0.80 and 16 %, respectively. These results showed improvements in the impacts from this technology, which is expected with the improvements of the production processes and cell and module efficiency.

2.3.2.2 Cadmium telluride technology

Considering solar modules using CdTe technology, a few LCA studies have been made. Most of the reports analysed in this review considered 1 kWh as the FU, but even with similar assumptions, the results are very different.

Table 5 shows the LCAs for CdTe technologies.

Table 5: Summary of LCA published of CdTe technologies (from the year 2000). Colours identify the different FU.

Technology/ System	Year	Impacts	FU	System boundaries	Assumptions				Main results	Ref.
					Insolation (kWh/m^2/yr)	PR	Eff. (%)	Lifetime (years)		
CdS/CdTe PV modules	2001	✓GWP ✓EPBT	1 kWh	Production (BOS), installation.	1430	0.81	10.3	20	GWP: 14 gCO$_{2eq}$/kWh EPBT: 1.7 years	[138]
CdTe PV modules	2005	✓GWP ✓EPBT	1 kWh	Production, transportation and waste treatment.	1800	0.80	9.0	30	GWP: 23.6 gCO$_{2eq}$/kWh EPBT: 1.2 years	[139]
Production of CdTe modules	2006	✓GWP ✓EPBT ✓Others	1 kWh	Cell/module production (BOS), installation.	1700	0.75	9.0	30	GWP: 25 gCO$_{2eq}$/kWh EPBT: 1.1 years	[140]
CdTe Large-scale PV System	2006	✓GWP ✓EPBT	1 kWh	Installation and use phase.	1702	0.7	9.0	30	GWP: 12.8 gCO$_{2eq}$/kWh EPBT: 1.9 years	[116]
CdTe PV modules	2007	✓GWP ✓EPBT	1 kWh	Module production (including BOS)	1700	0.75	9.0	20	GWP: 48 gCO$_{2eq}$/kWh EPBT: 1.5 years	[134]
CdTe PV systems	2016	✓GWP ✓EPBT ✓Others	1 kWh	Raw materials, production and system (BOS)	1000 - 2300	0.80	15.6	30	GWP: 12-14 gCO$_{2eq}$/kWh EPBT: 0.5-1.1 yrs	[121]
CdTe photovoltaic modules	2009	✓GWP ✓EPBT	1 m^2	Production (BOS), installation, use and end-of-life	1700	0.75	10.9	30	GWP: 40 gCO$_{2eq}$/m^2 EPBT: 0.84 years	[130]
CdTe PV systems in Europe	2011	✓GWP ✓EPBT ✓Others	1 m^2	Production (BOS), installation, use and end-of-life	1200 - 1700	0.8	10.9	30	GWP: 19 - 30 gCO$_{2eq}$/kWh EPBT: 0.7 – 1.1 years	[141]

Using values for insolation, performance ratio, efficiency and module lifetime equal to 1700 kWh/m^2/yr, 0.75, 9.0 % and 30 years, respectively, three studies have chosen dissimilar system boundaries. An LCA of CdTe solar modules conducted in 2006 considered the cell production, module assembly (including the BOS) and installation phases as within their system boundaries. The results from this study are 25 gCO$_{2eq}$/kWh for GWP and 1.1 years for EPBT [140]. In the same year, another study measured the impacts from a CdTe large-scale PV system using a different system boundary (including only the installation and use phases). The results from this analysis are a GWP impact of 12.8 gCO$_{2eq}$/kWh and an EPBT of 1.9 years [116]. Finally, an LCA including the module production and the BOS manufacturing processes in the system boundaries found a GWP impact of 48 gCO$_{2eq}$/kWh and an EPBT of 1.5 years (assuming a lifetime of 20 years) [134]. From these studies, it can be concluded that, because of the use of different system boundaries, the results for GWP and EPBT were found to be completely distinct.

In 2001 an environmental study of CdTe PV modules considered to be within its system boundaries cell production, module assembly (including the BOS) and installation phase. The LCA was based in isolation of 1430 kWh/m^2/yr, a performance ratio of 0.81, an efficiency of 10.3 % and 20 years of lifetime. The results are a GWP impact of 14 gCO$_{2eq}$/kWh and an EPBT of 1.7 years [138]. In 2005, another LCA on CdTe PV modules was conducted considering the production process, transportation, module manufacturing and waste treatment. The results for GWP and EPBT were 23.6 gCO$_{2eq}$/kWh and 1.2 years, respectively. In this case, the isolation was 1800 kWh/m^2/yr, performance ratio 0.80, efficiency 9.0 % and 30 years of a lifetime [139]. These both studies considered 1 kWh as the FU, but because they assumed different values for insolation, performance ratio, efficiency and lifetime, the results for GWP and EPBT are dissimilar and not directly comparable.

In 2009 [130] and 2011 [141], LCA studies of CdTe PV modules used 1 m^2 as the FU. These two reports considered very similar assumptions. The system boundaries were set from the production process (including the BOS), installation and use phase until the end-of-life. Both were based in isolation of 1700 kWh/m^2/yr, an efficiency of 10.9 % and 30 years of lifetime. The main difference between these studies was the performance ratio. Considering a performance ratio of 0.75, the calculated results for GWP and EPBT were 40 gCO$_{2eq}$/m^2 and 0.84 years, respectively [130]. Using a performance ratio of 0.8, those impacts were 30 gCO$_{2eq}$/kWh and 1.1 years, respectively [141]. These results show the influence of the assumptions in an LCA and how sensitive the calculations are to one small change in the assumptions, and that care must be taken in expressing calculations.

In 2016 a updated study used recent data and realistic assumption to calculate the GWP and EPBT for CdTe PV systems [121]. The considered improvements in module efficiency and manufacturing process yields showed reduction of these environmental

impacts compared to previous similar studies. The GWP calculated was 12-14 gCO_{2eq}/kWh and the EPBT value was 0.5-1.1 years assuming 1000 - 2300 kWh/m^2/yr as the irradiation value, performance ratio of 0.80, 30 years of lifetime and an efficiency of 15.6%. These results demonstrate the importance of improving the production processes and efficiencies for solar cells and modules, as well as the magnitude of updating the LCA assumptions and inventories, to better predict environmental impacts.

2.3.2.3 Amorphous-Si technology

Table 6 presents the LCA studies for s-Si technology.

Table 6: Summary of LCA published on a-Si technologies (from the year 2000).

Technology/ System	Year	Impacts	FU	System boundaries	Assumptions				Main results	Ref.
					Insolation (kWh/m^2/yr)	PR	Eff. (%)	Lifetime (years)		
a-Si PV System	2000	GWP EPBT	1 kWh	Cells and modules (BOS) production	1700	0.75	7.0	30	GWP: 50 gCO_{2eq}/kWh EPBT: 2.7 years	[113]
a-Si large-scale PV	2006	GWP EPBT	1 kWh	Modules (BOS), install., transp.	1702	0.70	6.9	30	GWP: 15.6 gCO_{2eq}/kWh EPBT: 2.5 years	[116]
a-Si Large-scale PV plant	2007	GWP EPBT	1 kWh	Production of the PV cells and modules (BOS).	1359	0.75	6.3	20	GWP: 34.3 gCO_{2eq}/kWh EPBT: 3.2 years	[117]

In 2000 an LCA on different PV systems, including a-Si, was conducted [113]. This study assumed the insolation of 1700 kWh/m^2/yr, a performance ratio of 0.75, an efficiency of 7.0 % and a lifetime of 30 years. The results for GWP and EPBT were 50 gCO_{2eq}/kWh and 2.7 years, respectively. The results from an LCA conducted in 2006 calculated a GWP impact of 15.6 gCO_{2eq}/kWh and 2.7 years of EPBT, considering as in its system boundaries the production of the PV modules (including the BOS), the installation and transportation of a large-scale a-Si PV system the [116]. This study considered insolation of 1702 kWh/m^2/yr, a performance ratio of 0.70, an efficiency of 6.9 % and 30 of a lifetime. The comparison of these two studies demonstrates the

variability of environmental impacts influenced by the different assumptions, even considering the same FU (1kWh).

In 2007 an LCA study of large-scale a-Si PV system was conducted but using very different assumption compared with the other assessments of a-Si technology. Considering as insolation, performance ratio, efficiency and lifetime of 1359 kWh/m^2/yr, 0.75, 6.3 % and 20 years, respectively, the results are a GWP impact of 34.3 gCO$_{2eq}$/kWh and an EPBT of 3.2 years [117]. The results calculated are quite different from the previous studies due to the assumptions made, mainly the insolation, and cannot be compared directly.

2.3.2.4 Dye-sensitised (DSSC) technology

Some LCA studies have been made for solar power systems using DSSC technology.

Most of the reports analysed in this review considered 1 kWh as the FU, but even with similar assumptions, the results are very different. The LCA studies for DSSC technologies are shown in Table 7.

Table 7: Summary of LCA published of dye-sensitised technologies (from the year 2000). Colours identify the different FU.

Technology/ System	Year	Impacts	FU	System boundaries	Assumptions				Main results	Ref.
					Insolation (kWh/m^2/yr)	PR	Eff. (%)	Lifetime (years)		
Liq. junction glass-glass DSSC	2006	✓GWP ✓EPBT	1 kWh	Raw materials, cell and module fabrication (BOS).	1700	0.75	8.0	5, 10 and 30	GWP: 120 – 20 gCO$_{2eq}$/kWh EPBT: 0.80 years	[142]
Liq. junction glass-glass DSSC	2007	✓GWP ✓EPBT ✓Others	1 kWh	Raw materials, cell and module fabrication (BOS).	1700	-	8.0	20	GWP: 40 gCO$_{2eq}$/kWh EPBT: 0.48 years	[143]
DSSC case study	2012	✓GWP ✓EPBT	1 kWh	Raw mat., cell and module (BOS), reuse/recycling.	1700	-	8.0	20	GWP: 22.3 gCO$_{2eq}$/kWh EPBT: 1.58 years	[144]
DSSC Grätzel prototype to up-scaled	2014	✓GWP ✓EPBT ✓Others	1g	Raw materials, cell and module fabrication (BOS).	1700, 1117 and 950	0.75	8.0	20	GWP: App. 21.5 gCO$_{2eq}$/kWh EPBT: App. 1.8 years	[145]

Two LCA studies considered liquid junction glass-glass DSSC devices, one published in 2006 [142] and the other in 2007 [143]. Both studies assumed the same FU, insolation and efficiency, which are 1 kWh of electricity delivered, 1700 kWh/m^2/yr and 8.0%, respectively. The results are different, mainly because the studies used dissimilar lifetimes for the PV devices. Considering 5, 10 and 30 years of lifetime, the results for GWP were 120 – 20 gCO$_{2eq}$/kWh, respectively, and the EPBT was 0.80 years [142]. Assuming a lifetime of 20 years the results for GWP and EPBT were 40 gCO$_{2eq}$/kWh and 0.48 years, respectively [143].

A case study in 2012 analysed the impacts from DSSC using the LCA methodology [144]. The assumptions were insolation of 1700 kWh/m^2/yr, efficiency of 8.0 and lifetime of 20 years. The results for a 1 kWh of electricity delivered (FU) were GWP of 22.3 gCO2eq/kWh and EPBT of 1.58 years which is in accordance with the previous LCA of DSSC analysed.

In 2014, another LCA study estimated the environmental impacts from a DSSC from prototype to up-scaled fabrication [145]. Considering three insolation values (1700, 1117 and 950 kWh/m^2/yr), efficiency of 8.0, performance ratio of 0.75 and lifetime of 20 years, the results for GWP and EPBT were approximately 21.5 gCO$_{2eq}$/kWh and 1.8 years, respectively, depending on the assumed insolation value.

2.3.2.5 Organic photovoltaics technology

Seven LCA studies for OPV were analysed in this review (Table 8). Most of them focus on EPBT and GWP and consider different lifetimes, including more than 5 years, which seems to be unrealistic [146], which is also true for DSSC.

Table 8: Summary of LCA published on organic PV technologies (from the year 2000). Colours identify the different FU.

Technology/ System	Year	Impacts	FU	System boundaries	Assumptions Insolation (kWh/m²/yr)	PR	Eff. (%)	Lifetime (years)	Main results	Ref.
OPV solar cells and module process	2010	✓GWP ✓EPBT	1 kWh	Raw materials, cell and module fabrication.	1700	0.8	5-10	15	GWP: 54.92 - 109.84 gCO$_{2eq}$/kWh EPBT: 2 - 4 years	[147]
Long-term OPV modules	2013	✓GWP ✓EPBT	1 kWh	Raw materials, cell and module, transp., use.	1700	0.75	10-15	20	GWP: 2 - 80 gCO$_{2eq}$/kWh EPBT: <0.5 years	[85]
Flexible OPV solar cells	2011	✓GWP ✓EPBT	1 m²	Raw materials, cell and module fabrication.	1700	0.8	2-3	15	GWP: 37.77 – 56.65 gCO$_{2eq}$/kWh EPBT: 0.32 – 4.34 ys	[148]
ITO-free flexible OPV solar cells	2012	✓GWP ✓EPBT	1 m²	Raw materials, cell and module fabric. and use.	1700	0.8	1-5	15	GWP: 137.68 - 55.07 gCO$_{2eq}$/kWh EPBT: 0.41 – 9.45 ys	[149]
OPV cells (3 scenarios)	2012	✓GWP ✓EPBT	1 m²	Raw materials, production phase and transportation.	1961 - 1990	0.8	3	15	GWP: 3 – 18 gCO$_{2eq}$/kWh EPBT: 101.35 - 19.59 days	[150]
Indium and silver free OPV solar cells	2013	✓GWP ✓EPBT ✓Others	1 m²	Raw materials and cell fabrication (roll-to-roll).	1700	0.85	2	5	GWP: 2350 - 3440 gCO$_{2eq}$/kWh EPBT: 0.29 – 0.52 years	[151]
OPV systems	2009	✓GWP ✓EPBT ✓Others	1 Wp	Raw materials, cell and module fabrication.	1000 - 1700	0.75	5	2.6 (min)	GWP: 132 gCO$_{2eq}$/kWh EPBT: 0.19 years	[152]
Laboratory plastic solar cell	2010	✓CO$_2$ ✓EPBT ✓Others	1 kWp	Raw materials and cell fabrication	1700	0.80	5-10	15	CO$_2$: 1120.35 and 2240.70 kgCO$_2$/kWp EPBT: 2 – 4 years	[147]

Reports from 2010 and 2013, based on the same FU (1 kWh), can be compared because of the similar assumptions made. The first study [147] considered the insolation of 1700 kWh/m²/yr, a performance ratio of 0.8, efficiency of 5 to 10 % and a lifetime of 15 years. The results from this analysis are and GWP from 54.92 to 109.84 gCO$_{2eq}$/kWh and an EPBT from 2 to 4 years. The second LCA [85] assumed the insolation of 1700 kWh/m²/yr, a performance ratio of 0.75, efficiency of 10 to 15% and a lifetime of 20 years. From this study, the GWP results go from 2 to 80 gCO$_{2eq}$/kWh, and the EPBT is lower than 0.5 years.

The majority of the OPV LCA studies analysed in this report considered 1m² as the FU. Two of them assumed insolation of 1700 kWh/m²/yr, a performance ratio of 0.8 and 15 years of lifetime, but different efficiencies. Considering efficiency values of 1 and 5% the results for GWP and EPBT were 137.68 - 55.07 gCO$_{2eq}$/kWh and 9.45 – 0.41 years, respectively [149]. Considering an efficiency of 2 to 3% the results for the same

impacts were 56.65 – 37.77 gCO_{2eq}/kWh and 4.34 – 0.32 years, respectively [148], which validates the influence of the efficiency of the cells on the GWP impact (in an inversely proportional relation). Besides, it can be concluded from this comparison that the EPBT depends on the process assumed.

Again using the same FU (1 m^2), other studies found different results due to their assumptions. In 2012 an LCA considering insolation of 1990 - 1961 kWh/m^2/yr, a performance ratio of 0.8, an efficiency of 3% and a 15 years lifetime calculate the impacts for GWP and EPBT as 3 – 18 gCO_{2eq}/kWh and 101.35 - 19.59 days, respectively [150]. The dissimilarity on these results, compared with the previous GWP and EPBT impacts, is mainly due to the use of different insolation.

In 2013 a study assuming a 5 years lifetime calculated the results for GWP and EPBT as being 2350 - 3440 gCO_{2eq}/kWh and 0.29 – 0.52 years, respectively [151]. The high GWP impacts are a consequence of the low (5 years) lifetime assumed (compared with the other LCA studies analysed). The EPBT values are lower due to the selected process, which is a roll-to-roll method that requires a low quantity of primary energy.

One LCA study has used significantly different assumptions, so their results can't be directly compared with the other reports analysed in this review. Assuming an FU described as 25 years of electricity production by PV systems with a power of 1 watt-peak (Wp), a insolation of 1000 to 1700 kWh/m^2/yr, a performance ratio of 0.75, an efficiency of 5% and a minimum lifetime of 2.6 their results were a GWP of 132 gCO_{2eq}/kWh and an EPBT of 0.19 years [152]. A similar study analysed laboratory scale organic cells and considered a functional unit of 1 kWp. The system boundaries assumed in this study are from raw materials to cell fabrication. The results, in this case, for EPBT are 2 – 4 years (assuming efficiencies of 5 and 10%, respectively) and the CO_2 emissions results are 1120.35 and 2240.70 $kgCO_2$/kWp [142].

2.3.2.6 Organic-inorganic halide perovskite technology

Table 9 shows the LCA studies for perovskite technologies analysed in this review.

Table 9: Summary of LCA published on perovskite technologies (from the year 2000).
Colours identify the different FU.

Technology/ System	Year	Impacts	FU	System boundaries	Assumptions				Main results	Ref.
					Insolation (kWh/m²/yr)	PR	Eff. (%)	Lifetime (years)		
Solution + vapour depos. perovskite	2015	✓GWP ✓EPBT ✓Others	1 kWh	Raw materials and cell fabrication.	1700	-	15.4, 11.5	1	GWP: 5.48 and 5.24 kgCO$_{2eq}$/kWh EPBT: 17.32-6.54 yrs	[153]
Tin- and Lead-Perovskite	2015	✓GWP ✓Others	1 kWh	Raw mat., cell fab landfill (Pb rec.).	1700	0.80	6.4 - 15.4	1	GWP: 5.48, 5.24 and 10.7 kg CO$_{2eq}$/kWh	[154]
TiO$_2$ and ZnO perovskite solar modules	2015	✓GWP ✓EPBT ✓Others	1 m²	Production, module manuf., use and landfill.	1960	0.80	9.10, 11.0	2	GWP: 82.5 and 60.1 g CO$_{2eq}$/kWh EPBT: 0.26 and 0.19 yrs	[155]
Perovskite PV cells from lab to fab	2016	✓GWP ✓EPBT ✓Others	1 m²	Raw materials, cell and module fabrication.	1700	0.75	15.0	5	GWP: 99 - 147 g CO$_{2eq}$/kWh EPBT: 1.05 - 1.54 yrs	[156]
Titania Perovskite	2015	✓GWP ✓Others	1 cm²	Raw materials and cell fabr.	1000 - 1863	0.75	6.5 – 25	20 - 30	GWP: 2.88 g CO$_{2eq}$/kWh	[157]
Lead halide perovskite solar cells	2018	✓GWP ✓Others	1 cm²	Raw materials, cell fabric., use and end-of-life.	1700	-	20	20	GWP: 0.517 – 0.0354 g CO$_{2eq}$/kWh	[158]
Lead halide perovskite solar cells	2018	✓Others	1 GWh	Raw materials, cell fabric., use and end-of-life.	1700	0.75	17	20	-	[159]

It is important to highlight that, because perovskite is still in development phases and, consequently, the life cycle inventories represent lab-scale synthesis which cannot be scaled-up to industrial production. The analysis of these results should take this fact into consideration to not be misinterpreted.

In 2015 two studies used the same FU (1 kWh). The first LCA is an environmental analysis of a solution and vapour deposited Pb perovskite solar cell [153]. This study assumed 1700 kWh/m²/yr for the insolation, 15.4 and 11.5 for the efficiencies and 1 year lifetime. From this analysis, the results for GWP and EPBT are 5.48 to 5.24 kgCO$_{2eq}$/kWh and 17.32 to 16.54 years, respectively. The second study assumed the same FU, insolation and lifetime, but focussed on another perovskite technology (tin-based cell) that has lower efficiency (6.4 %) and the GWP result for this new technology was 10.7 kgCO$_{2eq}$/kWh [154].

Two studies used 1m^2 as the FU. Assuming insolation of 1960 kWh/m^2/yr, a performance ratio of 0.80, an efficiency of 9.10 and 11.0 % and 2 years lifetime the calculated GWP is 82.5 and 60.1 gCO$_{2eq}$/kWh and the EPBT results are 0.266 and 0.193 years [155]. Considering the same FU (1m^2), but assuming as insolation, performance ratio, efficiency and lifetime, 1700 kWh/m^2/yr, 0.75, 15.0 % and 5 years, respectively, another analysis calculated a GWP impact of 99 to 147 g CO$_{2eq}$/kWh and the EPBT of 1.05 to 1.54 years [156]. Although assuming the same FU, these two studies can't be directly compared because the rest of their assumptions are diverse.

The last studies analysed [157] used 1cm^2 as the FU. The first one used insolation varying between 1000 to 1863 kWh/m^2/yr, a performance ratio of 0.75, efficiencies from 6.5 to 25 % and a lifetime of 20 to 30 years, finding a GWP impact of 2.88 gCO$_{2eq}$/kWh. Another study using the same FU, but different assumptions, found much lower impacts (0.517 – 0.0354 g CO$_{2eq}$/kWh) [158]. However, these impacts considered 20 to 30 years of lifetime for the modules, which is currently unrealistic because of the stability problems of this technology.

2.3.3 LCA of Si-based Tandem Technologies

Table 10 displays the summary of LCAs published on Si-based tandem technologies.

Table 10: Summary of LCA published on Tandem technologies (from the year 2000).
Colours identify the different FU.

Technology/ System	Year	Impacts	FU	System boundaries	Assumptions				Main results	Ref.
					Insolation (kWh/m^2/yr)	PR	Eff. (%)	Lifetime (years)		
InGaP/mc-Si modules	2003	✓GWP ✓EPBT ✓Others	1 kWp	Materials, cell /module prod.	-	-	25	-	GWP: - gCO$_{2eq}$/kWh EPBT: 5.3 years	[160]
Perovskite/Si tandem solar cells	2017	✓GWP ✓EPBT ✓Others	1 kWh	Materials, cell /module prod., use/landfill.	1700	0.75	24 – 27	20	GWP: 294 gCO$_{2eq}$/kWh EPBT: 1.3 – 1.7 years	[110]
Chalcogenide/Si tandem modules	2017	✓GWP ✓EPBT ✓Others	1 kWh	Materials, cell /module prod., use/landfill.	1700	0.75	22	20	GWP: 25 – 30 gCO$_{2eq}$/kWh EPBT: 1.3 – 1.4 years	[161]
Monolithic SHJ-PSC tandem cells	2017	✓GWP ✓Others	1 kWh	Materials, cell /module prod., use/end-of-life	1700	0.75	26 - 30	30	GWP: ≈ 0.05 – 0.08 kgCO$_{2eq}$/kWh	[162]
Si/perovskite	2017	✓GWP ✓EPBT ✓Others	1m^2	Materials, cell/module	1700	-	6	5	GWP:168.4gCO$_{2eq}$/kWh EPBT:13–13.5 months	[163]

In 2003 an LCA study of InGaP/multi-Si solar modules was produced. This report assumed a single PV module as the FU and considered the raw materials, cell and module production as the system boundaries. This study measured the EPBT, which was 5.3 years, considering the efficiency of 25 % [160].

In 2017 two LCA studies were made considering the same bottom layer (Si) and system boundaries from raw material, cell and module production, use phase until end-of-life (landfill). These reports assumed insolation of 1700 kWh/m^2/yr, a performance ratio of 0.75 and 20 years lifetime. The first one considered a perovskite solar cell top layer. In this case, the efficiency was 24 – 27 %, depending on the structure of the tandem cell. The results for GWP and EPBT were 294 gCO$_{2eq}$/kWh and 1.3 – 1.7 years (for different scenarios), respectively [110]. The other top layers studied were chalcogenide (including copper indium gallium selenide – CZTS, copper zinc tin sulfide – CZTS and silver zinc tin sulfide – AZTS) and the efficiency considered was 22%. In this case, the results for GWP and EPBT were 25 – 30 gCO$_{2eq}$/kWh and 1.3 – 1.4 years, respectively, depending on the top cell structure [161]. Comparing these two studies, it is observed that the change of the bottom cell reduced the environmental impacts considerably, mainly because of the different processes and materials studied.

A monolithic silicon heterojunction-perovskite (SHJ-PSC) tandem cell structure was analysed in 2017 [162]. Assuming a 1 kWh FU, an insolation of 1700 kWh/m^2/yr, a performance ratio of 0.75 and 30 years lifetime, as well as system boundaries from raw materials until the end-of-life, the calculated results for GWP are approximately 0.05 – 0.08 kgCO$_{2eq}$/kWh, depending on the efficiency.

Also in 2017, a comparative LCA was conducted relating different tandem structures using the perovskite technology [163]. The structures analysed were Si/perovskite (efficiency: 6%), CIGS/perovskite (efficiency: 19%), CZTS/perovskite (efficiency: 21%) and perovskite/perovskite (efficiency: 21%) tandem solar cells. All technologies

analysed considered insolation of 1700 kWh/m^2/yr, FU of 1 m^2 of cell area and 5 years lifetime. The GWP result for Si/perovskite was approximately 168.4 gCO$_{2eq}$/kWh and the EPBT 13–13.5 months.

2.3.4 Additional Impact Categories Other than GWP and EPBT

As mentioned, GWP is the most common impact category analysed in LCA studies. In the case of PV technologies, this impact is calculated to determine the effect of the analysed system in reducing GHG emissions during the manufacturing process as well as during electrical generation due to, for example, fossil fuel-based technologies [104].

However, the use of toxic or rare elements and the study of wastes and emissions from the PV cells and modules production processes requires consideration of more than just GWP and EPBT. There is a necessity to analyse different environmental categories that address toxicity, materials scarcity and other impacts from the PV technology's life cycle.

The environmental impact categories are intended to be complementary and to analyse all the aspects related to production processes and the use of products. Because of that, the ideal LCA study should present as many significant impact categories as possible to allow it to be complete and representative.

This review analysed a total of 56 LCA studies for silicon, thin-films and some sorts of tandem PV technologies. Through the detailed analysis of these studies, it can be observed that not all studies present results other than GWP and EPBT.

Table 11 shows the comparison between the number of LCA studies reviewed, which calculate GWP and EPBT, and the number of studies that also analysed other environmental impacts.

As shown in Table 11, approximately 52% (33 of 63) of the LCA studies analysed more environmental impacts than just GWP and EPBT. The detailed examination of them is shown in Table 12.

Table 11: Comparison between the number of LCA studies reviewed (TOTAL) and the studies that analysed not just GWP and EPBT, but also other environmental impacts (ADDITIONAL).

TECHNOLOGY	TOTAL	ADDITIONAL
Multi-Si	16	9
Mono-Si	8	4
Si (others)	2	1
Chalcogenide	5	2
CdTe	7	2
a-Si	3	0
DSSC	4	2
OPV	8	3
Perovskite	7	7
Si-based tandem	5	5
TOTAL	61	31

Table 12: Environmental impacts analysed in the LCA studies, other than GWP or EPBT.

ENVIRONMENTAL IMPACT	TOTAL
Abiotic Depletion Potential	22
Ozone Layer Depletion	18
Human Toxicity Potential	17
Ecotoxicity Potential	17
Photochemical Oxidation	14
Acidification potential	17
Eutrophication Potential	22
Land Use	8
Others	3

The most studied category beside GWP is the abiotic depletion potential (ADP). This category is related to non-living resources (including energy resources) such as metal ore and crude oil and it represents the consumption, without replacement, of these resources [164]. The impacts from the cells' and modules' production are related to the use of non-renewable elements such as Al, Cu, silver, chromium and nickel and fossil fuels, the latter being used for primary energy (electricity) generation during the manufacturing processes.

Ozone layer depletion is the indicator that describes the thinning of the stratospheric ozone layer as a result of anthropogenic emissions. The impacts are potentially harmful to human health, animal health, terrestrial and aquatic ecosystems. PV related processes, such as chemical vapour bath chamber cleaning, currently use tetrafluoroethylene as a proxy for CF_4, C_2F_6, SF_6, and NF_3 and it has been demonstrated to cause high ozone layer depletion if released [165]. For multicrystalline silicon solar cells, for example, it has been shown that this impact is dominated by the release of gases such as Halon (1301) and (1211) and carbon tetrachloride. These gases are mainly generated during the production stages of solar-grade Si and in the use (considering all life cycle) of Al and electricity and in the module production process [123].

As a consequence of the production process of PV cells and modules, for all technologies, toxic substances are emitted to the air, water and soil. The environmental impact caused by these processes can affect human health, fauna and flora. The HTP, for example, is an environmental impact category that provides approximations of the cumulative toxicological risk and potential effects associated with chemicals produced from a process or a product on human health [166]. Considering freshwater ecosystems, an example impact is the FEcP, which refers to the impact of toxic substances on water, describing fate, exposure and effects of toxic substances [42].

Besides toxic substances, adding excessive quantities of nutrients, nitrogen (N) and P to water and soil is also an important environmental impact. The consequence of these releases in freshwater, for example, is that they stimulate the rapid growth of plants and algae. Consequently, when these plants and algae die and decompose, they use up large amounts of oxygen, which reduces its availability to fish and other aquatic species [167]. The FEuP is the environmental category that calculates such impact.

2.3.5 Discussion

The LCA methodology is considered as one of the main relevant tools to assess the environmental impacts from a product or system. Therefore, LCA has been widely used in order to identify the environmental impacts from different areas, including renewable energies such as PV. The result is a large quantity of LCA studies, using different sets of assumptions, presenting a high variability in impact results for similar systems, which makes it difficult to compare them.

The greatest challenge is to find an ideal standard on which all LCA practitioners (in this case related to PV modules) can base themselves, allowing consistency, balance, quality and, most importantly, transparency of the study to enhance the reliability and reproducibility of the environmental results, which is mandatory in the LCA methodology. At this time, consensus is limited to a small number of PV technologies for which there are complete and reasonably recent inventory data available, but there is still room for improvement in order to standardise the results for the most common technologies and guide practitioners in future LCA studies for new PV technologies.

Currently, and based on this review, variations in LCA studies are still widespread and are related to assumptions implemented by each author [113]. Inconsistency in environmental impact results may also be related to the system boundary setting of each investigation, energy source selection during the process steps, different values

of assumed insolation, lifetime and performance ration and variations in the production processes used to manufacture the PV cells, PV modules and BOS components [117].

The efficiency, the performance ratio, the insolation and other assumptions are usually provided in the LCA reports, but in some cases, one or more are not, which makes comparison of results difficult. Besides, some results are presented only after normalisation, which obscures the contribution of each environmental impact and can cause differences in the final results.

This review considered LCA studies from the year 2000 and, to be able to compare the GWP and EPBT results, all values were normalised considering a performance ratio of 0.75 and insolation of 1700 $kWh/m^2/yr$, but retained different lifetimes, materials and production processes. This review considered 9 different PV technologies. A summary of all LCA results analysed is shown in Figures 11 and 12.
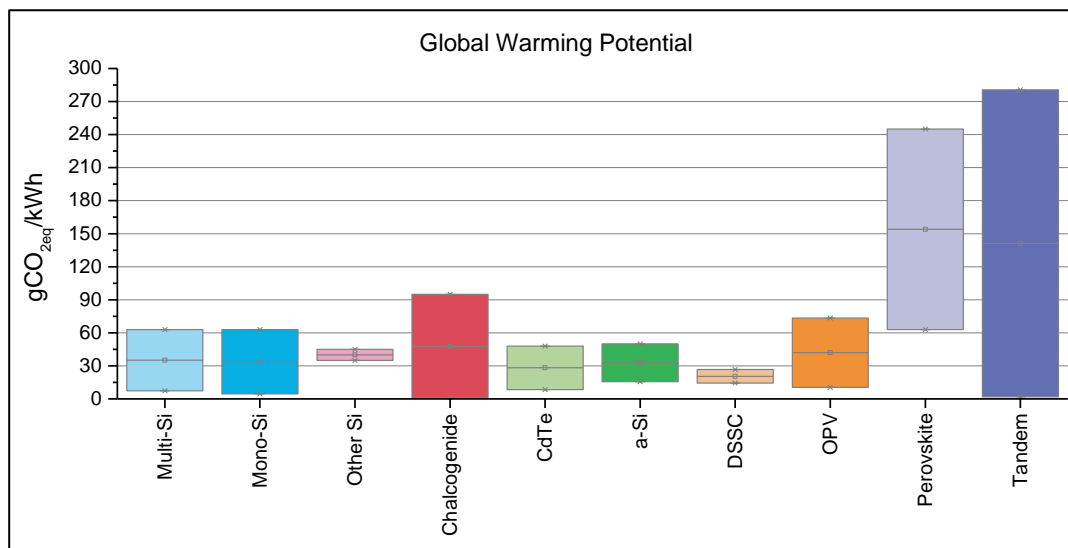
Figure 11: Variances of global warming potential results (in gCO$_{2eq}$/kWh) of LCA studies of various PV systems. Results from the normalisation of all LCA revised using the same insolation (1700 kWh/m^2/yr), performance ratio (0.75) and lifetime (30 years).
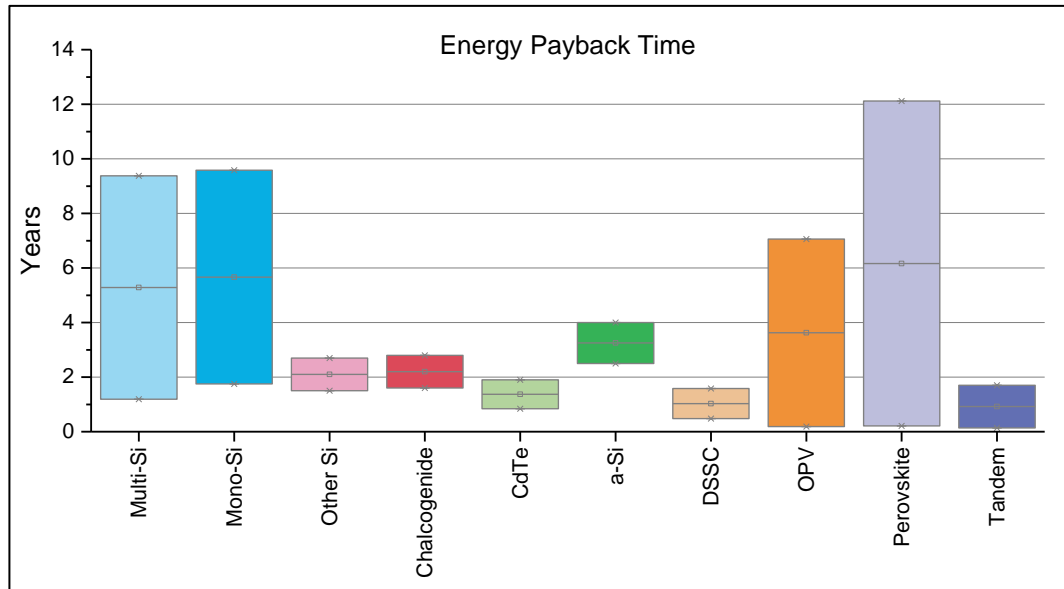
Figure 12: Variances of energy payback time results of LCA studies of various PV systems. Results from the normalisation of all LCA revised using the same insolation (1700 kWh/m^2/yr), performance ratio (0.75) and lifetime (30 years).

From Figures 11 and 12 it is found that tandem technologies present the lowest average impacts (0.92 years) compared with the other PV technologies. This result is reasonable considering that a tandem structure aims to get higher efficiencies, which impacts positively on the environmental impacts (either GWP or EPBT). It is important to notice that different technologies are considered in these studies, and the production processes and assumptions are not similar.

The results for GWP (Figure 11) show large variations for most of the technologies. The main reasons for that are the different assumptions made and the continuous update of the production process inventories and technologies. Particularly for multi-Si, there is a significant variation in the GWP impacts, which is a result of the high number of studies for this technology. These studies include diverse set of assumptions related to the production processes, materials usage and other important parameters that can strongly influence in the final results.

For the EPBT (Figure 12) there is a significant range from the lowest to the highest value, particularly for organic and perovskite technologies. The LCA studies for organic solar cells assume several manufacturing processes, as this technology has numerous alternative approaches. These differences influence the final results for EPBT, mainly because of the energy usage for each process. The perovskite solar cells are not mature enough to be competitive. This technology is promising, but still has stability issues and the manufacturing processes are diverse. Each LCA study focuses on one particular method and different lifetimes, which leads to very different results regarding environmental impacts.

It is essential to highlight that improvements in PV production processes and the efficiency of solar cells and modules should be taken into consideration when analysing environmental impacts. Developments should always be considered in LCA inventories, as this is vital in order to model a realistic and representative LCA study. The example given in this analysis is an LCA study published in 2016 [121], which uses recent and realistic assumptions, mainly for the efficiency of the most common technologies (single-Si, multi-Si, CdTe, and CIGS PV systems). This study presents up-to-date energy and environmental impact results and considers a range of categories, such as CED, GWP, ODP, AP and EPBT, where for the most common impact, GWP, the results are reduced compared with older studies described in this chapter (Tables 1, 2, 4 and 5). As discussed, these results validate the importance of constant improvements in efficiencies for solar cells and modules as well as production processes followed by the respective update in the LCA assumptions and inventories, to better predict environmental impacts.

The end of life and the transportation stages are not included in most LCA studies for any PV technology, mainly due to the lack of data for these steps of the processes in this field. However, the impacts from these phases can have important environmental

effects and should be included in LCA studies [168]. Attention should be paid to the research and data collection related to these processes, in order to build complete and broadly accepted inventories to be used in the LCA studies of PV technologies.

The use of fossil fuels as source of electricity represents a major contribution to the majority of the environmental impacts. Most of LCA studies for PV technologies assume that the cell and module production is located in China because it remains the biggest producer and customer for Si cells [169]. The electricity mix in China is based in approximately 72% on fossil fuels (coal) [170] and the environmental impacts related to this source of energy consider substances such as carbon dioxide (CO_2), carbon monoxide (CO), sulfur dioxide (SO_2), nitrogen oxides (NO_x), particulate matter (PM) and heavy metals (e.g. mercury). Similarly, the USA electricity mix is mainly based in fossil fuels, such as petroleum, natural gas, and coal that, combined, accounted for about 77.6% of the county's primary energy production in 2017 [171]. This value is similar to that for China and the estimated share of total final energy consumption worldwide in 2016, which is 79.5% [2]. If other locations with different electricity mixes are considered, the LCA results might change considerably. An LCA study considering the electricity mixes from China, Russia, Norway and the United States, for example, shown that there are significant differences in impacts such as cumulative energy demand (CED), GWP, acidification potential (AP) and ozone depletion potential (ODP) [121]. Because of that, it is important that LCA studies are transparent in relation to the location chosen for the study, as well as for other assumptions made. In the case of the calculations done for this thesis, I focussed on the realistic present case of mix for the country with dominant current manufacture and consumption of PV, China.

In order to avoid these discrepancies in LCA studies of PV cells, modules and systems, the IEA PVPS programme, for example, published a guideline whose mission is: "*To enhance the international collaborative efforts which facilitate the role of photovoltaic*

solar energy as a cornerstone in the transition to sustainable energy systems."[172].
The most important contribution from this guideline is to provide practitioners with complete inventory data for the main PV technologies industrially available today, based on assumptions such as definition of system boundaries, performance ratio and insolation to be used in the calculations.

The LCA transparency can affect the results significantly. According to the IEA-PVPS guideline: "*At a minimum, the following parameters should be reported: 1) On-plane irradiation level and location; 2) module-rated efficiency; 3) system's performance ratio; 4) time-frame of data; 5) type of system (e.g., roof-top, ground mount fixed tilt or tracker); 6) expected lifetime and degradation ratio for PV and BOS; 7) system's boundaries (whether capital goods, installation, maintenance, disposal, the transportation- and recycling-stages are included for both PV modules and balance-of-system (frame, mounting, cabling, inverter; for utility applications the transformer, site preparation, and maintenance)); 8) the place/country/region of production modeled (e.g., average grid, site specific power use (e.g., hydro, coal), and 9) explicit goal of the study (e.g., static or prospective LCA, prototype or commercial production, current performance or expected future development).*" [172].

Besides guidelines, there are some uncertainties that also have to be reduced. Most uncertainties are due to input data (parameter uncertainty), normative choices (scenario uncertainty) and the mathematical models involved (model uncertainty) [173]. There are techniques to identify and quantify these uncertainties, such as Monte Carlo simulation, which is a method that propagates known parameter uncertainties into an uncertainty distribution of the output variable [174].

The lack of data and data inaccuracy is one of the most important sources of LCA uncertainties, and the majority of the publicly available data are not the most current, which also results in uncertainties. There is a need for a development for a more

dynamic tool that allows reliable, confirmed data to be available more quickly and efficiently, so that inventory is not outdated, and the results can be as realistic and recent as possible.

In summary, the lack of recent and reliable data, as well as the importance of more LCA studies focusing on new technologies, as mentioned, opens a range of possible assessments related to emerging PV technologies. Potential improvements in LCA inventories, as well as developments in industrial processes that can create both ecologic and economic benefits, such as better efficiencies for solar cells and modules, need to be studied to standardise data and present more realistic results. After a careful literature review, a lack of consistency in LCA inventory data and results were identified, which motivated this research. Particularly for technology that present potential efficiency improvements for cells and modules, such as tandem structures and advanced Si technologies.

3 Life Cycle Assessment Methodology

Manufacturing a product can involve complicated process steps and the use of diverse materials. Each process or resource has its peculiarities and can come from many different sources, involving a specific series of inputs (material or energy which enters a unit process [39]) and outputs (material or energy which leaves a unit process [39]). Each one of these processes and the use of every material has potential environmental impacts. Several tools and methodologies can be used to calculate those effects.

LCA is a method accredited by the International Organisation for Standardisation (ISO). The LCA technique evaluates the environmental impacts of a process or a product across its entire lifecycle by compiling an inventory of relevant inputs and outputs of a product system, assessing the potential environmental effects associated with those flows and interpreting the results according to the objectives of the study [39].

Attributional and consequential approaches are the two different methods to perform an LCA study.

The attributional LCA evaluates one complete production-use chain, assigning emissions from each step of the process. This method is useful in benchmarking and comparing different technologies or products, for example. Which is the methodology used in this thesis.

The consequential LCA analyses a wider system, assessing the consequences of selecting one use of one material over another, which is useful for decision making at sector-wide or policy levels [175].

The results from an LCA study can assist in identifying opportunities to improve the environmental aspects of products at various points in their lifecycle, decision-making

in industry, governmental or non-governmental organisations, selection of relevant indicators of environmental performance and marketing [39]

The four main phases of any type of LCA are 1) goal and scope, 2) inventory analysis, 3) impact assessment and 4) interpretation [39].

3.1 Goal and Scope

According to the ISO-standardised LCA methodology [39], the objective of the goal definition is to establish the main purpose of the assessment in a clear and objective approach. The scope goes further, describing the assumptions and decisions to be made in the next steps of the study [176]. The LCA goal and scope definition describes the analysed product or system, the system boundaries, the assumptions and the FU [177].

This first step of an LCA is often underestimated, but it has the same importance for the study as the other steps, and it should be clear and well structured. The goal and scope must be defined before any collection of input and output data (inventory) because this is where the exact approach to be followed in the next steps is determined [176].

It is important to realise that an LCA model is a simplification of reality and it does not incorporate all the complexities that the real product or process might have. The challenge for an LCA practitioner is to develop the model as realistically as possible, considering assumptions that will not cause distortions or influence the results considerably. The goal and scope of the LCA are the first steps study to deal with this challenge.

3.1.1 System boundaries

The LCA study must describe the analysed process, presenting a diagram that includes all routes related to the analysis. The system boundaries indicate the inclusion and exclusion of unit processes, where the steps within borders are the processes to be analysed [178].

The system boundaries should also include detailed information, such as the technological system and nature, geographical area, time horizon, comparison between current life cycle and related life cycles of other technical systems and so on [178].

The definition of the system boundaries needs to consider as many steps of the process as possible, including the material and energy flows, the extraction of raw materials, and the production of intermediate feedstocks and the manufacture of equipment. The end of life is also essential and should embrace the disposal of products, by-products and wastes. The inclusion or exclusion of any of these steps can affect the outcome importantly, and should be clearly documented. There are different approaches to be taken when choosing the type of system boundaries [178]. The main possibilities are shown in Table 13.

Table 13: Variants of system boundaries approaches.

System boundary	Description
Cradle-to-grave	From resource extraction (cradle) to the end-of-life (EoL) or disposal phase (grave), considering all inputs and outputs for each process.
Cradle-to-cradle	The EoL phase is a recycling process, where new/different products are generated and relocated to the beginning of the process (cradle).
Cradle-to-gate	From resource extraction (cradle) to the factory gate (gate). The next steps, such as use and disposal phase, are not assessed.
Gate-to-gate	It looks at a specific sub-system that produces the final product only, not considering the production chain, but it can include transportation.

This analysis is initiated with the raw materials necessary for the cells' production and finishes at the modules' end of life (cradle-to-grave LCA). The analysed processes are shown within the system boundaries in Figure 13. Landfill disposal is assumed, because, even with some attempts at mass recycling of some types of modules [179], for the structures analysed in this LCA there is a lack of recycling technology, and consequently, a lack of data.
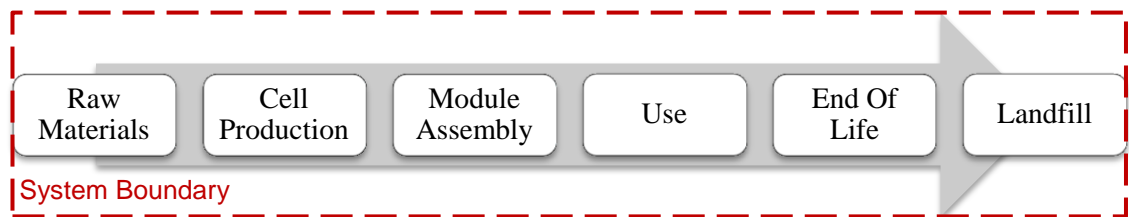
Figure 13: Processes within the LCA system boundaries.

3.1.2 Functional unit

The FU is a crucial element of an LCA and must be explicitly specified in the scope definition. This unit is a measure of the function of the studied products or system, and it provides a reference to which the inputs and outputs from the LCA inventory can be related [180].

The functional unit used for a project should be determined during the elaboration of the goal and scope definition, and the correct use of the FU enables the comparison of two or more different systems [177].

The FU to be used in this analysis is defined as 1kWh of generated electrical energy over the lifetime of the module, not just because this is the most common FU used to analyse PV systems (as discussed in Chapter 2), but also because it allows a fair and realistic comparison between different PV technologies.

3.2 Inventory analysis

Life Cycle Inventory (LCI) analysis is a methodology for estimating the consumption of resources and the quantities of waste and emissions generated by or otherwise attributable to a product's lifecycle [177].

The LCI analysis involves the compilation and quantification of inputs and outputs (inventory), for a given product system throughout its life cycle. The main steps of this phase are preparing for data collection, data collection, calculation procedures and allocation and recycling [177].

The data aggregation must be straightforward and homogeneous, and the LCI should be standardised in such a way that all inputs and outputs refer to the selected FU. The calculation procedures relate process data to the FU (matrix algebra), and the allocation method defines the multiple processes (multiple outputs, multiple inputs, re-use and recycling) [181].

The complete inventories for all structures analysed in this thesis, as well as their references, are presented in Appendix.

3.2.1 Challenges of data collection

The data collection for the LCI can be from a specific process which already had this information collected, or it can aim to create a new database. However, for these two cases, there are a few challenges to be overcome.

In the case of a known process or material, the owner or operator of the activity might have little or no previous experience in doing such a compilation of data. Thus this process may not have a traditional environmental data record or may even have no documented data at all. Similarly, the LCA practitioner may have little previous

knowledge of the process itself and not know which data are relevant or not for the environmental analysis [177].

Even more challenging is to create a new database, especially in research projects without the involvement of a manufacturing company. In this case, the access to primary data is even more limited, which forces the creation of an inventory from scratch. This process can introduce uncertainties, and some results can become irrelevant [177].

3.3 Impact assessment

Life Cycle Impact Assessment (LCIA) is a vital phase of an LCA study. The LCIA translates the data from the LCI to potential environmental impacts following a few steps: selection and definition of impact categories, classification and characterisation. There are also some non-compulsory stages that may be performed, such as normalisation [182].

In general, the LCIA process involves associating inventory data with specific environmental impacts and attempts to understand those impacts. The level of detail, choice of categories evaluated and methodologies used depend on the goal and scope of the study.

3.3.1 Impact categories, classification and characterisation

The first step of the LCIA is the selection of the environmental impact categories to be analysed, which should be in accordance with the goal of the study.

The environmental impacts are defined as a negative effect on human health or the environment, the depletion of resources or disturbance of any natural ecological biomes by a product or process (including the input and output flows) during its

lifecycle. The impact categories are the classes that represent the potential environmental issues of concern to which LCI analysis results may be assigned [39].

The calculation of category indicator results in LCA studies is called characterisation phase. The calculation is made by multiplying the quantity of each flow (inputs and outputs) by a characterisation factor, which is specific for each impact category and gives a quantitative representation of its importance for a particular impact category [183].

There are two main groups of choice for a category, which are midpoint-oriented and endpoint-oriented indicators. The midpoint-oriented are related to impacts that are relatively close to the interventions and have the advantage of relying primarily on scientific information and well-proven facts, which reduces the subjectivity and uncertainty involved in the calculations.

The endpoint-oriented indicators are broader and are related to the endpoint impacts. These have the advantage of presenting information more clearly, for instance, human health (endpoint) is more accessible to interpret than ozone layer depletion (midpoint) [183]. Some examples of midpoint and endpoint indicators, and their interactions, are shown in Figure 14.
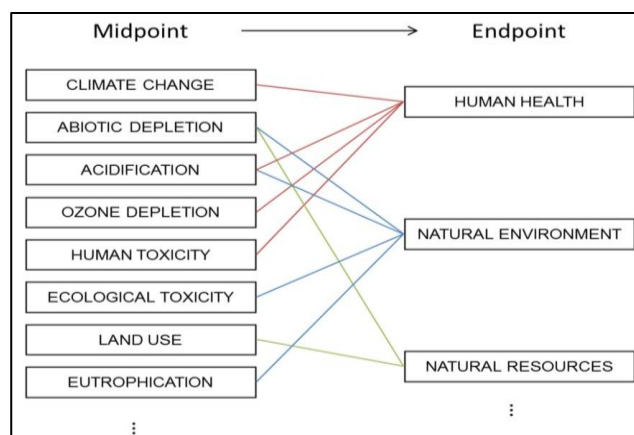
Figure 14: Examples of midpoint and endpoint indicators.

In the LCA classification step, the LCI results are correlated to the selected impact categories. In other words, in this phase, the inventory flows are assigned to the relevant impact categories among those chosen under the characterisation phase, giving their capability to contribute to different environmental issues.

The most commonly used impact categories are climate change, abiotic depletion, acidification, human and ecological toxicity, eutrophication, etcetera [183]. The impact categories are selected according to what was defined in the goal and scope.

There are different characterisation models for the LCA practice, which are described and critically analysed in the literature [111].

Examples of common characterisation methods are the Institute of Environmental Sciences of Leiden University (Centrum Milieukunde Leiden - CML), which is one of the most complete and most commonly used approaches, the ReCiPe method (which has this name because it provides a "recipe" to calculate life cycle impact category indicators) and the International Reference Life Cycle Data System (ILCD) [184-186].

3.3.2 Selected Impacts Categories (Midpoint)

Midpoint approaches generally present the environmental impacts in a qualitative form, offering statistics and review articles. Midpoint results are separated in several ecological category indicators with specific relevance, which is a more complex approach and usually focused on presenting the results for other LCA practitioners, who will understand all the different categories.

The CML characterisation method is used for midpoint impact categorisation based on the recommendation of best practice for LCAs undertaken in Australia [187]. The CML methodology have characterisation factors for more than 1700 different flows, and they are updated when new knowledge on substance level is available [184]. The choice of

impact categories to be analysed in an LCA study is based in which possible impacts the product or process might have on the environment.

Table 14 shows the selected impact categories for this LCA and is followed by the justification of each choice.

Table 14: Impact categories chosen to be analysed in this LCA.

Impact Category	Characterisation Unit
Global warming potential (GWP)	Kilograms of carbon dioxide equivalent (kg CO_2 eq.)
Human toxicity potential – cancer effects (HTP – CE)	Kilograms of 1,4-Dichlorobenzene equivalent (kg 1,4-DCB eq.)
Human toxicity potential – non-cancer effects (HTP – nCE)	Kilograms of 1,4-Dichlorobenzene equivalent (kg 1,4-DCB eq.)
Freshwater ecotoxicity potential (FEuP)	Kilograms of 1,4-Dichlorobenzene equivalent (kg 1,4-DCB eq.)
Freshwater eutrophication potential (FEuP)	Kilograms of phosphorus equivalent (kg PO_4 eq.)
Abiotic depletion potential (ADP)	Kilograms of antimony equivalent (kg Sb eq.)

GWP aims to compare the climate effects of emissions of different GHG to the atmosphere. This method was initially presented as analogous to the ozone depletion potential impact, to help assess the environmental impacts of substituting chlorofluorocarbons to hydrofluorocarbons [188, 189]. Later, the interest in its more extensive function and its use to relate the effects of CO_2 emissions with other GHG made this impact one of the most popular in environmental analysis.

The GHG of most importance in this category are carbon dioxide (CO_2), methane (CH_4) and nitrous oxide (N_2O), but other GHG are also included in the software calculations

when data are available. Human activities can also affect climate beneficially through the uptake of CO_2 into biomass and soils, countering the global-warming effect [187].

GWP is considered in this LCA to determine the effectiveness of the PV technologies in reducing GHG emissions during the manufacturing process as well as during electrical generation [104].

The impacts related to toxicity take into account the fate, route of exposure and toxicity impact of toxic substances when released to air, water or land. Categories of chemical substances commonly accounted for are pesticides, heavy metals, hormones and organic chemicals [190, 191]. Toxicity can affect humans and the environment.

HTP is the impact on human health caused by the emission of toxic substances to the environment [190]. This impact category captures the adverse effects of chemicals on human health, including both HTP-CE and HTP-nCE [192, 193].

Ecotoxicity refers to the impact on ecosystems, as a result of emissions of toxic substances to air, water and soil [42]. This category makes it possible to estimate ecotoxic effects on freshwater, marine and terrestrial environments. However, the majority of available ecotoxicological effect data is for freshwater species. Consequently, the FEcP is traditionally used to represent all aquatic ecosystems (freshwater, marine and terrestrial) [187].

The toxicity (human and freshwater) is evaluated in this LCA because of the use of toxic substances, such as heavy metals and organic chemicals during most of the processes from the extraction of the raw materials until the end-of-life of solar modules.

Eutrophication characterises the impacts of adding excessive quantities of macro-nutrients to air, water and soil. The macro-nutrients most commonly accounted for in this category are N, P and organic compounds. It can occur in aquatic and terrestrial environments, but the former is more commonly a problem [187].

The FEuP assesses the impacts of excessive macro-nutrients in freshwater, which causes the rapid growth of plants and algae, blockage of waterways and blooms of toxic blue-green algae. The consequence of this impact is the reduction of the amount of oxygen available to fish and other aquatic species. In extreme cases, it can lead to an oxygen-depleted environment that can only support a few species of anaerobic bacteria. It can also kill fish and other aquatic life and reduce the aesthetic and recreational value of the water body [167].

The FEuP is calculated in this LCA because of concerns about the possible emissions to freshwater, including nitrogen oxides, phosphate and nitrate, during the silicon treatment and cell manufacturing processes.

The ADP category is related to the non-living resources (including energy resources) such as iron ore and crude oil, which might be depleted. The concept of ADP was developed in 1995 as a characterisation factor based on global reserves and extraction rates of materials. In other words, abiotic depletion is the consumption of resources that are not renewed in nature and eventually will be depleted completely [164]. As solar cells (of any type) and modules are manufactured using several metals and other materials that are not renewable, it is crucial to analyse this impact category in this LCA study.

Other LCA metrics suggested by the IEA Methodology guidelines on life cycle assessment of photovoltaic electricity [107] but not included in this thesis are acidification potential (AP), which represent the impacts associated with changes in soil acidity as a consequence of the atmospheric deposition of sulphates, nitrates and phosphates, and ozone depletion potential (ODP), which defines the impacts caused by anthropogenic emissions on the thinning of the stratospheric ozone layer.

The AP is excluded due to the similarities with the eutrophication potential. The acidification impacts are linked to emissions such as sulphur dioxide, nitrogen oxides and ammonia, which are deposited in part near the emission sources and the eutrophication impacts are mainly linked to the transformation of NOx and NH3 emissions into nitrogen, which modifies the chemical balance of the ecosystems in which it is deposited [194]. It seems unlikely that a decision-maker could be misled in any any of my studied cases by exclusion of AP when I have included EP. The exclusion of ODP is mainly because GWP and ODP impacts are closely interrelated on a global scale. Atmospheric processes establish a linkage through certain gases, such as carbon dioxide, nitrous oxide, chlorofluorocarbons and methane, in promoting global warming and in depleting the ozone layer at the same time. Many gases emitted from man's industrial and agricultural activities can accumulate in the earth's atmosphere and ultimately contribute to alterations in the vertical distribution of stratospheric ozone, as well as to global warming [195]. This thesis focuses on GWP because this is an urgent and unsolved concern and one which primarily motivates PV research and development, whereas ozone depletion has been addressed already to a significant extent by the Montreal Protocol and PV has not been found to be a likely to make a significant contribution [196].

3.3.3 Selected Impacts Categories (Endpoint)

The ReCiPe characterisation factors are based on the most detailed and complete modelling available and are recommended for the calculation of endpoint impact in LCA studies by the International Reference Life Cycle Data System (ILCD) [111].

ReCiPe is a method used for calculating the environmental impacts at midpoint and endpoint level. The endpoint indicators, which are separated in 3 categories, show the

ecological effect on three higher aggregation levels, which are the effect on human health, biodiversity and resource scarcity [186].

The use of an endpoint indicator (the ReCiPe method in this LCA) contributes to a better understanding of the consequences of environmental impacts, accounting to current scientific knowledge. The insights obtained can be used to understand how to reduce the ecological effects even for non-LCA practitioners, as it presents a more summarised result, combining the midpoint indicators in a simplified representation of impacts.

3.3.4 Energy Payback Time

The EPBT for PV systems is defined as the time, normally in years, required for this system to generate the same amount of energy to compensate the primary energy input requirements during the PV cells and modules' manufacturing, assembly, transportation, installation, operation and maintenance [108]. The EPBT relates the total primary energy input of the PV module, which can include that for the BOS or not, depending on the goal and scope of the study, and the annual electricity generation by the PV system. The result of this calculation depends on several factors such as the type of PV module, manufacturing technologies, module conversion efficiency, installation location, etcetera [109].

This parameter is not an environmental impact, but it is often calculated in LCA studies of energy sources, such as PV solar modules. For this LCA the EPBT of all structures analysed are calculated considering the cumulative energy input for all the production process of the PV modules. The average grid conversion efficiency from primary energy to electricity is considerd to be 0.315, according to Ecoinvent [197].

Another important LCA indicator, related to the EPBT, is the CED, which describes the consumption of fossil, nuclear and renewable energy sources along the life cycle of a

product and it is an input for the EPBT calculation [172]. The EPBT calculates how long a PV system must operate to recover the energy that went into making the system in the first place, and it does not differ when the power plant is dominated by non-renewable electricity generation [198]. However, the consumption of electricity must take into consideration the associated generation of pollution and CO_2 from the electricity mix and, with that, an increasing share of renewable energies, which is expected in future power grid mixes, may change the interpretation of the EPBT values with the variation of the CED, which should be analysed.

This thesis focuses in the EPBT values, but future work is being developed in order to analyse the impact of different CED in the overall environmental impact of PV technologies such as c-Si and CdTe.

3.3.5 Normalisation and weighting

Differently from classification and characterisation, which are compulsory steps according to the ISO standards [39], normalisation and weighting are optional in the LCIA phase due to potential biases and subjective value choices.

Normalisation relates all categories analysed, delivering a single impact that agglomerates the relative contribution of each impact from the product system based on a reference situation (geographical, temporal, etc.) [199]. In other words, normalisation is calculating the magnitude of category indicator results relative to reference information.

Weighting as converting and possibly aggregating indicator results across impact categories using numerical factors based on value-choices [39]. This final step is perhaps the most debated, because of its subjectivity. Weighting entails multiplying the normalised effects of each of the impact categories with a weighting factor that

expresses the relative importance (value judgement) of the impact category, which can influence the results and conclusions of your LCA.

Normalisation and weighting are not part of the scope of the LCA conducted in this thesis.

3.3.6 Assumptions

For this LCA the assumption of similar module production is a simplification that allows the comparison between technologies, since some of them are not yet fully established. This assumption could be further explored when more robust methods of encapsulation for tandem solar cells are stablished.

The module materials considered are ethyl vinyl acetate (EVA), Al frame, polymer back-sheet (Tedlar® film-based backsheet is the industry standard), cover glass, tabbing and solder. In this work, Pb-containing solder interconnects, commonly used in Si PV modules, are included because this material still accounts for more than 90% of the PV market [32] for interconnection technologies.

Module efficiencies are generally slightly lower than cell efficiencies. In this LCA the module efficiencies are estimated, based on a 90% abs. ratio from cell to module [32], since module efficiencies have not been measured for the tandem technologies of interest.

The module area required to produce 1kWh of electricity (FU) is different for each solar module, depending on its efficiency, and it is calculated via Equation 1.

$$A = \frac{\varepsilon}{\eta.I.y.PR}$$
[1]

Where ε is the energy generated, η is the efficiency of the cell, I is the insolation, y is the lifetime (years), and PR is the performance ratio.

Insolation is the amount of solar radiation [200] received at the earth's surface per unit of horizontal surface area. For each location on the surface of the planet, an energy budget calculation is made using hourly visible radiation information, i.e. irradiances measured from a meteorological satellite [201, 202]. The values of insolation can be very different depending on the location. This LCA assumes 1700 kWh/m^2/year that is typical of southern European countries and representative of a world average in LCA studies of renewable energy [42].

PR is a value representing the degree of use of a PV system. It specifies the effect of losses on the PV system's rated output due to array temperature, incomplete utilisation of the irradiation, and system component inefficiencies or failures [200]. In other words, the PR is the relationship between the theoretical and the real performance of a PV system.

For comparison reasons we are considering China as the manufacturing location for all cells and modules studied. Coal-fired electricity generation in China, the world's largest coal consumer, accounts for more than 70% of its electricity mix (in 2018) and is expected to remain flat through 2040 [203].

3.4 Interpretation

The last step of an LCA study is interpretation in which the findings of the inventory analysis and the impact assessment are combined, consistent with the defined goal and scope, to reach conclusions and recommendations [39].

This step is essential since the key aim of an LCA is to provide decision-makers with comprehensive and understandable information. The interpretation component of the LCA should identify, quantify, check, and evaluate information derived from the assessment by analysing the results, reach conclusions, explain limitations, and provide recommendations based on the findings of the previous phases of the study [204]. The LCA data quality can be performed by using two main methods: sensitivity and uncertainty analysis [205].

3.4.1 Sensitivity analysis

Sensitivity analysis is the relative importance of an independent parameter related to the value of another (dependent variable) [206]. Often, sensitivity analysis is carried out in LCAs to test system boundaries, allocation approaches, parameter values and characterisation methods. It is a significant tool for studying the robustness of results and their sensitivity to uncertainty factors in LCA studies.

This analysis highlights the most critical parameters that determine whether data quality needs to be improved and to enhance the interpretation of results [205]. It is related to the uncertainty of data because it studies how the uncertainty of an environmental impact can be apportioned to different sources of uncertainty from the input flow, for example [207].

In this thesis the LCA presented include sensitivity analysis to evaluate different parameters depending on the technologies studied and their chlanges and uncertainties.

3.4.2 Uncertainty analysis

ISO 14040 [39] recommends LCA practitioners perform quantitative uncertainty analysis, but it is not mandatory. However, without characterising the possible

uncertainties, the reliability of the study is impaired. Uncertainties can be incomplete information, conflicting information, linguistic imprecision, variability, errors and so on [205].

LCA practitioners recognise the importance of uncertainty, and studies have addressed this issue [208, 209]. The Monte Carlo technique, for example, is used to quantify and update the LCA results. In this method, all uncertainty distributions that are defined in the flows, parameters and characterisation factors are taken into account for the simulation, which substitutes point estimates with random numbers obtained from probability density functions and then builds models of possible results [210].

In this thesis, the analysis of uncertainties is not included, but future work should include this parameter to better understand the oscillation on the results.

4 LCA of Perovskite/Si Tandem Solar Modules

The recently emerged perovskite solar cell, if implemented as part of a multi-junction tandem structure on the top of a Si solar cell, may provide a pathway for technological progress. The potential efficiency gain in the performance of the tandem designs is the primary motivation for developing perovskite/Si tandem solar cells [6] since the bandgaps of these two cells are suitable for that application.

In the PV field, the term perovskites refers mainly to a class of organic-inorganic hybrid methylammonium Pb halides ($CH_3NH_3PbX_3$). These perovskites have a direct bandgap, ranging from 1.5 to 2.2 eV [211], that covers the whole visible solar spectrum, and high optical absorption. Hence, the research in this area has been increasing and various demonstrations of two-terminal perovskite/Si tandems, which involve the fabrication of perovskite solar cells directly on a Si solar cells, have been reported [20-22].

There are published LCA studies of perovskite solar cells in a single-junction design, comparing different materials and processes (Table 15), but not for perovskite/Si tandem structures, to the best knowledge of the author, prior to this work [110]. This chapter compares the environmental impacts and the EPBT of three different designs of perovskite/Si tandem PV modules compared to Si solar modules.

Table 15: Summary of published LCA studies of perovskite solar cells in a single-junction design.

Reference	LCA Study
Espinosa et al.[153]	Perovskite solar cells manufactured by vapour and solution phase deposition processes.
Gong et al. [155]	Process 1: fluorine-doped tin oxide glass, Au cathode, and titanium dioxide. Process 2: indium tin oxide glass, Ag cathode, and zinc oxide thin film.
Serrano-Lujan et al. [154]	Tin-based and Pb-based perovskite solar cells. Material extraction and manufacturing. EoL by sensitivity analysis.
Zhang et al. [157]	Titanium dioxide nanotube-based perovskite solar cells, with laboratory-scale and upstream data.
Celik et al.[156]	Perovskite device structures using scalable manufacturing methods such as spray and co-evaporation.

4.1 Methods

This section complements the described LCA methodology (Chapter 3), including the specific information for the perovskite/Si tandem PV modules studied. The goal of this LCA is to assess the environmental impacts and the EPBT of three different designs of perovskite/Si tandem PV modules compared to Si solar modules.

The cell production is different depending on the tandem structure chosen. In this LCA three different architectures are analysed, as shown in Figure 15.

Tandem solar cells "a" and "b" (Figure 15) use the same bottom sub-cell, which is an HJS solar cell and the same perovskite cell structure for the top sub-cell, except the top electrode. Arrangement "a" uses Ag, while structure "b" uses Au as the top electrode (grid) for a "standard polarity" (p-on-n) perovskite cell. In these two cases, the perovskite cell consists of titanium dioxide (compact-TiO_2) for hole blocking and electron transport, a $CH_3NH_3PbI_3$ perovskite layer for photon absorption, Spiro-

OMeTAD for hole transport and molybdenum oxide (MoO$_3$) as a protective layer for subsequent sputter deposition of indium tin oxide (ITO) as a transparent conductive layer. For this work, the same durability for the Au and Ag devices is assumed for comparative purposes, even though lower stability has been reported for cells using Ag [212].

Sun light		
Ag · Ag · Ag	Au · Au · Au	Al · Al · Al
ITO	ITO	ITO
MoO$_3$	MoO$_3$	ZnO
Spiro-OMeTAD	Spiro-OMeTAD	PCBM
Perovskite Layer	Perovskite Layer	Perovskite Layer
TiO$_2$	TiO$_2$	PEDOT:PSS
HJS	HJS	ITO
Ag	Ag	Si (p-n junction)
		Al
a	b	c
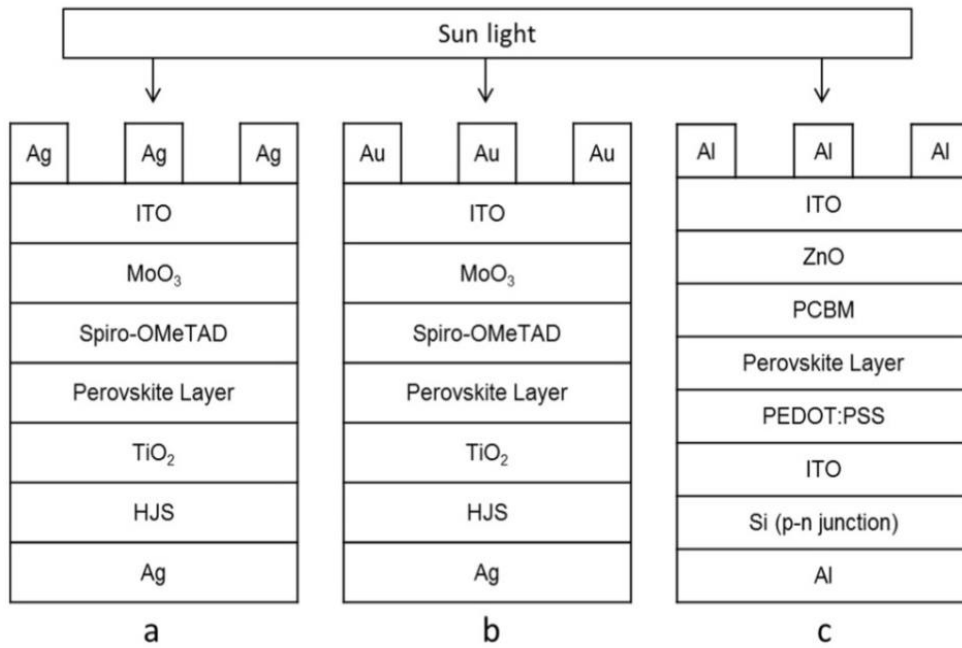
Figure 15: Different perovskite/Si tandem structures investigated.

For the HJS layer, a monocrystalline silicon wafer is assumed, with a layer of amorphous silicon on each side (deposited by PECVD) and a transparent conductive oxide (TCO), composed of indium-tin-oxide (ITO), layer on the top, deposited via sputtering. The inventory for this process sequence is public available [132].

The tandem structure "c" uses a bottom p-n junction Si solar cell (p-type substrate and n-type emitter), and a different perovskite cell structure using Al as the top electrode (grid). For the Si p-on-n junction, which remains the dominant (above 90% share)

commercial PV technology in the industry [213], this LCA assumes the multi-Si Al-BSF technology [33], because it is the current industry standard process [32]. The process sequences for perovskite/Si tandem solar cells using Ag, Au and Al is shown in Tables 16, 17 and 18, respectively.

Table 16: Process sequences for perovskite/Si solar cells (Ag for the front metal grid).

Step	Perovskite/silicon tandem Ag or Au technology	Ref.
1	Raw material purification (silica to metallurgical grade Si -MGS).	[52]
2	MGS purification into electronic grade silicon (EGS).	[52]
3	EGS conversion to boules by the Czochralski process (mono-Si).	[52]
4	Boules slicing into wafers.	[52]
5	Wafer cleaning and texturing.	[132]
6	Deposition of amorphous-Si (a-Si) layers on the front and back.	[132]
7	Deposition of TCO on the front of Si.	[132]
8	Ag onto the back side (screen printing).	[132]
9	TiO_2 deposition.	[155]
10	Perovskite layer deposition (spin coating) and heat treatment.	[214]
11	Hole selective material (spiro-MeOTAD) deposition (spin coating).	[215]
12	MoO_3 layer deposition (thermal evaporation).	[215]
13	Top ITO contact sputtering.	[215]
14	Ag (grid) deposition (evaporation) into the front side.	[215, 216]

Table 17: Process sequences for perovskite/Si solar cells (Au for the front metal grid).

Step	Perovskite/silicon tandem Ag or Au technology	Ref.
1	Raw material purification (silica to metallurgical grade Si -MGS).	[52]
2	MGS purification into electronic grade silicon (EGS).	[52]
3	EGS conversion to boules by the Czochralski process (mono-Si).	[52]
4	Boules slicing into wafers.	[52]
5	Wafer cleaning and texturing.	[132]
6	Deposition of amorphous-Si (a-Si) layers on the front and back.	[132]
7	Deposition of TCO on the front of Si.	[132]
8	Ag onto the back side (screen printing).	[132]
9	TiO_2 deposition.	[155]
10	Perovskite layer deposition (spin coating) and heat treatment.	[214]
11	Hole selective material (spiro-MeOTAD) deposition (spin coating).	[215]
12	MoO_3 layer deposition (thermal evaporation).	[215]
13	Top ITO contact sputtering.	[215]
14	Au (grid) deposition (evaporation) into the front side.	[215, 216]

Table 18: Process sequences for perovskite/Si solar cells (Al for the front metal grid).

Step	Perovskite/silicon tandem Al technology	Ref.
1	Raw material purification (silica to metallurgical grade Si -MGS).	[52]
2	MGS purification into electronic grade silicon (EGS).	[52]
3	Silicon ingot growth (casting of silicon blocks – multi-Si).	[52]
4	Slicing of ingot blocks into wafers.	[52]
5	Wafer cleaning and texturing.	[132]
6	Dielectric layer diffusion/deposition (antireflection coating).	[42]
7	Ag on the back side (screen printing), firing for contact formation.	[42]
8	Deposition of TCO on the front of Si.	[132]
9	Spin coating of PEDOT:PSS.	[214]
10	Perovskite layer deposition (spin coating) and heat treatment.	[214]
11	Application of PCBM electron transport layer (solution processing).	[214]
12	ZnO deposition.	[155]
13	Top ITO contact sputtering.	[215]
14	Al (grid) deposition (evaporation) into the front side.	[214]

From Tables 16, 17 and 18 it is important to note that these processes represent a synthesis on a laboratory scale and therefore the respective life cycle inventories generated cannot be extended to an industrial production ratio and consequently the use of these data should be careful, and the results may be irrelevant considering larger scales. Examples such as the use of Spiro-MeOTAD as an orifice transfer layer are accepted in cases of smaller (laboratory) scales, but in larger scales, it is known that this process is very expensive and unstable, therefore not realistic. New inventories and LCA studies should be further discussed when more realistic data for industrial scale are published for this technology.

The next step is the module assembly, which assumes the same encapsulation scheme and module assembly for all technologies (Si and tandem), although it is likely that a commercial thin-film perovskite module would be eventually produced slightly differently to current silicon modules [217].

As perovskite cells and, consequently, perovskite/Si tandem cells, are not yet stable, this study assumed a lifetime of one year for the perovskite layer. However, the effect of longer lifetime is explored in the sensitivity analysis, below.

The Si layer (either p-n junction or HJS) is assumed to have a lifetime of 25 years, which is the expected lifetime for PV modules replacement cycle [32].

To better understand the influence of the perovskite layer on the perovskite/Si tandem technology, this LCA considers two different scenarios that are explained in Figure 16.
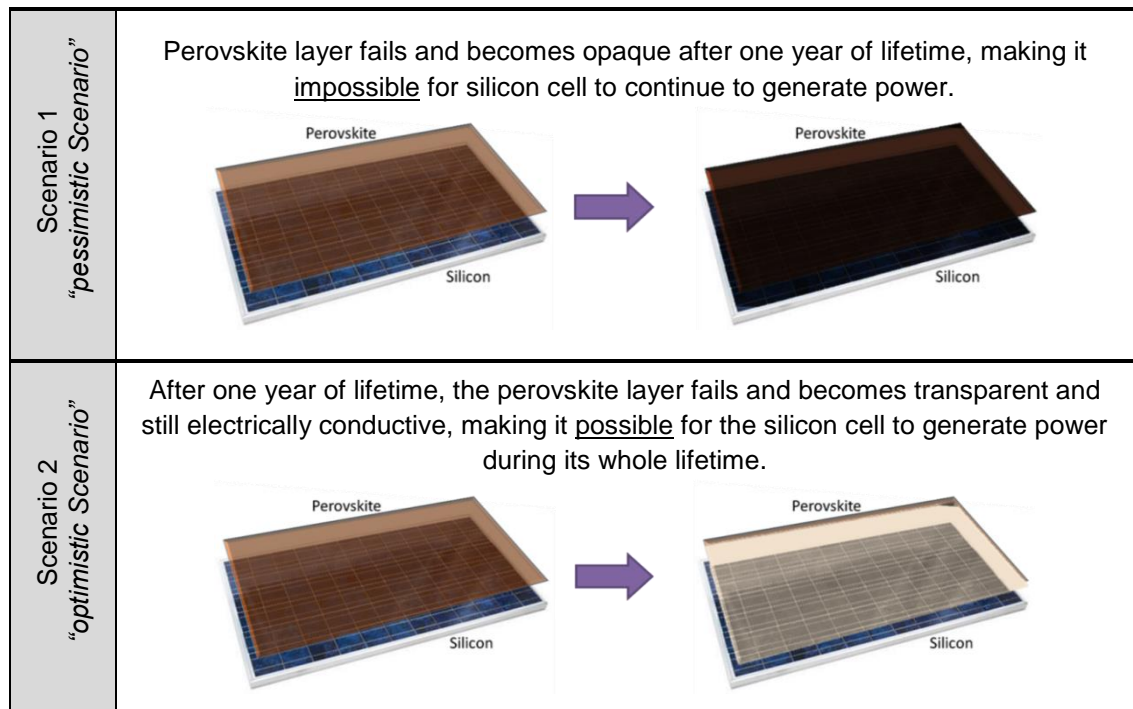
Figure 16: Scenarios considered for the perovskite layer in the perovskite/Si tandem structure.

Based on Equation 1, Tables 19 and 20 list the assumptions and the area required for each technology to produce 1kWh (FU) during the modules' lifetimes, considering Scenarios 1 and 2, respectively.

Table 19: Assumptions for Scenario 1 (Si = Silicon and PPK = Perovskite).

Parameters	Module	Si (p-n junction)	Si (HJS)	PPK(Ag)/Si Tandem	PPK(Au)/Si Tandem	PPK(Al)/Si Tandem
efficiency	-	0.18 [42]	0.20 [132]	0.27 [6, 218]	0.27 [6, 218]	0.24 [6, 219]
insolation	kWh/m^2/yr	1700	1700	1700	1700	1700
energy	kWh	1	1	1	1	1
lifetime	years	25	25	1	1	1
PR	-	0.75	0.75	0.75	0.75	0.75
area	m^2	0.174	0.154	2.93	2.93	3.30

(Scenario 1)

Table 20: Assumptions for Scenario 2 (Si = Silicon and PPK = Perovskite).

Parameters	Module	Si (p-n junction)	Si (HJS)	PPK(Ag)/Si Tandem	PPK(Au)/Si Tandem	PPK(Al)/Si Tandem
efficiency	-	0.180	0.204	0.207	0.207	0.182
insolation	kWh/m^2/yr	1700	1700	1700	1700	1700
energy	kWh	1	1	1	1	1
lifetime	years	25	25	25	25	25
PR	-	0.75	0.75	0.75	0.75	0.75
area	m^2	0.174	0.154	0.152	0.152	0.172

(Scenario 2)

The inventory for the main perovskite layers in the perovskite/Si tandem solar cells [153, 154] is presented in Appendix, including the inventory for the MoO_3 [220] (MoO_3/ITO stack) layers that need to be added in the tandem structures and the Si technologies analysed.

4.2 Results and Discussion

4.2.1 Global Warming Potential

The results for GWP are shown in Figures 17 and 18 (Scenarios 1 and 2, respectively).
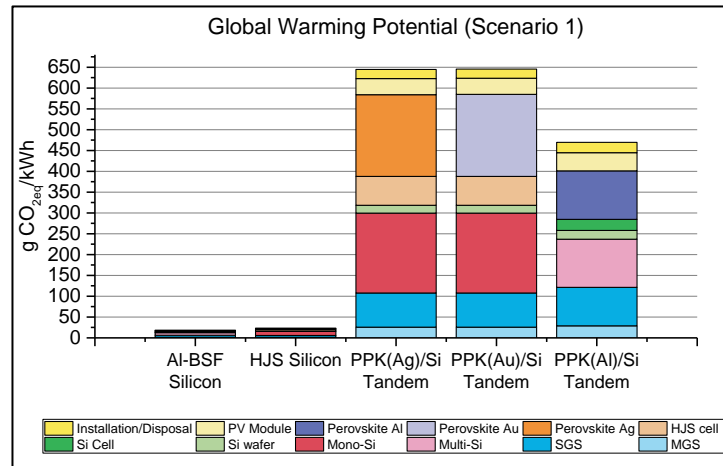
Figure 17: GWP results considering Scenario 1 (PPK = perovskite).
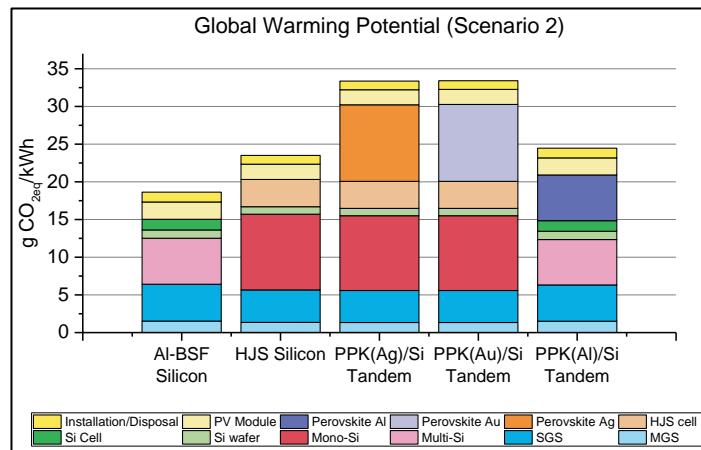
Figure 18: GWP results considering Scenario 2 (PPK = perovskite).

The comparison between Scenarios 1 and 2 indicates that the module lifetime has an important relationship with the generation of impacts in this category. The Si purification processes (for both p-n junction and HJS) demands a significant amount of primary energy, which is directly related to the GWP impact because of the generation

of GHG, considering that this energy comes primarily from coal combustion, assuming the electricity mix from China (approximately 70% coal). Fossil fuels comprise carbon and hydrogen predominantly and, when burned, oxygen combines with carbon to form CO_2 and with hydrogen to create water (H_2O). The energy produced is the result of the heat generated by these chemical reactions. The carbon content of the fuel determines the amount of CO_2 produced, and the quantity of heat created depends on its carbon and hydrogen content. Natural gas, for example, is mostly made of methane (CH_4), which has a high hydrogen content. Consequently, its combustion produces less CO_2 for the same amount of heat generated from burning other fossil fuels. Burning coal, which is the assumption made in this LCA for the reasons mentioned previously, for the same amount of energy produced, produces about twice the amount of CO_2 produced by burning gas [221]. This fact explains why the GWP impacts are predominantly related to the use of electricity.

Figure 17 (Scenario 1) considers that the tandem modules require replacement every year, and consequently, the quantity of Si used to produce the FU is much more significant (the cell area required is larger since that energy must be generated in just one year). Therefore, the impacts increase.

Comparing Figures 17 and 18 it can be seen that the impact is much lower for Scenario 2. This result is mainly due to the continuing operation of the Si layer of the tandem solar cells after the perovskite cell has failed. Additionally, comparing the two types of Si technology, it can be concluded that, for GWP, the p-n junction, without a perovskite top cell, has better environmental outcomes, mainly due to the differences between the process's steps used.

The impact from the perovskite layer is significant due to this short lifetime and is particularly serious in Scenario 1, in which the perovskite layer becomes opaque after one year. The short lifetime (in both Scenarios 1 and 2) doesn't allow a sufficiently

significant increase in the cell and module efficiency, compared with the single junction technologies, which, consequently, doesn't permit the top cell to diminish the environmental impacts significantly.

The GWP impacts from the ITO layer are a result of the massive energy consumption during its manufacturing process. A better environmental option for this layer is to replace it with FTO glass, that has much lower GWP impacts [155].

The elimination of the Spiro-OMeTAD layer, which requires a high energy consumption during its deposition process (2.76×10^{-2} kWh/cm^2), would reduce the overall GWP impacts. Options for lower GWP impacts, include replacement for the Spiro-OMeTAD layer by PEDOT:PSS (9.90×10^{-3} kWh/cm^2) or PCBM (5.00×10^{-5} kWh/cm^2) [153].

The metal grid processes also have significant GWP impacts, which are mostly due to the energy and material inputs required to process the ore (raw material) [222].

4.2.2 Human Toxicity Potential (Cancer and non-Cancer Effects)

The results for HTP-CE and for HTP-nCE, considering Scenarios 1 and 2, are shown in Figures 19-22.
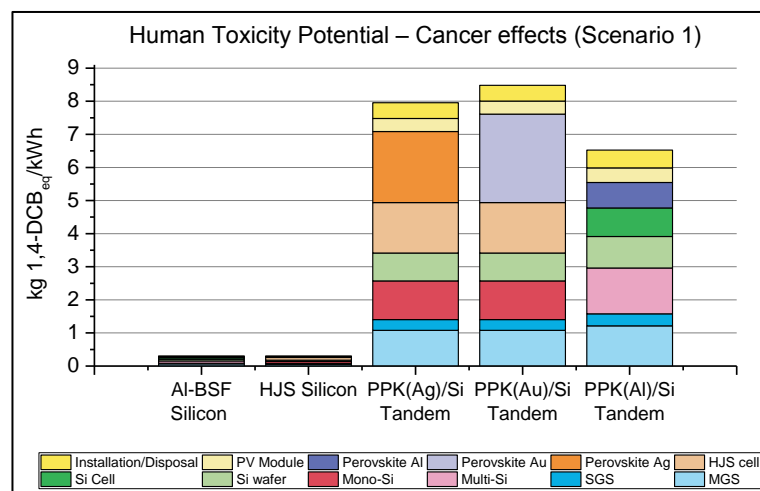
Figure 19: HTP-CE results (Scenario 1) (PPK = perovskite).
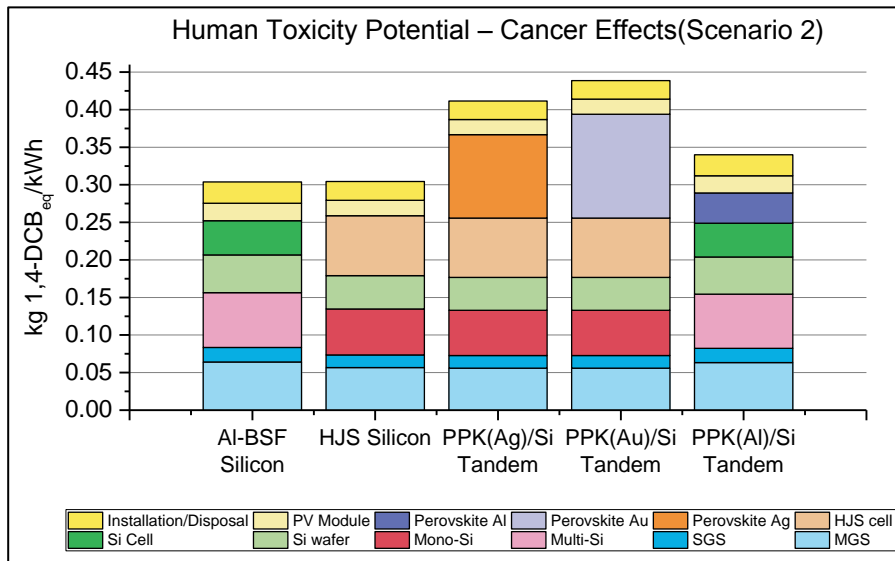
Figure 20: HTP-CE results (Scenario 2) (PPK = perovskite).
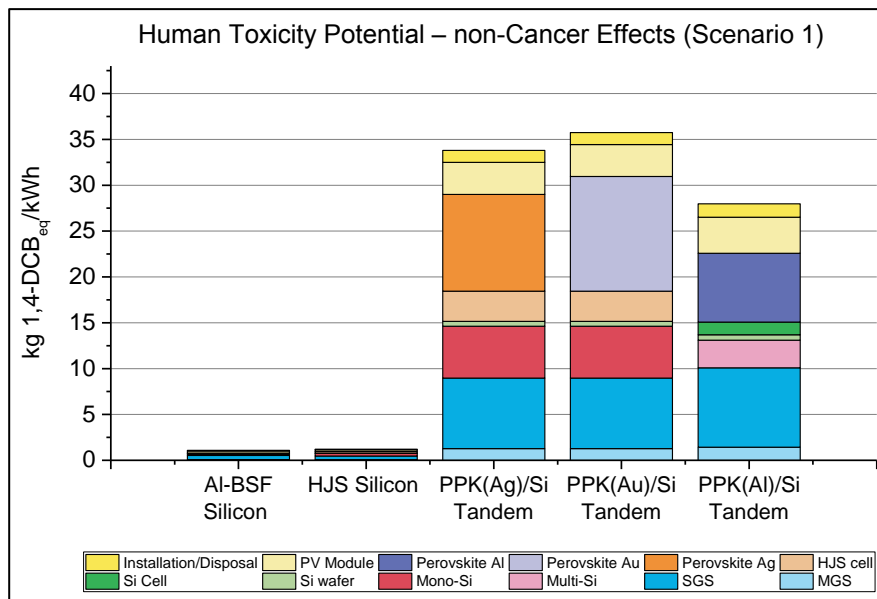
Figure 21: HTP-nCE results (Scenario 1) (PPK = perovskite).
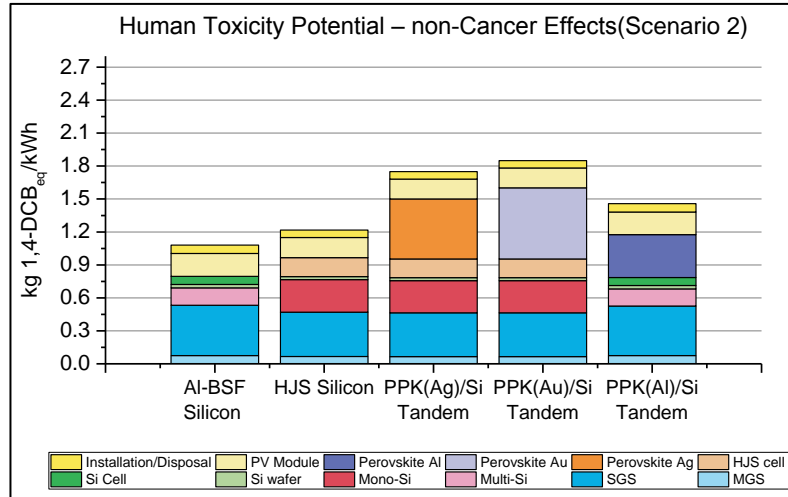
Figure 22: HTP-nCE results (Scenario 2) (PPK = perovskite).

The perovskite layer has the most significant impacts (both cancer and non-cancer effects) for the HTP category. The short lifetime of this component, similarly as for the GWP impact, is most influential in both Scenarios (1 and 2), which, again, shows the importance of research on the stability of the perovskite devices.

The HTP impacts (CE and nCE) are mainly from the perovskite absorbing layer and the spiro-OMeTAD deposition, mostly due to the use of solvents such as dimethylformamide and isopropanol (perovskite) and to the use of monochlorobenzene (spiro-OMeTAD), that are poisonous for humans [223]. Therefore, a perovskite cell structure that avoids solution processing of the hole transport layer and perovskite (possibly Pb-free [224-226]) layer might be a future structure optimised for minimum toxicity impacts. However, as mentioned, it is important to highlight that the use of Spiro-MeOTAD represents a laboratory scale procedure and is unlikely to be used in mass production due to its high cost and instability [92] and therefore the respective life cycle inventories, and consequent results generated, should be analysed with this in mind. For these results to be considered in an industrial scale production ratio, further device research, beyond the scope of this thesis, still needs to be done.

An important observation is the influence of the Au contact grid on both HTP-CE and HTP-nCE impacts, which can be seen when comparing the similar structures (perovskite/Si tandem Ag and Au). This environmental effect is related to the mining process of this material. Mercury (Hg) amalgamation for Au extraction is widespread from historical and ongoing mining practices. Examples of Hg pollution associated with Au mining have been shown in Canada, the US, Africa, China, Philippines, Siberia and South America [227]. Besides Hg, other heavy metals wastes produced from gold ore, such as Cu, Ag and Pb extraction are leached out in an uncontrolled manner into surrounding environments on exposure to water or through dispersal by wind. The presence of elevated concentrations of heavy metals in the environment is a severe issue due to their non-degradative nature, which makes them persistent and thereby exert long-term effects on the ecosystem and human health [228].

The difference between perovskite(Al)/Si and perovskite(Au)/Si tandem structures is subtle because both metals are used as a grid metal contact, so the amount of Au and Al is not very significant compared to an entire layer.

The impacts of Si (p-n and HJS) are mainly from the Si treatment processes. As already discussed, these processes require substantial amounts of electricity. The effects, in this case, are from the use of non-renewable sources of electricity, particularly for the mining process, plant operation and coal transportation [123, 229], which is the assumption for electricity usage.

The module fabrication process also has some HTP impacts. The substances that mostly contribute for this category are Pb, arsenic, and mercury, whose emissions to air are mainly generated from the electricity supply and glass production process for the modules [230]. Pb is also present in the solder, but the impacts are small compared with the use of coal-fired electricity. The disposal of these modules also has some significant impacts on human health, considering that all materials are assumed to go

to landfill. Particularly, Pb exhibits high cancer and non-cancer toxicity potential for humans [231].

The overall human toxicity impacts from perovskite(Al)/Si tandem are lower than the other perovskite/Si tandem studied, mainly because of the charge selective layer since PCBM has lower environmental impacts than Spiro-OMeTAD.

4.2.3 Freshwater Ecotoxicity Potential

The results for FEcP, considering Scenarios 1 and 2, are shown in Figures 23 and 24.
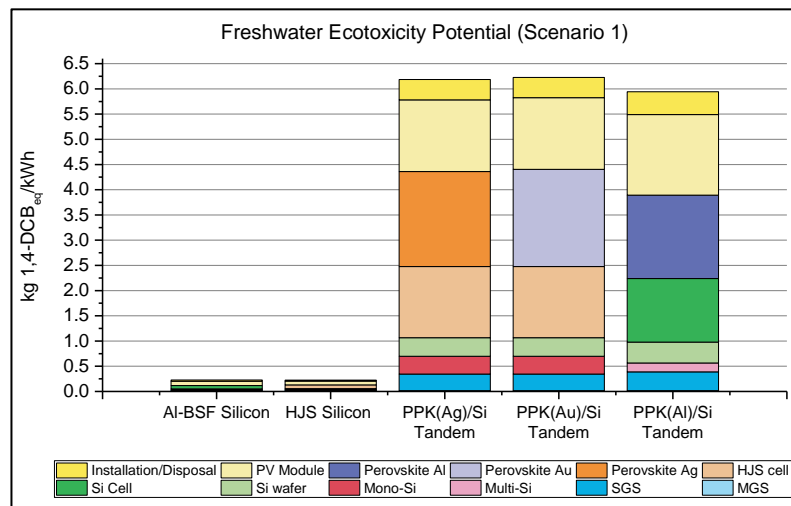
Figure 23: FEcP results (Scenario 1) (PPK = perovskite).
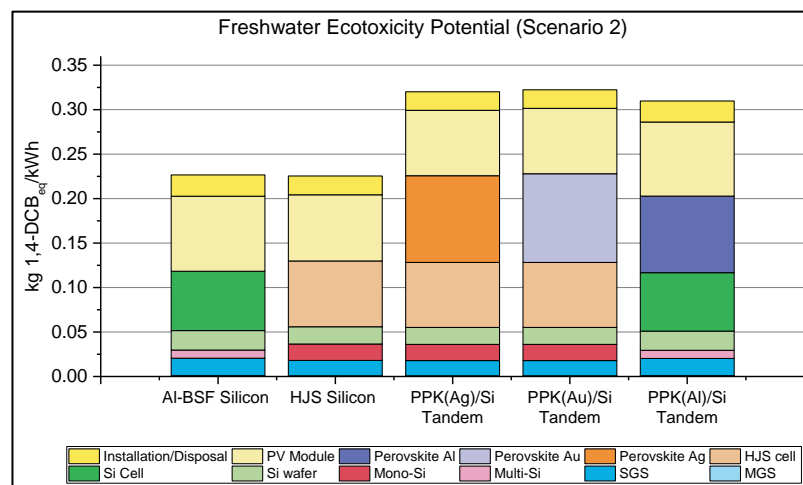
Figure 24: FEcP results (Scenario 2) (PPK = perovskite).

This category is essential due to concerns with the soluble Pb (II) salts content of the perovskite layer, which has a great FEcP contribution in the perovskite/Si tandem structures analysed. Thus, these results also further encourage research related to the Pb replacement in perovskite solar cells. Pb is a health hazard, since when inhaled (in the case of emission to air) it is stored in the bones, teeth and blood, and may damage liver, kidneys and brain affecting the health of children, unborn babies and adults [232]. The metabolism of arsenic in humans can result in the formation of dimethylarsenic acid (DMA), which is carcinogenic to mammals [233].

Strategies have been demonstrated to reduce the toxicity of Pb in perovskite technologies, such as the partial substitution of Pb by other low-toxic metal cations or completely Pb-free perovskite materials based on Sn (II), Sn (IV), Ge (II), Bi (III), Sb (III) and Cu (II) etc [234].

Besides Pb, solvents in the perovskite layer, the spiro-OMeTAD and the ITO layer also contribute to freshwater ecotoxicity. Particularly for ITO, the FEcP impact is from the emission of heavy metals (e.g. indium).

Specifically for the Au layer, the FEcP impact is due to the mining process of this metal, which includes As, Co, Cr, Hg, Zn etcetera as typical metal pollution associated with this activity, posing risks to soils, water and associated flora and fauna [235, 236]. These results motivate the development of perovskite and perovskite/Si tandem solar cells that eliminate Au.

The charge selective layer (PCBM and Spiro-MeOTAD) has an important influence in tandem structures for this category. The PCBM layer has better environmental outcomes for the FEcP category than Spiro-MeOTAD, mainly because Spiro-MeOTAD contains monochlorobenzene (solvent), which is a toxic substance. Also from the cell production and additionally from the module fabrication phases, the silver-based paste

(cells) and glass production (module) have major impacts in this category [93]. Comparing the three tandem structures, we can say that the one that has lower environmental impacts is the perovskite(Al)/Si tandem, because of the layer materials and deposition processes.

4.2.4 Freshwater Eutrophication Potential

The results for FEuP (Scenarios 1 and 2) are shown in Figures 25 and 26, respectively.
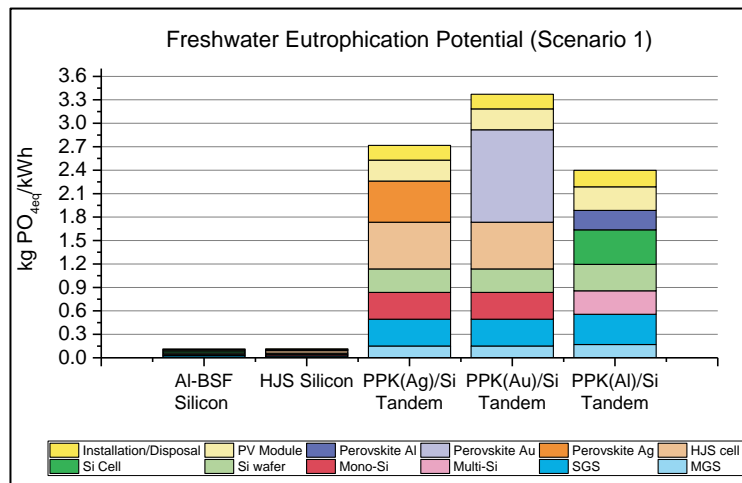
Figure 25: FEuP results (Scenario 1) (PPK = perovskite).
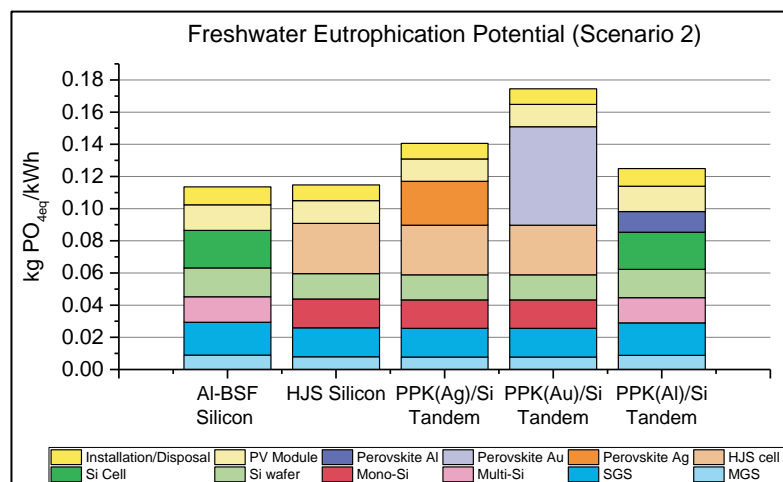
Figure 26: FEuP results (Scenario 2) (PPK = perovskite).

The perovskite layer contributes significantly to freshwater eutrophication because of the use of organic compounds (e.g., methylammonium iodide), which represent approximately 29% in perovskite/Si tandem Ag, 26% in perovskite/Si tandem Au and 57% in perovskite/Si tandem Al [110].

The bottom layers (Si p-n junction and HJS) of the three tandem structures have a significant influence on the FEuP impacts, mainly due to the emissions to air and freshwater, including nitrogen oxides, phosphate and nitrate during the silicon treatment and cell manufacturing processes. In the module production stage, encapsulant, backsheets and Al frame are the main contributors to this impact category because phosphate and nitrogen oxides are emitted during their production and life cycle.

4.2.5 Abiotic Depletion Potential

The ADP results (Scenarios 1 and 2) are shown in Figures 27 and 28, respectively.
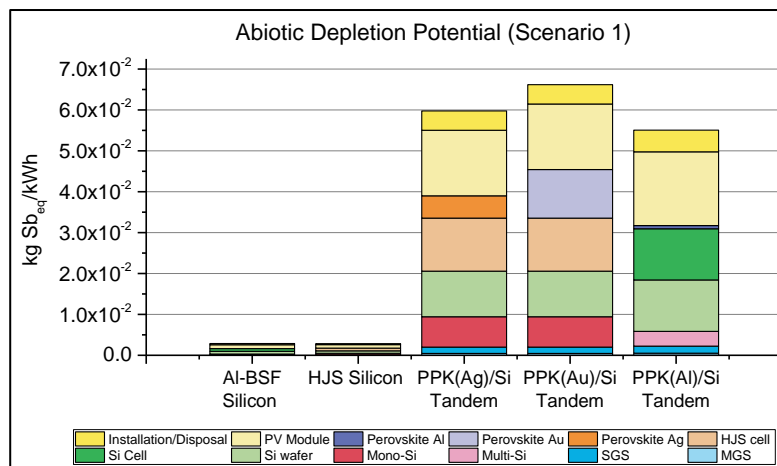
Figure 27: ADP results (Scenario 1) (PPK = perovskite).
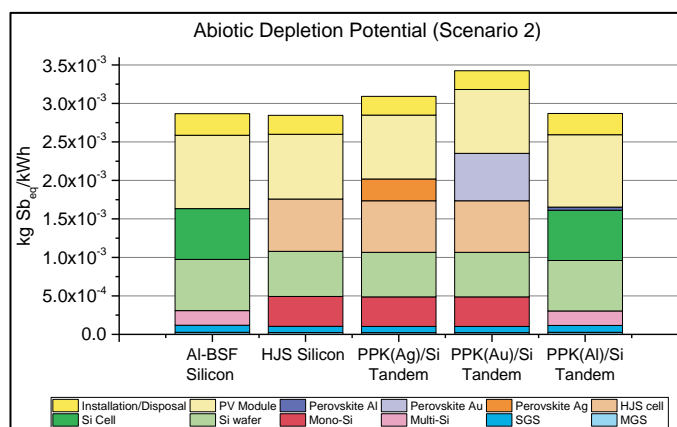
Figure 28: ADP results (Scenario 2) (PPK = perovskite).

Perovskite/Si tandems that use precious and scarcer metals than Al, such as Ag and Au, as the front contacts have higher ADP impacts than the tandem that uses Al. The Ag and Au layers represent 58 and 45% of the total ADP contributions in the tandem structures that use them, which is associated with their extraction processes – extraction from the ore and purification [153]. Particularly, the mining process of Au has a high environmental impact, especially for open-pit mining. Regardless of the method, metal extraction and refining stages impact on land use drastically [237].

The impacts from the modules are related to the use of metals such as Al, Ag, copper, chromium and nickel and also due to the burning of fossil fuels for primary energy (electricity) generation during manufacturing.

With this in mind, it is essential to develop future processes for recycling of these materials for reduced environmental impacts, including for ADP [238]. The ecological outcomes from the treatment of secondary (recycled raw materials) metals are much lower than in primary production [239].

The use of metals such as copper (tabbing material) and Ag in the cells and Al in the module production phase creates higher impacts compared with other materials (for all structures studied in this LCA). Specific Ag consumption is expected to be decreased by development of advanced processes and/or replacement with other metals [32].

4.2.6 Energy Payback Time

The EPBT results are shown in Table 21. These results are in acceptable agreement with those presented in the literature (Chapter 2) [156].

Table 21: Energy payback time (EPBT) for all structures studied.

Technology	Al-BSF Si	HJS Si	PPK(Ag)/Si	PPK(Au)/Si	PPK(Al)/Si
EPBT (years)	1.56	1.6	1.33	1.33	1.14

The EPBT of perovskite/Si tandem solar cells is better, compared to the respective Si cells, mainly because the efficiency of perovskite/Si tandem solar cells/modules is assumed to be higher than Si (either p-n junction or HJS) and most of the invested energy is recovered before the perovskite cell faults. These results are similar to other published EPBT analysis of PPK/Si tandem solar cells [162], some assumptions are a bit different, however they have a small impact in the final results.

The EPBT is related only with the energy use and production, and not consider the environmental impacts from the GHG emissions. Because of that, the EPBT results differ from the GWP impacts.

The steps that dominate the input energy are the SGS manufacturing process, thin-film deposition (PECVD a-Si in HJS) and TCO sputtering (HJS). Designs that replace or optimise these processes or that improve the energy conversion efficiency will improve the EPBT. It should be noted that the EPBT for the tandem structures exceeds the assumed life for perovskite top cell.

Studies about the impact of recycling of solar modules are showing that this process can improve the EPBT of several PV technologies [240]. The development of recycling processes can affect all the technologies studied in this work, and consequently generate better environmental outcomes for these solar devices.

4.2.7 Endpoint (ReCiPe) Impacts

As discussed previously, converting midpoints to endpoints simplifies the interpretation of the LCA results. However, with each aggregation step, uncertainty in the results increases so the interpretation of these results needs to be meticulous. The endpoint impacts for Si and perovskite/Si tandem solar modules are presented in Figures 29 and 30, considering Scenario 1 and Scenario 2, respectively.
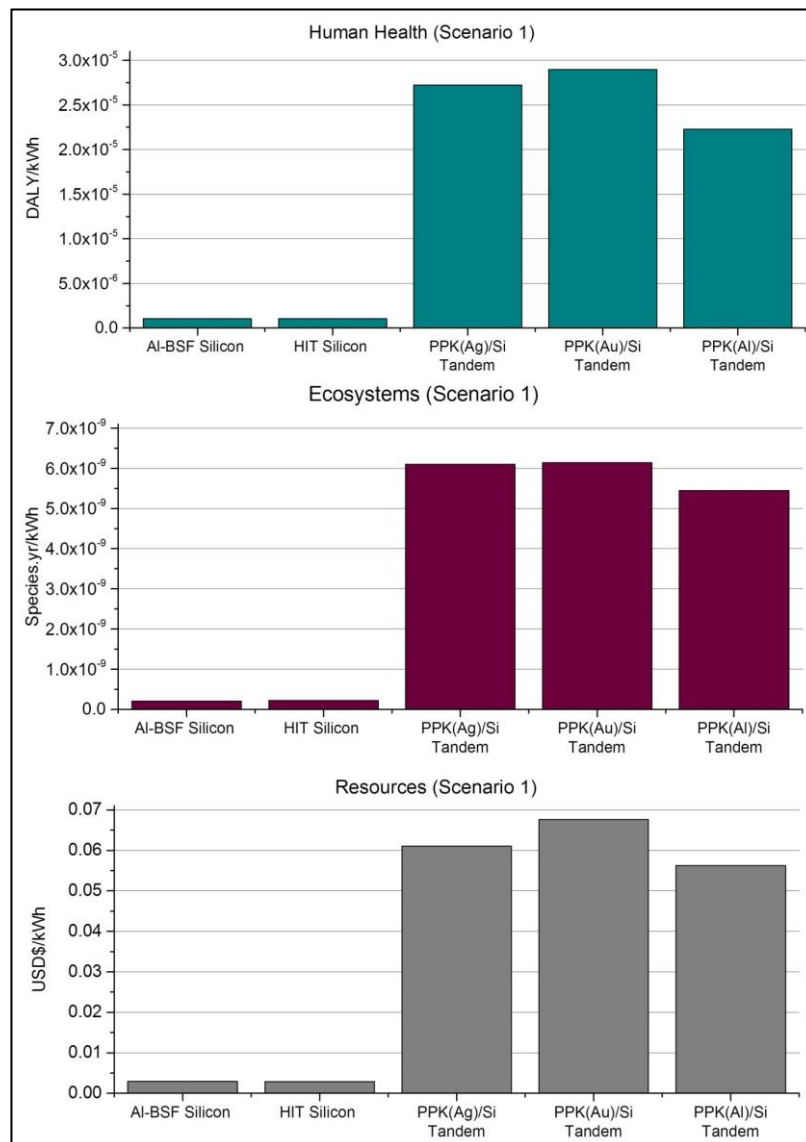
Figure 29: ReCiPe results for Scenario 1.
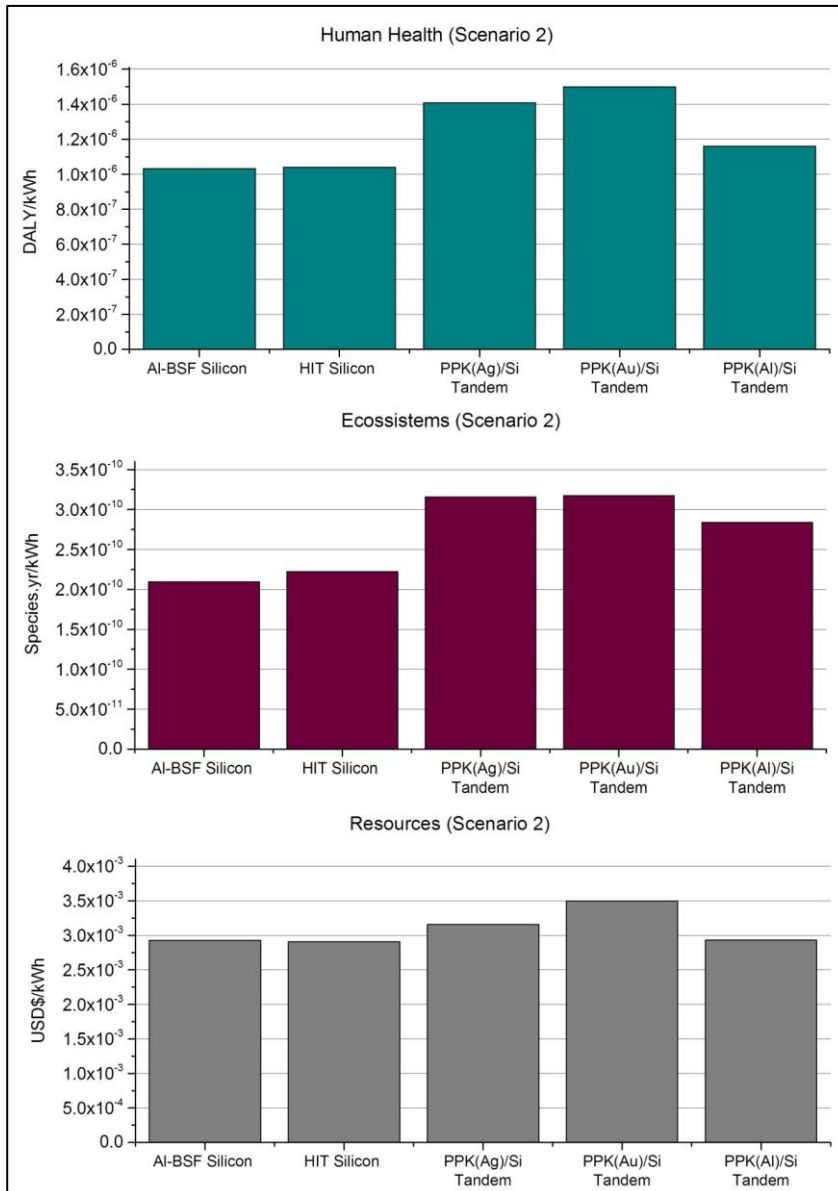
Figure 30: ReCiPe results for Scenario 2.

The comparison of the three ReCiPe indicators for Scenario 1 shows that the environmental impacts produced from the tandem structures studied are much worse than those from Si (both p-n junction and HJS). Also, it is again observed that the perovskite that uses Ag as the metal grid has higher ecological effects, mainly for human health and resources depletion. This impact covers several types of human health problems, such as respiratory issues, cancer potential, etc.

Considering Scenario 2, it can be observed that for all three ReCiPe indicators the environmental impacts produced from the perovskite/Si tandem solar modules are still worse when compared with Si (both p-n junction and HJS). As discussed in the interpretation of the midpoint impacts assessment (sub-chapters 4.2.1 to 4.2.5), the perovskite cell's lifetime has a significant influence on the environmental impacts. It can be stated that considering the assumptions made in this LCA, regarding efficiency and the possibility of having a "dead" transparent perovskite cell, it is incredibly essential for the reduction of the environmental impacts to have a combination of these two factors. These results confirm the importance of a longer lifetime and EoL transparency for the perovskite layer.

Besides transparency, the efficiency also has an important influence on the overall environmental impacts of the tandem solar modules analysed. The longest the top layer (perovskite) can last, the longest the high efficiency will be considered and, consequently, the environmental impacts decrease if compared with the lower efficiency of having just the bottom layer (Si) working. In order to estimate the lifetime for the perovskite layer required to be able to produce a tandem solar cell that can have lower environmental impacts than Si (p-n junction and HJS), we performed a sensitivity analysis predicting the overall impacts from the tandem structures and comparing with both Si technologies studied.

4.3 Sensitivity analysis

A sensitivity analysis determines how different values of an independent variable affect a dependent variable under a given set of assumptions.

Figures 31 and 32 present the sensitivity analysis for the perovskite/Si structures analysed considering Scenarios 1 and 2 respectively. These results are based in a perovskite layer lifetime of 1, 5, 10, 15, 20 and 25 years.
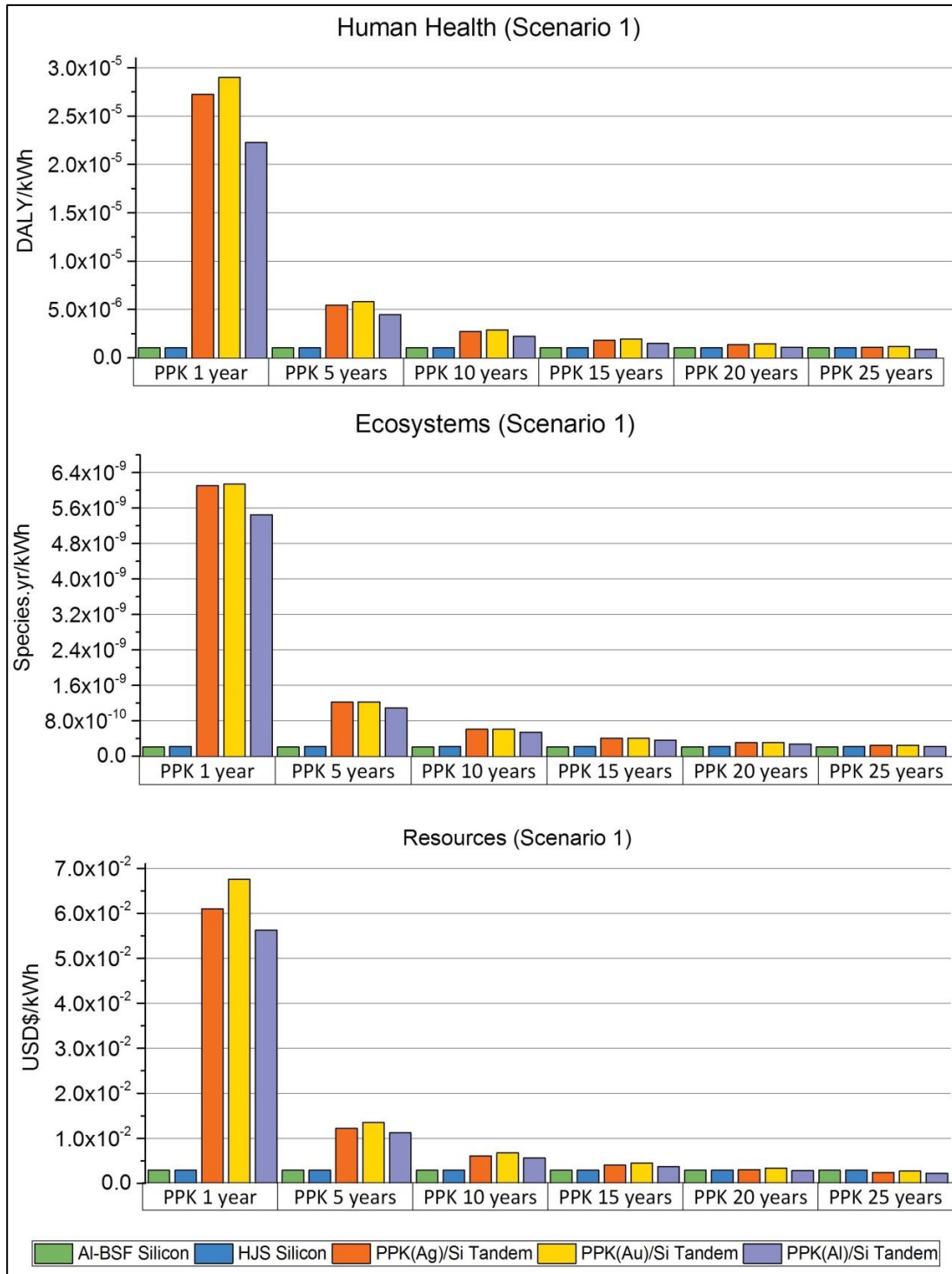
Figure 31: Sensitivity analysis of perovskite(Ag, Au and Al)/Si tandem devices considering Scenario 1 (the perovskite cell is assumed to become opaque and non-electrically conductive at the end of its lifetime, not allowing the Si cell to continue to operate for the rest of its lifetime). PPK = perovskite.
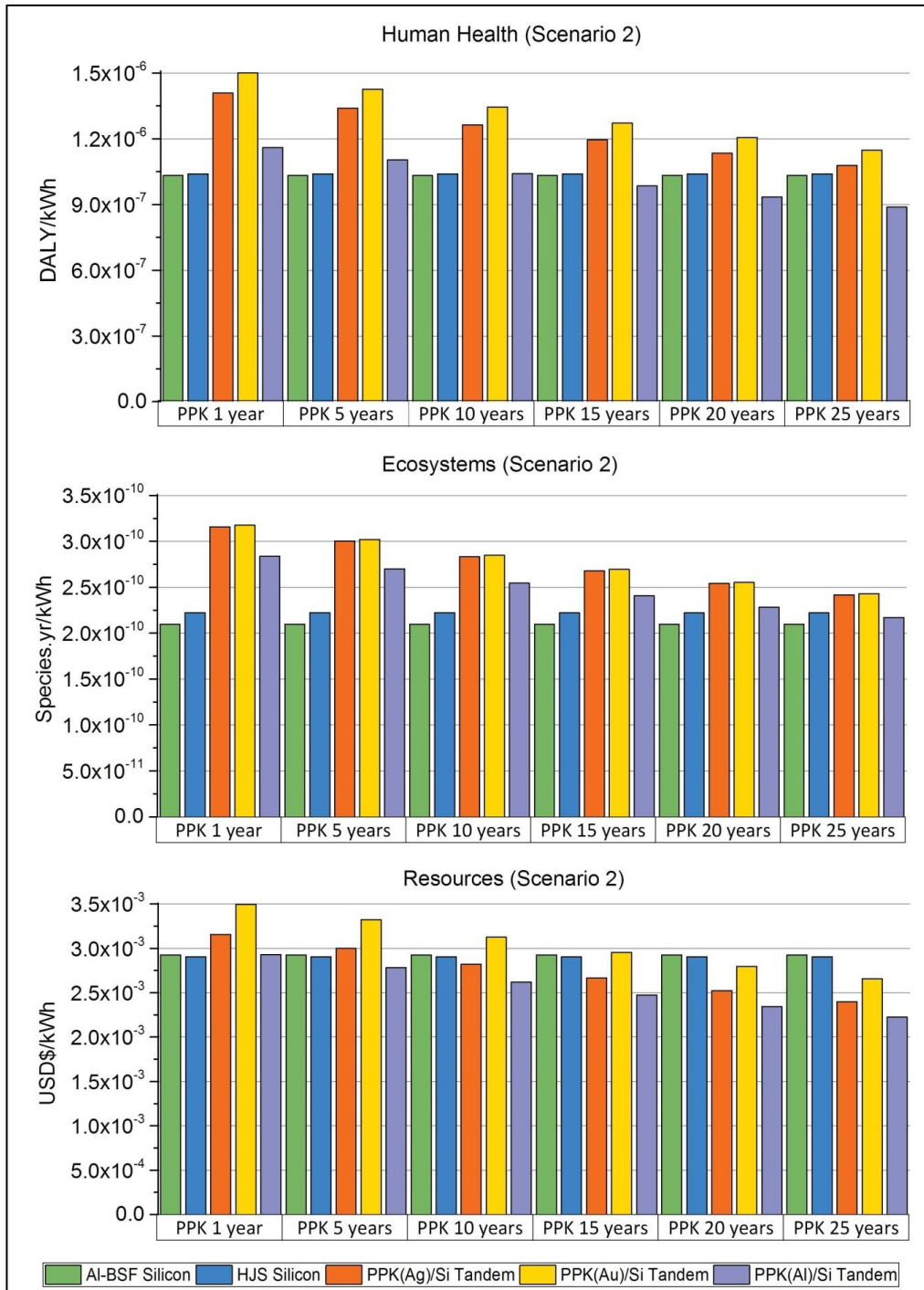
Figure 32: Sensitivity analysis of perovskite(Ag, Au and Al)/Si tandem devices considering Scenario 2 (the perovskite cell is assumed to become transparent and electrically conductive at the end of its lifetime, allowing the Si cell to continue to operate for the rest of its lifetime). PPK = perovskite.

The influence of the perovskite lifetime on the environmental impacts of perovskite/Si tandem solar modules is evident. The results confirm that the longer lifetime of the perovskite layer results in better environmental outcomes for both Scenarios (1 and 2).

Considering Scenario 1 (Figure 31) it can be observed that for human health and ecosystems the perovskite layer, even if it could reach a lifetime of 25 years, the impacts are still slightly worse than both types of Si studied. For resource depletion, the tandem structures need to reach at least 25 years to be able to produce equal or lower environmental impacts compared with Si (p-n junction and HJS).

Scenario 2 presents different results, which is expected due to the assumptions made (transparency and conductivity of the perovskite layer).

Considering human health, the perovskite(Al)/Si can match the impacts with Si (both p-n junction and HJS) if the perovskite layer can achieve 10 years or more lifetime. However, for the other two perovskites/Si structures (using Ag and Au as the metal grid) the impacts continue to be higher than Si single junction even if the perovskite layer reaches 25 years of lifetime.

For ecosystems, even if the perovskite layer reaches 25 years of a lifetime, the impacts are still higher than from Si p-n junction modules. The perovskite(Al)/Si tandem can compete with Si HJS, regarding endpoint ecosystems impacts, if the perovskite layer reaches a lifetime of 25 years.

Finally, considering resources depletion, both perovskite/Si using Ag and Al as the metal grid can achieve lower environmental impacts if the perovskite layer reaches a lifetime of 10 years compared with both types of Si. For perovskite(Au)/Si the lifetime to be achieved would be around 20, for the environmental impacts to be lower than for Si (p-n junction and HJS).

5 LCA of Chalcogenide/Si Tandem Solar Modules

Chalcogenide is a family of thin-film PV materials, with similar crystal structure, that includes compounds such as CdTe, CIS, CIGS and CZTS [241]. The bandgap of CdTe solar cells makes them not suitable for Si tandem structures [72].

CIGS is a semiconductor with very high optical absorption coefficient because it is a direct band gap material. Its band gap can be tuned between 1.0 and 2.4 eV by varying the In/Ga and Se/S ratios [15]. Best cell efficiency of approximately 15.7 ± 0.5 % has been achieved for high bandgap [28]. The possibility of a high band gap makes CIGS an attractive material in tandem solar cells [15]. Because of the progress in this technology, CIGS is already in production, as single material modules, with a small market share [242].

CZTS (kesterite) is very similar to CIGS in optoelectronic and crystallographic properties, as well as in methods of fabrication but it doesn't use indium, which is a scarce metal and an essential challenge for the CIGS technology [23]. Nevertheless, researchers are showing that CZTS is the most promising current alternative to CIGS [24] and CZTS/Si tandem cells are expected to be of increasing interest. The first step was to demonstrate CZTS epitaxy on Si, which has already been confirmed [25-27].

Recently, modifications of CZTS have been proposed where either Zn or Cu is replaced by other elements in order to produce higher band gaps [29]. One example is AZTS, wherein Ag replaces Cu [30]. The possibility of high bandgaps, where AZTS can achieve a direct band gap of 2.0 eV [31], makes AZTS/Si tandem solar cells an interesting possibility.

This chapter compares the environmental impacts and the EPBT of CIGS/Si, CZTS/Si and AZTS/Si tandem solar modules, compared with Si technologies. Up to this work

[161], LCA has not been reported for the chosen tandem solar modules, to the best of the authors' knowledge.

5.1 Methods

The LCA methodology is described in Chapter 3. This section complements the general description with detailed data for the chalcogenide/Si tandem PV modules analysed, assuming that these tandem solar cells have an ideal tunnel junction and neither electrical resistance nor optical loss at the interface between the top and bottom cells.

This LCA assumes an adjustment of the chalcogenide layers' thickness, which affects the quantities of materials, of the top cells to match the currents generated in each sub-cell of a tandem structure. 1µm is assumed for high bandgap CIGS, which is thinner than the normal absorber layer (i.e. 2 µm) [243]. For CZTS the first tandem experiments are focusing on demonstration of CZTS epitaxy on Si [25-27]. Based on these experiments a thickness of 0.5 µm is assumed in this analysis, which is approximately half of the normal absorber layer (i.e. 1 µm) for CZTS.

A thickness of 0.5 µm is also assumed for AZTS for an appropriate comparison in relation to environmental impacts. Besides that, for this technology it is shown that the use of a CdS buffer layer leads to device efficiencies less than 0.5%. This is why we are assuming that an alternative stack with a FTO and MoO_3 buffer layers, which can deliver a higher efficiency for this cell, is implemented [30]. HJS silicon is assumed as the bottom cell in this case [244]. The processes for the Si cells (p-n juntion and HJS) and modules are the same as assumed for the perovskite/Si LCA.

The architectures assessed are shown in Figure 33, where "a" represents CIGS on top of Si (p-n junction), "b" CZTS on top of Si (p-n junction) and "c" AZTS on top of Si (HJS) tandem solar cell structures.
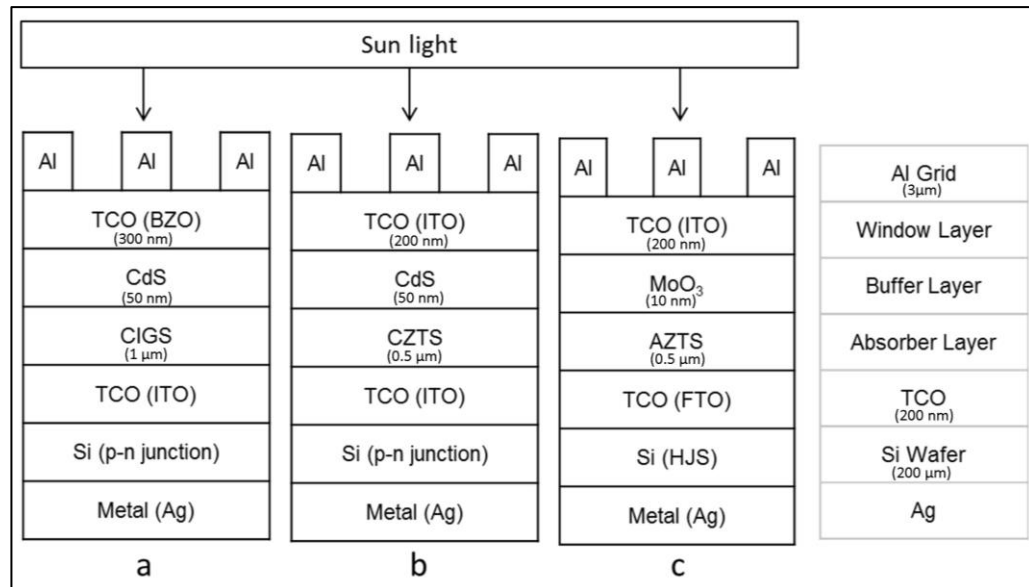
Figure 33: Different chalcogenide/Si tandem structures investigated (TCO = Transparent conductive layer, BZO = boron-doped tin oxide, ITO = indium tin oxide, FTO = fluorine-doped tin oxide, CdS - cadmium sulfide, MoO$_3$ = molybdenum oxide).

The lifetime, efficiencies and respective areas required to produce 1kWh of energy (FU) considered in this LCA are shown in Table 22.

Table 22: Parameters used for the structures studied.

Parameters \ Module		Si (p-n junction)	Si (HJS)	CIGS/Si Tandem	CZTS/Si Tandem	AZTS/Si Tandem
Efficiency	-	0.18 [42]	0.20 [132]	22* [245]	22* [245]	22* [245]
Insolation	kWh/m^2/yr	1700	1700	1700	1700	1700
Energy	kWh	1	1	1	1	1
Lifetime	years	25	25	25	25	25
PR	-	0.75	0.75	0.75	0.75	0.75
Area	m^2	0.17	0.15	0.14	0.14	0.14
*Assuming the same efficiency for comparison purposes.						

The inventory for the main chalcogenide layers in the tandem solar cells collected from the literature [153, 246] and from personal communications with researchers based at UNSW laboratories [247]. The complete inventory for the structures studied is presented in Appendix.

5.2 Results and Discussion

5.2.1 Global Warming Potential

The results for GWP impacts are shown in Figure 34.
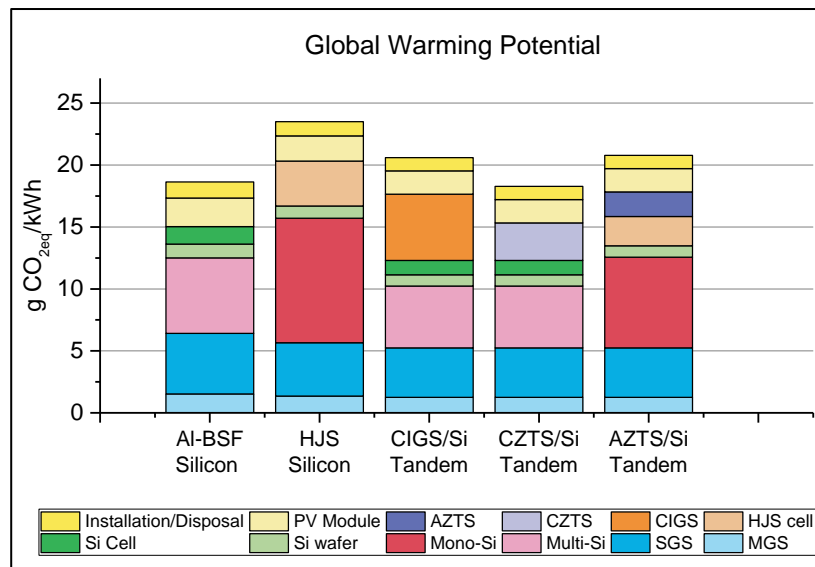
Figure 34: GWP (gCO$_{2eq}$/kWh) results for CIGS/Si, CZTS/Si and AZTS/Si tandem solar modules.

It can be seen that the most significant impact comes from the Si treatment processes, in particular, the production of SGS, multi-Si (p-n junction Si) and mono-Si (HJS), as already discussed in the LCA of perovskite/Si solar modules (Chapter 4), mercury emissions from the coal smoke are the main source of anthropogenic discharge and mercury pollution in atmosphere [248]

The GWP results also show some significant impacts from the top layers of the tandem solar cells studied. The production processes of CIGS, CZTS and AZTS are similar, however, as we are considering different thicknesses, the consumption of energy is higher for CIGS and, consequently, the GWP impacts are worse than for the other tandems studied.

Comparing with Si, the GWP impacts from CZTS/Si and AZTS/Si tandem structures are lower (p-n junction for CZTS/Si and HJS for AZTS/Si). However, the CIGS/Si tandem structure has worse impacts compared with both Si technologies studied. Electricity usage is the main contributor for this impact.

5.2.2 Human Toxicity Potential (Cancer and non-Cancer Effects)

The results for HTP-CE and HTP-nCE are shown in Figures 35 and 36, respectively.
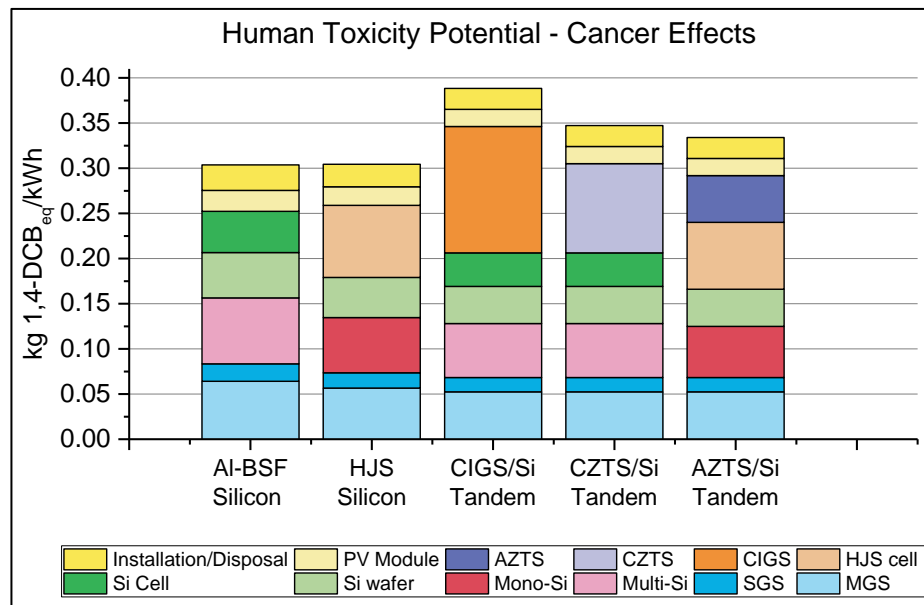
Figure 35: HTP-CE (kg 1,4-DCB$_{eq}$/kWh) results for CIGS/Si, CZTS/Si and AZTS/Si tandem solar modules.
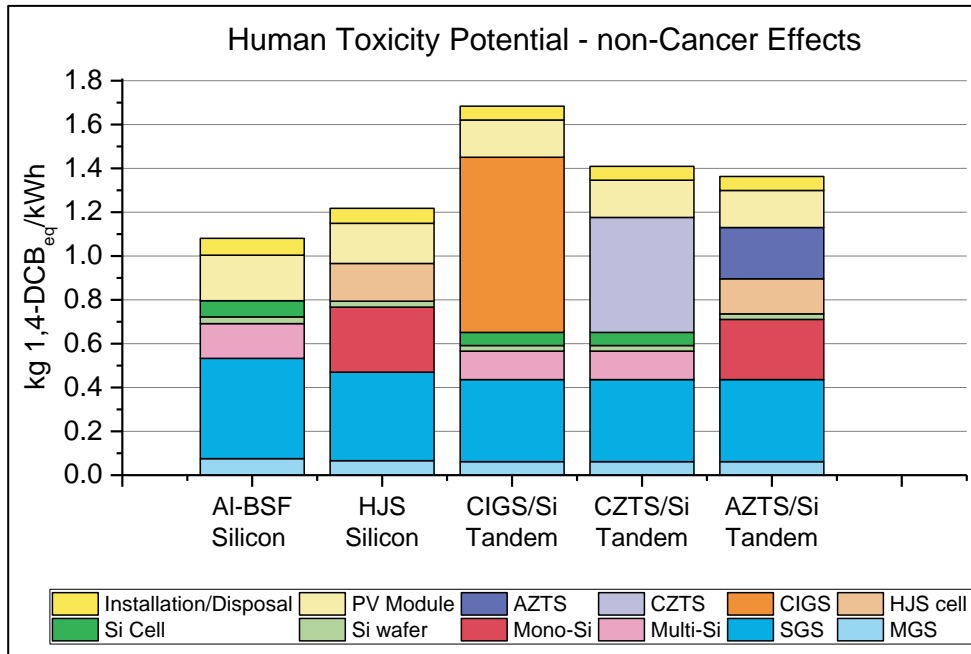
Figure 36: HTP-nCE (kg 1,4-DCB$_{eq}$/kWh) results for CIGS/Si, CZTS/Si and AZTS/Si tandem solar modules.

It can be observed that the impacts come predominantly from the same layers for both cancer and non-cancer effects and that the main contributor to these impacts is the Si production (SGS), similarly to the results of perovskite/Si tandem modules (chapter 4).

The impacts from the chalcogenide layers are also significant, particularly for CIGS. In the case of CIGS, the results come predominantly from the buffer layer (CdS), because of the presence of cadmium (Cd). There are three possible ways of cadmium absorption by humans: gastrointestinal, pulmonary and dermal [249]. Kidney damage has long since been described to be the main problem for patients chronically exposed to cadmium [250]. The respiratory system is affected severely by the inhalation of cadmium-contaminated air [251] and long-term occupational exposure to Cd may contribute to the development of lung cancer and high Cd exposure may induce kidney and bone damage [252, 253].

The use of indium and gallium in the CIGS layer also produce a significant environmental impact for human toxicity. Indium lung disease is recognised as a potentially fatal disease caused by the inhalation of indium-containing particles. Increased exposure has been linked with increased indium concentrations in blood serum or plasma, which has been linked with poor health outcomes [254-256]. Gallium exposure is growing, especially in occupational settings, and environmental exposure may be of concern near industries such as mining and smelting, coal combustion, and semiconductor manufacture [257].

5.2.3 Freshwater Ecotoxicity Potential

The results for FEcP are shown in Figure 37.
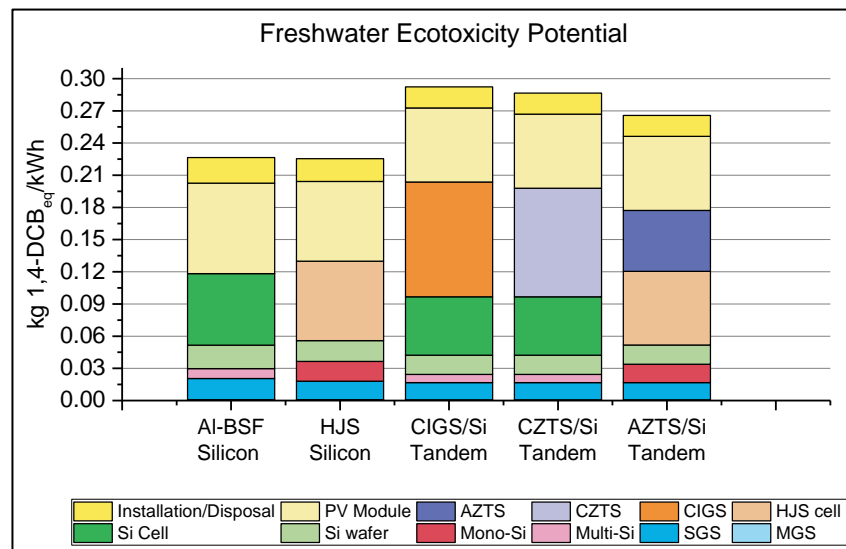
Figure 37: FEcP (kg 1,4-DCB$_{eq}$/kWh) results for CIGS/Si, CZTS/Si and AZTS/Si tandem solar modules.

In the case of CIGS and CZTS the toxic potential of Cd, from the CdS layer, raises environmental concerns. Cd induces apoptosis (i.e. a process of cell death that occurs in multicellular organisms) [258] and causes developmental deformities in fish [259].

Because of that, the CdS layer has a significant contribution to this impact category. The use of melamine-urea-formaldehyde in the CdS layer also contributes to local formaldehyde emissions, causing toxicity to freshwater [260].

The use of copper and indium in the CIGS layer, when in excess, can affect fish behaviour, causing stress and risking their lives [261, 262], increasing the FEcP impacts.

The most significant FEcP impacts, however, come from the SGS production processes, and the reasons were discussed in Chapter 4.

5.2.4 Freshwater Eutrophication Potential

The results for FEuP are shown in Figure 38.
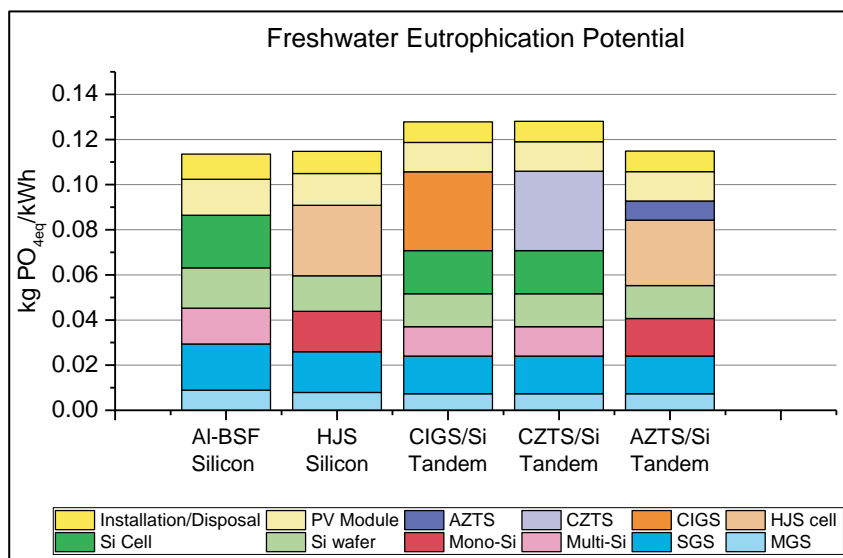
Figure 38: FEuP (kg PO$_{4eq}$/kWh) results for CIGS/Si, CZTS/Si and AZTS/Si tandem solar modules.

The FEuP impacts from the Si layers were presented in Chapter 4, but another important impact comes from the chemical bath deposition of CdS. This is because this

process uses ammonia, which is very toxic for aquatic organisms. Oxygen depletion and high ammonia concentrations under hypereutrophic conditions can lead to decreases in fish numbers as eutrophication rises [263-265].

5.2.5 Abiotic Depletion Potential

Figure 39 shows the ADP impacts for the processes studied in this LCA. It should be noted that primary energy consumption and abiotic resource depletion are highly related [266]. The use of electricity from non-renewable sources and metals in all the steps of these processes are the main reasons for these impact results.
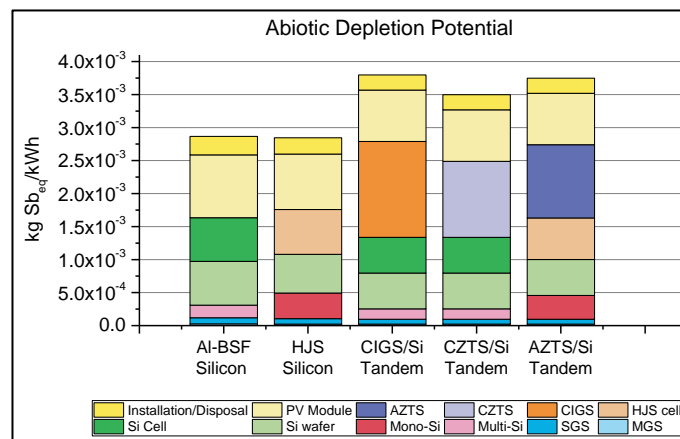
Figure 39: ADP (kg Sb$_{eq}$/kWh) results for CIGS/Si, CZTS/Si and AZTS/Si tandem solar modules.

The top cells (CIGS, CZTS and AZTS) have significant impacts in this category because of the depletion of scarce metals [267] , explained in Chapter 3.

In this context, the importance of the development of recycling processes for materials used in these cells is evident. It is not just environmentally beneficial to recycle these materials, but there is also a high-value recycling approach of some metals and other

materials used in PV modules. Besides the potentially harmful substances (e.g. Pb, cadmium, and selenium) that should be removed and contained during treatment, there are also rare materials (e.g. silver, tellurium, and indium) and materials with high embedded energy value (e.g. silicon, glass) that can be recovered and made available for future use through an efficient recycling process [268].

5.2.6 Energy Payback Time

The EPBT is calculated considering the efficiencies and lifetimes shown in Table 22. The results for the tandem technologies studied in this LCA are shown in Table 23.

Table 23: Energy Payback Time (EPBT) for the technologies studied in this LCA.

Technology	Al-BSF Si	HJS Si	CIGS/Si	CZTS/Si	AZTS/Si
EPBT (years)	1.56	1.6	1.4	1.29	1.39

The EPBT of chalcogenide/Si tandem solar cells are better than Si (p-n and HJS), which is in accordance with similar studies [105, 269]. The main reason for that result is because the efficiency of the tandem technologies is assumed to be higher than the efficiency of Si.

The process that dominates the input energy is the SGS manufacturing process. Designs that replace or optimise these processes or that improve the energy conversion efficiency will improve the EPBT. Besides, it has been shown that the impact of recycling of solar modules can improve the EPBT of several PV technologies [240].

As already explained in Chapter 4, the EPBT accounts for the energy use and production and not for the GHG emissions, therefore, they are different than GWP impacts.

5.3 Endpoint (ReCiPe) Impacts

The endpoint impacts, based on the ReCiPe method, for Si (p-n junction and HJS) and chalcogenide/Si tandem solar modules are presented in Figure 40.
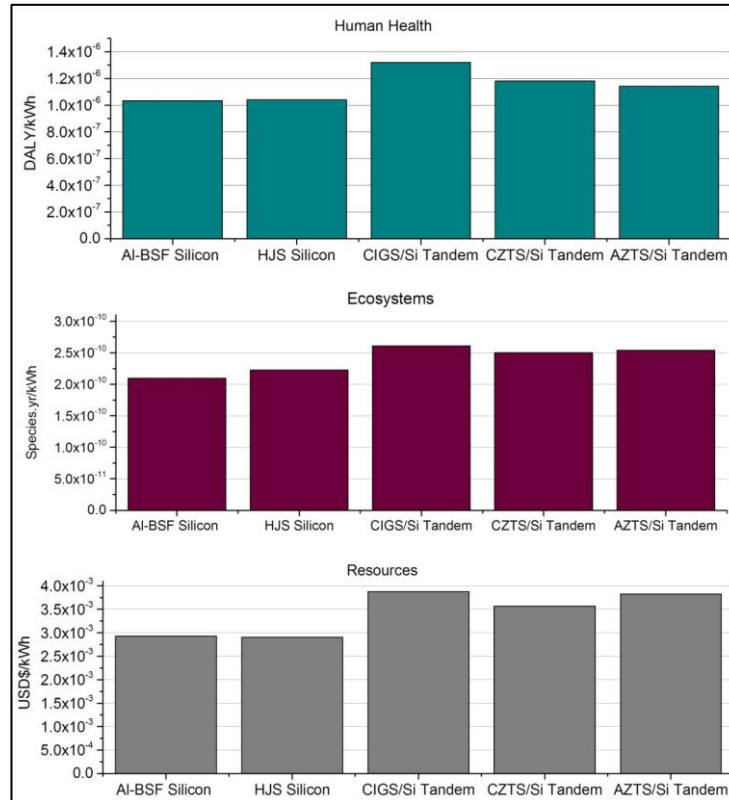
Figure 40: ReCiPe results for Si (p-n junction and HJS) and chalcogenide/Si tandem solar modules.

The ReCiPe indicators show that the environmental impacts produced from the tandem structures studied are slightly worse than those from Si (p-n junction and HJS). It is essential to highlight that these relative impacts might change considering different assumptions because the difference between the Si and tandem modules is not substantial and the input data for the thin films are less reliable for potential future mass production processes.

Also, it confirms that the CIGS/Si tandem solar modules have greater ecological effects, especially for human health and resources depletion. As discussed, the production processes of the top layers (CIGS, CZTS and AZTS) are comparable, but, the different thicknesses assumed in this LCA and the consequential dissimilar consumption of energy (a thicker layer needs more energy to be made) influence in the three endpoint impacts. As the ReCiPe method incorporated midpoint impacts such as GWP, the energy consumption influences the most in the overall endpoint impact assessment.

5.4 Sensitivity analysis

The stability of the tandem structures has been revealed to have a direct and important relationship with the environmental impacts (Chapter 4). When proposing new PV technologies, it is essential to look at the long-term outdoor stability of the modules, to be part of the existing PV market, since the consumer expects high performance from the solar modules in order to justify the investment [270].

The energy of the chemical bonds between the CIS semiconductor compounds, for example, is reasonably high, which leads to a decent chemical and thermal stability and reduces the risk of performance degradation over time [270].

Unfortunately, the knowledge of the lifetime of large-scale commercial CIGS modules is still limited, as is their degradation rates [271]. However, CIGS module warranties state that they retain 80% of their initial power after 20 years of field exposure [272]. With that in mind, the sensitivity analysis for the lifetime is not performed.

The analysis of the environmental impacts shows that, besides the Si processing, the top layer (chalcogenide technologies) also has an essential contribution to all categories. One of the reasons for that is the efficiency of these technologies. In order understand the influence of the efficiency of these top layers (CIGS, CZTS and AZTS),

a sensitivity analysis is performed (Figure 41), assuming efficiencies for the tandem solar cells from 22 to 28%.
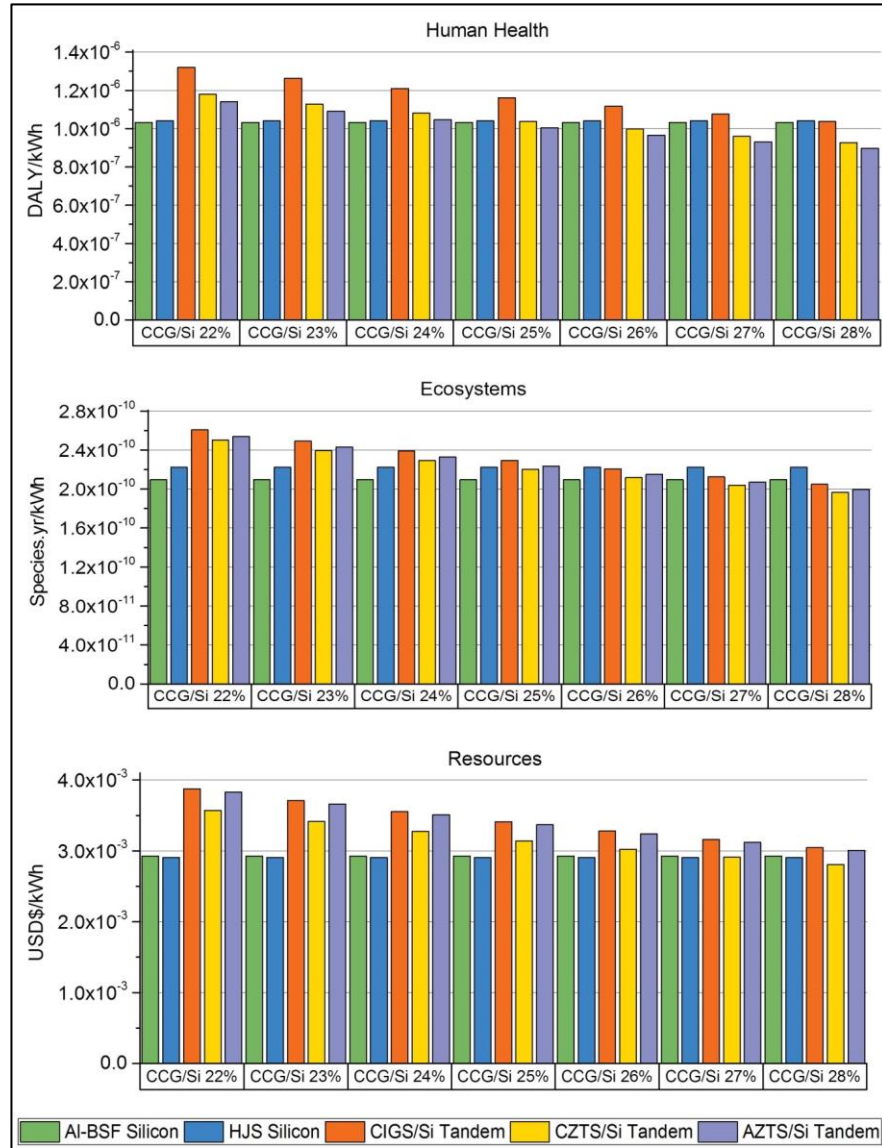
Figure 41: Sensitivity analysis assuming efficiencies from 22 to 28% for the chalcogenide/Si tandem solar cells. CCG = chalcogenide.

Considering human health, both CZTS/Si and AZTS/Si can match the impacts of Si (both p-n junction and HJS) if the tandem solar modules can achieve an efficiency of

25%. For the CIGS/Si structure, the impacts continue to be higher than Si (p-n junction and HJS) until the CIGS/Si module reaches around 28% of efficiency.

For ecosystems, all tandem structures have similar behaviour when the efficiency changes. For CIGS/Si, CZTS/Si and AZTS/Si the efficiency needed for the tandem solar modules to have equal or lower environmental impacts (related to ecosystems indicator) is around 26% or higher.

Finally, considering resources depletion, the CIGS/Si presents the lowest environmental impacts of the tandems and can have equal or lower environmental effects relative to Si in this category if the tandem modules can achieve around 27% of efficiency. For the other two structures studies (CIGS/Si and AZTS/Si), even with 28% of efficiency, the impacts are still slightly higher than both types of Si (p-n junction and HJS), mainly because of the use of silver.

Besides the efficiency, there is another parameter that can be further investigated. In this analysis the thickness of the top layers was assumed to be 1 µm for CIGS and 0.5 µm for CZTS and AZTS layers. The impacts from these layers are significant for most of the impacts categories assessed and, thus, shuld be explored.

In order to better understand the influence of the top layer thickness in the overall environmental impacts, different thicknesses for the chalcogenide layers are assumed (Table 24) and a sensitivity analysis is performed (Figure 42), based on the ReCiPe results (Human Health, Ecosystems and Resources).

Table 24: CIGS, CZTS and AZTS thicknesses assumed for the sensitivity analysis, considering the tandem solar modules assessed in this LCA.

Thickness	This LCA	10% thinner	20% thinner	30% thinner	40% thinner	50% thinner
CIGS	1 µm	0.9 µm	0.8 µm	0.7 µm	0.6 µm	0.5 µm
CZTS	0.5 µm	0.45 µm	0.4 µm	0.35 µm	0.3 µm	0.25 µm
AZTS	0.5 µm	0.45 µm	0.4 µm	0.35 µm	0.3 µm	0.25 µm
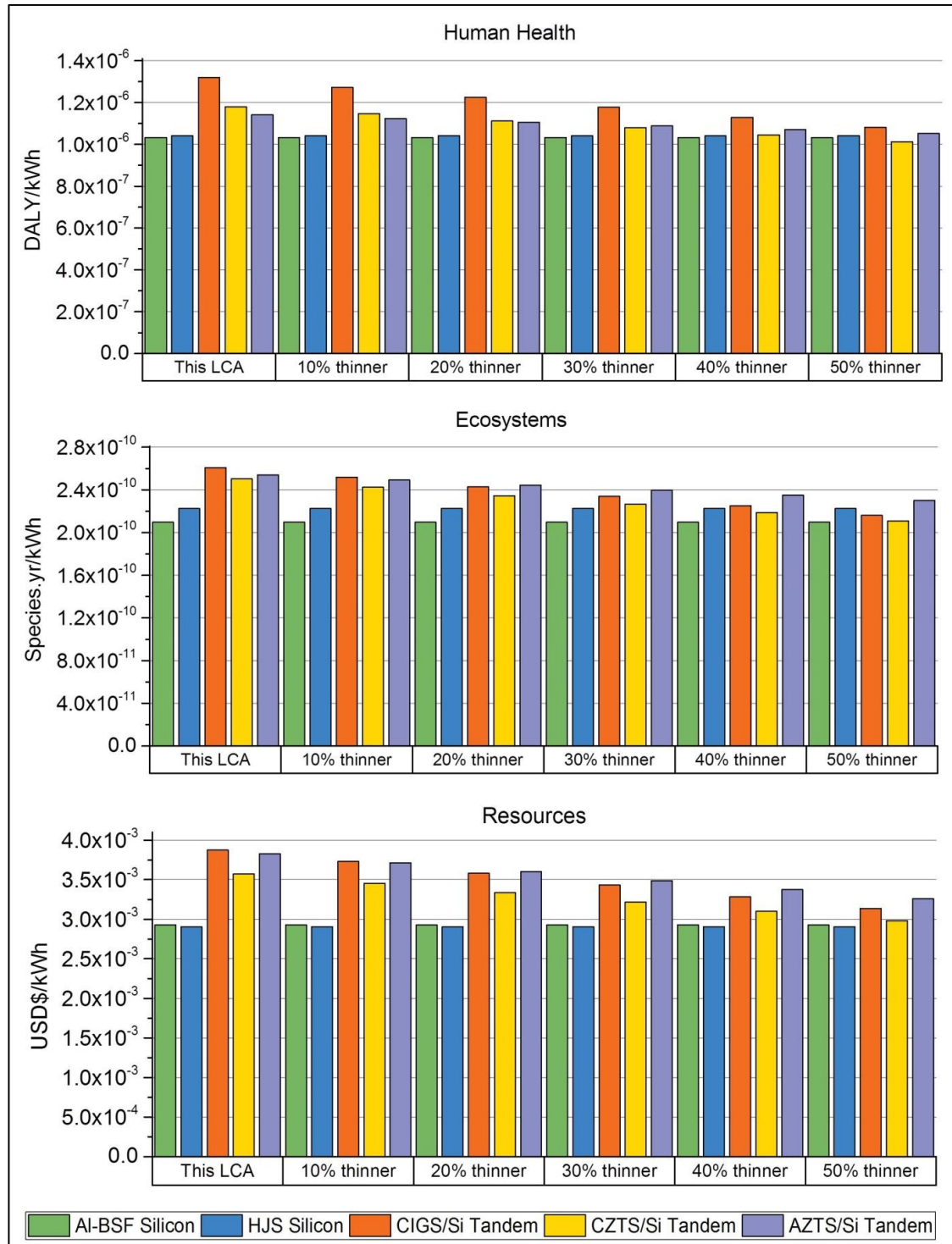
Figure 42: Sensitivity analysis assuming chalcogenide layer thickness reduction from 10 to 50% compared to the original thickness calculated in this LCA, which is 1μm for CIGS and 0.5μm for CZTS and AZTS.

For all ReCiPe categories, the tickness of the top layer (CIGS, CZTS and AZTS) is directly proportional to the envirnmental impacts.

For human health, both CZTS/Si and AZTS/Si can match the impacts with Si (both p-n junction and HJS) if the chalcogenide layer is 50% thiner that the previous calculeted (in this LCA 0.5 µm). The human health impacts for the CIGS/Si structure remain higher than Si (p-n junction and HJS) until even if the thickness is 50% reduced than the original (in this LCA 1 µm).

Analysing the effects on ecosystems, it can be seen that the CZTS impacts is the most affected by the thickness. However, even with 50% of the original thickness calculated in this LCA, none of the tandem structures is able to have lower ReCiPe ecosystems impacts then both Si technologies.

Considering the ReCiPe resources impacts, the AZTS/Si presents the highest results compared with the other structures analysed, mainly because of the use of silver.

It can be observed that, even with a reduction of 50% of the original thickness, all tandem solar modules still have higher impacts than both Si technologies.

5.5 Possibilities for environmental optimisation

There are several possibilities for environmental improvement in the production process of the technologies studied in this LCA, including the reduction of material consumption for the production of the cells, more efficient manufacturing processes and higher energy conversion efficiency.

One possibility to reduce the impacts of the Si treatment is to use different approaches such as the use of solar grade Si (SGS). The energy consumption to produce SGS is estimated to be 25-30 kWh/kg of product, which is a significant reduction, compared to the EGS production via the conventional Siemens (approximately 120-160 kWh/kg of

product) [273], but at some cost to efficiency. Besides that, most of the LCA studies of PV technologies consider the primary energy to produce the modules as being from mostly non-renewable sources, following the standard convention of assuming cells and modules are produced with electricity generated from the actual generator mix typical of the manufacturing regions [42, 129, 274]. However, as the PV prices falls and installations grow rapidly, it is possible to consider, instead, that they could be fabricated exclusively with the electricity from earlier PV modules that were produced from the same or similar facilities [275], which could lead to a new understanding of environmental impacts from solar modules. Examples of solar energy being directly linked to industrial and horticultural businesses already exist in Australia [276-279] and others are planned [280].

Besides, recycling could lead to economic and environmental benefits [281, 282], particularly with metals recovery [283], or the separation of the PV wafers for their potential reuse in new panels. It is estimated that the reuse of the cells from a standard PV module (72 cells of dimension 125 mm x 125 mm, Tedlar as backside foil and an Al frame) implied an overall reduction of the GWP by 59.2 kg CO_{2eq}, for example [281].

Until now, the total amount of reclaimable material from thin-film solar cells has been low (not including module materials and frame and glass), which makes it unlikely that the recovery of elements from spent modules is economically warranted [268]. However, the environmental impacts of disposal should be considered [284].

Processes for recycling thin-film solar modules have been already developed, mostly for CdTe and CIGS technologies. The recovery of semiconductor materials from CIGS thin-film modules was demonstrated, showing the possibility of thermal and mechanical separation of the cover glass and subsequent chemical treatment [285]. After that, valuable metals can be recycled from CdTe and CIGS modules through

hydrometallurgical and pyrometallurgical processes that can recover Cu, In, Ga and Se [286-288].

Besides these improvements, some significant impacts come from the CdS layer in CIGS/SI and CZTS/Si tandem technologies. It can be seen in the results (HTP – cancer and non-cancer, FEuP and FEcP) that changing this layer for MoO_2, for example, can reduce the environmental impacts. Environmental improvements may be achieved for all layers, and with this discussion, we aim to encourage researchers to keep searching for materials that can yield cells with high efficiency but having reduced environmental costs.

6 LCA of Advanced Si Solar Modules

Chapters 4 and 5 presented LCA of different possibilities for Si-based tandem solar cells. In both those studies the main impacts come from the Si treatment processes, mostly because of the intense use of electricity.

Continuous developments are being reported for PV materials and, especially for c-Si wafer solar cells and there are many variations of the existing production processes that are intended to improve module performance [32].

The Al-BSF [33] is the current industry standard process but the PERC technology [34] is gaining significant share in the world market and is expected to replace Al-BSF as the dominant technology in the future (around 60% share expected in 2027) [32]. So, attention is focussed on the silicon bottom cells in this Chapter, exploring the impacts from different choices for production.

These technologies experience degradation processes due to multiple mechanisms. One example is light induced degradation degradation (LID), which is caused by the charge carriers generated by illumination and can severely impact the cells' performance [61]. The interactions with hydrogen of impurities and defects within Si have been intensely studied for decades [60].

The hydrogenation process, in which atomic hydrogen is forced into the silicon material, has recently become better understood and more controllable and offers improvements to the electrical performance and stability of Si solar cells from different feedstocks [289, 290]. The laser hydrogenation [291] (LH) and the hydrogenation in a firing furnace [290] (FH) processes are included in the analyses in this Chapter.

Until now, LCA has not been reported for PERC or the hydrogenation processes considered, to the best of the author's knowledge, prior to this work [292, 293]. This

Chapter presents a comparative environmental analysis, including EPBT, of Al-BSF and PERC solar modules considering SGS, EGS and UMG-Si feedstocks, as well as the ecological effects of hydrogenation (LH and FH) methods.

6.1 Methods

This section describes the specific information for PERC solar cells and two different hydrogenation processes, as an addition to the LCA methodology described in Chapter 3.

6.1.1 Goal and Scope Definition

The aim of this chapter is to compare the environmental impacts and the EPBT of Al-BSF and PERC solar modules using different Si feedstocks. After that, using the same functional unit (FU), the best results are selected and the impacts of these modules with and without the addition of hydrogenation processes are compared.

Figure 43 shows the Al-BSF and PERC structures studied.
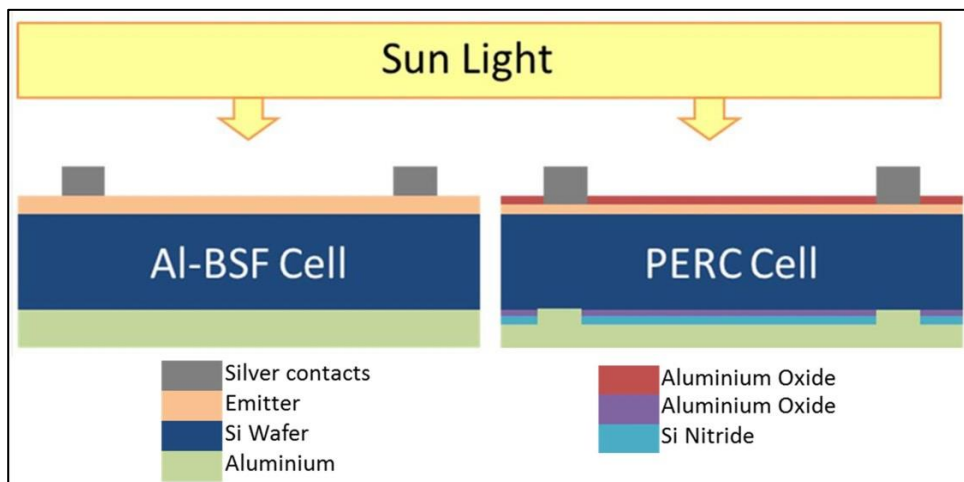
Figure 43: Al-BSF and PERC basic structures.

Table 25 shows the process steps for Al-BSF and PERC technologies.

Table 25: Al-BSF and PERC production process steps.

Al-BSF	PERC	Data Source
Treatment of MGS to achieve a purity of 99%.		[40]
EGS, SGS and UMG-Si.		[35, 40, 42, 294]
Crystal growth (mono c-Si) via Czochralski (CZ) process.		[40, 295]
Si wafer production (sawing and cleaning).		[40]
PV cells production steps, including rear Screen print Ag/Al, front Screen Print Ag and standard Firing	Al-BSF cells production steps + Rear Passivation Layers and Dielectric Openings processes	Al-BSF: [40, 42, 296, 297] PERC: [34, 296]
Module fabrication and Installation		[40, 42]
Disposal of inert material to landfill (no direct emissions).		[40]

Table 26 presents the efficiencies, lifetimes and other important parameters used to compare these two PV technologies.

Table 26: Parameters used for the Al-BSF and PERC technologies studied.

Cell technology		Al-BSF	Al-BSF	Al-BSF	PERC	PERC	PERC
Si Feedstock Parameters		EGS	SGS	UMG-Si	EGS	SGS	UMG-Si
Initial module eff.		0.180 [32]	0.171 [298]	0.165 [299]	0.191 [32]	0.182 [32]	0.180 [299]
insolation	kWh/m^2/yr	1700	1700	1700	1700	1700	1700
energy	kWh	1	1	1	1	1	1
lifetime	years	25	25	25	25	25	25
PR	-	0.75	0.75	0.75	0.75	0.75	0.75
area	m^2	0.174	0.183	0.190	0.164	0.172	0.174
*Assumed efficiencies based on a 90% abs. ratio from cell to module efficiency.							

A module with low degradation rate can be expected to produce more electrical power over its lifetime than for one with a high degradation rate, for the same initial power rating. Light-induced degradation (LID) impacts the performance of solar cells and the primary cause is the interaction of boron with oxygen atoms present in the Si, resulting in a reduction in the performance of the material [300].

The level of this type of degradation is also dependent on the quality of Si material used [300, 301]. The LID mechanism is less apparent for multi-Si cells, compared to mono-Si, because they have a lower concentration of oxygen. For mono-Si the LID effects are significant and cause considerable performance reduction of cells made on p-type Czochralski (Cz) grown Si [302].

PERC cells that use mono-Si are more sensitive to LID, compared with Al-BSF cells. The high degradation that occurs in PERC is mainly due to the stronger dependence of efficiency on bulk lifetime in high-efficiency solar cell structures [303, 304]. But, the LID degradation process in PERC is strong in the first year of exposure and then slows [305], although researchers have also used linear degradation simplifications [61].

This LCA assumes the worst case for PERC, in which all the degradation occurs in the first year. The resulting equivalent average lifetime efficiency is estimated, based on the assumption of 0.5% abs. [300] degradation per year over a 25-year lifetime for Al-BSF technology from initial efficiencies, as shown in Table 26.

The avoidance of some degradation processes can be achieved by hydrogenation processes, as already discussed. The advanced hydrogenation techniques considered in this chapter are the LH and the FH processes, which have been successfully tested in Si solar cells.

The LH process [291] activates and then passivates defects in the Si solar cells using high-intensity laser illumination [61]. This process allows complete stabilisation of

degradation mechanisms related to boron–oxygen reactions in solar cells [289]. The FH process [290] controls the charge state of the hydrogen through in-furnace illumination in the contact firing step. For this LCA we are assuming a conventional industrial firing process [290].

The assumptions for initial module efficiency, module lifetime and the process steps for hydrogenation methods are shown in Table 27. The PERC technology is chosen to be analysed, because the LID effects in this type of cell are more significant when compared with Al-BSF, as mentioned previously in this chapter.

Table 27: Parameters used for the hydrogenation techniques studied (considering PERC cells).

Cell technology		PERC LH	PERC LH	PERC LH	PERC FH	PERC FH	PERC FH
Si Feedstock Parameters		EGS	SGS	UMG-Si	EGS	SGS	UMG-Si
Initial module eff.		0.211	0.202	0.200	0.211	0.202	0.200
insolation	kWh/m^2/yr	1700	1700	1700	1700	1700	1700
energy	kWh	1	1	1	1	1	1
lifetime	years	25	25	25	25	25	25
PR	-	0.75	0.75	0.75	0.75	0.75	0.75
area	m^2	0.157	0.165	0.171	0.147	0.154	0.159
*Assumed efficiencies based on a 90% abs. ratio from cell to module efficiency.							

6.1.2 Inventory Analysis

For a generic p-type mono-Si PERC implementation [34], the inventory is based on estimations using equipment information from manufacturers indicating the throughput and electricity usage [296]. The process data for UMG-Si are collected from the literature [35] and are based on a pilot plant, which can be considered very similar to an industrial plant in terms of equipment dimensions [306]. These inventories are

shown in the appendix, as are the specific data for both hydrogenation processes (LH and FH).

6.2 Results and Discussion (PERC Technology)

6.2.1 Global Warming Potential - PERC

The results for GWP impacts are shown in Figure 44.
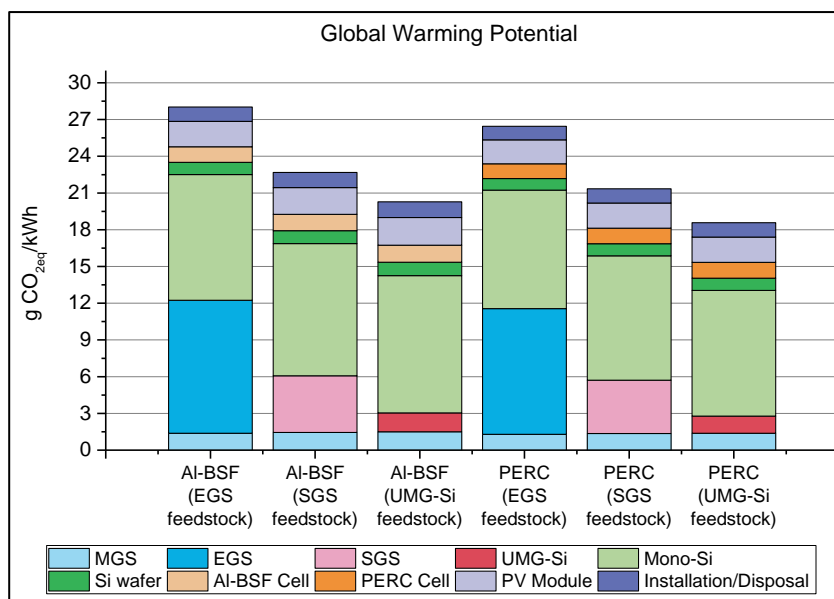
Figure 44: GWP (gCO$_{2eq}$/kWh) results for Al-BSF and PERC solar modules.

The GWP results show that the most significant impacts arise from the growing of mono-Si and the EGS processes, in accordance with Chapter 4 and 5.

The influence of the mono-Si ingots is primarily due to the Czochralski (CZ) process, which was briefly discussed in the perovskite/Si LCA (Chapter 4). In this case it represents approximately 35%, 45% and 51% of the total GWP impact for EGS, SGS and UMG-Si, respectively.

Comparing the different Si feedstocks, the modules that use SGS and UMG-Si have better environmental outcomes compared with EGS, due to the lower use of energy during the Si purification process.

The efficiency improvements due to the PERC technology also influence the environmental outputs. This is because of the lower energy usage required to produce the smaller module area required to collect the same amount of solar-derived energy (1 kWh - FU of this LCA) during the module's lifetime.

6.2.2 Human Toxicity Potential (Cancer and non-Cancer Effects) - PERC

The results for HTP-CE and HTP-nCE are shown in Figures 45 and 46, respectively.
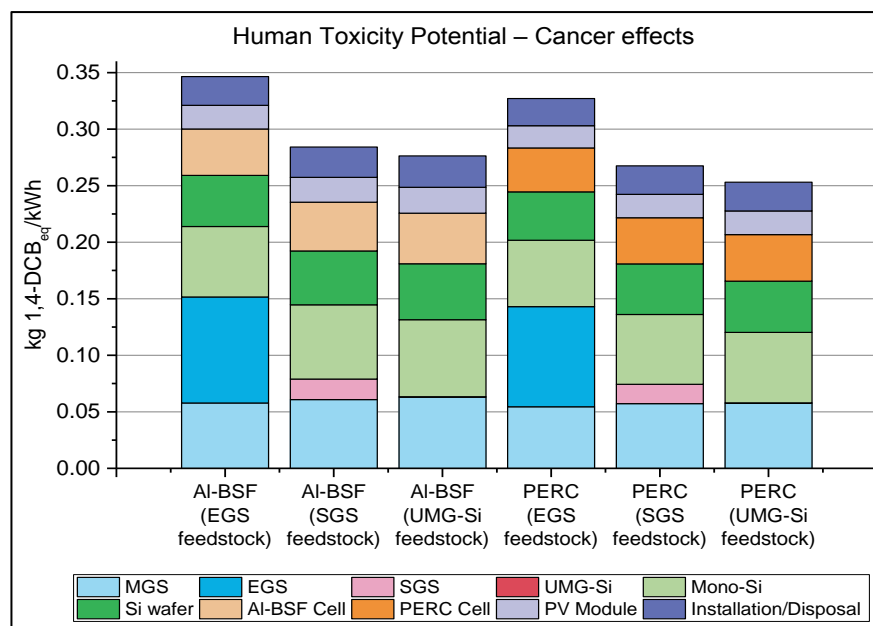
Figure 45: HTP-CE (kg 1,4-DCB$_{eq}$/kWh) for Al-BSF and PERC modules.
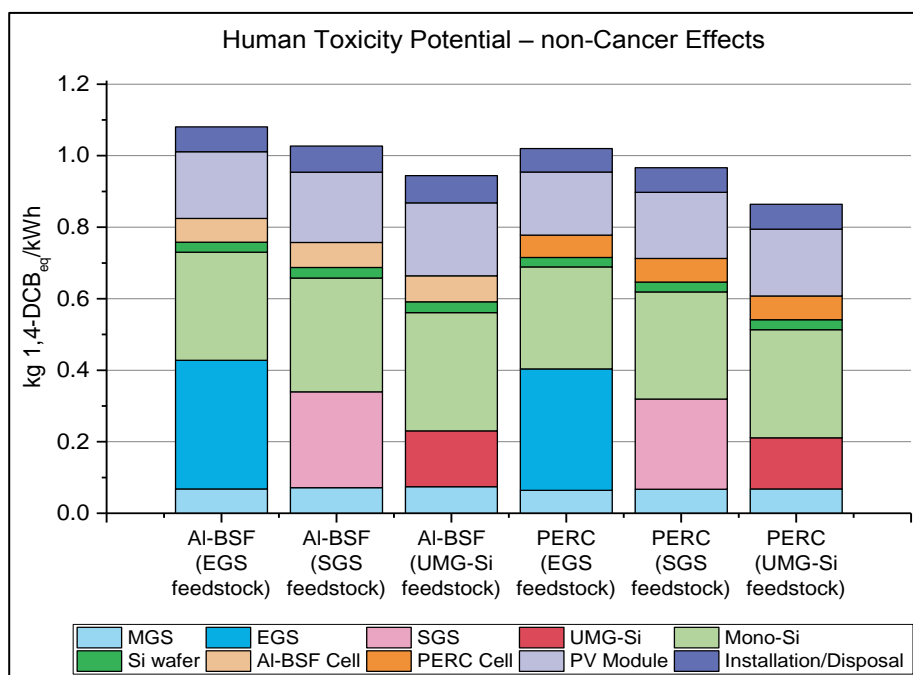
Figure 46: HTP-nCE (kg 1,4-DCBeq/kWh) for Al-BSF and PERC modules.

As the previous chapters (perovskite/Si and chalcogenide/Si LCAs), the most significant HTP impacts are from the mono c-Si ingot growth process, considering both cancer and non-cancer effects. As already discussed, these impacts are a consequence of the substantial amounts of electricity required by the CZ process [123, 229].

The cell and module fabrication processes also present some significant impacts for this category, as mentioned in the Chapters 4 and 5.

The impacts of the disposal step on human health are related to the assumption that the modules go to landfill. Particularly, lead exhibits high cancer and non-cancer toxicity potential for humans [231]. It is important to highlight that impacts from landfills and their human toxicity potentials (e.g. from heavy metals) have uncertainties and these results must be interpreted with caution [307]. It can also be seen that the use of the PERC technology reduces these impacts, mainly due to its improved efficiency.

6.2.3 Freshwater Ecotoxicity Potential - PERC

The results for FEcP are shown in Figure 47.
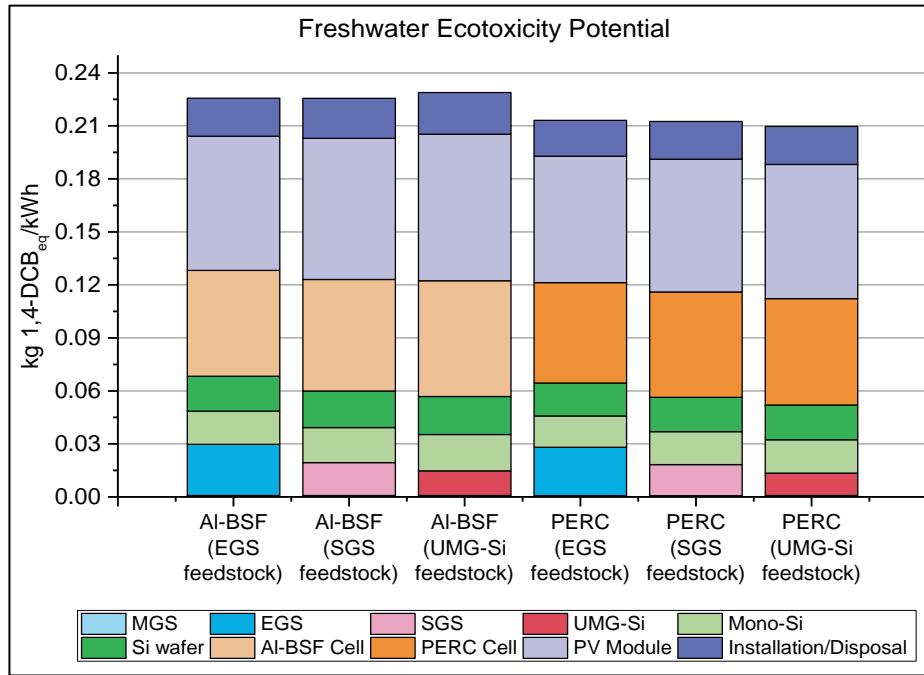
Figure 47: FEcP (kg 1,4-DCB$_{eq}$/kWh) results for Al-BSF and PERC solar modules.

It can be seen that UMG-Si generates similar environmental impacts for this category, compared with the other Si feedstocks analysed (EGS and SGS). Therefore, since the UMG-Si produces cells, and consequently modules, with lower efficiency, the FEcP impacts of the modules using UMG-Si feedstock are higher per FU.

As already discussed in Chapter 4, the cell production and module fabrication phases have the most important FEcP impact, which are mainly from the silver-based paste and glass production, respectively [93].

6.2.4 Freshwater Eutrophication Potential - PERC

The results for FEuP are shown in Figure 48.
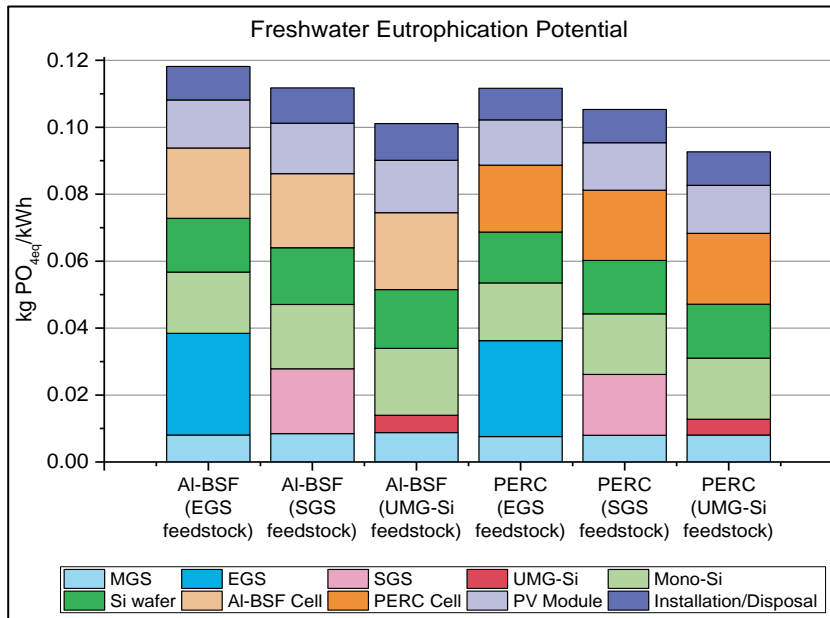
Figure 48: FEuP (kg PO$_{4eq}$/kWh) results for Al-BSF and PERC solar modules.

This impact is dominated by emissions to air and freshwater, including nitrogen oxides, phosphate and nitrate arising from the Si purification treatment and cell manufacturing processes. In the module production stage, encapsulant, backsheets and aluminium frame are the main contributors to this impact category because phosphate and nitrogen oxides are emitted during their production and life cycle, as already presented in Chapters 4 and 5.

The PERC solar modules present lower impacts when compared with the similar Al-BSF Si feedstock structure. The main factor for these effects is the better efficiency from the PERC technology, coupled with the low incremental impacts from the additional steps that this technology requires.

6.2.5 Abiotic Depletion Potential - PERC

Figure 49 shows the ADP impacts for the technologies studied in this LCA.
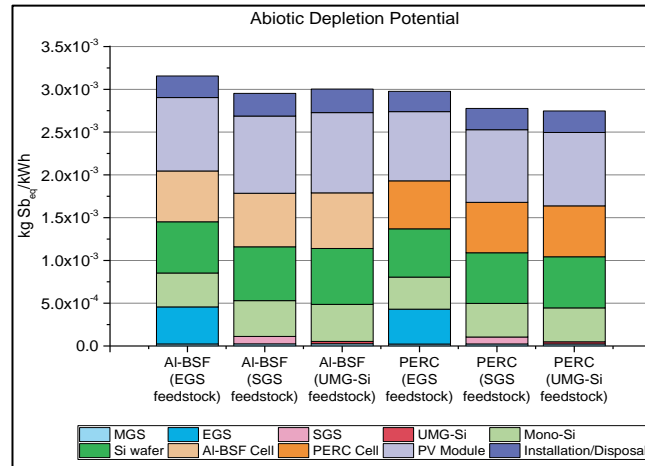
Figure 49: ADP (kg Sb$_{eq}$/kWh) results for Al-BSF and PERC solar modules.

The impacts are mainly from the use of metals, such as copper and silver in the cells and Al in the module production phase, which was mentioned in Chapters 4 and 5.

As it can be seen, the EGS has higher impacts because this process uses more energy per FU when compared with SGS and UMG-Si and that the modules that use PERC solar cells have lower impacts related to abiotic depletion compared with Al-BSF, mainly because of the higher efficiency of the PERC technology.

6.2.6 Energy Payback Time - PERC

Considering the parameters shown in Table 26, the EPBT results are shown in Table 28.

Table 28: EPBT results for mono-Si Al-BSF and PERC (EGS, SGS and UMG-Si feedstock).

Technology	Al-BSF (EGS)	Al-BSF (SGS)	Al-BSF (UMG-Si)	PERC (EGS)	PERC (SGS)	PERC (UMG-Si)
EPBT (years)	1.55	1.47	1.51	1.38	1.31	1.27

The higher EPBT value for EGS is a consequence of the more intensive use of energy per FU in the EGS refinement process than for SGS and UMG-Si, and the higher efficiency does not sufficiently compensate for it. Both higher efficiencies and the use of less energy during the process produce better EPBT results from the PERC structures that use SGS and UMG-Si, whose results are similar to each other.

6.2.7 Endpoint (ReCiPe) Impacts - PERC

The endpoint impacts, based on the ReCiPe methodology, are presented in Figure 50 for Al-BSF and PERC solar modules using different Si feedstocks.
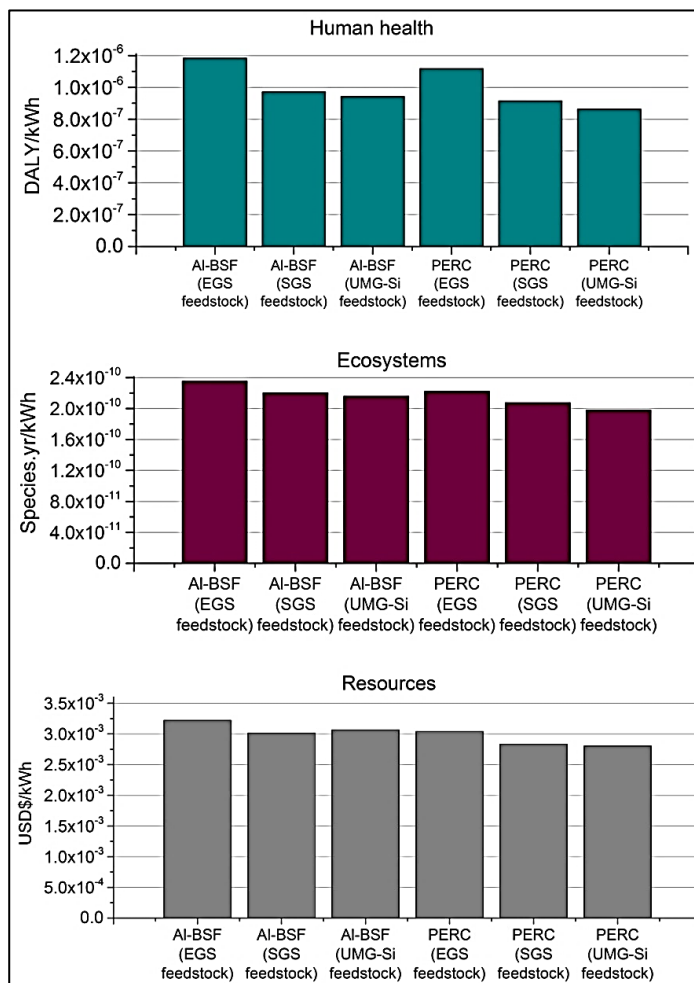
Figure 50: ReCiPe results for Al-BSF and PERC with different Si feedstocks.

The comparison of the three ReCiPe indicators verifies that, for the assumptions made for and the data collected in this LCA, the lowest environmental outcomes are from the modules with PERC cells using SGS or UMG-Si, with a slight advantage for UMG-Si feedstock.

As discussed in the previous LCA chapters, energy use influences in most of the assessed impact categories, such as global warming and toxicity potential and, consequently, it influences all three impact categories considered in the ReCiPe method. Because of that, all endpoint categories analysed are strongly affected by energy usage.

6.3 Results and Discussion (Hydrogenation Process)

The results show that, mainly because of the higher efficiency, PERC solar modules have lower environmental impacts than the Al-BSF technology. However, besides efficiency gains, the examination of the influence of the degradation processes is also important in order to reach even lower ecological effects.

The environmental results considering LH and FH processes, compared with PERC without hydrogenation are shown in Figure 51.
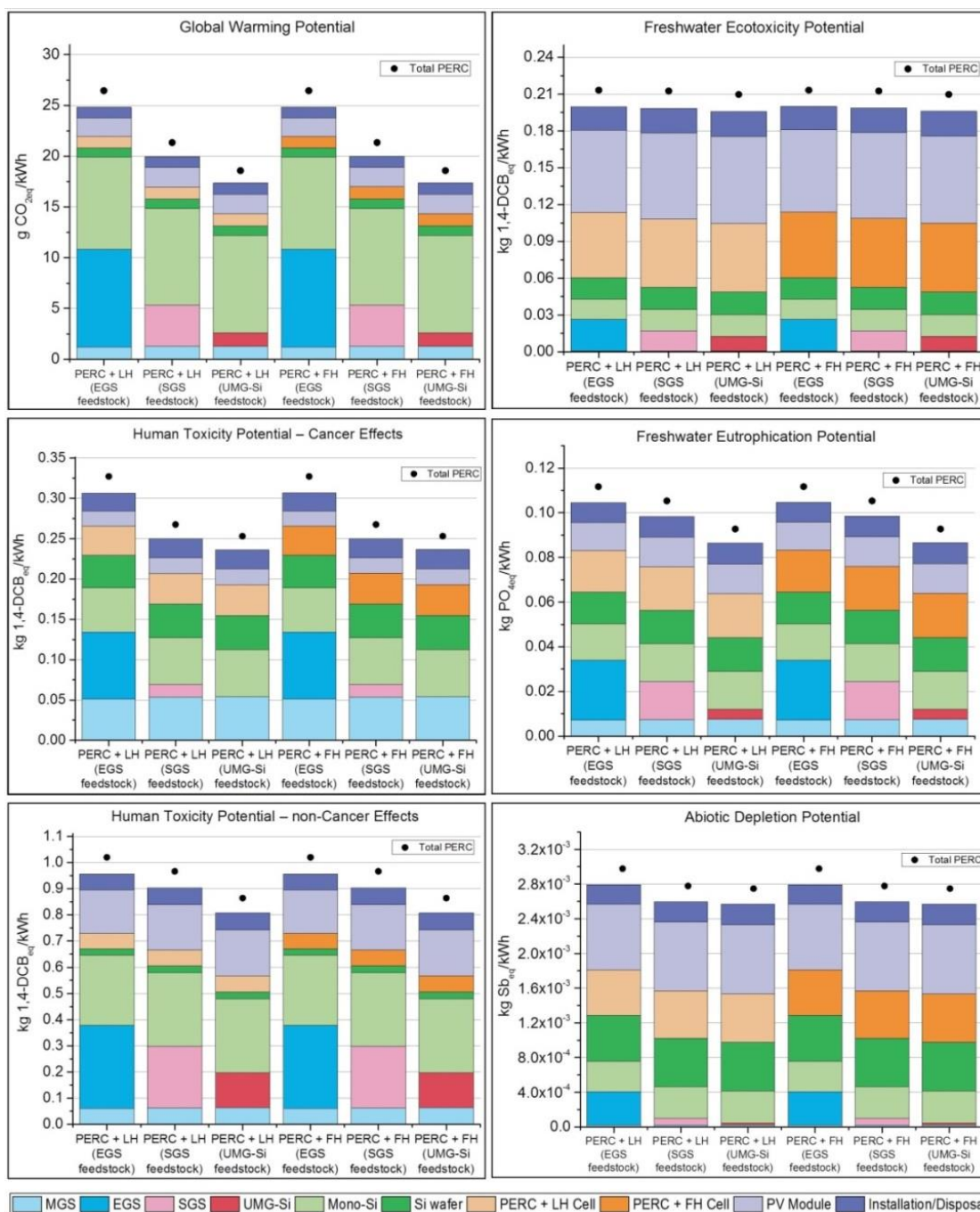
Figure 51: Environmental impacts results for PERC with LH and FH solar modules, where the black dots represent the total impacts from the PERC technology (with the respective Si feedstock), previously presented in this chapter

Compared with PERC, it can be seen that the application of both hydrogenation processes, and the consequential reduction of the degradation process of the cells,

results in lower GWP impacts for the three different Si feedstocks analysed. The contribution to the environmental costs of the additional steps (laser hydrogenation or hydrogenation in a firing furnace) is minimal compared with the impacts from other process steps.

6.3.1 Energy Payback Time – Hydrogenation

Considering Table 27, the EPBT results are shown in Table 29.

Table 29: EPBT results for PERC with LH and FH solar modules.

Cell technology	PERC LH	PERC LH	PERC LH	PERC FH	PERC FH	PERC FH
Si Feedstock	EGS	SGS	UMG-Si	EGS	SGS	UMG-Si
EPBT (years)	1.35	1.28	1.25	1.35	1.28	1.25

Considering the hydrogenation processes, the EPBT presents a positive change if compared with the PERC technology without hydrogenation (Table 28), considering the respective Si feedstocks. The improved performance of these modules results in lower EPBT, which shows the importance of hydrogenation not only for the best environmental results but also for the efficient use of input energy.

From these analyses, we can see that the best results are shown by the PERC (UMG-Si) with hydrogenation (either LH or FH), because of the lower usage of energy during the Si treatment process and increase in the efficiency of the devices.

6.3.2 Endpoint (ReCiPe) Impacts – Hydrogenation

The endpoint impacts for PERC with LH and FH solar modules using different Si feedstocks are presented in Figure 52, based in the ReCiPe methodology.

It can be observed that the hydrogenation processes (LH and FH) have positive effects on the outcomes in all categories (human health, ecosystems and resources) when

compared with PERC solar modules and the respective Si feedstock. The degradation reduction (benefit over the lifetime) and the improvement in the efficiency result in low environmental impacts.
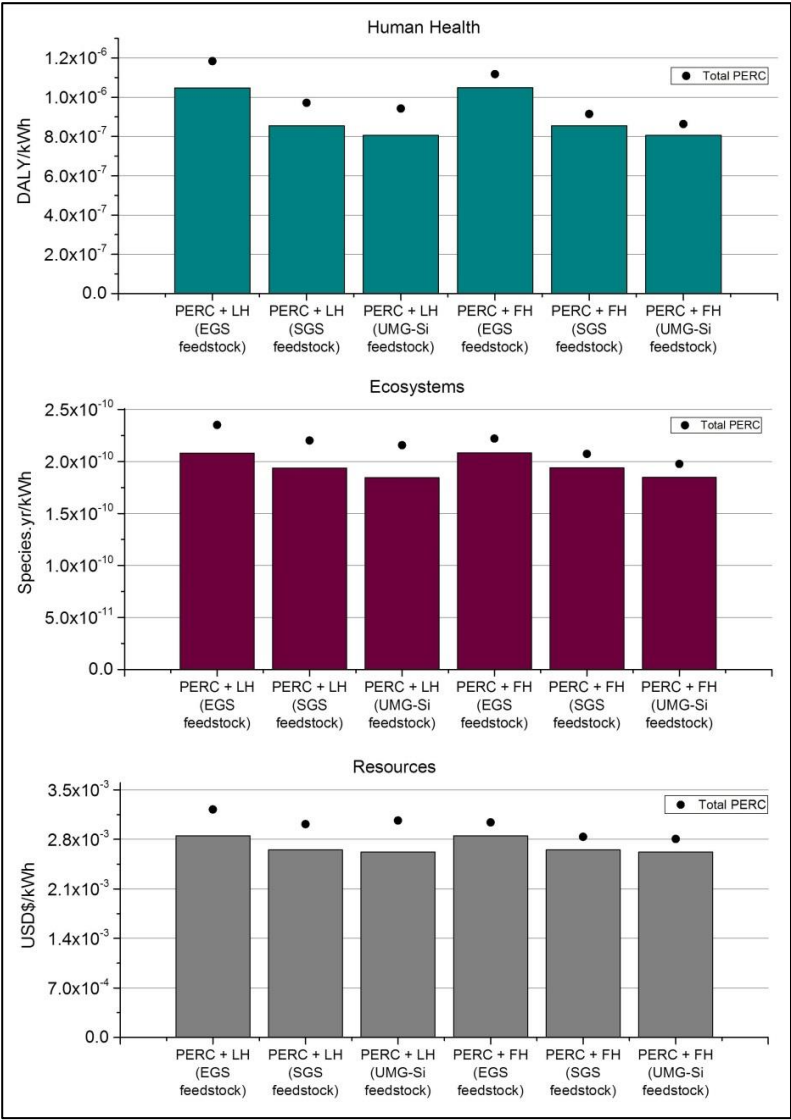
Figure 52: ReCiPe results for PERC with LH and FH solar modules, where the black dots represent the total impacts from the PERC technology (with the respective Si feedstock), previously presented in this chapter.

6.4 Possibilities for environmental optimisation

The recycling of cells and modules materials can conduce to environmental benefits [283]. Different methods for recycling Si-based modules that can achieve a good recovery of the range of materials in these modules are being developed worldwide [308-312]. Because c-Si leads the market [79], the trend is that the processes for recycling this technology will improve faster than for other technologies. The most common recycling process for c-Si modules, which is commercially available in Europe [313], can recover about 80% of materials from these modules, and the recuperated materials can also have high commercial value through the industrialisation of more complex processes that are currently being studied at laboratory scale [314, 315], although the economic costs are still high.

Moreover, the use of renewable energy as the main primary source of electricity in all processes studied would reduce the environmental impacts. The main problems with consuming power from non-renewable sources are the impacts related to the extraction of the raw materials (e.g. coal, petroleum and natural gas) and the emissions during the electricity production process.

The environmental impacts directly depend on the lifetime of the PV cells and modules and on their stability, which is affected by several degradation processes, such as potential-induced degradation [316], moisture-induced degradation [317] and light-induced degradation [318]. The environmental investigation conducted in this chapter verifies the benefits from the hydrogenation technique, which can lead to low environmental impacts when compared with cells that present degradation through the LID mechanism.

Both efficiency and lifetime are challenges that are being actively addressed by the research community, and the costs and benefits of improvements should be further

studied from an environmental point of view. The guidance provided by the results of

an LCA is essential in the search for better technologies.

7 Discussion and Conclusions

The current world electricity supply chains are dominated by the use of sources that consume significant quantities of non-renewable materials and fossil fuels, and, as a consequence have a lot of environmental impacts, such as carbon emissions and abiotic depletion. Considerable effort is being made worldwide trying to decarbonise that inappropriate energy system, aiming to reduce by 2050 the global GHG emission by, at least, 80% [319, 320].

Electricity is indispensable in modern civilisations, and emissions data related to electricity generation, such as kg of CO_2 per energy production, are often used for accounting and reporting purposes, not just for the R&D community but also for the general public. The electricity sector needs to reduce its emissions even more, and the aim is 85% reduction by 2050 to accomplish the *global warming emission reduction target* [321]. To achieve this goal, the investment in several sectors related to renewable electricity supply is growing, including hydro, thermal and PV solar, onshore and offshore wind, biomass and geothermal.

According to the Intergovernmental Panel on Climate Change (IPCC) [322], in 2014, the world's CO_{2eq} emissions were approximately 27 Gt from multiple sources, of which 37% (about 10 Gt) were from the electricity sector. The International Energy Agency (IEA) has warned that emissions in 2018 are set to rise (Figure 53) [323].
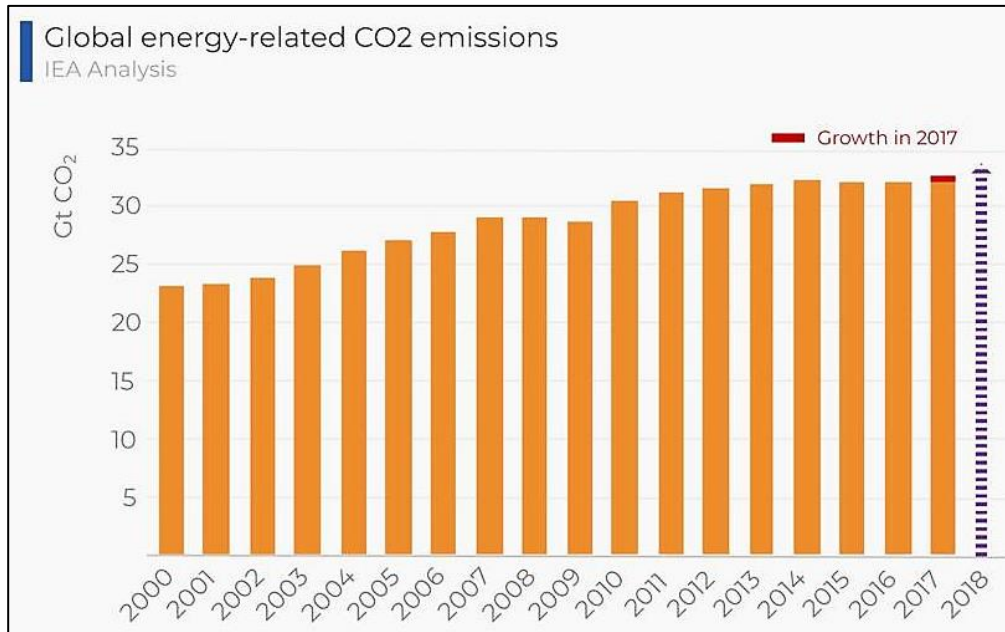
Figure 53: Predictions from the International Energy Agency (IEA) [323] for the global energy-related CO$_2$ emission from 2000 to 2018 (Figure from [294]).

There are several different electrical generation methods, each having advantages and disadvantages related to the operational cost, environmental impacts, and other factors. Each one of them produces different quantities of GHG emissions during construction, operation (including fuel supply activities), and decommissioning processes. There is a variety of opportunities to reduce GHG emissions associated with electricity generation, transmission, and distribution, such as increasing the efficiency of existing power plants (renewable or non-renewable), fuel switching and use of renewable energy sources, improving the energy utilization of the end-user, investing in carbon capture sequestration and storage etcetera [324].

Most probably, there will never be one single perfect technology for the whole world, but instead, a range of the most suitable energy sources depending on the location, application, power demand and available infrastructure. PV technology can be

considered one of those sustainable energy options comparing the CO_{2eq} emissions from other sources of energy (Figure 54), for example.
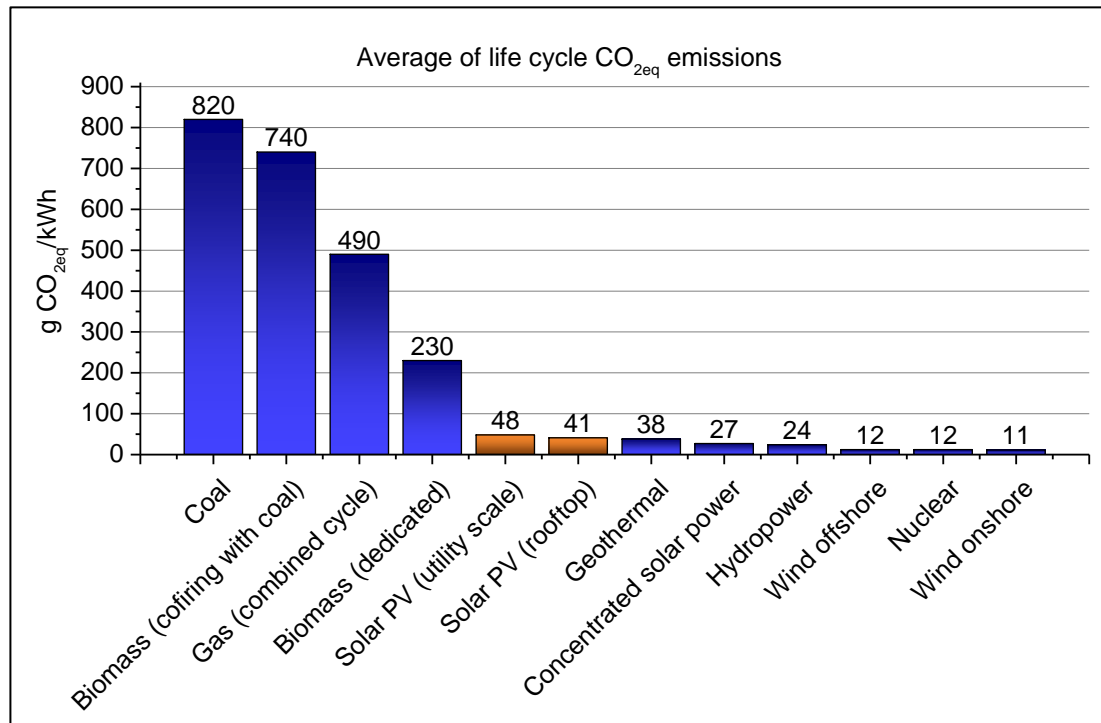
Figure 54: Average of life cycle CO_{2eq} emissions from commercially available electricity supply technologies in gCO2eq/kWh [322].

In comparison with nuclear and wind technologies, the current PV emissions are still relatively high, especially when installed at low-irradiation regions. Therefore, the development of this technology is essential to maintain the sustainable goal of PV solar modules and ensure good prospects for further reduction of the GHG emissions and other environmental impacts. Besides, solar PV has important advantages when compared with other renewable sources of energy, such as low maintenance costs (solar energy systems generally don't require a lot of maintenance apart from occasional cleaning), can be installed in cities, on factory roofs, other buildings

etcetera, and, although solar systems require an upfront investment for their installation, they otherwise operate silently and unobtrusively at very low costs [322].

In this thesis, LCA studies were conducted assessing GWP, HTP-CE, HTP-nCE, FEcP, FEuP, ADP and EPBT impacts of Si-based tandem solar modules, including perovskite/Si tandem (using Ag, Au and Al as metal contacts) and chalcogenide/Si tandem (considering CIGS, CZTS and AZTS top cells) solar modules as well as advanced technologies for Si-based solar modules such as the PERC structure and hydrogenation processes (LH and FH).

The results were briefly discussed in Chapters 4, 5 and 6, but will be further examined in this chapter, which also drawn conclusions to this thesis.

7.1 Silicon-based tandem solar modules

Through the analyses of the LCA studies conducted for perovskite/Si and chalcogenide/Si tandem devices, it becomes clear that the most significant impacts come from the Si bottom cell, mostly due to the intense use of electricity during the Si treatment processes. Alternative methods should be studied to find new routes that can produce good quality materials using lower quantities of energy. These results are in line with the literature, as presented in Chapter 2.

Comparing the Si bottom layer technologies, p-n junction Si (multi-Si feedstock) modules have lower GWP, HTP-nCE and FEuP impacts compared with HJS (mono-Si feedstock), mainly because of the use of the different Si purification processes. For the other categories considered, which are HTP-CE, FEcP and ADP, the impacts are similar, but also related to the use of mono-Si and multi-Si feedstocks. The processes

to fabricate these types of Si require different amounts of energy input, as mentioned in Chapter 2, which is related to the environmental impact because of the assumption that the primary energy comes from coal combustion, considering the electricity mix from China (approximately 70% of coal).

As mentioned, when coal is burned it releases several toxins and pollutants to air, land and water. Among these substances, there are Hg, Pb, sulfur dioxide, nitrogen oxides, particulates, and various other heavy metals that might affect human health, such as through asthma and breathing difficulties, brain damage, heart problems, cancer, neurological disorders, and premature death, as well as the environment.

For the perovskite/Si structures, the lifetime of the perovskite top cells used in the tandem structures is the key point for better environmental outcomes and has a drastic influence in all impact categories analysed in Chapter 4. For the majority of them, the perovskite/Si tandem devices have poorer environmental outcomes compared with Si (p-n junction and HJS), mainly because of the stability of the perovskite layer and energy use during the Si production process. The transparency and electrical conductivity of the perovskite layers after failure, if they could be engineered, would also contribute to lower ecological impacts. For the majority of the impact categories analysed, the most significant environmental impacts from the perovskite cell comes from the Au grid and Spiro-OMeTAD (due to the solvents used), which requires further development of perovskite solar cells, while maintaining cell performance.

Considering the major influence of the cell lifetime on the environmental impacts of perovskite top cells, a sensitivity analysis was performed considering scenario 2 ("*after one year of lifetime, the perovskite layer fails and becomes transparent and still electrically conductive, making it possible for the Si cell to generate power during its whole lifetime*") by varying the lifetime for perovskite cells. The results from this

analysis verify that the longer lifetime of the perovskite layer increases the total efficiency of the device for longer, resulting in better environmental outcomes.

From the analysis presented in Chapter 4 the tandem structure offering the best environmental outcomes is the perovskite/Si tandem using a p-n junction Si solar cell (rather than an HJS cell), Spiro-free perovskite cell and Al (rather than Ag or Au) as the top electrode. The EPBT results show that perovskite/Si tandem solar cells outperform Si technologies, mainly because the efficiency of perovskite/Si tandem solar modules is assumed to be higher than Si single junction (either p-n junction or HJS) modules. As mentioned, the EPBT is related with the energy consumption and production, not considering the environmental impacts from the GHG emissions. Because of that, the EPBT results differ from the GWP impacts. However, it is important to highlight that the EPBT results are higher than 1 year, and currently the perovskite technologies are not able to last that long. The EPBT was calculated considering efficiencies of 27% for perovskite (Ag and Au)/Si (HJS) tandem and 24% for perovskite (Al)/Si (p-n junction) tandem solar modules.

The LCA of chalcogenide/Si is presented in Chapter 5 and the GWP results show that the CZTS/Si and AZTS/Si tandem structures studied have lower impacts than than the corresponding Si single junction modules (considering p-n junction Si for CZTS/Si and HJS for AZTS/Si). However, the CIGS/Si tandem structure has worse impacts compared with both Si technologies studied, considering the assumptions made. These impacts are mainly due to the energy use during the production processes of the chalcogenide solar cells. The production processes of CIGS, CZTS and AZTS are similar but different thicknesses are assumed, which results in distinct consumptions of energy in manufacture. The thickness of the CIGS layer is assumed to be greater than that of CZTS and AZTS and, consequently, the GWP impacts are worse for the

CIGS/Si tandem structure than for the other modules studied, as discussed in Chapter 5.

The main HTP (CE and nCE), FEcP and FEuP impacts come from the CdS layer, as a consequence of the presence of cadmium (Cd) in its composition. This layer is verified to be toxic not just for humans but also for fauna and flora. Much work has already been done to try to replace this buffer layer in CIS and CIGS solar cells, but there is still a lot to be done in this area to find a reliable and effective replacement for CdS. Replacing the CdS buffer layer will reduce the environmental impacts from this cells, so we suggest researchers keep focusing on alternative buffer layers to CdS with the same efficiency, but without the use of toxic substances.

The ADP results show that the use of metals and other materials is also a problem. The recycling of toxic elements as well as scarce metals is significant to reduce the environmental impacts in all categories evaluated, especially ADP. Specifically for CIGS, indium is a crucial element, and its scarcity is a concern for scaling up CIGS module production to the terawatt level.

Additionally, in order understand the influence of the efficiency of the chalcogenide top layers studied, a sensitivity analysis was performed, assuming efficiencies for the tandem solar cells (CIGS/Si, CZTS/Si and AZTS/Si) from 22 to 28%. Considering ReCiPe categories, this analysis showed, unsurprisingly, that the greater the efficiency, the smaller the impacts. Also, particularly for resources depletion, the CIGS/Si presents the lowest environmental impacts of the tandems and can have equal or lower ecological effects in this category if the tandem modules can achieve around 27% efficiency.

Besides the efficiency, the effect of thickness of the chalcogenide layers was also analysed, because the impacts from these layers are significant for most of the impacts

categories assessed. The results showed that, for all ReCiPe categories, the thickness of the top layer (CIGS, CZTS and AZTS) is directly proportional to the environmental impacts.

7.2 Advanced silicon-based solar modules

Chapter 6 presented an LCA of PERC technology and different hydrogenation processes considering SGS, EGS and UMG-Si feedstocks, and the results demonstrate that the increase in the performance of PV modules can result in better environmental impacts when considering most of the categories analysed and, as already discussed, the most significant overall impacts come from the Si treatment processes.

PV modules with PERC solar cells using SGS or UMG-Si feedstocks present lower GWP impacts compared with Al-BSF using all analysed Si feedstocks and PERC using EGS feedstock. The use of PERC technology with UMG-Si show the best outcomes, compared with the other modules studied in this LCA, which encourages studies of cell and module performance improvements using low quality Si. These conclusions are reinforced by the analysis of the EPBT that shows the importance of the effective use of energy input. It was observed that the structures using EGS present higher EPBT than the structures that use SGS or UMG-Si feedstocks, which is mainly due to the intensive use of energy in the EGS process compared to the other Si feedstocks. The lowest EPBT value is from the modules using UMG-Si, mainly because of the low use of energy during the Si treatment process compared with the other feedstocks analysed.

Significant human and freshwater toxicity impacts come from the cell (both Al-BSF and PERC) and module fabrication processes. The main substances that contribute in

these environmental categories are Pb, arsenic, copper, nickel and mercury, although emissions to air and freshwater are mostly generated from the silver paste in cell production, glass production process for the modules and the overall electricity usage during these processes.

The key finding of the analysis of the PERC technology is that the improvements in the modules' efficiency through the adoption this type of solar cell and the use of low electricity input for the Si feedstock (SGS and UMG-Si) result in lower environmental impacts when compared with Al-BSF cells and EGS feedstock. It is essential to emphasise that a small contribution to low environmental impacts arises from the PERC improvements in the cell/module efficiency, while the most significant is from the use of Si feedstock (SGS or UMG-Si).

The hydrogenation process also shows that the improved efficiency and the benefits over the lifetime, due to the reduction of the LID effects from the hydrogenation processes (LH and FH), positively influence the environmental outputs when compared with PERC cells without hydrogenation. Besides that, for all impact categories analysed, the UMG-Si combined with the hydrogenation process result in lower environmental outcomes when compared with the other Si feedstocks assessed. Regarding EPBT, the modules using hydrogenated solar cells show lower values, which demonstrate the importance of these processes not only for the best environmental results but also for the effective use of energy input.

7.3 Summary

Conducting LCAs on new technologies is indispensable in the search for materials and processes that have the lowest environmental impacts possible, which was reinforced in this thesis. The energy use during the Si treatment is the main contributor to the majority of the ecological effects assessed.

The impacts from the disposal of solar modules are not significant compared with the impacts of the production processes. However, recycling methods should also be studied, aiming to reduce the environmental effects of these processes further, and to protect against reputational damage.

Besides that, further research and analysis must be done regarding processes under development for recycling modules that can achieve a good recovery rate for materials [308-311]. In this thesis the environmental impacts from recycling methods were not considered. Future work will focus on LCA for recycling processes, assessing different techniques such as mechanical, thermal and chemical routes.

8 Additional Contribution and Recommendations for Future Work

The global annual market for solar photovoltaic modules has grown at a compound annual rate of 40% from 1997 (114.1 MWp) to 2017 (93.9 GWp) [325]. In 2016, the cumulative global PV waste was projected to reach between 43.5 and 250 thousand tonnes in that year and to rise to between 1.7 and 8.0 million tonnes by 2030 [268]. Predictions indicate that by 2050 that volume will increase to around 6 million tonnes annually. These estimations are shown in Figure 55.
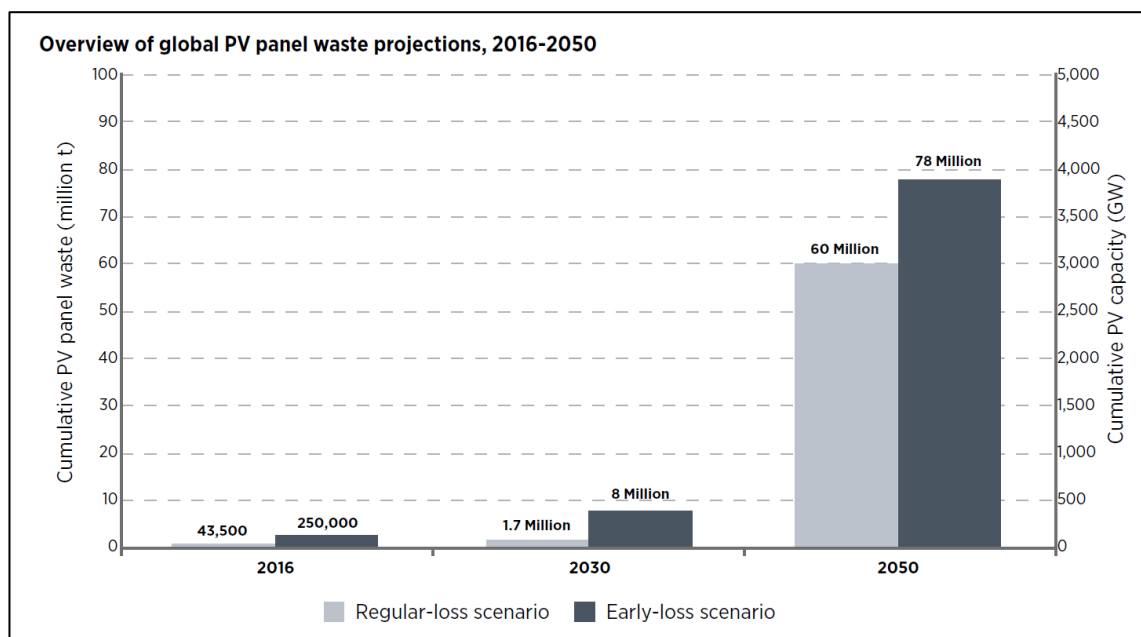
Figure 55: Overview of global PV panel waste projections, 2016-2050 (Figure adapted from [268]).

With the expected acceleration of installation rates, waste from PV panels is a growing concern and an environmental obstacle to be overcome. On the other hand, it unlocks

a range of opportunities to create processes that can convert this rejected material into economic gains and ecological benefits. For this to happen, there must be adequate end-of-life (EoL) management technologies and policies for PV systems and, particularly, PV modules [268].

It is well known that today most of the PV modules go to landfill when they reach their EoL, mainly because recycling processes are not economically feasible and regulation in most countries is not yet established for this matter [268]. The late or non-inclusion of PV waste within countries' waste legislation is usually related to the so-far low quantities of EoL PV modules, due to their long lifetime (up to 25-30 years or more) and low historical installation rates [309]. Regarding the financial aspects, the volume of waste PV modules being taken to recycling facilities is currently insignificant compared to the amount of other electronic wastes [326] and, so, the technology developed for recycling PV waste is still unable to generate profits.

The majority of LCA studies of solar modules focus on the production and operation phases, with an emphasis on the energy requirements of these processes, which have been shown to have an essential contribution to environmental impacts [42]. However, lately, there has been increasing interest and research on the effects of the recycling processes for PV modules. Several studies focus on CdTe modules [116, 130, 134, 138-141], mainly aiming to recover cadmium and tellurium, which are toxic and rare, respectively. Other studies focus on the impacts of a specific recycling process for c-Si technologies [311, 327], and some of them compare recycling process with other scenarios, such as landfill [328] and incineration [329].

The main recommendation from this thesis is to conduct a complete LCA study that analyses the possible EoL scenarios for c-Si PV modules, assuming different pathways to understand the impacts of these EoL options. To do that, it is also important to build

a comprehensive inventory for each scenario, which is currently lacking in the PV and LCA communities.

This chapter presents a preliminary study comparing the environmental impacts from landfill, incineration, reuse and recycling of EoL c-Si solar modules [168], considering results described in the literature. This assessment aims to present an overview of options for PV waste management based on the environmental benefits or disadvantages produced by each EoL possibility.

Although it is a preliminary analysis, the results can indicate the best direction to be taken from an ecological perspective, including the possible recovery of materials and reuse during the initial steps of solar cell and module production.

8.1 Methods

In this study, we are assuming the following module materials which are commonly used in c-Si PV modules (not considering the junction box, as it can be easily removed and can go to normal e-waste recycling plants): silicon wafer cells with silver (Ag)-based and Al contacts, ethylene vinyl acetate (EVA) encapsulant, Al frame, polymer back-sheet, cover glass, tinned copper tabbing and Pb- and tin (Sn)-containing solder.

It has been shown that, for a recycling plant that is 400km from the collection point, truck transportation has some important environmental impacts, mainly for abiotic depletion [311]. However, these results are calculated only for a specific transport type and location. This chapter considers the transportation phase separately from the environmental analysis because it does not depend on the recycling technology but the collection system and distances. It is crucial to highlight that the lack of data results in reliance on a considerable number of assumptions and, thus, the results should be used with caution.

The assessment of the environmental impacts was performed using the LCA methodology discribed in Chapter 3, Methodology, with the aid of GaBi software, version 6 [41]. The calculations are based on data collected from the literature and the Ecoinvent database, version 2 [197]. For a clearer understanding of the LCA endpoint results, the ReCiPe (2016) method is used [186]. The functional unit is defined as 1 kg of Si-based PV waste modules.

8.2 EoL Options for c-Si Solar Modules

The four different PV module EoL approaches analysed in this LCA are landfill, incineration, reuse and recycling.

8.2.1 Landfill

EoL PV modules can generate pollutants, especially the leaching of metals to the environment, if they are not correctly handled [283, 330]. However, the literature presents very few experimental studies about the environmental consequences of the landfilling of c-Si PV modules, with most focusing on the presence of Pb and Ag in the modules [282, 283, 310].

Studies analysing and predicting the future resource availability of materials (mostly metals) demonstrate the need for a proactive systems approach to natural resources scarcity and consequent price increases [331].

In most of the cases, before going to landfill, the PV module is separated from the BOS, which allows the specific components to be separated, based on their waste types. The BOS components are often neglected in LCA studies, but there are a few results for the impacts of these materials [332, 333]. The BOS components' impacts are predominantly carcinogens and ecotoxicity, mainly from the plastic parts, attributable to the release of toxic substances and contaminants into the air or

percolation into the ground during their manufacturing process and when they are placed in landfill, affecting the water and the soil [334].

8.2.2 Incineration

Incinerating solar modules, as for electronic waste in general, is very harmful to the environment because this process releases toxic heavy metals such as Pb into the atmosphere. Some of the materials contained in solar modules are known to be persistent and accumulative when released to the ecosystem, which means long-term effects to humans, fauna and flora.

The benefit of this method is that EoL modules don't need to be separated from other commercial or industrial waste. On the other hand, this process abolishes the chances of recovering raw materials. The impacts of municipal waste incineration and subsequent disposal of the residue at a landfill for inert waste were already assessed and published in the literature [329], but the inventory for this process was not made publicly available.

8.2.3 Reuse

Reuse is also a prioritised choice in the waste management hierarchy and, for PV modules, this process involves repair [335]. The improvement of c-Si solar modules is feasible, depending on the condition of the materials. Typically, methods of repairing modules involve applying a new Al frame or replacing the junction box. It can also be a solution to replace diodes, plugs, sockets and more [268]. Subsequently, the product receives a new label with new guarantees (in compliance with national laws).

The repaired module can have a new lifetime of approximately 15 years but with lower efficiency (around 1 – 2%) [336, 337]. By lengthening their life, the industry avoids manufacture of replacement modules. The problem with this scenario is that even with

inferior environmental outcomes due to the longer lifetime, the modules still have an EoL and the impacts eventually occur. Also, regulations may have changed and these modules are no longer compliant, when ready for reinstallation.

8.2.4 Recycling

Different techniques for recycling solar modules are being developed for all PV technologies. Specifically for c-Si, there are various possibilities for recycling and good results can be achieved with alternative or combined recycling processes. Generally, the first step is to mechanically separate the Al frame and the junction box from the rest of the module. The next stage is to delaminate or remove the encapsulant material, which is usually EVA. Several techniques can be used in this phase [268], including thermal [338, 339], chemical (organic and inorganic) [310, 340, 341] and mechanical recycling processes [311].

The most common process for recycling c-Si modules, which is commercially available in Europe [313], is based on a mechanical method for the extraction of the remaining materials of the module. However, the maximum amount of recovered materials from this process is currently about 80%, which is insufficient for future regulation requirements [342] and the value of the recovered resources is lower than that of the original raw materials [313]. Recently the European company PV Cycle has achieved a recycling rate of 96% for c-Si PV modules using a new process that combines mechanical and thermal treatments [343].

During the thermal process, the EVA and backsheet (Tedlar®) layers are burned, producing heavy smoke that can be noxious and harmful and cannot be emitted into the air. Therefore, in this study, we are considering the treatment of exhaust gas as essential in the pursuit of an environmentally friendly process [338, 339]. The same assumption is made for the chemical process, as we are considering that the

174

backsheet is removed from the module after the chemical treatment. Assuming Tedlar® as the backsheet, it is proven that it has a decent thermal stability in the range of approximately -70°C to 100°C and loses its strength at 260°C to 300°C, which is not hot enough for the EVA to start to decompose and, so, the Tedlar can be separated first from EVA [338].

8.3 Process Descriptions and Inventory Data

Figure 56 shows a process flow diagram for possible c-Si EoL scenarios and the description of each process, which are a compilation of the best results found in the literature.
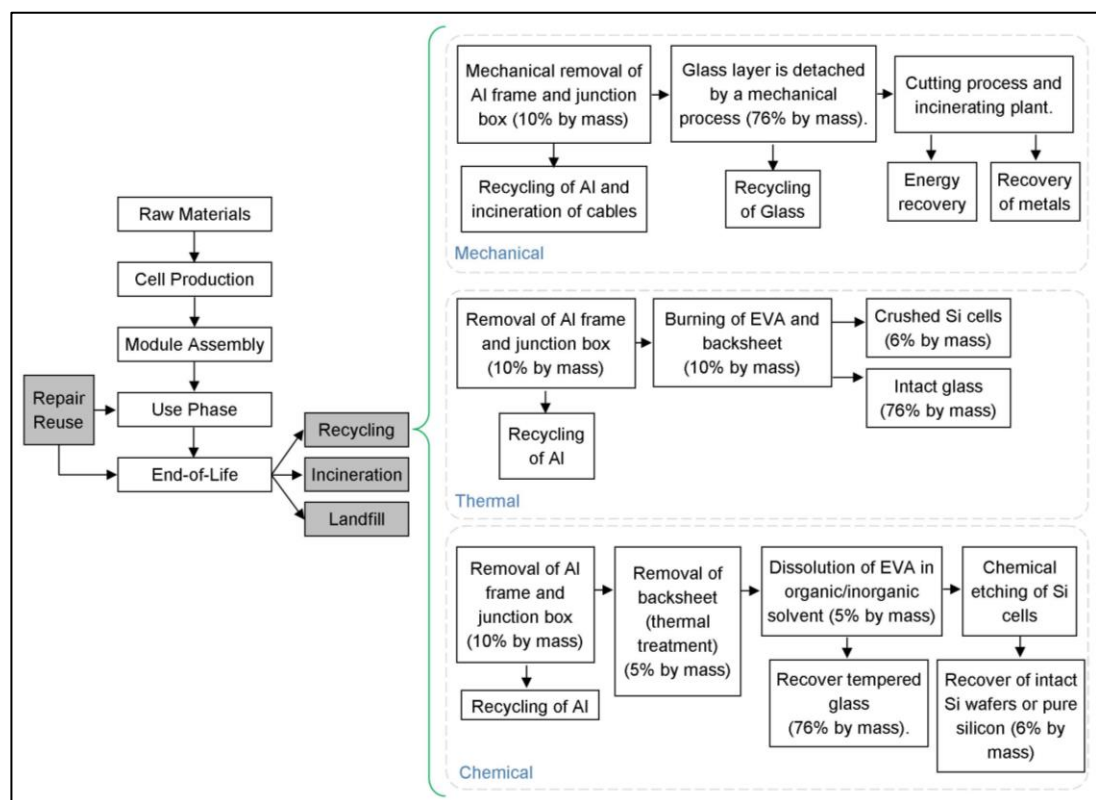
Figure 56. Simplified process flow diagram for c-Si module manufacturing and possible EoL scenarios. Where EVA = ethylene-vinyl-acetate, Al = aluminium, Ag = silver, Si = silicon and ARC = anti-reflection coating.

The impacts from the landfill, incineration and reuse scenarios are not thoroughly studied yet, but the Ecoinvent database [40] has a comprehensive database for plastic and some specific metals.

For the recycling scenario, the considered processes are thermal [338, 339] and chemical [310, 327, 340, 341] methods, which are compared with the mechanical approach that is already published [311], but with the transportation impacts excluded from all processes. These recycling processes start with the mechanical separation of the junction box and Al frame, which can be recycled and reused. We are not considering the Al frame, the cables and the plastic parts in our recycling processes because they usually are sent to separate plants for further treatment [311].

The thermal process inventory is based on the controlled burning of EVA (400 – 500°C), assuming the glass can be recovered without breaking and could be directly used again as a module component [338, 339]. A nitrogen atmosphere, which excludes oxygen and prevents the chemical oxidation of the EVA layer [282, 344], is assumed. In this process, it is expected that most of the cells break due to the excessive pressure from the gasses released during the burning process [338], but they can be reused as raw material for ingot growth (we are assuming that 100% of the raw silicon is from this recycling process). There is also a 100% recovery of Ag from the solar cells [338]. Tests with thermal treatment under air showed a significant temperature increase and the carbonisation of the EVA.

The chemical route assumed in this study starts with softening the EVA layer by a thermal process, as already explained [338]. The most promising organic solvents used for this reaction are tetrahydrofuran, o-dichlorobenzene and toluene. Toluene is the cheapest and more stable among these options and therefore, is the most commonly used chemical for dissolving EVA and it is our assumption in this report. The assumption is that this process is carried out at 80°C temperature, as that was proved

to be more effective compared with room temperature [340]. After this step, the glass is completely recovered and directly used again as a module component. In the next stage, it is possible to recover the intact Si wafers from the cells by using a combination of chemicals. Subsequently, potassium hydroxide is used to remove Al metal coatings, and a mixture of nitric acid, hydrogen fluoride and acetic acid to remove other metals, anti-reflection coatings and p-n junctions. The metals (including Si) are assumed to be reused in new cells [327] and that 80% of the unbroken Si wafer can be recycled into new cells.

For the mechanical approach, the Full Recovery End of Life Photovoltaic (FRELP) process [311] is used for the calculations. This project aims to test and develop innovative technologies for 100% recycling of EoL PV modules in an economically viable way [312]. The impacts of this process are calculated based on the published "gate-to-gate" LCA that assesses the potential environmental effects related to the FRELP recycling process [311], excluding the impacts from transportation.

8.4 Results and Discussion

A summary of all results is calculated using the ReCiPe method [186] for the effects on human health, ecosystems and resources (Figure 57).
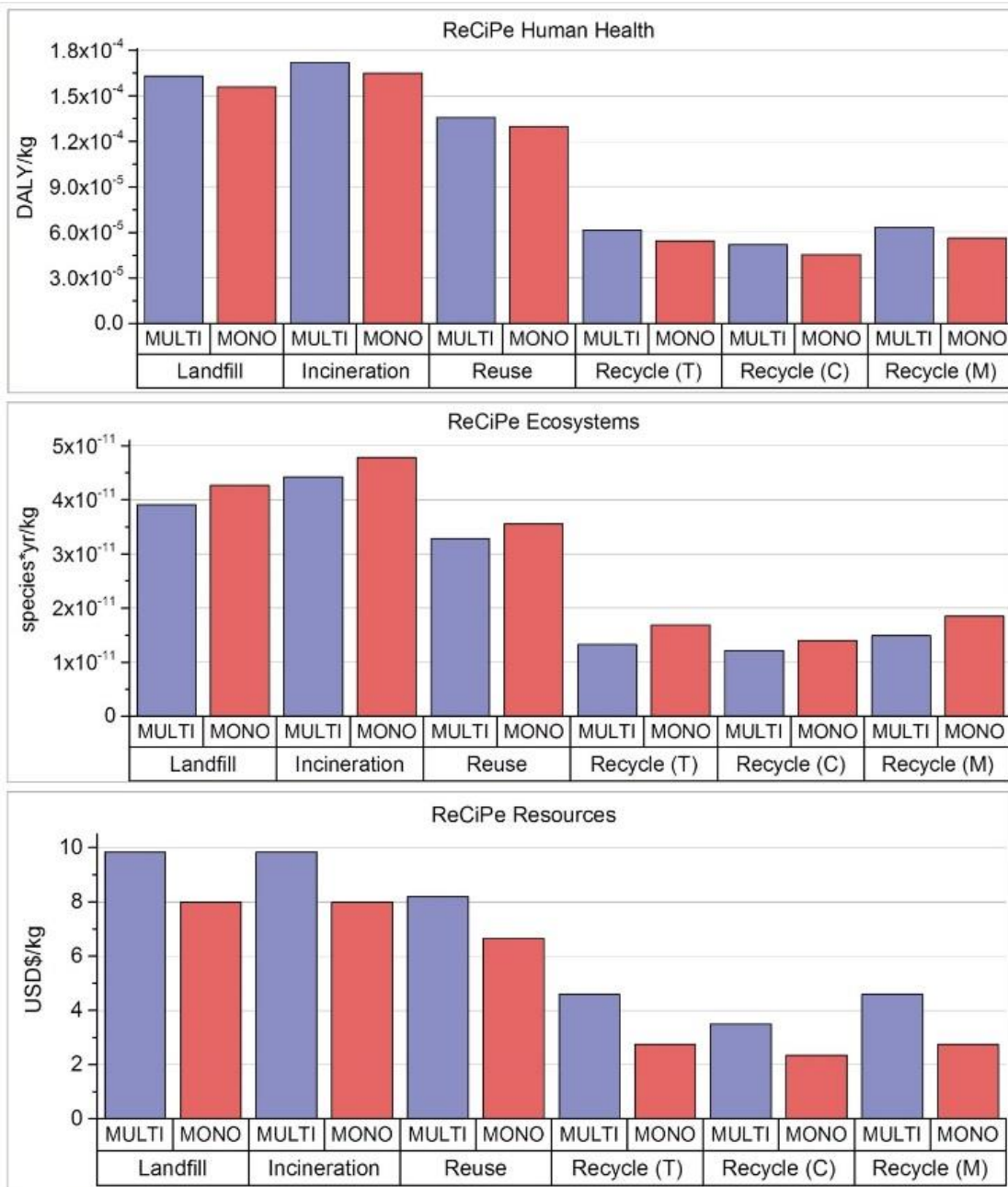
Figure 57: ReCiPe results for effects on Human Health, Ecosystems and Resources (from top to bottom, respectively). Where (T) = Thermal, (C) = Chemical and (M) = Mechanical.

The comparison of the ReCiPe indicators shows that lower environmental impacts can be achieved through recycling methods. That result is mainly due to the recycling and reuse of part of the raw materials such as Si and Ag from the cells and glass and Al

from the frame, which confirms the importance of high-value recycling processes compared to other disposal solutions.

It can also be observed that the incineration process produces the worst impacts compared with the other EoL scenarios, mainly because this process uses more primary energy than the other methods. It is important to highlight that this analysis is not considering any thermal energy or electricity produced by the incineration process, so, no energetic benefit is included in this scenario.

The chemical approach shows low impacts. However, there should be cautious use of toxic chemicals in any environmental analysis. The reuse of the solvent (in this case toluene) in multiple processes is possible and should be used again to recycle new PV modules.

From the analysis of Figure 57, it can also be observed that reuse seems to be a better option compared to the landfill and incineration scenarios. Also, besides reducing impacts, the extra lifetime considered in the reuse scenario also allows more time for recycling technologies to be ready. Besides, the repaired PV modules can be alternatively resold as used panels at a reduced market price of approximately 70% of the original sales price [268], which creates an excellent opportunity for a significant secondary market for used PV modules.

A more detailed analysis is presented in Figures 58 and 59. For the chemical process, it is assumed in this LCA that unbroken Si wafers can be recovered and reused to produce new cells, for mechanical and thermal recycling processes, it is considered that crushed Si cells can be recovered and reprocessed in the ingot growth process. The possibility of reuse of Si as raw material or of intact wafers to produce new solar cells is beneficial regarding environmental outcomes from the entire process.
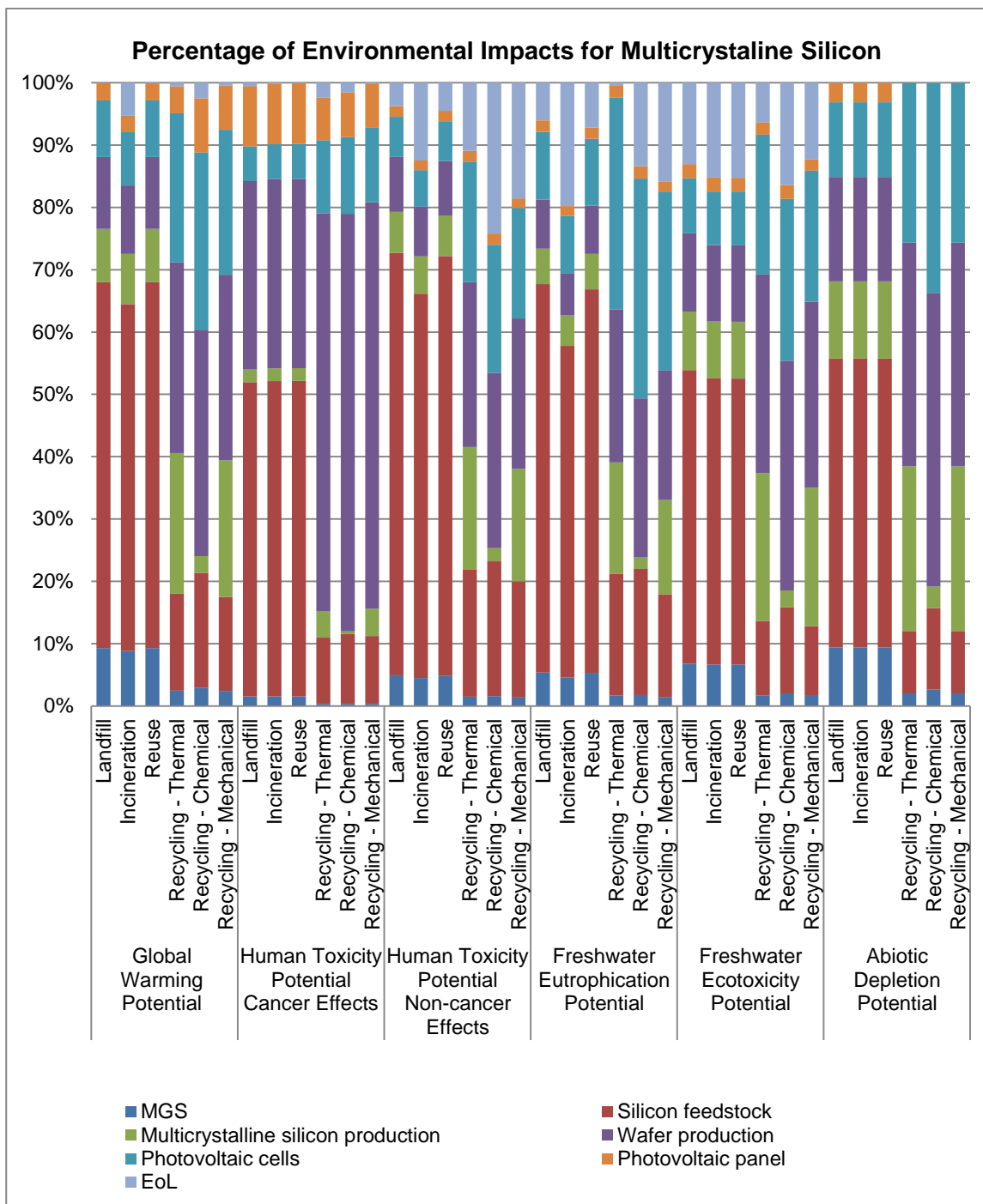
Figure 58: Relative environmental impacts for different end-of-life scenarios considering multicrystalline silicon solar modules, considering landfill, incineration, reuse and recycling (thermal, chemical and mechanical) but excluding transport.
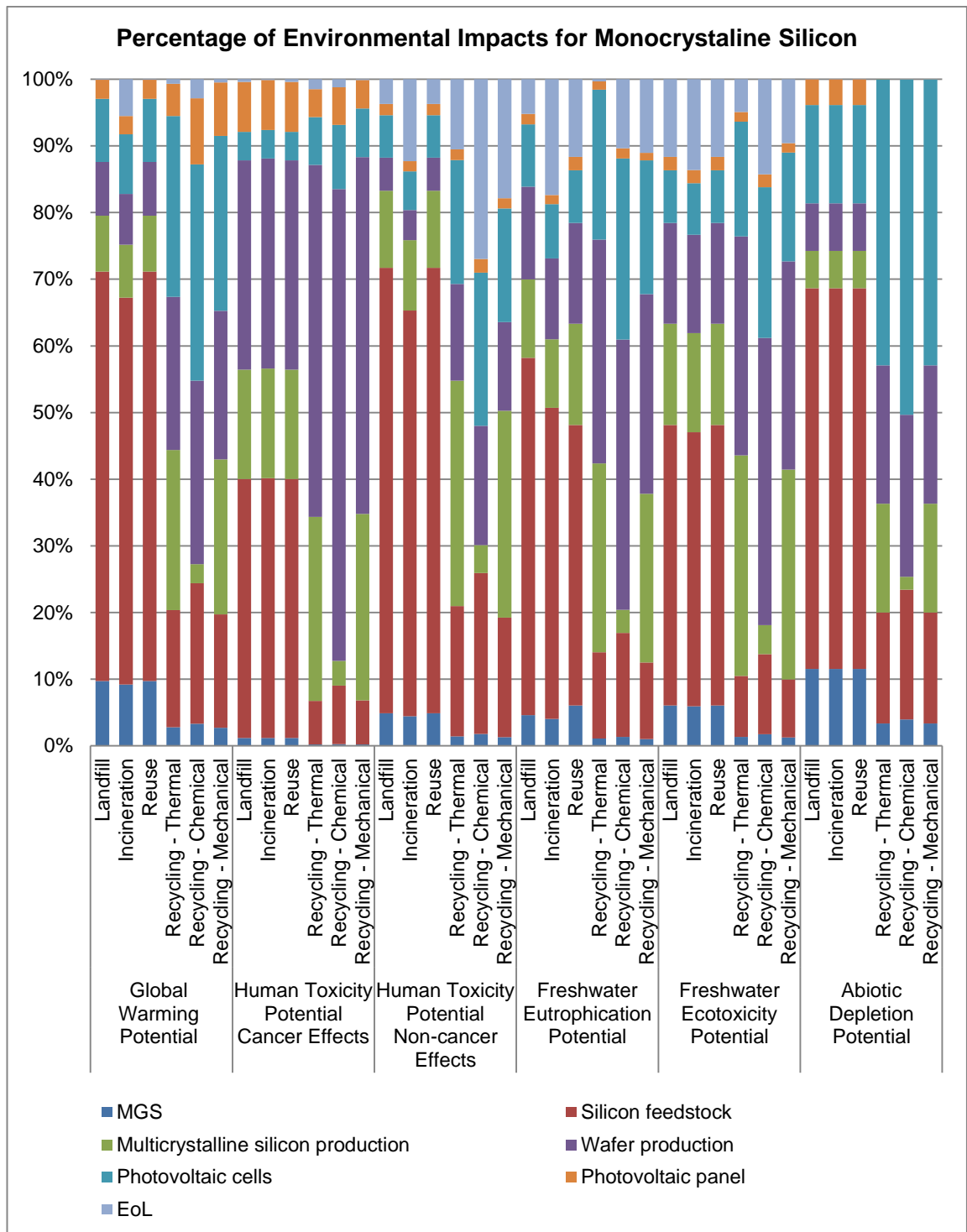
Figure 59: Relative environmental impacts for different end-of-life scenarios considering monocrystalline silicon solar modules, considering landfill, incineration, reuse and recycling (thermal, chemical and mechanical) but excluding transport.

Considering Figures 58 and 59 the GWP impacts are mostly produced by the Si feedstock (in this case, 50% of SGS and 50% of EGS) due to the high energy requirement for these processes [42]. The chemical recycling process can recover intact Si wafers and reuse them to produce solar cells. The thermal and mechanical treatments can recover crushed Si solar cells and reprocess them by ingot growth, and it would probably be economically advantageous as well. The possibility of reuse Si as raw material or intact wafers to produce new solar cells would be beneficial regarding environmental outcomes from the entire process, as well as the recovery of unbroken and clean glass [268].

It is evident that the overall results from the recycling processes are environmentally favourable when compared with the other scenarios analysed in this study, but some additional aspects should be taken into consideration. Lower environmental impacts may be achieved with more complex recycling methods that can recover other elements (mostly metals) and reuse them in new solar cells and modules. The European directive regarding electronic waste management, which includes PV modules, highlights the importance of recycling potentially harmful substances and rare materials as an environmental solution [342].

Additionally, the substances used during the chemical recycling treatment studied (tetrahydrofuran, o-dichlorobenzene and toluene, which is the most commonly used) present serious issues related to human health and can be risky for fauna and flora as well. Tetrahydrofuran is a carcinogen and when in contact with humans or animals, can cause severe diseases and even death. This substance is mobile in the environment causing contamination of water, soil and air [345]. The o-dichlorobenzene is not carcinogenic but, otherwise, has serious environmental and health effects [346]. Toluene is also toxic for both humans and animals for acute (short-term) and chronic (long-term) exposures. It can cause several illnesses, but there is insufficient

information to assess the carcinogenic potential of this substance. It is an environmentally hazardous material that can affect soil and water, causing long-lasting effects in aquatic organisms [347].

Finally, transportation could have added some impacts to these possible EoL scenarios [311], but these data depend entirely on the location of the modules and their final destination. These impacts can be negligible if the sites for the collection of the PV panels, treatment and disposal are assumed to be in the same area, but in most of the cases, the data for transport mode and distance is difficult to assess for the general case [268].

It is important to notice that significant impacts on the different categories related to the transport of the PV waste to the site were calculated for the FRELP process [311], for example. The contribution of transport was shown to be relevant in that particular case, and it should be considered. As the location of the EoL treatment plant was not set in this study, Figures 60, 61 and 62 show an estimated distance necessary for the recycling process to still have lower environmental impacts compared to the other EoL options analysed. For this analysis, only terrestrial transportation (Ecoinvent inventory for "lorry 16-32 t") was considered, and different distances ware investigated from the collection point to the EoL treatment facility.
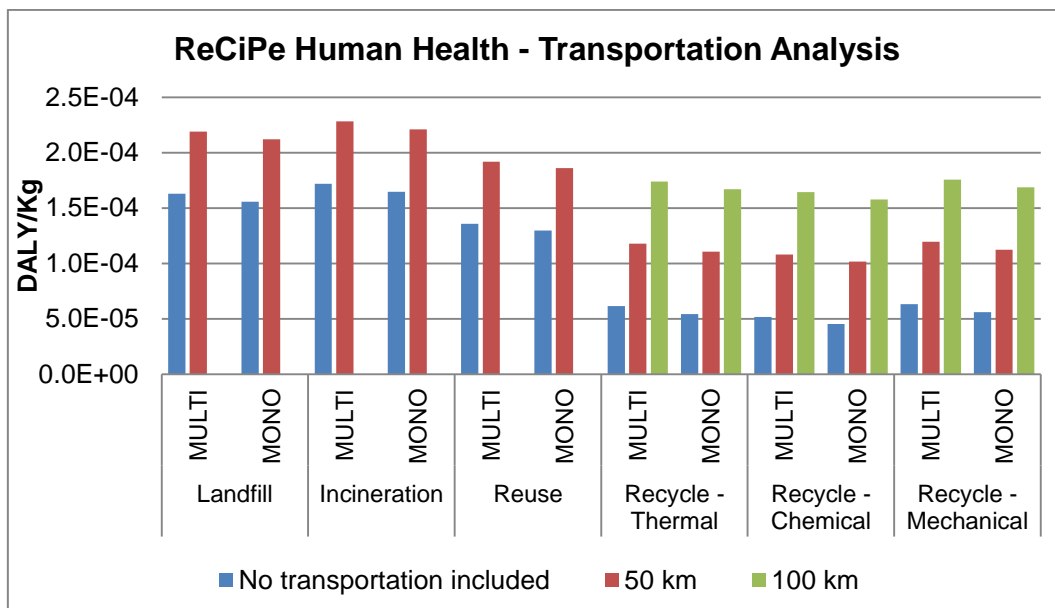
Figure 60: Inclusion of transportation on the final results for the EoL scenarios analysed for Human Health (ReCiPe), considering that the landfill and incineration plants are within 50 km from the collection point in all cases.
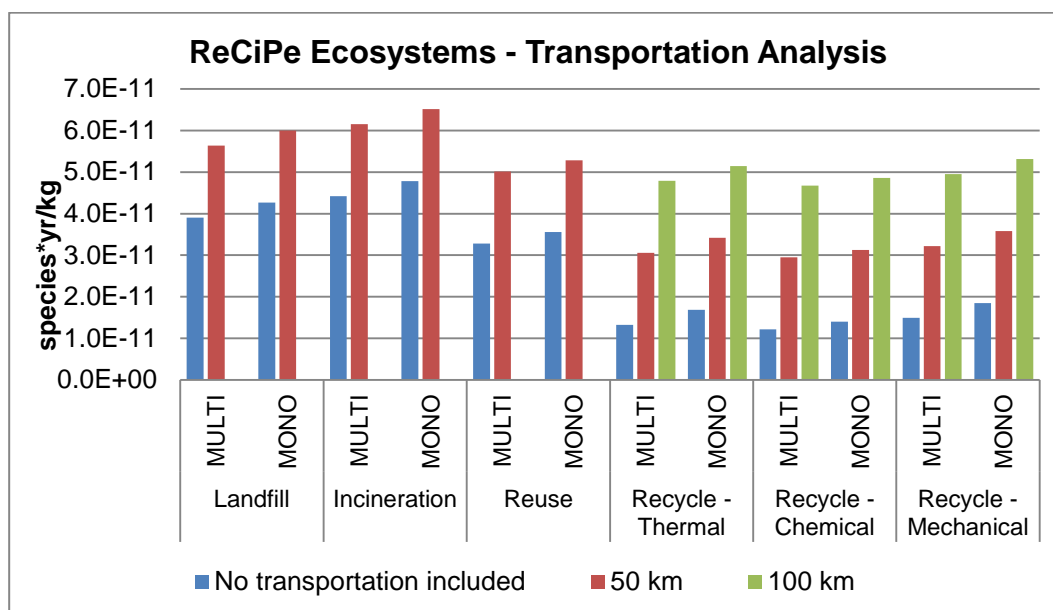
Figure 61: Inclusion of transportation on the final results for the EoL scenarios analysed for Ecosystems (ReCiPe), considering that the landfill and incineration plants are within 50 km from the collection point in all cases.
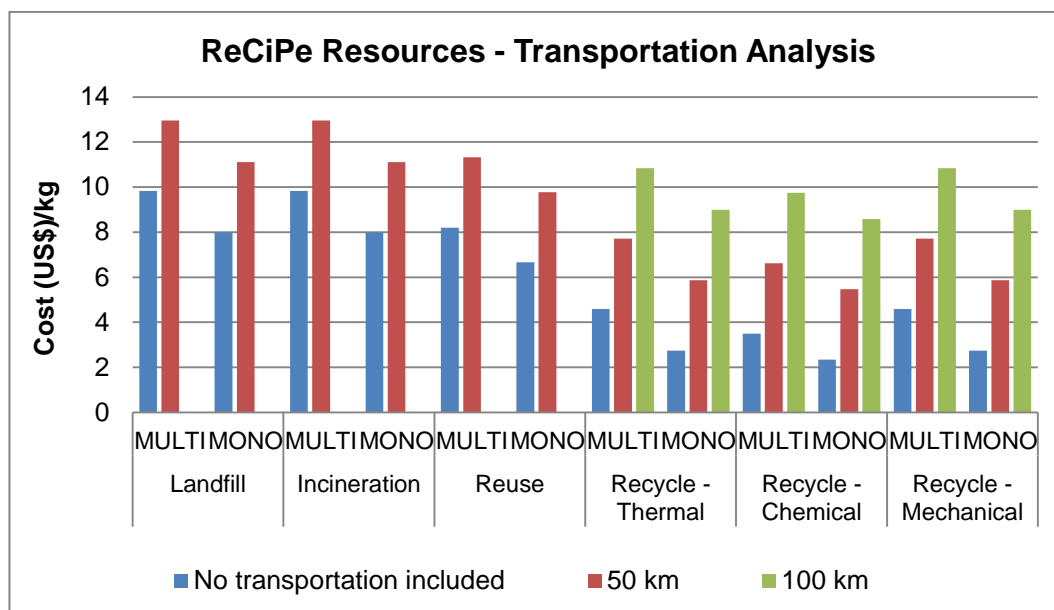
Figure 62: Inclusion of transportation on the final results for the EoL scenarios analysed for Resources (ReCiPe), considering that the landfill and incineration plants are within 50 km from the collection point in all cases

The inclusion of transportation increases the overall results for all three ReCiPe environmental categories, which is in line with other studies [311]. It is important to highlight that the impacts from the transportation will depend not only on the distance from the collection point to the EoL treatment facility but also on the transportation mode.

The analysis of ReCiPe human health and ecosystems, effects shows that the recycling plant needs to be within a maximum distance of 80 km for recycling to have lower impacts, considering human health and ecosystems than the other EoL scenarios (if they are assumed to be located 50 km from the collection point).

The ReCiPe resources effects show that the related impacts are strongly influenced by the transportation stage in all EoL scenarios analysed. In this case, for the distance of 100 km, the recycling processes are still better environmental options compared with some other choices, but it appears that it will be essential to develop portable or fixed

recycling processes that can be located reasonably close to the places where modules reach EoL.

8.5 Conclusions

This chapter presented the preliminary results for the analysis of the environmental impacts of PV modules EoL scenarios such as landfill, incineration, reuse and recycling (mechanical, thermal and chemical methods).

The results validate the environmental benefits of the recycling processes when compared with other possible scenarios for all categories, considering the assumptions made in this LCA. The main reason for that is the recovery of materials such as glass and Si that can be reused to manufacture new solar cells and modules.

The ADP impacts from the recycling processes are still higher than the other EoL scenarios. This outcome could be lower with the adoption of more complex recycling processes that can recycle more substances, such as Pb. Especially for thermal recycling, it is vital to include a combination of other methods after the recovery of the glass. Studies show that the combination of thermal and chemical processes can achieve good recycling rates and recover almost all materials from solar modules [311, 329, 348].

Another critical concern is the use of toxic substances during the chemical recycling treatment. Chemicals such as tetrahydrofuran, o-dichlorobenzene and toluene were considered in this chapter because they show the most promising recycling results. However, these substances present serious issues related to human health, fauna and flora. Alternative chemicals should be tested to decrease possibilities of environmental impacts associated with chemical routes for recycling solar modules.

Transportation can add significant environmental impacts to all scenarios analysed. This LCA suggested that, if the landfill or incineration plants are within 50 km from the collection point and if we require that ReCiPe human health and ecosystems impacts should be better than the other options studied, the maximum distance from the collection point to the recycling facility (all methods), should be 80 km for road transport. The implications for ReCiPe resources are also heavily impacted by transportation and, in this case, a distance of 100 km shows the recycling processes as the best environmental option, if road transport is assumed.

In summary, the key finding of this preliminary study is that the possibility of recycling materials from solar modules may result in lower environmental impacts when compared with landfill, incineration and reuse, based on the assumptions made in this LCA, but attention should be given to the transportation for all cases. Small fixed or portable recycling facilities could be considered, as could less damaging transport modes than road trucks. Attention should be given, too, to reducing the use of toxic substances during the chemical routes for recycling.

Further studies regarding possible recycling routes should be made to create a comprehensive inventory specific to PV modules for all possible EoL scenarios. Also, other technologies should be analysed, even before their industrialisation to be prepared to handle this type of waste.

List of Publications

Journal Articles

Lunardi, M.M; Ho-Baillie, A.W.Y.; Alvarez-Gaitan, J.P.; Moore, S. and Corkish, R. "A life cycle assessment of perovskite/silicon tandem solar cells." Progress in Photovoltaics: Research and Applications 25.8 (2017), 679-695.

Lunardi, M.M.; Moore, S.; Alvarez-Gaitan, J.P.; Yan, C.; Hao, X. and Corkish R. "A comparative life cycle assessment of chalcogenide/Si tandem solar modules." Energy 145 (2018), 700-709.

Lunardi, M.M.; Alvarez-Gaitan, J.P.; Chang, N. and Corkish, R. "Life cycle assessment on PERC solar modules." Solar Energy Materials and Solar Cells, 187 (2018),154-159.

Lunardi, M.M.; Alvarez-Gaitan, J.P.; Bilbao, J.I. and Corkish, R. "Comparative Life Cycle Assessment of End-of-Life Silicon Solar Photovoltaic Modules." Applied Sciences 8, no. 8 (2018), 1396.

Lunardi, M.M.; Needell, D.R.; Bauser, H.; Phelan, M.; Atwater, H.A. and Corkish, R. "Life Cycle Assessment on Tandem LSC-Si Device", Under Review for Energy.

Lunardi, M.M.; Alvarez-Gaitan, J.P.; Bilbao, J.I. and Corkish, R. "Life Cycle Assessment of Silicon-Based Tandem Solar Photovoltaics and their End-of-Life" Indonesian Journal of Life Cycle Assessment and Sustainability, V. 2, no. 1, (2018).

Conference Articles

Lunardi, M.M.; Alvarez-Gaitan, J.P.; Chang, N. and Corkish, R. "Life Cycle Assessment on Advanced Silicon Solar Modules" Asia-Pacific Solar Research Conference, Melbourne, December 2017.

Lunardi, M.M.; Alvarez-Gaitan, J.P.; Chang, N. and Corkish, R. "Life Cycle Assessment of Hydrogenation Processes on Silicon Solar Modules" 7th World Conference on Photovoltaic Energy Conversion, June 2018.

Lunardi, M.M.; Alvarez-Gaitan, J.P.; Bilbao, J.I. and Corkish, R. "Life Cycle Assessment of Silicon-Based Tandem Solar Photovoltaics and their End-of-Life" The International Conference Series on Life Cycle Assessment (ICSoLCA), October 2018.

Book Chapters

Lunardi, M.M.; Alvarez-Gaitan, J.P; Bilbao, J.I. and Corkish, R. "A Review of Recycling Processes for Photovoltaic Modules." In Solar Panels and Photovoltaic Materials. IntechOpen, Chapter 2, 2018.

Conference Oral Presentations

Asia-Pacific Solar Research Conference (APSRC) 2015 (Brisbane): LCA of Perovskite/Si tandem solar cells (preliminary results)

Asia-Pacific Solar Research Conference (APSRC) 2016 (Canberra): A LCA of perovskite/Si tandem solar cells

Asia-Pacific Solar Research Conference (APSRC) 2017 (Melbourne): Life Cycle Assessment on Advanced Silicon Solar Modules

Asia-Pacific Solar Research Conference (APSRC) 2018 (Sydney): A comparative LCA of end-of-life silicon solar modules

Conference Poster Presentations

European Photovoltaic Solar Energy Conference and Exhibition (EU PVSEC) – Amsterdam 2017: Lunardi, M.M.; Moore, S.; Alvarez-Gaitan, J.P.; Yan, C.; Hao, X. and Corkish R. "A LCA of Chalcogenide/Si Tandem Solar Modules".

IEEE Photovoltaic Specialist Conference, World Conference on Photovoltaic Energy Conversion (WCPEC-7) - Hawaii 2018 (presented by Richard Corkish): Lunardi, M.M.; Alvarez-Gaitan, J.P.; Chang, N. and Corkish, R. "LCA on Hydrogenation Processes on Silicon Solar Modules".

References

1.   United Nations, *Adoption of the Paris Agreement*, 21st meeting of the Conference of the Parties, 2015, Paris.

2.   REN21, *Renewables 2018 Global Status Report*. 2018.

3.   Frankl, P., et al., *International energy agency technology roadmap: solar photovoltaic energy*. 2010.

4.   Shockley, W. and Queisser, H.J. *Detailed balance limit of efficiency of p‑n junction solar cells*. Journal of applied physics, 1961. **32**(3): p. 510-519.

5.   Green, M.A. *Silicon wafer-based tandem cells: The ultimate photovoltaic solution?* in *SPIE OPTO*. 2014. International Society for Optics and Photonics.

6.   Almansouri, I., Ho-Baillie, A. and Green, M.A. *Ultimate efficiency limit of single-junction perovskite and dual-junction perovskite/silicon two-terminal devices*. Japanese Journal of Applied Physics, 2015. **54**(8).

7.   Wanlass, M., et al., *Practical considerations in tandem cell modeling*. Solar Cells, 1989. **27**(1): p. 191-204.

8.   Barber, G.D., et al., *Utilization of Direct and Diffuse Sunlight in a Dye-Sensitized Solar Cell - Silicon Photovoltaic Hybrid Concentrator System*. Journal of Physical Chemistry Letters, 2011. **2**(6): p. 581-585.

9.   Seo, J.H., et al., *High Efficiency Inorganic/Organic Hybrid Tandem Solar Cells*. Advanced Materials, 2012. **24**(33): p. 4523-4527.

10.   Yang, J., Banerjee, A. and Guha, S. *Triple-junction amorphous silicon alloy solar cell with 14.6% initial and 13.0% stable conversion efficiencies*. Applied Physics Letters, 1997. **70**(22): p. 2975-2977.

11.   Keppner, H., et al., *Microcrystalline silicon and micromorph tandem solar cells*. Applied physics A, 1999. **69**(2): p. 169-177.

12.   Yamaguchi, M., *III–V compound multi-junction solar cells: present and future*. Solar energy materials and solar cells, 2003. **75**(1-2): p. 261-269.

13.   Lee, M.M., et al., *Efficient Hybrid Solar Cells Based on Meso-Superstructured Organometal Halide Perovskites*. Science, 2012. **338**(6107): p. 643-647.

14.   Kim, H.S., Im, S.H. and Park, N.G. *Organolead Halide Perovskite: New Horizons in Solar Cell Research*. Journal of Physical Chemistry C, 2014. **118**(11): p. 5615-5625.

15.   Polman, A., et al., *Photovoltaic materials: Present efficiencies and future challenges*. Science, 2016. **352**(6283): p. aad4424.

16.   Bailie, C.D., et al., *Semi-transparent perovskite solar cells for tandems with silicon and CIGS*. Energy & Environmental Science, 2015. **8**(3): p. 956-963.

17.   Löper, P., et al., *Organic–inorganic halide perovskite/crystalline silicon four-terminal tandem solar cells*. Physical Chemistry Chemical Physics, 2015. **17**(3): p. 1619-1629.

18.   Todorov, T., et al., *Perovskite-kesterite monolithic tandem solar cells with high open-circuit voltage*. Applied Physics Letters, 2014. **105**(17): p. 173902.

19. Bremner, S., Levy, M. and Honsberg, C.B. *Analysis of tandem solar cell efficiencies under AM1. 5G spectrum using a rapid flux calculation method.* Progress in photovoltaics: Research and Applications, 2008. **16**(3): p. 225-233.

20. Twidell, J. and Weir, T. *Renewable energy resources*. 2015: Routledge.

21. Owens, J., *Life cycle assessment.* J. of Industrial Ecology, 1997. **1**(1): p. 37-49.

22. Efficiency, E., *What is the energy payback for PV?* National Renewable Energy Laboratory, 2004.

23. Redlinger, M., Eggert, R. and Woodhouse, M. *Evaluating the availability of gallium, indium, and tellurium from recycled photovoltaic modules.* Solar Energy Materials and Solar Cells, 2015. **138**: p. 58-71.

24. Abolghasemi, H., *The solar energy industry (PV) and it's future.* World Scientific News, 2016. **52**: p. 195-206.

25. Song, N., et al., *Epitaxial Cu2ZnSnS4 thin film on Si (111) 4° substrate.* Applied Physics Letters, 2015. **106**(25): p. 252102.

26. Shin, B., et al., *Epitaxial growth of kesterite Cu 2 ZnSnS 4 on a Si (001) substrate by thermal co-evaporation.* Thin Solid Films, 2014. **556**: p. 9-12.

27. Oishi, K., et al., *Growth of Cu 2 ZnSnS 4 thin films on Si (100) substrates by multisource evaporation.* Thin Solid Films, 2008. **517**(4): p. 1449-1452.

28. Green, M.A., et al., *Solar cell efficiency tables (version 52).* Prog Photovolt Res Appl., 2018(26): p. 427–436.

29. Malerba, C., et al., *CZTS stoichiometry effects on the band gap energy.* Journal of alloys and compounds, 2014. **582**: p. 528-534.

30. Gershon, T., et al., *Photovoltaic Device with over 5% Efficiency Based on an n-Type $Ag_2ZnSnSe_4$ Absorber.* Advanced Energy Materials, 2016.

31. Jing, T., et al., *Electronic Structure and Photocatalytic Water-Splitting Properties of $Ag_2ZnSn (S_{1-x} Se_x)_4$.* The Journal of Physical Chemistry C, 2015. **119**(50): p. 27900-27908.

32. ITRPV, *International Technology Roadmap for Photovoltaic Results 2017*. 2018.

33. Narasinha, S. and Rohatgi, A. *Optimized aluminum back surface field techniques for silicon solar cells*, in *Photovoltaic Specialists Conference, 1997., Conference Record of the Twenty-sixth IEEE*. 1997, IEEE. p. 63-66.

34. Green, M.A., *The passivated emitter and rear cell (PERC): From conception to mass production.* Solar Energy Materials and Solar Cells, 2015. **143**: p. 190-197.

35. Dubey, S., Jadhav, N.Y. and Zakirova, B. *Socio-economic and environmental impacts of silicon based photovoltaic (PV) technologies.* Energy Procedia, 2013. **33**: p. 322-334.

36. Khattak, C.P., Joyce, D.B. and Schmid, F. *A simple process to remove boron from metallurgical grade silicon.* Solar energy materials and solar cells, 2002. **74**(1-4): p. 77-89.

37. Forster, M., et al., *Ga co-doping in Cz-grown silicon ingots to overcome limitations of B and P compensated silicon feedstock for PV applications.* physica status solidi (c), 2011. **8**(3): p. 678-681.

38. Energiewende, A., *Current and Future Cost of Photovoltaics: Long-term Scenarios for Market Development, System Prices and LCOE of Utility-scale PV Systems.* Study prepared by Fraunhofer Institute for Solar Energy Systems, 2015.

39. International Organization for Standardization, *ISO 14040: Environmental Management-Life Cycle Assessment-Principles and Framework.* 1997.

40. Jungbluth, N., et al., *Photovoltaics - Part XII*, R.E.e.a. In Dones, Editor. 2010, ecoinvent report No. 6-XII.

41. *GaBi LCA Software.* 2016. Available from: <http://www.gabi-software.com/australia/index/>, Acessed on: 20/01/2016.

42. Frischknecht, R., et al., *Life Cycle Inventories and Life Cycle Assessment of Photovoltaic Systems.* International Energy Agency (IEA) PVPS Task 12, Report T12, 2015. **4**.

43. Archer, M.D. and Green, M.A. *Clean electricity from photovoltaics.* Vol. 4. 2014: World Scientific.

44. Parida, B., Iniyan, S. and Goic, R. *A review of solar photovoltaic technologies.* Renewable and sustainable energy reviews, 2011. **15**(3): p. 1625-1636.

45. Becquerel, A., *Recherches sur les effets de la radiation chimique de la lumière solaire au moyen des courants électriques.* Comptes Rendus de LAcadémie des Sciences, 1839. **9**: p. 145-149.

46. Kazmerski, L.L., *Photovoltaics: a review of cell and module technologies.* Renewable and sustainable energy reviews, 1997. **1**(1): p. 71-170.

47. Hersch, P. and Zweibel, K. *Basic photovoltaic principles and methods.* 1982, Solar Energy Research Inst., Golden, CO (USA).

48. Smits, F.M., *History of Silicon Solar-Cells.* Ieee Transactions on Electron Devices, 1976. **23**(7): p. 640-643.

49. Loferski, J.J., *The first forty years: a brief history of the modern photovoltaic age.* Progress in photovoltaics: research and applications, 1993. **1**(1): p. 67-78.

50. Hammonds, M., *Getting power from the sun.* Chemistry & Industry, 1998(6): p. 219-222.

51. Kalogirou, S.A., *Solar energy engineering: processes and systems.* 2013: Academic Press.

52. Luque, A. and Hegedus, S.*Handbook of photovoltaic science and engineering.* 2011: John Wiley & Sons.

53. Coiante, D. and Barra, L. *Can Photovoltaics Become an Effective Energy Option.* Solar Energy Materials and Solar Cells, 1992. **27**(1): p. 79-89.

54. Dovey, C., *Australia's solar champions face an uncertain future*, in *The Monthly.* 2016.

55. World Energy Council, *Survey of energy resources 2007.* Retrieved on 20 of January, 2009.

56. Markvart, T. and Castañer, L. *Practical handbook of photovoltaics: fundamentals and applications.* 2003: Elsevier.

57. Bakhiyi, B., Labreche, F. and Zayed, J. *The photovoltaic industry on the path to a sustainable future - Environmental and occupational health issues.* Environment International, 2014. **73**: p. 224-234.

58.   De Wolf, S., et al., *High-efficiency silicon heterojunction solar cells: A review.* green, 2012. **2**(1): p. 7-24.

59.   Zhao, J., et al., *19.8% efficient "honeycomb" textured multicrystalline and 24.4% monocrystalline silicon solar cells.* Applied Physics Letters, 1998. **73**(14): p. 1991-1993.

60.   Sopori, B., *Silicon solar-cell processing for minimizing the influence of impurities and defects.* Journal of Electronic Materials, 2002. **31**(10): p. 972-980.

61.   Hallam, B., et al., *Techniques for mitigating light-induced degradation (LID) in commercial silicon solar cells.* Photovoltaics International, 2016. **33**: p. 37–46.

62.   Phylipsen, G. and Alsema, E. *Environmental life-cycle assessment of multicrystalline silicon solar cell modules.* 1995: Department of Science, Technology and Society, Utrecht University.

63.   Pizzini, S., et al., *On the Effect of Impurities on the Photovoltaic Behavior of Solar Grade Silicon II. Influence of Titanium, Vanadium, Chromium, Iron, and Zirconium on Photovoltaic Behavior of Polycrystalline Solar Cells.* Journal of the Electrochemical Society, 1986. **133**(11): p. 2363-2373.

64.   Pizzini, S., Acciarri, M. and Binetti, S. *From electronic grade to solar grade silicon: chances and challenges in photovoltaics.* physica status solidi (a), 2005. **202**(15): p. 2928-2942.

65.   Bye, G. and Ceccaroli, B. *Solar grade silicon: Technology status and industrial trends.* Solar Energy Materials and Solar Cells, 2014. **130**: p. 634-646.

66.   de Wild-Scholten, M., et al. *LCA comparison of the Elkem Solar metallurgical route and conventional gas routes to solar silicon.* in *Proceedings of the 23rd European photovoltaic solar energy conference, Valencia, Spain.* 2008.

67.   Mukashev, B., et al., *Upgrading Metallurgical Grade Silicon to Solar Grade Silicon.* Eurasian Chemico-Technological Journal, 2014. **16**(4): p. 309-313.

68.   Sarti, D. and Einhaus, R. *Silicon feedstock for the multi-crystalline photovoltaic industry.* Solar Energy Materials and Solar Cells, 2002. **72**(1-4): p. 27-40.

69.   Ranjan, S., et al., *Silicon solar cell production.* Computers & Chemical Engineering, 2011. **35**(8): p. 1439-1453.

70.   Heine, C. and Morf, R.H. *Submicrometer gratings for solar energy applications.* Applied Optics, 1995. **34**(14): p. 2476-2482.

71.   van Sark, W., Korte, L. and Roca, F. *Physics and technology of amorphous-crystalline heterostructure silicon solar cells.* 2012. Springer.

72.   Shah, A., et al., *Photovoltaic technology: the case for thin-film solar cells.* science, 1999. **285**(5428): p. 692-698.

73.   Chopra, K., Paulson, P. and Dutta, V. *Thin‐film solar cells: an overview.* Progress in Photovoltaics: Research and applications, 2004. **12**(2-3): p. 69-92.

74.   Tawada, Y., Yamagishi, H. and Yamamoto, K. *Mass production of large-area integrated thin-film silicon solar-cell module*, in *Thin-Film Solar Cells*. 2004, Springer. p. 150-162.

75.   Yamamoto, K., *Very thin film crystalline silicon solar cells on glass substrate fabricated at low temperature.* IEEE Transactions on Electron Devices, 1999. **46**(10): p. 2041-2047.

76. Yang, J., et al. *Recent progress in amorphous silicon alloy leading to 13% stable cell efficiency*. in *Photovoltaic Specialists Conference, 1997., Conference Record of the Twenty-Sixth IEEE*. 1997. IEEE.

77. Mai, Y., et al., *Improvement of open circuit voltage in microcrystalline silicon solar cells using hot wire buffer layers*. Journal of Non-Crystalline Solids, 2006. **352**(9-20): p. 1859-1862.

78. Lechner, P. and Schade, H. *Photovoltaic thin‐film technology based on hydrogenated amorphous silicon*. Progress in Photovoltaics: Research and Applications, 2002. **10**(2): p. 85-97.

79. International Energy Agency - Photovoltaic Power Systems Programme (IEA-PVPS), *Snapshot of Global Photovoltaic Markets*, in IEA Photovoltaic Power Systems Programme Report T1-29. 2016.

80. Aberle, A.G., *Thin-film solar cells*. Thin solid films, 2009. **517**(17): p. 4706-4710.

81. Song, T., Moore, A. and. Sites, J.R *Te Layer to Reduce the CdTe Back-Contact Barrier*. IEEE Journal of Photovoltaics, 2018. **8**(1): p. 293-298.

82. Phipps, G., Mikolajczak, C. and Guckes, T. *Indium and gallium: long-term supply*. Renewable energy focus, 2008. **9**(4): p. 56-59.

83. Grätzel, M., *Dye-sensitized solar cells*. Journal of Photochemistry and Photobiology C: Photochemistry Reviews, 2003. **4**(2): p. 145-153.

84. Hagfeldt, A. and Vlachpoulos, N. *Dye-sensitized solar cells*, in *The Future of Semiconductor Oxides in Next-Generation Solar Cells*. 2018, Elsevier. p. 183-239.

85. Darling, S.B. and You, F. *The case for organic photovoltaics*. Rsc Advances, 2013. **3**(39): p. 17633-17648.

86. Mazzio, K.A. and Luscombe, C.K. *The future of organic photovoltaics*. Chemical Society Reviews, 2014. **44**(1): p. 78-90.

87. Xiao, Z., Jia, X. and Ding, L. *Ternary organic solar cells offer 14% power conversion efficiency*. Sci. Bull, 2017. **62**(23): p. 1562-1564.

88. Tanenbaum, D.M., et al., *The ISOS-3 inter-laboratory collaboration focused on the stability of a variety of organic photovoltaic devices*. Rsc Advances, 2012. **2**(3): p. 882-893.

89. Green, M.A., Ho-Baillie, A. and Snaith, H.J. *The emergence of perovskite solar cells*. Nature Photonics, 2014. **8**(7): p. 506-514.

90. Yang, W.S., et al., *High-performance photovoltaic perovskite layers fabricated through intramolecular exchange*. Science, 2015. **348**(6240): p. 1234-1237.

91. Hodes, G., *Perovskite-based solar cells*. Science, 2013. **342**(6156): p. 317-318.

92. Rong, Y., et al., *Challenges for commercializing perovskite solar cells*. Science, 2018. **361**(6408): p. eaat8235.

93. Chen, P.Y., et al., *Environmentally responsible fabrication of efficient perovskite solar cells from recycled car batteries*. Energy & Environmental Science, 2014. **7**(11): p. 3659-3665.

94. Yoshida, S., *Tandem solar cell*. 1991, Google Patents.

95. Sameshima, T., et al., *Multi junction solar cells stacked with transparent and conductive adhesive*. Japanese Journal of Applied Physics, 2011. **50**(5R): p. 052301.

96. Zhao, L., et al., *Novel mechanically stacked multi-junction solar cells applying ultra-thin III-V cells and wafer based germanium cell.* ECS Transactions, 2010. **27**(1): p. 1123-1128.

97. Corporation, S., *Sharp Develops Concentrator Solar Cell with World's Highest Conversion Efficiency of 43.5%.* 2012. Available at: <http://sharp-world.com/corporate/news/120531.html>, Acessed on: 04/06/2016.

98. Zhang, S., et al., *335-W world-record p-type monocrystalline module with 20.6% efficient PERC solar cells.* IEEE Journal of Photovoltaics, 2016. **6**(1): p. 145-152.

99. Yoshikawa, K., et al., *Silicon heterojunction solar cell with interdigitated back contacts for a photoconversion efficiency over 26%.* Nature Energy, 2017. **2**(5): p. 17032.

100. Duda, M. and Shaw, J.S. *Life cycle assessment.* Society, 1997. **35**(1): p. 38-43.

101. Maycock, P. *The development of photovoltaics as a power source of large scale terrestrial application.* in *Thirteenth IEEE Photovoltaic Specialists Conference-1978.* 1978.

102. Eliot, P., Lasnier, F. and Pergeline. V. *Future of photovoltaics for residential applications in France.* in *Photovoltaic Solar Energy Conference.* 1981. Springer.

103. Kim, H.C., et al., *Life cycle greenhouse gas emissions of thin-film photovoltaic electricity generation.* Journal of Industrial Ecology, 2012. **16**(s1): p. S110-S121.

104. Hsu, D.D., et al., *Life cycle greenhouse gas emissions of crystalline silicon photovoltaic electricity generation.* Journal of Industrial Ecology, 2012. **16**(s1): p. S122-S135.

105. Bhandari, K.P., et al., *Energy payback time (EPBT) and energy return on energy invested (EROI) of solar photovoltaic systems: A systematic review and meta-analysis.* Renewable and Sustainable Energy Reviews, 2015. **47**: p. 133-141.

106. Louwen, A., et al., *Re-assessment of net energy production and greenhouse gas emissions avoidance after 40 years of photovoltaics development.* Nature Communications, 2016. **7**: p. 13728.

107. Frischknecht, R., et al., *Methodology guidelines on life cycle assessment of photovoltaic electricity.* 2016, National Renewable Energy Laboratories (NREL), Golden, CO (United States).

108. Fthenakis, V., et al. *Update of PV energy payback times and life-cycle greenhouse gas emissions.* in *24th European Photovoltaic Solar Energy Conference and Exhibition.* 2009.

109. Knapp, K. and Jester, T. *Empirical investigation of the energy payback time for photovoltaic modules.* Solar Energy, 2001. **71**(3): p. 165-172.

110. Lunardi, M.M., et al., *A life cycle assessment of perovskite/silicon tandem solar cells.* Progress in Photovoltaics: Research and Applications, 2017. **25**(8): p. 679-695.

111. International Reference Life Cycle Data System, *ILCD handbook Recommendations for Life Cycle Impact Assessment in the European context-based on existing environmental impact assessment models and factors, First edit. ed.* Publication Office of the European Union, 2011.

112. Fthenakis, V. and Kim, H.C. *Photovoltaics: Life-cycle analyses.* Solar Energy, 2011. **85**(8): p. 1609-1628.

113. Alsema, E., *Energy pay-back time and CO2 emissions of photovoltaic systems.* Progress in photovoltaics: research and applications, 2000. **8**(1): p. 17-25.

114. Ito, M., et al., *A preliminary study on potential for very large-scale photovoltaic power generation (VLS-PV) system in the Gobi desert from economic and environmental viewpoints.* Solar Energy Materials and Solar Cells, 2003. **75**(3-4): p. 507-517.

115. Battisti, R. and Corrado, A. *Evaluation of technical improvements of photovoltaic systems through life cycle assessment methodology.* Energy, 2005. **30**(7): p. 952-967.

116. Ito, M., et al., *A comparative study on cost and life‑cycle analysis for 100 MW very large‑scale PV (VLS‑PV) systems in deserts using m‑Si, a‑Si, CdTe, and CIS modules.* Progress in Photovoltaics: research and applications, 2008. **16**(1): p. 17-30.

117. Pacca, S., Sivaraman, D. and Keoleian, G.A. *Parameters affecting the life cycle performance of PV technologies and systems.* Energy Policy, 2007. **35**(6): p. 3316-3326.

118. Graebig, M., Bringezu, S. and Fenner, R. *Comparative analysis of environmental impacts of maize–biogas and photovoltaics on a land use basis.* Solar Energy, 2010. **84**(7): p. 1255-1263.

119. Sumper, A., et al., *Life-cycle assessment of a photovoltaic system in Catalonia (Spain).* Renewable and sustainable energy reviews, 2011. **15**(8): p. 3888-3896.

120. Desideri, U., et al., *Life Cycle Assessment of a ground-mounted 1778 kWp photovoltaic plant and comparison with traditional energy production systems.* Applied Energy, 2012. **97**: p. 930-943.

121. Leccisi, E., Raugei, M. and Fthenakis, V. *The Energy and environmental performance of ground-mounted photovoltaic systems—A timely update.* Energies, 2016. **9**(8): p. 622.

122. Alsema, E. and de Wild, M.J. *Environmental impact of crystalline silicon photovoltaic module production.* MRS Online Proceedings Library Archive, 2005. **895**.

123. Fu, Y., Liu, X. and Yuan, Z. *Life-cycle assessment of multi-crystalline photovoltaic (PV) systems in China.* Journal of Cleaner Production, 2015. **86**: p. 180-190.

124. Hong, J., et al., *Life cycle assessment of multicrystalline silicon photovoltaic cell production in China.* Solar Energy, 2016. **133**: p. 283-293.

125. Jungbluth, N., et al., *Life cycle assessment for emerging technologies: case studies for photovoltaic and wind power (11 pp).* The International Journal of Life Cycle Assessment, 2005. **10**(1): p. 24-34.

126. Stoppato, A., *Life cycle assessment of photovoltaic electricity generation.* Energy, 2008. **33**(2): p. 224-232.

127. Desideri, U., et al., *Comparative analysis of concentrating solar power and photovoltaic technologies: technical and environmental evaluations.* Applied energy, 2013. **102**: p. 765-784.

128. Reich, N., et al., *Greenhouse gas emissions associated with photovoltaic electricity from crystalline silicon modules under various energy supply options.* Progress in Photovoltaics: Research and Applications, 2011. **19**(5): p. 603-613.

129. Alsema, E. and de Wild-Scholten, M. *The real environmental impacts of crystalline silicon PV modules: an analysis based on up-to-date manufacturers data.* in *Presented at the 20th European Photovoltaic Solar Energy Conference.* 2005.

130. de Wild-Scholten, M. *Energierücklaufzeiten für PV-module und systeme energy payback times of PV modules and systems.* in *Workshop Photovoltaik-Modultechnik.* 2009.

131. Perez, M.J., et al., *Façade–integrated photovoltaics: a life cycle and performance assessment case study.* Progress in Photovoltaics: Research and Applications, 2012. **20**(8): p. 975-990.

132. Louwen, A., et al., *Life‐cycle greenhouse gas emissions and energy payback time of current and prospective silicon heterojunction solar cell designs.* Progress in Photovoltaics: Research and Applications, 2014. **23**(10), pp.1406-1428.

133. Green, M.A., et al., *Crystalline silicon on glass (CSG) thin-film solar cell modules.* Solar energy, 2004. **77**(6): p. 857-863.

134. Raugei, M., Bargigli, S. and Ulgiati, S. *Life cycle assessment and energy pay-back time of advanced photovoltaic modules: CdTe and CIS compared to poly-Si.* Energy, 2007. **32**(8): p. 1310-1318.

135. Collier, J., Wu, S. and Apul, D. *Life cycle environmental impacts from CZTS (copper zinc tin sulfide) and Zn 3 P 2 (zinc phosphide) thin film PV (photovoltaic) cells.* Energy, 2014. **74**: p. 314-321.

136. Mokhtarimehr, M., Forbes, I. andPearsall, N. *Environmental assessment of vacuum and non-vacuum techniques for the fabrication of Cu2ZnSnS4 thin film photovoltaic cells.* Japanese Journal of Applied Physics, 2018. **57**(8S3): p. 08RC14.

137. White, T.P., Lal, N.N. and Catchpole, K.R. *Tandem solar cells based on high-efficiency c-Si bottom cells: top cell requirements for> 30% efficiency.* IEEE Journal of Photovoltaics, 2014. **4**(1): p. 208-214.

138. Kato, K., et al., *A life-cycle analysis on thin-film CdS/CdTe PV modules.* Solar Energy Materials and Solar Cells, 2001. **67**(1-4): p. 279-287.

139. Fthenakis, V. and Kim, H.C. *Energy use and greenhouse gas emissions in the life cycle of CdTe photovoltaics.* MRS Online Proceedings Library Archive, 2005. **895**.

140. Alsema, E., de Wild-Scholten, M. and Fthenakis, V. *Environmental impacts of PV electricity generation-a critical comparison of energy supply options.* in *21st European Photovoltaic Solar Energy Conference.* 2006.

141. Held, M. and Ilg, R. *Update of environmental indicators and energy payback time of CdTe PV systems in Europe.* Progress in photovoltaics: research and applications, 2011. **19**(5): p. 614-626.

142. Veltkamp, A. and de Wild-Scholten, M. *Dye sensitised solar cells for large-scale photovoltaics; the determination of environmental performances.* Renewable Energy, Makuhari Messe, Japan, 2006: p. 9-13.

143. de Wild-Scholten, M. and Veltkamp, A. *Environmental life cycle analysis of dye sensitized solar devices; status and outlook.* in *22nd European Photovoltaic Solar Energy Conference, Milan, Italy.* 2007.

144. Parisi, M.L., Sinicropi, A. and Basosi, R. *Life cycle assessment of thin film non conventional photovoltaics the case of dye sensitized solar cells.* in *25th International Conference on Efficiency, Cost, Optimization, Simulation and Environmental Impact of Energy Systems.* 2012.

145. Parisi, M.L., Maranghi, S. and Basosi, R. *The evolution of the dye sensitized solar cells from Grätzel prototype to up-scaled solar applications: A life cycle assessment approach.* Renewable and Sustainable Energy Reviews, 2014. **39**: p. 124-138.

146. Cheng, P. and Zhan, X. *Stability of organic solar cells: challenges and strategies.* Chemical Society Reviews, 2016. **45**(9): p. 2544-2582.

147. García‑Valverde, R., Cherni, J.A. and Urbina, A. *Life cycle analysis of organic photovoltaic technologies.* Progress in Photovoltaics: Research and Applications, 2010. **18**(7): p. 535-558.

148. Espinosa, N., et al., *A life cycle analysis of polymer solar cell modules prepared using roll-to-roll methods under ambient conditions.* Solar Energy Materials and Solar Cells, 2011. **95**(5): p. 1293-1302.

149. Espinosa, N., et al., *Life cycle assessment of ITO-free flexible polymer solar cells prepared by roll-to-roll coating and printing.* Solar Energy Materials and Solar Cells, 2012. **97**: p. 3-13.

150. Yue, D., et al., *Deciphering the uncertainties in life cycle energy and environmental analysis of organic photovoltaics.* Energy & Environmental Science, 2012. **5**(11): p. 9163-9172.

151. Espinosa, N., et al., *OPV for mobile applications: an evaluation of roll-to-roll processed indium and silver free polymer solar cells through analysis of life cycle, cost and layer quality using inline optical and functional inspection tools.* Journal of Materials Chemistry A, 2013. **1**(24): p. 7037-7049.

152. Roes, A., et al., *Ex‑ante environmental and economic evaluation of polymer photovoltaics.* Progress in Photovoltaics: Research and Applications, 2009. **17**(6): p. 372-393.

153. Espinosa, N., et al., *Solution and vapour deposited lead perovskite solar cells: Ecotoxicity from a life cycle assessment perspective.* Solar Energy Materials and Solar Cells, 2015. **137**: p. 303-310.

154. Serrano-Lujan, L., et al., *Tin‑and Lead‑Based Perovskite Solar Cells under Scrutiny: An Environmental Perspective.* Advanced Energy Materials, 2015. **5**(20).

155. Gong, J., Darling, S.B. and You, F.Q. *Perovskite photovoltaics: life-cycle assessment of energy and environmental impacts.* Energy & Environmental Science, 2015. **8**(7): p. 1953-1968.

156. Celik, I., et al., *Life Cycle Assessment (LCA) of perovskite PV cells projected from lab to fab.* Solar Energy Materials and Solar Cells, 2016.

157. Zhang, J., et al., *Life cycle assessment of titania perovskite solar cell technology for sustainable design and manufacturing.* ChemSusChem, 2015. **8**(22): p. 3882-3891.

158. Alberola-Borràs, J.A., et al., *Relative impacts of methylammonium lead triiodide perovskite solar cells based on life cycle assessment.* Solar Energy Materials and Solar Cells, 2018. **179**: p. 169-177.

159. Billen, P., et al., *Comparative evaluation of lead emissions and toxicity potential in the life cycle of lead halide perovskite photovoltaics.* Energy, 2019. **166**: p. 1089-1096.

160. Meijer, A., et al., *Life‑cycle assessment of photovoltaic modules: comparison of mc‑Si, InGaP and InGaP/mc‑Si solar modules.* Progress in Photovoltaics: Research and Applications, 2003. **11**(4): p. 275-287.

161. Lunardi, M.M., et al., *A comparative life cycle assessment of chalcogenide/Si tandem solar modules.* Energy, 2018. 145, pp.700-709.

162. Itten, R. and Stucki, M. *Highly efficient 3rd generation multi-junction solar cells using silicon heterojunction and perovskite tandem: prospective life cycle environmental impacts.* Energies, 2017. **10**(7): p. 841.

163.   Celik, I., et al., *Environmental analysis of perovskites and other relevant solar cell technologies in a tandem configuration.* Energy & Environmental Science, 2017. **10**(9): p. 1874-1884.

164.   Guinée, J.B. and Heijungs, R. *A proposal for the definition of resource equivalency factors for use in product life‑cycle assessment.* Environmental toxicology and chemistry, 1995. **14**(5): p. 917-925.

165.   Stamford, L. and Azapagic, A. *Life cycle environmental impacts of UK shale gas.* Applied energy, 2014. **134**: p. 506-518.

166.   Jolliet, O., et al., *IMPACT 2002+: a new life cycle impact assessment methodology.* The International Journal of Life Cycle Assessment, 2003. **8**(6): p. 324-330.

167.   Smith, V.H., Tilman, G.D. and Nekola, J.C. *Eutrophication: impacts of excess nutrient inputs on freshwater, marine, and terrestrial ecosystems.* Environmental pollution, 1999. **100**(1): p. 179-196.

168.   Lunardi, M.M., et al., *Comparative Life Cycle Assessment of End-of-Life Silicon Solar Photovoltaic Modules.* Applied Sciences, 2018. **8**(8): p. 1396.

169.   Hutchins, M., *Cell manufacturer ranking.* 2018: PV Magazine.

170.   West, B., *Chinese coal-fired electricity generation expected to flatten as mix shifts to renewables.* 2017, EIA's International Energy Outlook 2017.

171.   U.S. Energy Information Administration, *The United States uses a mix of energy sources.* 2018. Available at: < https://www.eia.gov/energyexplained>, Acessed on: 05/07/2017.

172.   Fthenakis, V., et al., *Methodology Guidelines on Life Cycle Assessment of Photovoltaic Electricity. Subtask 20" LCA", IEA PVPS Task 12.* 2011.

173.   Huijbregts, M.A., et al., *Evaluating uncertainty in environmental life-cycle assessment. A case study comparing two insulation options for a Dutch one-family dwelling.* Environmental science & technology, 2003. **37**(11): p. 2600-2608.

174.   Huijbregts, M.A., et al., *Framework for modelling data uncertainty in life cycle inventories.* The International Journal of Life Cycle Assessment, 2001. **6**(3): p. 127.

175.   Rödger, J.-M., et al., *Life cycle assessment.* Biochar in European Soils and Agriculture: Science and Practice, 2016: p. 184.

176.   Curran, M.A., *Overview of goal and scope definition in life cycle assessment*, in *Goal and Scope Definition in Life Cycle Assessment.* 2017, Springer. p. 1-62.

177.   Rebitzer, G., et al., *Life cycle assessment: Part 1: Framework, goal and scope definition, inventory analysis, and applications.* Environment international, 2004. **30**(5): p. 701-720.

178.   Tillman, A.M., et al., *Choice of system boundaries in life cycle assessment.* Journal of Cleaner Production, 1994. **2**(1): p. 21-29.

179.   Cucchiella, F. and Rosa, P. *End-of-Life of used photovoltaic modules: A financial analysis.* Renewable and Sustainable Energy Reviews, 2015. **47**: p. 552-561.

180.   Weidema, B., et al., *The product, functional unit and reference flows in LCA.* Environmental News, 2004. **70**: p. 1-46.

181.   Klöpffer, W. and Grahl, B. *Life Cycle Inventory Analysis*, in *Life Cycle Assessment (LCA): A Guide to Best Practice.* 2014. p. 63-180.

182. Margni, M. and Curran, M.A. *Life cycle impact assessment.* Life cycle assessment handbook: a guide for environmentally sustainable products, 2012: p. 67-104.

183. Hauschild, M.Z. and Huijbregts, M.A. *Introducing life cycle impact assessment*, in *Life Cycle Impact Assessment.* 2015, Springer. p. 1-16.

184. Guinée, J.B., *Handbook on life cycle assessment operational guide to the ISO standards.* The international journal of life cycle assessment, 2002. **7**(5): p. 311.

185. European Commission - Joint Research Centre, *International reference life cycle data system (ILCD) handbook e general guide for life cycle assessment e detailed guidance.* Institute for Environment and Sustainability, 2010.

186. Mark A.J. Huijbregts, et al., *ReCiPe2016: a harmonized life cycle impact assessment method at midpoint and endpoint level.* . 2016.

187. Renouf, M., et al., *Best Practice Guide for Life Cycle Impact Assessment (LCIA) in Australia.* Australian Life Cycle Assessment Society, 2015.

188. Rogers, J.D. and Stephens, R.D. *Absolute infrared intensities for F-113 and F-114 and an assessment of their greenhouse warming potential relative to other chlorofluorocarbons.* Journal of Geophysical Research: Atmospheres, 1988. **93**(D3): p. 2423-2428.

189. Fisher, D.A., et al., *Model calculations of the relative effects of CFCs and their replacements on stratospheric ozone.* Nature, 1990. **344**(6266): p. 508.

190. Hauschild, M.Z., Olsen, S.I. and Wenzel, H. *Human toxicity as a criterion in the environmental assessment of products*, in *Environmental Assessment of Products. Volume 2: Scientific Background.* 1998, Chapman & Hall. p. 315-444.

191. Hauschild, M.Z., Jolliet, O. and Huijbregts, M.A. *A bright future for addressing chemical emissions in life cycle assessment.* The International Journal of Life Cycle Assessment, 2011. **16**(8): p. 697.

192. Mckone, E.G.H., Pease, W.S. and T. E, *Environmental Policy Analysis: Evaluating Toxic Impact Assessment Methods: What Works Best.* Environmental science & technology, 1998. **32**(5): p. 138A-144A.

193. Hertwich, E.G., et al., *Human toxicity potentials for life-cycle assessment and toxics release inventory risk screening.* Environmental Toxicology and Chemistry, 2001. **20**(4): p. 928-939.

194. Bouwman, L., *Global assessment of acidification and eutrophication of natural ecosystems.* Vol. 6. 1999: UNEP/Earthprint.

195. Worrest, R.C., Smythe, K.D. and Tait, A.M. *Linkages between climate change and stratospheric ozone depletion.* 1989, Environmental Protection Agency, Washington, DC (USA). Office of Research ….

196. Montreal Protocol, *Montreal protocol on substances that deplete the ozone layer.* Washington, DC: US Government Printing Office, 1987. **26**: p. 128-136.

197. Jungbluth, N., Stucki, M. and Frischknecht, R. *Photovoltaics. Sachbilanzen von Energiesystemen: Grundlagen für den ökologischen Vergleich von Energiesystemen und den Einbezug von Energiesystemen in Ökobilanzen für die Schweiz.* 2009, ecoinvent report.

198. Raugei, M., *Energy pay-back time: methodological caveats and future scenarios.* Progress in Photovoltaics: Research and Applications, 2013. **21**(4): p. 797-801.

199. Laurent, A. and Hauschild, M.Z. *Normalisation*, in *Life Cycle Impact Assessment*, M.Z. Hauschild and M.A.J. Huijbregts, Editors. 2015, Springer Netherlands: Dordrecht. p. 271-300.

200. International Electrotechnical Commission, *International Standard IEC 61724: Photovoltaic system performance monitoring and Guidelines for measurements, data exchange and analysis*. 1998, IEC.

201. Ahrens, C.D., *Meteorology today: an introduction to weather, climate, and the environment*. 2012: Cengage Learning.

202. Magee, S., *Solar Irradiance and Insolation for Power Systems*. 2010: Steven Magee.

203. U.S. Energy Information Administration, *International Energy Outlook 2018*. 2018.

204. Zampori, L., et al., *Guide for interpreting life cycle assessment result*. 2016, EUR.

205. Guo, M. and Murphy, R. *LCA data quality: sensitivity and uncertainty analysis*. Science of the total environment, 2012. **435**: p. 230-243.

206. Saltelli, A., Chan, K. and Scott, E.M. *Sensitivity analysis*. Vol. 1. 2000: Wiley New York.

207. Saltelli, A., *Sensitivity analysis for importance assessment*. Risk analysis, 2002. **22**(3): p. 579-590.

208. Owens, J.W., *LCA impact assessment categories*. The International Journal of Life Cycle Assessment, 1996. **1**(3): p. 151-158.

209. Huijbregts, M.A., *Application of uncertainty and variability in LCA*. The International Journal of Life Cycle Assessment, 1998. **3**(5): p. 273.

210. Lo, S.C., Ma, H.W. and Lo, S.L. *Quantifying and reducing uncertainty in life cycle assessment using the Bayesian Monte Carlo method*. Science of the total environment, 2005. **340**(1-3): p. 23-33.

211. Noh, J.H., et al., *Nanostructured TiO 2/CH 3 NH 3 PbI 3 heterojunction solar cells employing spiro-OMeTAD/Co-complex as hole-transporting material*. Journal of Materials Chemistry A, 2013. **1**(38): p. 11842-11847.

212. Han, Y., et al., *Degradation observations of encapsulated planar CH 3 NH 3 PbI 3 perovskite solar cells at high temperatures and humidity*. Journal of Materials Chemistry A, 2015. **3**(15): p. 8139-8147.

213. Burger, B., et al., *Photovoltaics report*. Fraunhofer Institute for Solar Energy Systems, Freiburg, 2014. **24**.

214. You, J., et al., *Low-temperature solution-processed perovskite solar cells with high efficiency and flexibility*. 2014.

215. Albrecht, S., et al., *Monolithic perovskite/silicon-heterojunction tandem solar cells processed at low temperature*. Energy & Environmental Science, 2016. **9**(1): p. 81-88.

216. Hao, F., et al., *Lead-free solid-state organic-inorganic halide perovskite solar cells*. Nature photonics, 2014. **8**(6): p. 489-494.

217. Yang, J., et al., *Effect of various encapsulants for frameless glass to glass Cu (In, Ga)(Se, S) 2 photovoltaic module*. RSC Advances, 2015. **5**(63): p. 51258-51262.

218. Huang, F., et al., *Gas-assisted preparation of lead iodide perovskite films consisting of a monolayer of single crystalline grains for high efficiency planar solar cells*. Nano Energy, 2014. **10**: p. 10-18.

219. Zhang, L.Q., et al., *Highly efficient and stable planar heterojunction perovskite solar cells via a low temperature solution process.* Journal of Materials Chemistry A, 2015. **3**(23): p. 12133-12138.

220. International Molybdenum Association, since 1989. Available from: <http://www.imoa.info/index.php.>, Acessed on 08/10/2016.

221. Cui, X., Hong, J. and Gao, M. *Environmental impact assessment of three coal-based electricity generation scenarios in China.* Energy, 2012. **45**(1): p. 952-959.

222. Norgate, T. and Haque, N. *Using life cycle assessment to evaluate some environmental impacts of gold production.* Journal of Cleaner Production, 2012. **29**: p. 53-63.

223. Meek, M., Giddings, M. and Gomes, R. *Monochlorobenzene: evaluation of risks to health from environmental exposure in Canada.* Journal of Environmental Science & Health Part C, 1994. **12**(2): p. 409-415.

224. Noel, N.K., et al., *Lead-free organic–inorganic tin halide perovskites for photovoltaic applications.* Energy & Environmental Science, 2014. **7**(9): p. 3061-3068.

225. Takahashi, Y., et al., *Charge-transport in tin-iodide perovskite CH 3 NH 3 SnI 3: origin of high conductivity.* Dalton Transactions, 2011. **40**(20): p. 5563-5568.

226. Chiarella, F., et al., *Combined experimental and theoretical investigation of optical, structural, and electronic properties of C H 3 N H 3 Sn X 3 thin films (X= Cl, Br).* Physical Review B, 2008. **77**(4): p. 045129.

227. Eisler, R., *Mercury hazards from gold mining to humans, plants, and animals*, in *Reviews of environmental contamination and toxicology*. 2004, Springer. p. 139-198.

228. Fashola, M., Ngole-Jeme, V. and Babalola, O. *Heavy metal pollution from gold mines: environmental effects and bacterial strategies for resistance.* International journal of environmental research and public health, 2016. **13**(11): p. 1047.

229. Atilgan, B. and Azapagic, A. *Life cycle environmental impacts of electricity from fossil fuels in Turkey.* Journal of Cleaner Production, 2015. **106**: p. 555-564.

230. Chen, W., et al., *Environmental impact assessment of monocrystalline silicon solar photovoltaic cell production: a case study in China.* Journal of Cleaner Production, 2016. **112**: p. 1025-1032.

231. European Commission, *Directive 2008/98/EC of the european parliament and of the council of 19 november 2008 on waste and repealing certain directives (waste framework directive).* LexUriServ. do, 2008.

232. Yun, Y.H., et al., *The association of self-leadership, health behaviors, and posttraumatic growth with health-related quality of life in patients with cancer.* Psycho-Oncology, 2014. **23**(12): p. 1423-1430.

233. Bissen, M. and Frimmel, F.H. *Arsenic—a review. Part I: occurrence, toxicity, speciation, mobility.* Acta hydrochimica et hydrobiologica, 2003. **31**(1): p. 9-18.

234. Lyu, M., et al., *Addressing Toxicity of Lead: Progress and Applications of Low‐Toxic Metal Halide Perovskites and Their Derivatives.* Advanced Energy Materials, 2017. **7**(15): p. 1602512.

235. Qasim, B., et al., *Potentially toxic element phytoavailability assessment in Technosols from former smelting and mining areas.* Environmental Science and Pollution Research, 2015. **22**(8): p. 5961-5974.

236. Otomo, P.V., Wahl, J. and Maboeta, M.S. *The enchytraeid reproduction test (ERT): a potentially quick and affordable tool for the assessment of metal contaminated soils in emerging economies.* Bulletin of environmental contamination and toxicology, 2013. **91**(5): p. 545-548.

237. Brearley, F.Q. and Thomas, A.D. *Land-use Change Impacts on Soil Processes: Tropical and Savannah Ecosystems.* 2015: CABI.

238. Simon, F.G., Holm, O. and Berger, W. *Resource recovery from urban stock, the example of cadmium and tellurium from thin film module recycling.* Waste management, 2013. **33**(4): p. 942-947.

239. Hagelüken, C. and Meskers, C. *Technology challenges to recover precious and special metals from complex products.* in *R'09 World Congress, Davos, Switzerland, Conference Start Date.* 2009.

240. Goe, M. and Gaustad, G. *Strengthening the case for recycling photovoltaics: An energy payback analysis.* Applied Energy, 2014. **120**: p. 41-48.

241. Green, M.A., *Thin-film solar cells: review of materials, technologies and commercial status.* Journal of Materials Science: Materials in Electronics, 2007. **18**(1): p. 15-19.

242. Gifford, J., *The weekend read: CIGS is back, back again*, in *PV magazine.* 2018: Available at: <https://www.pv-magazine.com/.>, Acessed on: 02/11/2018.

243. Kim, K., et al., *Simulations of chalcopyrite/c-Si tandem cells using SCAPS-1D.* Solar Energy, 2017.

244. Bush, K.A., et al., *23.6%-efficient monolithic perovskite/silicon tandem solar cells with improved stability.* Nature Energy, 2017. **2**: p. 17009.

245. Coutts, T.J., et al., *Critical issues in the design of polycrystalline, thin‑film tandem solar cells.* Progress in Photovoltaics: Research and Applications, 2003. **11**(6): p. 359-375.

246. Bekkelund, K., *A comparative life cycle assessment of PV solar systems.* 2013, Institutt for energi-og prosessteknikk.

247. Hao, X. and Yan, C. *UNSW Laboratories.* Personal comunication. 2016.

248. Zahir, F., et al., *Low dose mercury toxicity and human health.* Environmental toxicology and pharmacology, 2005. **20**(2): p. 351-360.

249. Godt, J., et al., *The toxicity of cadmium and resulting hazards for human health.* Journal of occupational medicine and toxicology, 2006. **1**(1): p. 22.

250. Barbier, O., et al., *Effect of heavy metals on, and handling by, the kidney.* Nephron Physiology, 2005. **99**(4): p. p105-p110.

251. Seidal, K., et al., *Fatal cadmium-induced pneumonitis.* Scandinavian journal of work, environment & health, 1993: p. 429-431.

252. Järup, L. and Åkesson, A. *Current status of cadmium as an environmental health problem.* Toxicology and applied pharmacology, 2009. **238**(3): p. 201-208.

253. Satarug, S., et al., *Cadmium, environmental exposure, and health outcomes.* Ciencia & saude coletiva, 2011. **16**(5): p. 2587-2602.

254. Cummings, K.J., et al., *Respirable indium exposures, plasma indium, and respiratory health among indium‑tin oxide (ITO) workers.* American journal of industrial medicine, 2016. **59**(7): p. 522-531.

255. Cummings, K.J., et al., *Indium lung disease.* CHEST Journal, 2012. **141**(6): p. 1512-1521.

256. Cummings, K.J., et al., *Serial evaluations at an indium-tin oxide production facility.* American journal of industrial medicine, 2013. **56**(3): p. 300-307.

257. White, S.J.O. and Shine, J.P. *Exposure Potential and Health Impacts of Indium and Gallium, Metals Critical to Emerging Electronics and Energy Technologies.* Current environmental health reports, 2016. **3**(4): p. 459-467.

258. Chan, P. and Cheng, S. *Cadmium-induced ectopic apoptosis in zebrafish embryos.* Archives of toxicology, 2003. **77**(2): p. 69-79.

259. Cheng, S.H., et al., *Cellular and molecular basis of cadmium-induced deformities in zebrafish embryos.* Environmental Toxicology and Chemistry, 2000. **19**(12): p. 3024-3031.

260. Silva, D.A.L., et al., *Environmental performance assessment of the melamine-urea-formaldehyde (MUF) resin manufacture: a case study in Brazil.* Journal of Cleaner Production, 2015. **96**: p. 299-307.

261. De Boeck, G., et al., *Swimming performance and energy metabolism of rainbow trout, common carp and gibel carp respond differently to sublethal copper exposure.* Aquatic toxicology, 2006. **80**(1): p. 92-100.

262. Shaw, B.J. and Handy, R.D. *Dietary copper exposure and recovery in Nile tilapia, Oreochromis niloticus.* Aquatic Toxicology, 2006. **76**(2): p. 111-121.

263. Vaccaro, R., *Available nitrogen and phosphorus and the biochemical cycle in the atlantic off new-england.* Journal of Marine Research, 1963. **21**(3): p. 284-301.

264. Thomas, W.H., *surface nitrogenous nutrients and phytoplankton in the northeastern tropical pacific ocean.* Limnology and Oceanography, 1966. **11**(3): p. 393-400.

265. Ryther, J.H. and Dunstan, W.M. *Nitrogen, phosphorus, and eutrophication in the coastal marine environment.* Science, 1971. **171**(3975): p. 1008-1013.

266. van Oers, L. and Guinée, J. *The Abiotic Depletion Potential: Background, Updates, and Future.* Resources, 2016. **5**(1): p. 16.

267. Mancini, L., De Camillis, C. and Pennington, D. *Security of Supply and Scarcity of Raw Materials.* Towards a Methodological Framework for Sustainability Assessment.

268. Weckend, S., Wade, A. and Heath, G. *End-of-life management Solar Photovoltaic Panels.* 2016, IRENA and IEA-PVPS.

269. Ebhota, W.S. and Jen, T.C. *Photovoltaic Solar Energy: Potentials and Outlooks.* in *ASME 2018 International Mechanical Engineering Congress and Exposition.* 2018. American Society of Mechanical Engineers.

270. Powalla, M. and Bonnet, D. *Thin-film solar cells based on the polycrystalline compound semiconductors CIS and CdTe.* Advances in OptoElectronics, 2007. **2007**.

271. Theelen, M. and Daume, F. *Stability of Cu (In, Ga) Se2 solar cells: A literature review.* Solar Energy, 2016. **133**: p. 586-627.

272. Theelen, M., et al., *Stability of CIGS solar cells under illumination with damp heat and dry heat: A comparison.* Solar Energy Materials and Solar Cells, 2017. **166**: p. 262-268.

273. de Wild-Scholten, M. and Alsema, E. *Towards cleaner solar PV: Environmental and health impacts of crystalline silicon photovoltaics.* Refocus, 2004. **5**(5): p. 46-49.

274.   Amponsah, N.Y., et al., *Greenhouse gas emissions from renewable energy sources: A review of lifecycle considerations.* Renewable & Sustainable Energy Reviews, 2014. **39**: p. 461-475.

275.   Slesser, M. and I. Hounam, *Solar energy breeders.* Nature, 1976. **262**: p. 244-245.

276.   Vorrath, S. *"No need for new coal:" Sun Metals formally opens solar farm in "George" town.* 2018. Available from: <https://reneweconomy.com.au/no-need-for-new-coal-sun-metals-formally-opens-solar-farm-in-george-town-26798/>, Acessed on: 17/08/2018.

277.   Parkinson, G. *Victoria's biggest solar farm reaches financial close, to power steel works.* 2018. Available from: <https://reneweconomy.com.au/victorias-biggest-solar-farm-reaches-financial-close-to-power-steel-works-11109/>, Acessed on: 27/07/2018.

278.   Parkinson, G. *Steel giant BlueScope turns to solar with major PPA deal.* 2018. Available from: <https://reneweconomy.com.au/steel-giant-bluescope-turns-to-solar-with-major-ppa-deal-37396/.>, Acessed on: 20/07/2018.

279.   Mendes, J.J. *Nectar Farms and Sundrop Farms are blazing a trail.* 2018. Available from: <https://reneweconomy.com.au/nectar-farms-sundrop-farms-blazing-trail-64882/>, Acessed on: 21/03/2018.

280.   Parkinson, G. *Gupta launches 1GW renewable plan at Cultana solar project.* 2018. Available from: <https://reneweconomy.com.au/gupta-launches-1gw-renewable-plan-at-cultana-solar-project-67819/>, Acessed on: 15/08/2018.

281.   Wambach, K., Müller, A. and Alsema, E. *Life cycle analysis of a solar module rec ycling process.* in *20th European Photovoltaic Solar Energy Conference, Barcelona, Spain.* 2005.

282.   Frisson, L., et al. *Recent improvements in industrial PV module recycling.* in *16th European Photovoltaic Solar Energy Conference.* 2000.

283.   Fthenakis, V.M., *End-of-life management and recycling of PV modules.* Energy Policy, 2000. **28**(14): p. 1051-1058.

284.   Jewell, S.K., Suzette, M. , *Mineral Commodity Summaries 2016*, ed. G.S. Interior Department. 2016: Government Printing Office. 196.

285.   Kushiya, K., Ohshita, M. and Tanaka. M. *Development of recycling and reuse technologies for large-area Cu (InGa) Se/sub 2/-based thin-film modules.* in *Photovoltaic Energy Conversion, 2003. Proceedings of 3rd World Conference on.* 2003. IEEE.

286.   Huot, J.-Y. and Suys. M. *Recycling of solar Thin Film PV modules and scraps, and closed-loop use of metals.* in *Innovationsforum Life-Cycle-Strategien und Recycling für Seltene Metalle mit strategischer Bedeutung.* 2011.

287.   Oosterhof, H., *Recycling of scarce metals at Umicore, 2011.* Freiberg, Germany, 2011.

288.   Meskers, C., et al. *Recycling Technologies to close the loop for PV materials.* in *25th European Photovoltaic Solar Energy Conference and Exhibition, 5th World Conference on Photovoltaic Energy Conversion, Valencia, Spain, 6th.* 2010.

289.   Hallam, B., et al., *The role of hydrogenation and gettering in enhancing the efficiency of next‑generation Si solar cells: An industrial perspective.* physica status solidi (a), 2017.

290.   Hallam, B.J., et al., *Advanced bulk defect passivation for silicon solar cells.* IEEE Journal of Photovoltaics, 2014. **4**(1): p. 88-95.

291. Hallam, B.J., et al., *Hydrogen passivation of BO defects in Czochralski silicon.* Energy Procedia, 2013. **38**: p. 561-570.

292. Lunardi, M.M., et al., *Life Cycle Assessment on Advanced Silicon Solar Modules*, in *Asia-Pacific Solar Research Conference*. 2017: Melbourne.

293. Lunardi, M.M., et al., *Life cycle assessment on PERC solar modules.* Solar Energy Materials and Solar Cells, 2018. **187**: p. 154-159.

294. Kraiem, J., et al. *High performance solar cells made from 100% UMG silicon obtained via the PHOTOSIL process*. in *Photovoltaic Specialists Conference (PVSC), 2010 35th IEEE*. 2010. IEEE.

295. Jiménez-González, C., Kim, S. and Overcash, M.R. *Methodology for developing gate-to-gate life cycle inventory information.* The International Journal of Life Cycle Assessment, 2000. **5**(3): p. 153-159.

296. Solar Industrial Research Facility (SIRF), Library Walk, Kensington NSW 2033, Sydney, Australia. 2017.

297. Innolas Solutions, *ILS-TT turntable machine for various applications*. 2017. Available from: <http://www.innolas-solutions.com/products/ils-tt/>, Acessed on: 06/09/2017.

298. Li, M., et al. *Review of New Technology for Preparing Crystalline Silicon Solar Cell Materials by Metallurgical Method*. in *IOP Conference Series: Earth and Environmental Science*. 2017. IOP Publishing.

299. Rougieux, F., et al., *High efficiency UMG silicon solar cells: impact of compensation on cell parameters.* Progress in Photovoltaics: Research and Applications, 2016. **24**(5): p. 725-734.

300. Sopori, B., et al. *Understanding light-induced degradation of c-Si solar cells*. in *Photovoltaic Specialists Conference (PVSC), 2012 38th IEEE*. 2012. IEEE.

301. Schmidt, J. and Bothe, K. *Structure and transformation of the metastable boron-and oxygen-related defect center in crystalline silicon.* Physical review B, 2004. **69**(2): p. 024107.

302. Fischer, H. *Investigation of photon and thermal changes in silicon solar cells*. in *Conference Record of the 10^< th> IEEE Photovoltaic Specialists Conference, 1973*. 1973.

303. Cho, E., et al. *Light-induced degradation free and high efficiency p-type indium-doped PERC solar cells on Czochralski silicon*. in *Photovoltaic Specialist Conference (PVSC), 2015 IEEE 42nd*. 2015. IEEE.

304. Lee, K., et al. *Natural recovery from LID: Regeneration under field conditions*. in *Proceedings of the 31st European Photovoltaic Solar Energy Conference and Exhibition*. 2015.

305. Chang, M., et al., *Light induced degradation of p-mono perc from ingot, cell, module to system*, in *32nd European Photovoltaic Solar Energy Conference and Exhibition*. 2016: Munich.

306. Hoffmann, V., et al. *First results on industrialization of Elkem solar silicon at Pillar JSC and Q-Cells*. in *Proceedings of the 23rd European Photovoltaic Solar Energy Conference, Valencia, Spain*. 2008.

307. Woo, S.H., Lee, D.S. and Lim, S.R. *Potential resource and toxicity impacts from metals in waste electronic devices.* Integrated environmental assessment and management, 2016. **12**(2): p. 364-370.

308.	Shin, J., Park, J. and Park, N. *A method to recycle silicon wafer from end-of-life photovoltaic module and solar panels by using recycled silicon wafers.* Solar Energy Materials and Solar Cells, 2017. **162**: p. 1-6.

309.	Granata, G., et al., *Recycling of photovoltaic panels by physical operations.* Solar Energy Materials and Solar Cells, 2014. **123**: p. 239-248.

310.	Kang, S., et al., *Experimental investigations for recycling of silicon and glass from waste photovoltaic modules.* Renewable Energy, 2012. **47**: p. 152-159.

311.	Latunussa, C.E., et al., *Life Cycle Assessment of an innovative recycling process for crystalline silicon photovoltaic panels.* Solar Energy Materials and Solar Cells, 2016. **156**: p. 101-111.

312.	SASIL. *Full Recovery End of Life Photovoltaic – FRELP*. 2014. Available from: <https://frelp.info/>, Acessed on: 05/02/2018.

313.	PVCycle, *Breakthrough in PV module recycling*. 2016 February 18th, 2016. Available from: <http://www.pvcycle.org/press/breakthrough-in-pv-module-recycling/>, Acessed on: 15/12/2017.

314.	Kadro, J.M., et al., *Proof-of-concept for facile perovskite solar cell recycling.* Energy & Environmental Science, 2016. **9**(10): p. 3172-3179.

315.	Lunardi, M.M., et al., *A Review of Recycling Processes for Photovoltaic Modules*, in *Solar Panels and Photovoltaic Materials*, B. Zaidi, Editor. 2018, IntechOpen.

316.	Naumann, V., et al., *Potential-induced degradation at interdigitated back contact solar cells.* Energy Procedia, 2014. **55**: p. 498-503.

317.	Kim, T.H., Park, N.C. and Kim, D.H. *The effect of moisture on the degradation mechanism of multi-crystalline silicon photovoltaic module.* Microelectronics Reliability, 2013. **53**(9-11): p. 1823-1827.

318.	Schmidt, J. *Light-induced degradation in crystalline silicon solar cells*. in *Solid State Phenomena*. 2004. Trans Tech Publ.

319.	United Nations Framework Convention on Climate Change (UNFCCC), *Aggregate effect of the intended nationally determined contributions: an update.* Available from: <http://unfccc.int/resource/docs/2016/cop22/eng/02.pdf>, Accessed on: 23/11/2016.

320.	Rogelj, J., et al., *Paris Agreement climate proposals need a boost to keep warming well below 2 C.* Nature, 2016. **534**(7609): p. 631.

321.	Wigley, T., *The Paris warming targets: emissions requirements and sea level consequences.* Climatic Change, 2018. **147**(1-2): p. 31-45.

322.	Bruckner, T., et al., *Energy Systems, Annex II: Metrics & Methodology*, in *Climate Change 2014: Mitigation of Climate Change*. 2014, Fifth Assessment Report of the Intergovernmental Panel on Climate Change

323.	Internation Energy Agency (IEA), *World Energy Outlook 2017 - Executive Summary.* 2017: p. 13.

324.	United States Environmental Protection Agency, *Sources of Greenhouse Gas Emissions*. 2018.

325.	Mints, P., *The solar flare, Issue 4*. 2018, SPV Market Research.

326.	Monier, V. and Hestin, M. *Study on photovoltaic panels supplementing the impact assessment for a recast of the WEEE directive.* Final Report, ENV. G, 2011. **4**: p. 6.

327. Vellini, M., Gambini, M. and Prattella, V. *Environmental impacts of PV technology throughout the life cycle: Importance of the end-of-life management for Si-panels and CdTe-panels.* Energy, 2017. **138**: p. 1099-1111.

328. Huang, B., et al., *Environmental influence assessment of China's multi-crystalline silicon (multi-Si) photovoltaic modules considering recycling process.* Solar Energy, 2017. **143**: p. 132-141.

329. Müller, A., Wambach, K. and Alsema, E. *Life cycle analysis of solar module recycling process.* MRS Online Proceedings Library Archive, 2005. **895**.

330. Berger, W., et al., *A novel approach for the recycling of thin film photovoltaic modules.* Resources, Conservation and Recycling, 2010. **54**(10): p. 711-718.

331. Choi, J.K. and Fthenakis, V. *Crystalline silicon photovoltaic recycling planning: macro and micro perspectives.* Journal of Cleaner Production, 2014. **66**: p. 443-449.

332. Gerbinet, S., Belboom, S. and Léonard, A. *Life Cycle Analysis (LCA) of photovoltaic panels: A review.* Renewable and Sustainable Energy Reviews, 2014. **38**: p. 747-753.

333. Stamford, L. and Azapagic, A. *Environmental Impacts of Photovoltaics: The Effects of Technological Improvements and Transfer of Manufacturing from Europe to China.* Energy Technology, 2018. **6**(6): p. 1148-1160.

334. Zhong, Z., Song, B. and Loh, P. *LCAs of a polycrystalline photovoltaic module and a wind turbine.* Renewable Energy, 2011. **36**(8): p. 2227-2237.

335. Barnes, L.L., *Environmental Impact of Solar Panel Manufacturing and End-of-Life Management: Technology and Policy Options.* 2017, Champaign, IL: Illinois Sustainable Technology Center.

336. Yamashita, K., Miyazawa, A. and Sannomiya. H. *Reserch and Development on Recycling and Reuse Treatment Technologies for Crystalline Silicon Photovoltaic Modules.* in *Photovoltaic Energy Conversion, Conference Record of the 2006 IEEE 4th World Conference on.* 2006. IEEE.

337. Schmauder, J., et al., *First steps towards an automated repairing of solar cells by laser enabled silicon post-processing.* Proc. EU-PVSEC, 2012.

338. Wang, T.Y., Hsiao, J.C. and Du, C.H. *Recycling of materials from silicon base solar cell module.* in *Photovoltaic Specialists Conference (PVSC), 2012 38th IEEE.* 2012. IEEE.

339. Komoto, K. *Developments on PV Recycling in Japan.* in *24th European Photovoltaic Solar Energy Conference.* 2014. Hamburg.

340. Doi, T., et al., *Experimental study on PV module recycling with organic solvent method.* Solar energy materials and solar cells, 2001. **67**(1): p. 397-403.

341. Park, J. and Park, N. *Wet etching processes for recycling crystalline silicon solar cells from end-of-life photovoltaic modules.* RSC Advances, 2014. **4**(66): p. 34823-34829.

342. European Union., *Directive 2012/19/EU of the European Parliament and of the Council of 4 July 2012 on waste electrical and electronic equipment (WEEE).* Official Journal of the European Union, 2012: p. L 197/38-71.

343. Kenning, T. *PV Cycle achieves record 96% recycle rate for silicon-based PV modules.* 2016. Available from: <https://www.pv-tech.org/news/pv-cycle-achieves-record-96-recycle-rate-for-silicon-based-pv-modules>, Acessed on: 17/05/2018.

344. Born, M. and Wambach, K. *Pyrolysis of EVA and its application in recycling of photovoltaic modules.* Journal of Environmental Sciences, 2004. **16**(6): p. 889-893.

345. Fowles, J., et al., *A review of the toxicological and environmental hazards and risks of tetrahydrofuran.* Critical reviews in toxicology, 2013. **43**(10): p. 811-828.

346. Housingsworth, R., et al., *Toxicity of o-Dichlorobenzene. Studies on Animals and Industrial Experience.* Arch. Indust. Health, 1958. **17**(3): p. 180-87.

347. Integrated Risk Information System (IRIS), *Toluene*, National Center for Environmental Assessment, 2005, U.S. Environmental Protection Agency - National Center for Environmental Assessment: Washington.

348. Radziemska, E., et al., *Chemical, thermal and laser processes in recycling of photovoltaic silicon solar cells and modules.* Ecological Chemistry and Engineering. S, 2010. **17**(3): p. 385-391.

349. Fthenakis, V.M., Kim, H.C. and Alsema, E. *Emissions from photovoltaic life cycles.* Environmental science & technology, 2008. **42**(6): p. 2168-2174.

350. Peng, J., Lu, L. and Yang, H. *Review on life cycle assessment of energy payback and greenhouse gas emission of solar photovoltaic systems.* Renewable and sustainable energy reviews, 2013. **19**: p. 255-274.

351. Ecoinvent database, *Ecoinvent data v2.1. Technical report.* Swiss Centre for Life Cycle Inventories: Dübendorf, Switzerland.

LIFE CYCLE ASSESSMENT OF SILICON BASED TANDEM AND ADVANCED SILICON SOLAR MODULES

Marina Monteiro Lunardi

APPENDIX

LIST OF TABLES

212

Inventory Tables

Table 0-1: Silicon p-n junction multi-crystalline solar cell inventory (for 1 m^2 cell area) [40].

Flow		Unit	Quantity
Metallurgical grade silicon (MGS)			
Inputs	Electricity (medium voltage)	kWh	11.0
	Wood chips (mixed, u=120%)	m^3	0.00325
	Hard coal	MJ	23.1
	Graphite	kg	0.1
	Charcoal	kg	0.17
	Petroleum coke	kg	0.5

	Flow	Unit	Quantity
	Silica sand	kg	2.7
	Oxygen (liquid)	kg	0.02
	Slag from MG silicon	kg	0.025
Outputs	MGS	kg	1
	Heat (waste)	MJ	71.3
	Carbon monoxide	kg	0.00138
	Carbon dioxide	kg	5.19
	Nitrogen oxides	kg	0.00974
	Particulates (>10um)	kg	0.00775
	Silicon	kg	0.00751
	Sulphur dioxide	kg	0.0122
	Hydrogen sulfide	kg	0.0005
	Hydrogen fluoride	kg	0.0005
	Non-methane volatile organic compounds (NMVOC)	kg	0.000096

	Flow	Unit	Quantity
	Solar grade silicon (SGS) – Siemens process		
Inputs	MGS	kg	1.13
	Hydrochloric acid (30%)	kg	1.60
	Hydrogen (liquid)	kg	0.0501
	Sodium hydroxide (50%)	kg	0.348
	Electricity (medium voltage)	kWh	110.00
	Heat (1MW)	MJ	185.00
Outputs	*SGS*	*kg*	*1*
	Absorbable organic halogen as Cl (AOX)	kg	0.0000126
	Biological oxygen demand (BOD5)	kg	0.000205
	Chemical oxygen demand (COD)	kg	0.00202
	Chloride	kg	0.0360
	Nitrogen	kg	0.000208
	Sodium (ion)	kg	0.0338
	Dissolved organic carbon (DOC)	kg	0.000910

	Flow	Unit	Quantity
	Multi-Crystalline silicon production		
Inputs	Water	m³	0.943
	Electricity (medium voltage)	kWh	15.5
	Argon (liquid)	kg	1
	Helium	kg	0.0000776
	Sodium hydroxide (50%)	kg	0.005
	Nitrogen (liquid)	kg	0.0304
	Ceramic tiles	kg	0.214
	Silicon (production mix)	kg	0.7
Outputs	*Multi-crystalline silicon*	*kg*	*1*
	Heat (waste)	MJ	55.8

	Flow	Unit	Quantity
	Multi-Crystalline silicon wafer production		
Inputs	*Multi-crystalline silicon*	*kg*	*1*
	Electricity (medium voltage)	kWh	20.8
	Natural gas	MJ	4.00
	Water	kg	164.00
	Silicon (multi-Si)	kg	1.02
	Silicon carbide	kg	0.620
	Silicon carbide (recycling)	kg	1.41
	Flat glass	kg	0.0408
	Sodium hydroxide (50%)	kg	0.0150
	Hydrochloric acid (30%)	kg	0.00270
	Acetic acid (98%)	kg	0.0390

	Flow	Unit	Quantity
	Triethylene glycol	kg	0.218
	Triethylene glycol (recycling)	kg	1.95
	Dipropylene glycol monomethyl ether	kg	0.300
	Alkylbenzene sulfonate (petrochemical)	kg	0.240
	Acrylic binder (34%)	kg	0.00385
	Brass	kg	0.00744
	Steel (low-alloyed)	kg	0.797
	Wire drawing (steel)	kg	0.805
Outputs	*Multi-crystalline silicon wafer*	m²	*1*
	silicon wafer waste (disposal)	kg	0.170
	Heat (waste)	MJ	74.9
	Chemical Oxygen Demand (COD)	kg	0.0295
	Biological Oxygen Demand (BOD5)	kg	0.0295
	Dissolved Organic Carbon (DOC)	kg	0.0111
	Total Organic Carbon (TOC)	kg	0.0111
	Flow	**Unit**	**Quantity**
	Photovoltaic cells (Si) production		
Inputs	Water	kg	251.00
	Electricity (medium voltage)	kWh	14.4
	Natural gas	MJ	0.247
	Light fuel oil	MJ	0.00270
	Multi-Si wafer	m²	1.04
	Metallization paste (front side)	kg	0.00912
	Metallization paste (back side)	kg	0.00534
	Metallization paste (back side – aluminium)	kg	0.0596
	Ammonia (liquid)	kg	0.00892
	Phosphoric acid (70%)	kg	0.00863
	Phosphoryl chloride	kg	0.0274
	Isopropanol	kg	0.000810
	Solvents (organic – unspecified)	kg	0.0113
	Calcium chloride ($CaCl_2$)	kg	0.0315
	Hydrochloric acid (30%)	kg	0.00859
	Hydrogen fluoride	kg	0.403
	Nitric acid (50%)	kg	0.293
	Sodium hydroxide (50%)	kg	0.0707
	Lime (hydrated)	kg	0.218
	Hydrogen peroxide (50%)	kg	0.000452
	Sulphuric acid (liquid)	kg	0.101
	Potassium hydroxide	kg	0.0300
	Ammonium sulphate	kg	0.0210
	Oxygen (liquid)	kg	0.00822
	Nitrogen (liquid)	kg	1.35
	Silicon tetrahydride	kg	0.00261
Outputs	*Photovoltaic cells (multi-si)*	m²	*1*
	PV cell production effluent (wastewater treat. - class 3)	m³	0.0789
	Waste Si wafer production (residual material landfill)	kg	2.74
	Solvents mixture (hazard waste incineration)	kg	0.0108
	Heat (waste)	MJ	51.8
	Hydrogen fluoride	kg	0.000690
	Ammonia	kg	0.000522
	Carbon dioxide	kg	0.682
	Hydrogen	kg	0.000444
	Silicon	kg	0.000147
	Non-methane volatile organic compounds (NMVOC)	kg	0.000353
	Water	kg	5.96
	Nitric acid	kg	0.000119

	Nitrogen oxides		kg	0.0160

Table 0-2: Inventory for HIT solar cells (per 1 m^2 cell area) using mono-crystalline silicon [132].

		Flow	Unit	Quantity
Metallurgical grade silicon (MGS)	Inputs	Electricity (medium voltage)	kWh	11.0
		Wood chips (mixed, u=120%)	m^3	0.00325
		Hard coal	MJ	23.1
		Graphite	kg	0.1
		Charcoal	kg	0.17
		Petroleum coke	kg	0.5
		Silica sand	kg	2.7
		Oxygen (liquid)	kg	0.02
		Slag from MG silicon	kg	0.025
	Outputs	MGS	kg	1
		Heat (waste)	MJ	71.3
		Carbon monoxide	kg	0.00138
		Carbon dioxide	kg	5.19
		Nitrogen oxides	kg	0.00974
		Particulates (>10um)	kg	0.00775
		Silicon	kg	0.00751
		Sulphur dioxide	kg	0.0122
		Hydrogen sulfide	kg	0.0005
		Hydrogen fluoride	kg	0.0005
		Non-methane volatile organic compounds (NMVOC)	kg	0.000096
Solar grade silicon (SGS) – mod. Siemens process	Inputs	MGS	kg	1.13
		Hydrochloric acid (30%)	kg	1.60
		Hydrogen (liquid)	kg	0.0501
		Sodium hydroxide (50%)	kg	0.348
		Electricity (medium voltage)	kWh	110.00
		Heat (1MW)	MJ	185.00
	Outputs	*SGS*	*kg*	*1*
		Absorbable organic halogen as Cl (AOX)	kg	0.0000126
		Biological oxygen demand (BOD5)	kg	0.000205
		Chemical oxygen demand (COD)	kg	0.00202
		Chloride	kg	0.0360
		Nitrogen	kg	0.000208
		Sodium (ion)	kg	0.0338
		Dissolved organic carbon (DOC)	kg	0.000910
Mono-Crystalline silicon production	Inputs	*SGS*	*kg*	*0.781*
		Water	m^3	5.09
		Electricity (medium voltage)	kWh	68.2
		Natural gas (burned in industrial furnace low-NOx)	MJ	68.2
		Tap water	kg	94.1
		Water (deionised)	kg	4.01
		Argon (liquid)	kg	1
		Hydrogen fluoride	kg	0.01
		Nitric acid (50% in H$_2$O)	kg	0.0668
		Sodium hydroxide (50% in H$_2$O)	kg	0.0415
		Ceramic tiles	kg	0.167
		Lime (hydrated)	kg	0.0222
	Outputs	*CZ single crystalline silicon*	*kg*	*1*
		Heat (waste)	MJ	246
		Hydroxide	kg	0.367
		BOD5, Biological Oxygen Demand	kg	0.13
		COD, Chemical Oxygen Demand	kg	0.13

		DOC, Dissolved Organic Carbon	kg	0.0405
		TOC, Total Organic Carbon	kg	0.0405
		Nitrogen oxides	kg	0.0339
		Nitrate	kg	0.0835
Texturing/Cleaning	Inputs	CZ single crystalline silicon	m^2	1
		Water (deionized)	L	33.43
		Electricity	kWh	0.647
		Hydrogen fluoride	kg	0.095
		Sodium hydroxide	kg	0.156
		Hydrogen peproxide	kg	0.056
		Hydrochloride acid	kg	0.061
		Ammonia	kg	0.011
		Compressed air	m^3	0.25
	Outputs	Fluid waste to treatment	L	33.5
Thin-film deposition	Inputs	Electricity	kWh	6.59
		Water	L	394.0
		Silane	g	1.62
		Hydrogen	g	2.42
		Oxygen	g	0.26
		NF3 (for cleaning)	g	2.2
	Outputs	Gaseous waste to abatement	L	29.0
TCO Sputtering	Inputs	Electricity	kWh	6.3
		Water	L	511.82
		ITO	g	2.74
Metalization Screen printing	Inputs	Electricity	kWh	0.524
		Compressed air	m^3	1.096
		Silver paste	g	29.6
Metalization Screen printing	Inputs	Electricity	kWh	0.131
		Compressed air	m^3	0.274
Curing	Inputs	Electricity	kWh	0.31
Gas Abatement	Inputs	Electricity	kWh	0.045
		Water	L	1.2
		Oxygen	g	5.1
		Nitrogen	g	4.3
		Propane	g	3.3
		Compressed air	m^3	14.0

Table 0-3: Material inventory for 1 cm2 of perovskite (Ag, Al and Au) solar cells. Where "I" are inputs and "O" are outputs [153, 154].

			Materials and processes	Amount	Unit
			Front electrode – FTO (1 cm^2)		
I			Fluorine	3.21E-08	kg
I			Oxygen (liquid)	4.29E-05	kg
I			Tin	1.04E-06	kg
I			Flat glass (uncoated)	1.54E-04	kg
I			Electricity (low voltage)	4.82E-02	kWh
I			Anti-reflex-coating (solar glass)	1	cm^2
	I		Glass etching plant	2.00E-11	p
	I		Water (deionised)	1.00E-03	kg
	I		Hydrochloric acid (reaction of hydrogen with chlorine)	1.33E-05	kg
	I		Zinc	2.00E-06	kg
	I		Electricity (low voltage)	1.20E-04	kWh
	I		Heat (from natural gas)	6.53E-04	MJ
	O		Water	1.50E-07	m^3
	O		Chlorine	5.00E-07	kg
	O		Refinery sludge	2.50E-06	kg
	O		Wastewater (unpolluted)	1.00E-06	m^3
			Front electrode – ITO (1 m^2)		
I			ITO glass	1.54	kg
I			Ethanol	2.58E-02	kg
I			Deionized water	3.27E-02	kg
O			Ethanol	2.58E-02	kg
			n-type material - TiO$_2$ (1 cm^2)		
I			Electricity (low voltage)	4.86E-03	kWh
I			TiO$_2$	3.76E-05	kg
	O		Isopropanol (GLO) market for	1.13E-04	kg
	I		Water (deionised)	1.69E-05	kg
	I		Titanium isopropoxide	1.34E-04	kg
		O	Hydrochloric acid (30% solution)	6.86E-05	kg
		I	Isopropanol	1.13E-04	kg
	I		Titanium tetrachloride	8.92E-05	kg
		I	Chlorine	1.17E-04	kg
		I	Carbon black	1.69E-05	kg
		I	Ilmenite (54% titanium dioxide)	7.13E-05	kg
		O	Iron (III) chloride (40% solution)	7.63E-05	kg
		O	Carbon monoxide	3.95E-05	kg
			n-type material – PEDOT:PSS (1 cm^2)		
I			PEDOT:PSS	7.57E-07	kg
I			Electricity (low voltage)	9.9E-03	kWh
O			2-propanol	2.27E-03	kg
O			Waste water	7.62E-07	kg
O			PEDOT:PSS	7.99E-09	kg

	Materials and processes			Amount	Unit
O	Propylene glycol			4.59E-05	kg

Perovskite layer (1 cm^2) – Spin coated					
P	Electricity (low voltage)			6.21E-02	kWh
I	Perovskite (by vapour deposition)			2.55E-07	kg
	I	Methylammonium iodide (CH$_3$NH$_3$I)		3.33E-07	kg
		I	Ethylamine	1.18E-10	kg
		I	Methanol	1.03E-09	kg
		I	HI	1.16E-09	kg
		I	Diethyl ether	8.00E-11	kg
		I	Electricity (low voltage)	6.18E-10	kWh
	I	Lead chloride, PbCl$_2$		1.47E-07	kg
		O	Sodium nitrate	4.32E-11	kg
		I	Sodium chloride	2.97E-11	kg
		I	Water, deionised	7.07E-11	kg
		I	Electricity, low voltage (DK) market for	3.29E-12	kWh
		I	Lead(II) nitrate	8.42E-11	kg
			I	Lead	5.98E-11	kg
			I	Nitric acid (50% solution)	8.42E-11	kg
			I	Electricity (low voltage)	8.26E-12	kWh
			O	Water (deionised)	7.33E-11	kg
Hole transport material - Spiro-OMeTAD (1 cm^2)					
I	Monochlorobenzene			2.81E-06	kg
I	Water (deionised)			4.50E-07	kg
I	Spiro-MeOTAD			1.88E-06	kg
	I	Toluene (liquid)		2.10E-06	kg
	I	Nitrogen (liquid)		1.76E-05	kg
	I	Ethyl acetate		1.69E-06	kg
	I	Water (deionised)		3.76E-05	kg
	I	Magnesium sulfate		3.01E-06	kg
	I	Electricity (low voltage)		2.61E-06	kWh
	I	3,4'-dimethoxydiphenylamine		1.98E-06	kg
		I	Aniline	1.97E-06	kg
		I	Toluene (liquid)	2.09E-06	kg
		I	Nitrogen (liquid)	1.85E-05	kg
		I	Ethyl acetate	1.78E-06	kg
		I	Water (deionised)	3.96E-05	kg
		I	Magnesium sulfate	3.17E-06	kg
		I	Electricity (low voltage)	1.02E-05	kWh
		I	4-bromoaniline	3.29E-06	kg
			I	Bromine	1.51E-06	kg
			I	Aniline	1.78E-06	kg
		I	Sodium tert-butoxide	2.31E-06	kg
			I	1-butanol	1.78E-06	kg

Materials and processes						Amount	Unit
			I		Sodium	5.26E-07	kg
		I		Tris(dibenzylideneacetone)dipalladium(0)		1.47E-06	kg
		I		Palladium chloride PdCl$_2$		1.54E-09	kg
			I		Palladium	9.78E-10	kg
			I		Electricity (low voltage)	2.14E-09	kWh
			I		Aqua regia	5.63E-10	kg
				I	Nitric acid (50% solution)	1.41E-10	kg
				I	Hydrochloric acid (30% solution)	4.22E-10	kg
		I		Methanol		1.74E-07	kg
		I		Trichloromethane		2.62E-07	kg
		I		Diethyl ether production		1.78E-07	kg
		I		Water		1.47E-05	kg
		I		Acetone (liquid)		1.47E-05	kg
		I		Electricity (low voltage)		4.69E-07	kWh
		I		Dibenzylideneacetone (C$_{17}$H$_{14}$O)		6.75E-09	kg
			I		Benzaldehyde	4.28E-09	kg
			I		Acetone (liquid)	1.17E-09	kg
			I		Sodium hydroxide (50% solution)	8.08E-09	kg
			I		Ethyl acetate	3.23E-09	kg
			I		Solvent (organic)	1.51E-11	kg
			I		Ethanol (from ethylene)	5.10E-08	kg
			I		Water (ultrapure)	2.16E-07	kg
			I		Electricity (low voltage)	2.69E-11	kWh
		I		Sodium acetate		5.72E-09	kg
			I		Acetic acid (98% solution)	4.19E-09	kg
			I		Sodium hydroxide (50% solution)	2.79E-09	kg
			O		Water	1.26E-09	kg
		I		Tri-tert-butylphosphine		5.22E-08	kg
			I		Tert-butyl amine	4.55E-08	kg
			I		Phosphane	2.12E-08	kg
			O		Ammonia (liquid)	1.40E-08	kg
			O		Hydrogen	5.20E-10	kg
		O		Acetone		5.22E-07	kg
		O		Wastewater		2.09E-08	m^3
		O		Spent solvent mixture		1.76E-04	kg
	I			2,2`, 7,7`-Tetrabromo-9-9`-spirobi[9H-fluorene]		1.22E-06	kg
		I		9-Fluorenone		7.24E-08	kg
			I		Polycarboxylates (40% active substance)	9.44E-08	kg
			I		Sulfuric acid	3.48E-09	kg
			I		Electricity (low voltage)	3.54E-10	kWh
		I		Magnesium		9.88E-06	kg
		I		Water (ultrapure)		4.02E-06	kg
		I		Diethyl ether		1.13E-06	kg

Materials and processes						Amount	Unit
		I	Ammonia (liquid)			6.33E-08	kg
		I	Acetic acid (98% solution)			5.22E-08	kg
		I	Hydrochloric acid (30% solution)			2.88E-11	kg
		I	Bromine			2.63E-08	kg
		I	Iron (III) chloride (without water)			3.16E-10	kg
		I	Dichloromethane			1.61E-08	kg
		I	4-Bromobiphenyl			7.31E-09	kg
			I	Acetic acid (98% solution)		6.01E-09	kg
			I	Trifluoroacetic acid		9.47E-10	kg
			I	Bromine		2.24E-09	kg
			I	Biphenyl		9.82E-10	kg
				I	Oxygen (liquid)	1.02E-10	kg
				I	Benzene	9.95E-10	kg
				O	Water	1.15E-10	kg
		I	Electricity (low voltage)			2.14E-06	kWh
	I	Sodium tert-butoxide				1.11E-06	kg
	I	Tris(dibenzylideneacetone)dipalladium(0)				1.48E-06	kg
	I	Tri-tert-butylphosphine				5.25E-08	kg
I	Tert-butylpyridine					1.86E-07	kg
	I	Pyridine				7.69E-08	kg
	O	Lithium				5.61E-09	kg
	I	Tert-butyllithium				6.22E-08	kg
		I	1-butanol			7.20E-08	kg
		I	Lithium			6.72E-09	kg
I	Lithium bis(trifluoromethanesulphonyl)imide					1.87E-07	kg
	I	Lithium amides				2.97E-07	kg
		I	Lithium			8.96E-08	kg
		I	Ammonia (liquid)			2.20E-07	kg
		O	Hydrogen			1.30E-08	kg
	O	Ammonia				1.10E-07	kg
I	Nitrogen (liquid)					4.91E-03	kg
I	Electricity (low voltage)					2.76E-02	kWh
Hole transport material - PCBM (1 cm^2)							
I	PCBM					1.54E-08	kg
I	Electricity (low voltage)					5.00E-05	kWh
ZnO ink (1kg)*							
I	Zinc Oxide (ZnO)					7.13E-03	kg
I	Acetic acid (C2H4O2)					1.05E-02	kg
I	Hydrogen peroxide (H2O2)					8.00E-05	kg
I	Potassium hydroxide (KOH)					9.64E-03	kg
I	n-Butanol (C4H10O)					8.27E-01	kg
I	Methanol (CH4O)					1.24E+00	kg
I	Chloroform					1.08E-01	kg
O	Waste					3.35E-2	kg

Materials and processes		Amount	Unit
I	Heat consumption	1.40E+00	MJ
I	Electricity consumption	4.11E+00	kWh
Back electrode – Ag (1cm^2)			
I	Silver	1.50E-07	kg
I	Electricity (low voltage)	2.16E-02	kWh
Back electrode – Al (1cm^2)			
I	Aluminium (ingot)	9.18E-08	kg
I	Electricity (low voltage)	2.16E-02	kWh
Back electrode – Au (1cm^2)			
I	Gold	1.88E-05	kg
I	Electricity (low voltage)	1.63	kWh

* We are using a thickness ZnO thickness of 25 nm (PCEs in excess of 14%), because further increases in the thickness of the ZnO layer did not result in any improvements in device performance (Liu and Kelly, 2014).

Table 0-4: Material inventory for 1 kg of MoO$_3$ [220].

	1 kg MoO$_3$	Unit
Inputs	Coal (in ground)	kg
	Iron (Fe, ore)	kg
	Limestone (CaCO$_3$, in ground)	kg
	Molybdenum (in ore)	kg
	Natural Gas (in ground)	kg
	Oil (in ground)	kg
	Uranium (U, ore)	kg
	Water Used (total)	m^3
	Total Primary Energy	MJ
Air Emissions	Ammonia (NH$_3$)	g
	Carbon Dioxide (CO$_2$, fossil)	g
	Carbon Monoxide (CO)	g
	Hydrocarbons (unspecified)	g
	Hydrogen Chloride (HCl)	g
	Hydrogen Cyanide (HCN)	g
	Hydrogen Sulfide (H$_2$S)	g
	Lead (Pb)	g
	Mercury (Hg)	g
	Metals (unspecified)	g
	Methane (CH$_4$)	g
	Molybdenum (Mo)	g
	Nitrogen Oxides (NO$_x$ as NO$_2$)	g
	Particulates (unspecified)	g
	Sulfur Oxides (SO$_x$ as SO$_2$)	g
	Zinc (Zn)	g
Water Effluents	Aluminum (Al3+)	g
	Ammonia (NH4+, NH$_3$, as N)	g
	BOD5 (Biochemical Oxygen Demand)	g
	Cadmium (Cd++)	g
	Chlorides (Cl-)	g
	Chromium (Cr III, Cr VI)	g
	Copper (Cu+, Cu++)	g
	Cyanide (CN-)	g
	Fluorides (F-)	g
	Iron (Fe++, Fe3+)	g
	Lead (Pb++, Pb4+)	g
	Manganese (Mn II, Mn IV, Mn VII)	g
	Mercury (Hg+, Hg++)	g
	Metals (unspecified)	g
	Molybdenum (Mo II, Mo III, Mo IV, Mo V, Mo VI)	g
	Nickel (Ni++, Ni3+)	g
	Nitrate (NO3-)	g
	Oils (unspecified)	g
	PAH, unspecified	g
	Phosphates (PO4 3-, HPO4--, H2PO4-, H3PO4, as P)	g
	Silicon Dioxide (SiO$_2$)	g
	Sulfate (SO4--)	g
	Suspended Matter (unspecified)	g
	Zinc (Zn++)	g
Solid mat's	Tailings	kg
	Waste: total industrial	kg
	Waste: inert mineral waste	kg

Table 0-5: Module assembly inventory (for 1 m^2 of module) [42].

		Flow	Unit	Quantity
Photovoltaic panel	Inputs	Electricity (medium voltage)	kWh	3.73
		Diesel	MJ	0.00875
		Water	kg	5.03
		Flat glass (tempering)	kg	8.81
		Wire drawing (copper)	kg	0.103
		Photovoltaic cell Si or Tandem (perovskite/Si) cell	m^2	0.935
		Aluminium alloy (AlMg$_3$)	kg	2.13
		Tin	kg	0.0129
		Lead	kg	0.000725
		Diode	kg	0.00281
		Polyethylene (HDPE – granulate)	kg	0.0238
		Solar glass (low-iron)	kg	8.81
		Copper	kg	0.103
		Glass fibre reinforced plastic (polyamide)	kg	0.295
		Ethylvinyl acetate (foil)	kg	0.875
		Polyvinyl fluoride (film)	kg	0.112
		Polyethylene terephthalate (granulate)	kg	0.346
		Silicone product	kg	0.122
		Corrugated board (mixed fibre)	kg	0.763
		1-propanol	kg	0.0159
		Hydrogen fluoride	kg	0.0624
		Isopropanol	kg	0.000147
		Potassium hydroxide	kg	0.0514
		Soap (detergent)	kg	0.0116
	Outputs	*Photovoltaic panel*	*m^2*	*1*
		Municipal solid waste (22.9% water – incineration)	kg	0.0300
		Polyvinyl fluoride (0.2% water – incineration)	kg	0.112
		Plastics (mixture, 15.3% water – incineration)	kg	1.64
		Mineral oil (10% water - hazard waste incineration)	kg	0.00161
		Sewage (wastewater treatment - class 2)	m^3	0.00503
		Heat (waste)	MJ	13.4
		Non-methane volatile organic compounds (NMVOC)	kg	0.00806
		Carbon dioxide	kg	0.0218

Table 0-6: Inventory for landfill (for 1 kg of glass/inert waste) [351].

Inputs	Quantity	Unit
Landfill of glass/inert waste	1.00E+00	kg
Air	2.34E-01	kg
Antimony	3.62E-15	kg
Barium sulphate	1.22E-17	kg
Basalt	8.89E-10	kg
Bauxite	9.11E-07	kg
Bentonite	4.56E-06	kg
Biotic Production	1.54E-06	kg/a
Biotic Production - Occupation	2.73E-04	kg
Calcium chloride	1.25E-15	kg
Carbon dioxide	1.17E-03	kg
Chromium	2.06E-08	kg
Clay	3.35E-02	kg
Coalbed methane (in MJ)	3.00E-06	MJ
Cobalt	5.88E-13	kg
Colemanite ore	7.27E-07	kg
Copper	1.40E-07	kg
Crude oil (in MJ)	1.07E-01	MJ
Dolomite	5.77E-07	kg
Erosion Resistance	-4.56E-07	kg/a
Erosion Resistance - Occupation	9.59E-05	kg
Feldspar (aluminium silicates)	4.50E-23	kg
Ferro manganese	6.81E-19	kg
Fluorspar (calcium fluoride; fluorite)	1.43E-07	kg
Gold	1.47E-12	kg
Granite	4.50E-23	kg
Graphite	1.64E-12	kg
Groundwater Replenishment	1.55E-04	(mm*m2)/a
Groundwater Replenishment - Occupation	5.68E-02	mm*m2
Gypsum	2.32E-07	kg
Hard coal (in MJ)	1.66E-02	MJ
Heavy spar ($BaSO_4$)	1.47E-09	kg
Ilmenite (titanium ore)	8.70E-09	kg
Inert rock	1.34E-02	kg
Iridium	1.09E-15	kg
Iron	6.11E-04	kg
Kaolin ore	4.32E-08	kg
Land Occupation	3.34E-04	m2*yr
Land Transformation	8.62E-06	sqm
Lead	6.11E-08	kg
Lignite (in MJ)	8.27E-03	MJ
Limestone (calcium carbonate)	1.14E-03	kg
Magnesit (Magnesium carbonate)	6.91E-08	kg

Magnesium	2.39E-09	kg
Magnesium chloride leach (40%)	1.63E-05	kg
Manganese	8.20E-07	kg
Manganese ore	-5.04E-14	kg
Mechanical Filtration	-1.27E-05	cm*m2/d
Mechanical Filtration	2.30E-01	cm*m²
Mercury	2.11E-18	kg
Molybdenum	1.42E-09	kg
Natural Aggregate	2.95E-02	kg
Natural gas (in MJ)	4.44E-02	MJ
Nickel	-7.36E-09	kg
Nitrogen	6.68E-14	kg
Occup. as Convent. arable land	3.65E-04	m2*yr
Occup. as Forest land	-4.69E-17	m2*yr
Oil sand (10% bitumen) (in MJ)	6.33E-05	MJ
Oil sand (100% bitumen) (in MJ)	5.52E-05	MJ
Olivine	7.69E-18	kg
Osmium	1.33E-15	kg
Oxygen	6.82E-07	kg
Palladium	1.93E-14	kg
Peat (in MJ)	4.00E-06	MJ
Phosphorus	-5.24E-06	kg
Physicochemical Filtration	-3.86E-06	(cmol*m2)/kg
Physicochemical Filtration - Occupation	2.48E-04	(cmol*m2*a)/kg
Pit Methane (in MJ)	2.72E-04	MJ
Platinum	3.26E-14	kg
Potashsalt, crude (hard salt, 10% K_2O)	-3.29E-05	kg
Potassium chloride	4.18E-15	kg
Primary energy from geothermics	5.14E-06	MJ
Primary energy from hydro power	1.37E-03	MJ
Primary energy from solar energy	1.39E-02	MJ
Primary energy from waves	4.68E-15	MJ
Primary energy from wind power	2.40E-03	MJ
Primary forest	2.71E-14	kg
Pyrite	8.24E-10	kg
Quartz sand (silica sand; silicon dioxide)	2.33E-02	kg
Raw pumice	3.19E-09	kg
Rhodium	3.29E-15	kg
Ruthenium	6.44E-15	kg
Secondary fuel	6.55E-04	MJ
Secondary fuel renewable	3.21E-04	MJ
Shale gas (in MJ)	5.84E-06	MJ
Silicon	2.64E-09	kg
Silver	7.09E-11	kg
Sodium chloride (rock salt)	2.05E-04	kg

Sodium nitrate	1.03E-25	kg
Sodium sulphate	2.97E-16	kg
Soil	1.41E-02	kg
Stone from mountains	7.38E-06	kg
Sulphur	1.28E-13	kg
Talc	1.76E-11	kg
Tantalum	3.42E-11	kg
Tight gas (in MJ)	8.64E-06	MJ
Tin	4.85E-18	kg
Tin ore	1.43E-09	kg
Titanium	5.43E-11	kg
Titanium ore	9.38E-17	kg
Uranium natural (in MJ)	7.10E-03	MJ
Vanadium	2.08E-10	kg
Water (ground water)	2.13E-01	kg
Water (lake water)	1.27E-01	kg
Water (rain water)	8.59E-01	kg
Water (river water)	7.44E+00	kg
Water (sea water)	7.07E-03	kg
Zinc	3.91E-08	kg
Zirconium	4.09E-16	kg
Outputs		
High radioactive waste	3.65E-09	kg
Low radioactive wastes	5.63E-08	kg
Medium radioactive wastes	2.84E-08	kg
Radioactive tailings	2.73E-06	kg
1,1,1-Trichloroethane	5.83E-19	kg
1,2-Dibromoethane	4.20E-24	kg
1,3,5-Trimethylbenzene [NMVOC]	1.61E-21	kg
1-Butylene (Vinylacetylene) [NMVOC]	4.86E-20	kg
1-Pentene [NMVOC]	1.72E-19	kg
1-Tetradecane [NMVOC]	1.26E-23	kg
1-Tridecane [NMVOC]	3.93E-23	kg
1-Undecane [NMVOC]	1.84E-23	kg
2,2,4-Trimethylpentane [NMVOC]	3.13E-20	kg
2,2-Dimethylbutane [NMVOC]	3.32E-20	kg
2,4-Dimethylpentane [NMVOC]	1.30E-20	kg
2-Methyl-1-butene [NMVOC]	1.25E-19	kg
2-Methylpentane [NMVOC]	2.25E-19	kg
3-Methylpentane [NMVOC]	1.13E-19	kg
Acenaphthene [NMVOC]	5.68E-13	kg
Acenaphthene – fresh water	9.13E-12	kg
Acenaphthene – sea water	2.49E-12	kg
Acenaphthylene	1.12E-12	kg
Acenaphthylene - fresh water	3.92E-12	kg

Acenaphthylene - sea water	1.07E-12	kg
Acetaldehyde (Ethanal) [NMVOC]	2.04E-10	kg
Acetic acid [NMVOC]	2.28E-09	kg
Acetic acid - sea water	2.07E-18	kg
Acetic acid - fresh water	1.13E-11	kg
Acetochlor - fresh water	1.65E-17	kg
Acetochlor - air	2.64E-16	kg
Acetone (dimethylcetone) [NMVOC]	1.91E-10	kg
Acid (calculated as H+)	6.53E-11	kg
Acrolein [NMVOC]	9.89E-13	kg
Acrylonitrile [NMVOC]	3.52E-16	kg
Acrylonitrile - fresh water	1.86E-18	kg
Adsorbable organic (AOX) - sea water	1.64E-15	kg
Adsorbable organic (AOX) - fresh water	5.22E-08	kg
Alachlor	2.68E-11	kg
Aldehyde (unspecified) [NMVOC]	2.67E-11	kg
Alkane (unspecified) [NMVOC]	5.15E-09	kg
Alkane (unspecified) - fresh water	1.89E-18	kg
Alkene (unspecified) [NMVOC]	4.44E-09	kg
Aluminium - air	1.79E-11	kg
Aluminium (+III) - fresh water	1.33E-08	kg
Aluminium (+III) - industrial soil	4.57E-13	kg
Aluminium (+III) - sea water	1.48E-13	kg
Aluminium oxide (dust)	7.55E-11	kg
Americium (Am241)	3.82E-08	Bq
Ammonia - industrial soil	2.94E-10	kg
Ammonia - fresh water	6.49E-09	kg
Ammonia - air	6.46E-07	kg
Ammonia - sea water	2.06E-17	kg
Ammonium – air	2.62E-12	kg
Ammonium (total N) - fresh water	1.37E-16	kg
Ammonium / ammonia - sea water	4.00E-14	kg
Ammonium / ammonia - fresh water	4.60E-07	kg
Ammonium nitrate - air	5.32E-20	kg
Anthracene - fresh water	1.71E-11	kg
Anthracene - sea water	4.66E-12	kg
Anthracene – air	1.54E-13	kg
Antimony - fresh water	1.39E-12	kg
Antimony - industrial soil	1.53E-17	kg
Antimony – air	1.55E-11	kg
Antimony (Sb124) - fresh water	1.11E-05	Bq
Antimony (Sb124) – air	3.86E-07	Bq
Antimony (Sb124) - fresh water	1.26E-05	Bq
Argon - air	3.26E-09	kg
Argon (Ar41) – air	0.01646	Bq

Aromatic hydrocarbons - fresh water	1.19E-10	kg
Aromatic hydrocarbons - sea water	1.81E-11	kg
Arsenic (+V) - fresh water	6.79E-09	kg
Arsenic (+V) – air	2.47E-10	kg
Arsenic (+V) - industrial soil	1.59E-14	kg
Arsenic (+V) - sea water	1.75E-09	kg
Arsenic trioxide – air	7.62E-16	kg
Atrazine - air	4.63E-16	kg
Atrazine - fresh water	2.89E-17	kg
Barium - fresh water	5.59E-08	kg
Barium – air	5.09E-10	kg
Barium - sea water	1.53E-08	kg
Barytes - sea water	1.41E-17	kg
Benomyl – air	6.93E-13	kg
Benomyl - fresh water	4.33E-14	kg
Benzene [NMVOC]	1.25E-08	kg
Benzene - fresh water	2.10E-08	kg
Benzene - sea water	5.73E-09	kg
Benzo-a-anthracene - fresh water	1.05E-12	kg
Benzo-a-anthracene - sea water	2.86E-13	kg
Benzo{a}anthracene	7.78E-14	kg
Benzo{a}pyrene	5.49E-13	kg
Benzo{ghi}perylene	6.95E-14	kg
Benzofluoranthene	1.39E-13	kg
Benzofluoranthene - fresh water	1.27E-13	kg
Benzofluoranthene - sea water	3.49E-14	kg
Beryllium - fresh water	3.53E-13	kg
Beryllium - industrial soil	2.16E-19	kg
Beryllium - sea water	1.32E-18	kg
Beryllium – air	3.01E-12	kg
Biological oxy. demand (BOD) - fresh water	1.75E-06	kg
Biological oxygen demand (BOD) - sea water	1.81E-09	kg
Biphenyl [NMVOC]	1.73E-23	kg
Boron - air	6.25E-16	kg
Boron - fresh water	5.49E-09	kg
Boron - sea water	1.12E-17	kg
Boron compounds (unspecified) – air	4.35E-09	kg
Bromate - fresh water	6.03E-21	kg
Bromide - industrial soil	2.99E-15	kg
Bromine - fresh water	4.16E-17	kg
Bromine - air	8.75E-10	kg
Butadiene [NMVOC]	4.41E-20	kg
Butane [NMVOC]	1.96E-18	kg
Butane (n-butane) [NMVOC]	2.43E-07	kg
Butene [NMVOC]	7.35E-11	kg

Cadmium (+II) - sea water	7.49E-10	kg
Cadmium (+II) - agricultural soil	2.09E-10	kg
Cadmium (+II) - air	3.12E-10	kg
Cadmium (+II) - industrial soil	1.05E-12	kg
Cadmium (+II) - fresh water	2.94E-09	kg
Calcium (+II) - fresh water	4.05E-06	kg
Calcium (+II) - industrial soil	6.29E-10	kg
Calcium (+II) - sea water	2.32E-15	kg
Caprolactam [NMVOC]	1.82E-14	kg
Carbofuran – air	3.81E-14	kg
Carbofuran - fresh water	2.38E-15	kg
Carbon (C14) – air	0.020955	Bq
Carbon (C14) - sea water	0.003563	Bq
Carbon (C14) - fresh water	6.14E-06	Bq
Carbon dioxide – air	0.01278	kg
Carbon dioxide (biotic) - air	0.00126	kg
Carbon dioxide (land use change) –air	2.30E-05	kg
Carbon disulphide – air	1.36E-18	kg
Carbon monoxide - air	4.95E-05	kg
Carbon, organically bound - fresh water	6.31E-06	kg
Carbonate - sea water	9.61E-07	kg
Carbonate - fresh water	2.63E-06	kg
Cesium (Cs134) - fresh water	4.38E-06	Bq
Cesium (Cs134) - sea water	4.28E-05	Bq
Cesium (Cs134) – air	6.76E-08	Bq
Cesium (Cs137) – air	6.63E-08	Bq
Cesium (Cs137) - fresh water	1.90E-05	Bq
Cesium (Cs137) - sea water	0.000572	Bq
Chemical oxy. demand (COD) - fresh water	6.50E-06	kg
Chemical oxy. demand (COD) - sea water	9.19E-08	kg
Chlorate - fresh water	3.05E-16	kg
Chloride - fresh water	0.000302	kg
Chloride - sea water	7.59E-05	kg
Chloride - industrial soil	4.85E-07	kg
Chloride (unspecified) - to air	5.01E-09	kg
Chlorinated hydrocarbons - fresh water	2.25E-18	kg
Chlorine – air	3.61E-08	kg
Chlorine - fresh water	2.70E-14	kg
Chlorine - industrial soil	1.29E-14	kg
Chlorine (dissolved) - fresh water	1.26E-08	kg
Chloromethane (methyl chloride) – air	6.26E-18	kg
Chloromethane - fresh water	4.48E-17	kg
Chromium (+III) - fresh water	3.37E-10	kg
Chromium (+III) – air	6.20E-12	kg
Chromium (+III) - agricultural soil	4.57E-09	kg

Chromium (+III) - industrial soil	3.29E-15	kg
Chromium (+VI) – air	1.14E-17	kg
Chromium (+VI) - fresh water	1.31E-09	kg
Chromium (+VI) - industrial soil	8.95E-19	kg
Chromium (unspecified) - sea water	2.75E-09	kg
Chromium (unspecified) - industrial soil	6.38E-14	kg
Chromium (unspecified) - agricultural soil	-2.10E-11	kg
Chromium (unspecified) – air	4.32E-10	kg
Chromium (unspecified) - fresh water	1.02E-08	kg
Chrysene	1.91E-13	kg
Chrysene - fresh water	3.83E-12	kg
Chrysene - sea water	1.05E-12	kg
cis-2-Pentene [NMVOC]	1.29E-19	kg
Clean gas – air	0.002409	kg
Cobalt - fresh water	8.71E-11	kg
Cobalt - industrial soil	1.57E-14	kg
Cobalt - sea water	5.73E-15	kg
Cobalt – air	3.87E-11	kg
Cobalt (Co58) – air	2.73E-07	Bq
Cobalt (Co58) - fresh water	6.33E-05	Bq
Cobalt (Co60) – air	7.25E-07	Bq
Cobalt (Co60) - fresh water	5.65E-05	Bq
Cobalt (Co60) - sea water	6.85E-05	Bq
Copper (+II) - sea water	6.06E-10	kg
Copper (+II) - industrial soil	7.75E-14	kg
Copper (+II) - fresh water	4.44E-09	kg
Copper (+II) - agricultural soil	4.33E-09	kg
Copper (+II) – air	4.27E-10	kg
Cresol (methyl phenol) - fresh water	2.02E-19	kg
Cresol (methyl phenol) - sea water	1.55E-19	kg
Cumene (isopropylbenzene) [NMVOC]	1.79E-19	kg
Curium (Cm alpha) - fresh water	5.07E-08	Bq
Cyanide - fresh water	3.47E-10	kg
Cyanide - sea water	5.11E-17	kg
Cyanide (unspecified) – air	1.03E-10	kg
Cyclohexane [NMVOC]	3.39E-13	kg
Cyclopentane [NMVOC]	2.20E-20	kg
Decane [NMVOC]	7.62E-22	kg
Deltamethrin - fresh water	9.27E-14	kg
Deltamethrin – air	1.48E-12	kg
Detergent (unspecified) - fresh water	7.96E-22	kg
Dibenz(a)anthracene	4.33E-14	kg
Dicamba - air	1.77E-17	kg
Dicamba - fresh water	1.11E-18	kg
Dichloroethane (ethylene dichloride) – air	3.16E-22	kg

Dichloroethane - fresh water	6.61E-24	kg
Dichloromethane – air	1.93E-15	kg
Dichloropropane - fresh water	4.24E-25	kg
Diethylamine [NMVOC]	-1.01E-19	kg
Different pollutants - industrial soil	1.34E-20	kg
Dimethenamid - air	5.24E-17	kg
Dimethenamid - fresh water	3.28E-18	kg
Dimethylamine [NMVOC]	3.06E-16	kg
Dioxins (unspec.) – air	2.41E-16	kg
Dodecane [NMVOC]	4.11E-23	kg
Dust (> PM10) - Particles to air	5.61E-07	kg
Dust (PM10) - Particles to air	4.12E-09	kg
Dust (PM2,5 - PM10) - Particles to air	0.000194	kg
Dust (PM2.5) - Particles to air	3.91E-06	kg
Ethane [NMVOC]	6.89E-07	kg
Ethanol [NMVOC]	3.86E-10	kg
Ethene (ethylene) [NMVOC]	4.32E-11	kg
Ethyl benzene [NMVOC]	4.40E-09	kg
Ethyl benzene - fresh water	1.14E-09	kg
Ethyl benzene - sea water	3.12E-10	kg
Exhaust - air	0.093269	kg
Fipronil - Pesticides to air	1.80E-18	kg
Fipronil - Pesticides to fresh water	1.13E-19	kg
Fluoranthene - fresh water	1.19E-12	kg
Fluoranthene [NMVOC]	5.04E-13	kg
Fluoranthene - sea water	3.25E-13	kg
Fluorene [NMVOC]	1.60E-12	kg
Fluoride - industrial soil	5.33E-10	kg
Fluoride - fresh water	2.52E-06	kg
Fluoride – air	3.73E-09	kg
Fluoride - sea water	5.22E-11	kg
Fluorine – air	1.00E-12	kg
Fluorine - fresh water	8.22E-12	kg
Formaldehyde (methanal) - fresh water	6.81E-15	kg
Formaldehyde (methanal) [NMVOC]	1.25E-08	kg
Glyphosate - fresh water	2.70E-18	kg
Glyphosate – air	4.33E-17	kg
Halon (1301) – air	3.00E-20	kg
Hazardous waste (deposited)	5.84E-08	kg
Heavy metals to air (unspecified)	8.15E-12	kg
Heavy metals to water (unspecified)	3.20E-17	kg
Helium - air	4.02E-13	kg
Heptane (isomers) [NMVOC]	5.85E-09	kg
Hexamethylene diamine (HMDA) [NMVOC]	4.36E-22	kg
Hexane (isomers) [NMVOC]	4.94E-08	kg

Hexane (isomers) - sea water	1.69E-20	kg
Hexane (isomers) - fresh water	2.21E-20	kg
Hydrocarbons (unspecified) - sea water	2.92E-15	kg
Hydrocarbons (unspecified) - fresh water	1.48E-10	kg
Hydrocarbons (unspecified) [VOC]	5.80E-08	kg
Hydrocarbons, aromatic [NMVOC]	7.54E-11	kg
Hydrocarbons, chloro-/fluoro – air	3.98E-15	kg
Hydrocarbons, halogenated – air	1.32E-15	kg
Hydrogen – air	1.34E-05	kg
Hydrogen arsenic (arsine) – air	6.32E-14	kg
Hydrogen bromine (hydrobromic acid) – air	2.26E-14	kg
Hydrogen chloride – air	3.53E-07	kg
Hydrogen chloride - fresh water	1.26E-11	kg
Hydrogen cyanide (prussic acid) – air	1.36E-12	kg
Hydrogen cyanide - fresh water	2.12E-18	kg
Hydrogen fluoride - to air	1.44E-08	kg
Hydrogen fluoride - fresh water	3.77E-08	kg
Hydrogen iodide – air	2.13E-21	kg
Hydrogen peroxide - fresh water	2.75E-09	kg
Hydrogen phosphorous – air	2.17E-14	kg
Hydrogen sulphide – air	4.64E-08	kg
Hydrogen-3, Tritium - air	0.057635	Bq
Hydrogen-3, Tritium - sea water	4.681625	Bq
Hydrogen-3, Tritium - fresh water	1.173935	Bq
Hydroxide - fresh water	2.19E-12	kg
Indeno[1,2,3-cd]pyrene	5.18E-14	kg
Inert gases	2.56E-25	Bq
Inorganic dissolved matter - fresh water	2.92E-18	kg
Inorganic salts and acids - fresh water	2.97E-24	kg
Iodide - fresh water	1.45E-18	kg
Iodine (I129) - fresh water	5.57E-06	Bq
Iodine (I129) - air	8.62E-08	Bq
Iodine (I131) – air	0.000538625	Bq
Iodine (I131) - fresh water	2.22E-06	Bq
Iodine (I131) - sea water	0.000626	Bq
Iron - sea water	1.43E-13	kg
Iron - fresh water	1.42E-06	kg
Iron – air	4.97E-09	kg
Iron - industrial soil	1.73E-11	kg
Iron ion (+III) - fresh water	5.89E-17	kg
iso-Butane [NMVOC]	6.39E-19	kg
iso-Pentane [NMVOC]	2.52E-18	kg
Isopropanol [NMVOC]	1.92E-11	kg
Krypton (Kr85) - air	0.121205	Bq
Krypton (Kr85m) – air	0.089492	Bq

Lanthanides – air	8.78E-20	kg
Lead (+II) - sea water	5.21E-10	kg
Lead (+II) - fresh water	3.98E-09	kg
Lead (+II) - air	3.90E-09	kg
Lead (+II) - agricultural soil	6.77E-09	kg
Lead (+II) - industrial soil	1.47E-13	kg
Lead (Pb210) – air	2.52E-05	Bq
Lead dioxide – air	2.60E-17	kg
Magnesium - sea water	3.17E-10	kg
Magnesium - fresh water	1.69E-07	kg
Magnesium - industrial soil]	2.67E-11	kg
Magnesium chloride - fresh water	7.57E-12	kg
Magnesium ion (+II) - fresh water	7.30E-14	kg
Mancozeb - air	4.03E-12	kg
Mancozeb - fresh water	2.52E-13	kg
Manganese (+II) - sea water	2.29E-14	kg
Manganese (+II) – air	7.07E-09	kg
Manganese (+II) - fresh water	6.66E-09	kg
Manganese (+II) - industrial soil	1.63E-13	kg
Manganese (Mn54) - fresh water	5.69E-06	Bq
Mercaptan (unspecified) [NMVOC]	2.67E-12	kg
Mercury (+II) - industrial soil	3.36E-16	kg
Mercury (+II) - sea water	4.27E-12	kg
Mercury (+II) - agricultural soil	4.57E-11	kg
Mercury (+II) – air	1.07E-08	kg
Mercury (+II) - fresh water	7.56E-11	kg
meta-Cresol [NMVOC]	1.99E-15	kg
Metal ions (unspecific) - fresh water	2.98E-11	kg
Metals (unspecified) - fresh water	1.93E-15	kg
Metals (unspecified) – air	6.00E-17	kg
Methacrylate [NMVOC]	4.91E-16	kg
Methane (group VOC)	2.28E-05	kg
Methane (biotic) (group VOC)	7.85E-10	kg
Methanol - fresh water	-6.57E-09	kg
Methanol [NMVOC]	4.01E-10	kg
Methomyl - fresh water	7.00E-17	kg
Methomyl – air	1.12E-15	kg
Methyl bromide – air	1.74E-18	kg
Methyl cyclopentane [NMVOC]	4.49E-20	kg
Methyl methacrylate (MMA) [NMVOC]	7.64E-14	kg
Methyl tert-butylether [NMVOC]	1.26E-19	kg
Molybdenum - sea water	5.94E-20	kg
Molybdenum – air	1.93E-11	kg
Molybdenum - fresh water	4.46E-10	kg
Naphthalene - sea water	1.80E-10	kg

Naphthalene – air	1.68E-11	kg
Naphthalene - fresh water	6.59E-10	kg
n-Butyl acetate [NMVOC]	1.71E-18	kg
Nickel (+II) - industrial soil	4.05E-13	kg
Nickel (+II) - sea water	9.72E-10	kg
Nickel (+II) - agricultural soil	2.26E-09	kg
Nickel (+II) - air	4.84E-10	kg
Nickel (+II) - fresh water	6.80E-09	kg
Nitrate - sea water	2.61E-09	kg
Nitrate - fresh water	4.50E-06	kg
Nitric acid - industrial soil	4.46E-17	kg
Nitrite - sea water	1.94E-11	kg
Nitrite - fresh water	1.47E-12	kg
Nitrogen - industrial soil	1.28E-15	kg
Nitrogen - fresh water	8.02E-12	kg
Nitrogen (as total N) - fresh water	3.31E-11	kg
Nitrogen (atmospheric nitrogen) - air	6.54E-06	kg
Nitrogen dioxide – air	1.08E-07	kg
Nitrogen monoxide – air	8.87E-07	kg
Nitrogen organic bounded - fresh water	6.53E-07	kg
Nitrogen oxides – air	7.39E-05	kg
Nitrogenous Matter - fresh water	6.44E-09	kg
Nitrogentriflouride – air	5.57E-14	kg
Nitrous oxide (laughing gas) – air	2.47E-07	kg
NMVOC (unspecified) [NMVOC]	7.47E-06	kg
Nonane [NMVOC]	2.01E-22	kg
Octane [NMVOC]	3.22E-09	kg
Oil (unspecified) - sea water	2.92E-08	kg
Oil (unspecified) - fresh water	2.33E-07	kg
Oil (unspecified) - industrial soil	3.00E-13	kg
Organic chlorine compounds (group VOC)	8.13E-19	kg
Organic chlorine compounds - fresh water	2.09E-17	kg
Organic compounds dissol.- fresh water	9.74E-17	kg
Organic compounds - fresh water]	1.30E-06	kg
Overburden (deposited)	0.021628	kg
Oxygen - air	0.000514	kg
Palladium – air	3.45E-20	kg
para-Cresol [NMVOC]	1.97E-15	kg
Pentachlorophenol (PCP) - fresh water	4.54E-15	kg
Pentane (n-pentane) [NMVOC]	1.05E-07	kg
Phenanthrene	5.10E-12	kg
Phenol (hydroxy benzene) – sea water	5.80E-09	kg
Phenol (hydroxy benzene) [NMVOC]	6.62E-12	kg
Phenol (hydroxy benzene) - fresh water	2.14E-08	kg
Phosphate - fresh water	1.01E-07	kg

Phosphorus - sea water	3.48E-13	kg
Phosphorus - fresh water	2.51E-07	kg
Phosphorus - industrial soil	2.45E-11	kg
Plutonium (Pu alpha) - fresh water	1.52E-07	Bq
Plutonium (Pu alpha) – air	9.49E-13	Bq
Polonium (Po210) – air	3.78E-05	Bq
Polychlorinated biphenyls (PCB) - air	1.14E-13	kg
Polychlorinateddibenzo-p-dioxins - fresh water	1.40E-24	kg
Polychlorinated dibenzo-p-dioxins - air	2.86E-16	kg
Polycyclic aromatic hydrocarbons (carcinogenic)	8.96E-11	kg
Polycyclic aromatic hydrocarbons - fresh water	2.51E-12	kg
Polycyclic aromatic hydrocarbons - industrial soil	1.90E-13	kg
Potassium - sea water	3.14E-16	kg
Potassium - fresh water	-3.10E-07	kg
Potassium (+I) - industrial soil	5.46E-11	kg
Propane [NMVOC]	9.57E-07	kg
Propene (propylene) [NMVOC]	7.39E-10	kg
Propionic acid (propane acid) [NMVOC]	2.21E-13	kg
Propylene glycol methyl ether acetate [NMVOC]	3.70E-12	kg
Protactinium (Pa234m) - fresh water	5.17E-05	Bq
Protactinium (Pa234m) – air	1.11E-08	Bq
R 11 (trichlorofluoromethane) – air	4.82E-17	kg
R 114 (dichlorotetrafluoroethane) - air	2.35E-13	kg
R 116 (hexafluoroethane) - air	6.97E-13	kg
R 12 (dichlorodifluoromethane) – air	1.04E-17	kg
R 124 (chlorotetrafluoroethane) – air	1.75E-18	kg
R 125 (pentafluoroethane) - air	2.70E-13	kg
R 13 (chlorotrifluoromethane) - air	6.51E-18	kg
R 134a (tetrafluoroethane) - air	1.73E-13	kg
R 143 (trifluoroethane) - air	2.41E-13	kg
R 22 (chlorodifluoromethane) - air	5.80E-14	kg
R 23 (trifluoromethane) - air	1.86E-12	kg
R 245fa - air	4.79E-12	kg
R32 (difluoromethane) - air	4.05E-14	kg
Radioactive emissions (general) – air	3.36E-11	Bq
Radioactive isotopes - fresh water	3.10E-13	Bq
Radium (Ra224) - fresh water	7.24E-16	Bq
Radium (Ra226) - fresh water	0.198084	Bq
Radium (Ra226) - air	0.000148	Bq
Radium (Ra228) - fresh water	1.45E-15	Bq
Radon (Rn222) - air	10.86163	Bq
Rhodium - air	3.33E-20	kg
Ruthenium (Ru106) - sea water	0.001926	Bq
Ruthenium (Ru106) - fresh water	9.21E-06	Bq
Scandium - air	4.41E-20	kg

Selenium - industrial soil	4.75E-17	kg
Selenium - fresh water	7.54E-11	kg
Selenium - air	2.70E-10	kg
Silicate particles -fresh water	3.67E-13	kg
Silicium tetrafluoride - air	1.02E-14	kg
Silicon dioxide (silica) - fresh water	2.36E-13	kg
Silicon dioxide (silica) - Particles to air	1.69E-12	kg
Silver - sea water	1.76E-19	kg
Silver - fresh water	1.74E-10	kg
Silver - air	1.79E-11	kg
Silver (Ag110m) - fresh water	1.42E-05	Bq
Sodium (+I) - sea water	3.62E-08	kg
Sodium (+I) - industrial soil	7.30E-11	kg
Sodium (+I) - fresh water	5.56E-06	kg
Sodium chloride (rock salt) - fresh water	6.01E-10	kg
Sodium hypochlorite - fresh water	6.78E-07	kg
Sodium sulphate - fresh water	5.61E-08	kg
Soil loss by erosion into water – fresh water	6.23E-05	kg
Solids (dissolved) - fresh water	7.26E-09	kg
Solids (suspended) - sea water	1.44E-06	kg
Solids (suspended) - fresh water	1.43E-05	kg
Spoil (deposited)	0.006950074	kg
Strontium - industrial soil	2.08E-15	kg
Strontium - sea water	3.76E-11	kg
Strontium - air	1.71E-18	kg
Strontium - fresh water	4.59E-09	kg
Strontium (Sr90) - sea water	9.68E-05	Bq
Strontium (Sr90) - fresh water	6.40E-07	Bq
Styrene [NMVOC]	5.03E-12	kg
Sulphate - sea water	4.05E-07	kg
Sulphate - industrial soil	4.90E-12	kg
Sulphate - fresh water	1.11E-05	kg
Sulphide -sea water	1.75E-07	kg
Sulphide - industrial soil	2.93E-11	kg
Sulphide - fresh water	6.40E-07	kg
Sulphite - fresh water	1.66E-09	kg
Sulphur - industrial soil	2.77E-12	kg
Sulphur -sea water	4.45E-12	kg
Sulphur - air	4.10E-12	kg
Sulphur - fresh water	2.12E-14	kg
Sulphur dioxide - air	3.72E-05	kg
Sulphur hexafluoride - air	6.75E-17	kg
Sulphur trioxide - fresh water	1.30E-11	kg
Sulphur trioxide - air	1.08E-09	kg
Sulphuric acid - fresh water	2.92E-12	kg

Sulphuric acid - air	3.97E-12	kg
Tailings (deposited)	0.000160	kg
Tantalum - fresh water	1.63E-17	kg
Tellurium - air	3.55E-13	kg
Terbufos - fresh water	1.24E-18	kg
Terbufos - air	1.99E-17	kg
Tetrachloroethene - sea water	2.49E-20	kg
Tetrachloroethene - fresh water	6.04E-17	kg
Tetrachloroethene - air	1.13E-17	kg
Tetrafluoromethane - air	7.22E-12	kg
Thallium - fresh water	2.67E-14	kg
Thallium – air	2.51E-12	kg
Thorium (Th228) - fresh water	2.90E-15	Bq
Thorium (Th230) - fresh water	0.004519	Bq
Thorium (Th230) - air	3.78E-05	Bq
Thorium (Th234) - fresh water	5.17E-05	Bq
Thorium (Th234) - air	1.14E-08	Bq
Tin (+IV) - sea water	2.11E-19	kg
Tin (+IV) - fresh water	1.21E-16	kg
Tin (+IV) - air	1.17E-10	kg
Tin oxide - air	7.85E-23	kg
Titanium - sea water	2.15E-20	kg
Titanium - fresh water	7.04E-11	kg
Titanium - air	9.41E-11	kg
Toluene (methyl benzene) - sea water	3.49E-09	kg
Toluene (methyl benzene) - fresh water	1.27E-08	kg
Toluene (methyl benzene) [NMVOC]	2.93E-09	kg
Tot. diss. organic bounded C - fresh water	9.75E-13	kg
Tot. diss. organic bounded C - sea water	1.81E-09	kg
Total organic bounded C - fresh water	4.01E-08	kg
Total organic carbon - air	2.00E-20	kg
trans-2-Butene [NMVOC]	9.72E-20	kg
trans-2-Pentene [NMVOC]	2.41E-19	kg
Trichloroethene (isomers) – air	4.67E-13	kg
Trichloromethane (chloroform) - fresh water	6.04E-17	kg
Triethylene glycol - fresh water	7.95E-19	kg
Trifluralin - fresh water	7.60E-13	kg
Trifluralin - air	1.22E-11	kg
Tungsten - fresh water	1.13E-12	kg
Unused prim. Ener. (geothermal) - fresh water	1.33E-10	MJ
Unused prim. Ener. (hydropower) - fresh water	0.000205	MJ
Unused prim. Ener. (solar) - air	0.002343	MJ
Unused prim. Ener. (wind power) - air	0.00144	MJ
Uranium - fresh water	0.000380	Bq
Uranium (total) - air	8.59E-11	Bq

Uranium (U234) - sea water	5.70E-06	Bq
Uranium (U234) - fresh water	0.000141	Bq
Uranium (U234) - air	1.05E-05	Bq
Uranium (U235) - fresh water	9.19E-06	Bq
Uranium (U235) - air	1.79E-06	Bq
Uranium (U238) - sea water	5.70E-06	Bq
Uranium (U238) - fresh water	0.000140	Bq
Uranium (U238) - air	1.14E-05	Bq
Used air - air	0.001421	kg
Vanadium (+III) - sea water	1.59E-17	kg
Vanadium (+III) - fresh water	9.67E-11	kg
Vanadium (+III) - air	9.74E-10	kg
Vinyl chloride (VCM) - fresh water	5.72E-15	kg
Vinyl chloride (VCM) - air	2.98E-13	kg
Waste (deposited)	1.001409	kg
Waste heat - sea water	6.34E-06	MJ
Waste heat - fresh water	0.003294	MJ
Waste heat [Other emissions to air]	0.021772	MJ
Water (evapotranspiration) - air	0.123735	kg
Water (waste water) - fresh water	2.07E-08	kg
Water (cooling water) - fresh water	0.188391	kg
Water (rain water) - fresh water	0.740942	kg
Water (turbined) -fresh water	7.357480	kg
Water (river water, waste) - fresh water	0.200200	kg
Water (sea water, cooling) - sea water	0.007015	kg
Water (sea water, waste) - sea water	6.09E-05	kg
Water vapour - air	0.032965	kg
Xenon (Xe131m) - air	0.012286	Bq
Xenon (Xe133) - air	0.199603	Bq
Xenon (Xe133m) - air	0.009198	Bq
Xenon (Xe135) - air	0.337445	Bq
Xenon (Xe135m) - air	0.017486	Bq
Xenon (Xe137) - air	0.058375	Bq
Xenon (Xe138) - air	0.064098	Bq
Xylene (dimethyl benzene) [NMVOC]	2.06E-08	kg
Xylene (isomers) - sea water	1.25E-09	kg
Xylene (isomers) - fresh water	4.55E-09	kg
Xylene (1,3-Dimethylbenzene) [NMVOC]	3.28E-20	kg
Xylene (1,2-Dimethylbenzene) [NMVOC]	3.18E-21	kg
Zinc (+II) - industrial soil	2.70E-13	kg
Zinc (+II) - sea water	1.89E-11	kg
Zinc (+II) - fresh water	7.70E-09	kg
Zinc (+II) - agricultural soil	1.77E-08	kg
Zinc (+II) - air	7.86E-10	kg
Zinc sulphate - air	1.33E-12	kg

References - APPENDIX

[1] N. Jungbluth, M. Stucki, R. Frischknecht, S. Buesser, Photovoltaics - Part XII, in: R.E.e.a. In Dones (Ed.), ecoinvent report No. 6-XII, 2010.

[2] A. Louwen, W. Sark, R. Schropp, W. Turkenburg, A. Faaij, Life-cycle greenhouse gas emissions and energy payback time of current and prospective silicon heterojunction solar cell designs, Progress in Photovoltaics: Research and Applications, (2014).

[3] N. Espinosa, L. Serrano-Luján, A. Urbina, F.C. Krebs, Solution and vapour deposited lead perovskite solar cells: Ecotoxicity from a life cycle assessment perspective, Solar Energy Materials and Solar Cells, 137 (2015) 303-310.

[4] L. Serrano-Lujan, N. Espinosa, T.T. Larsen-Olsen, J. Abad, A. Urbina, F.C. Krebs, Tin-and Lead-Based Perovskite Solar Cells under Scrutiny: An Environmental Perspective, Advanced Energy Materials, 5 (2015).

[5] in, 2016.

[6] R. Frischknecht, R. Itten, P. Sinha, M. de Wild-Scholten, J. Zhang, V. Fthenakis, H. Kim, M. Raugei, M. Stucki, Life Cycle Inventories and Life Cycle Assessment of Photovoltaic Systems, International Energy Agency (IEA) PVPS Task 12, Report T12, 4 (2015).

[7] E. CENTRE, Ecoinvent data v2.1. Technical report., in, Swiss Centre for Life Cycle Inventories, Dübendorf, Switzerland.